Instituto de Parasitología y Biomedicina
"López-Neyra"

Universidad de Granada

"Estudio de la localización de la proteína CD38 en microdominios de membrana del linfocito T: función en la sinapsis inmunológica"

TESIS DOCTORAL

PILAR MUÑOZ FERNÁNDEZ

Granada, 2007

Editor: Editorial de la Universidad de Granada
Autor: Pilar Muñoz Fernández
D.L.: Gr. 1693 - 2007
ISBN: 978-84-338-4409-5

Índice

II.II Pavón, E.J., Muñoz, P., Lario, A., Longobardo, V., Carrascal, M., Abián, J., Martín, A.B., Arias, S.A., Callejas-Rubio, J.L., Sola, R., Navarro-Pelayo, F., Raya-Álvarez, E., Ortego-Centeno, N., Zubiaur, M., and Sancho, J.
Proteomics 2006 (6); S282-S292
"Proteomic analysis of plasma from patients with systemic lupus erythematosus: Increased presence of haptoglobin α2 polypeptide chains over the α1 isoforms".

II.III Caparrós, E., Muñoz, P., Sierra-Filardi, E., Serrano-Gómez, D., Puig-Kröger, A., Rodríguez-Fernández, J.L., Mellado, M., Sancho, J., Zubiaur, M., and Corbí, A.
Blood 2006 (107)10;3950-3958
"DC-SIGN ligation on dendritic cells results in ERK and PI3K activation and modulates cytokine production".

II.IV Dominguez-Soto, L., Aragoneses-Fenoll, L., Martín-Gayo, E., Martínez-Prats, L., Colmenares, M., Naranjo-Gómez, M., Borrás, F.E., Muñoz, P., Zubiaur, M., Toribio, M.L., Delgado, R., and Corbí, A.
Blood 2007 (109)12;5337-5345
"The DC-SIGN-related lectin LSECtin mediates antigen capture and pathogen binding by human myeloid cells".

Abreviaturas

Aa: Aminoácido

celulas NK: Células *Natural Killer*

NAD^+: Nicotín-adenin-dinucleótido

$NAD(P)^+$: Nicotín-adenin-dinucleótido fosfato

ADPR: Adenosín-difosfato-ribosa

ADPRc: Adenosín-difosfato-ribosa cíclico

ATP: Adenosín-trifosfato

RyR: Receptor de rianodina

TRPM2: Melastatin-related transient receptor potential channel 2.

LAK: Lymphokine-activated killer cells. Se obtienen a partir de PBLs de sangre periférica humana tras la eliminación de células B y macrófagos, percoll, adhesión a plástico y diferenciación con IL2 durante 10 dias.

APC: Célula presentadora del antígeno

SNP: Single-nucleotide-polymorphism. Polimorfismo debido al cambio de un nucleótido

RARE: Elemento de respuesta a ácido retinoico

GPI: glicosil-fosfatidil-inositol.

NGD^+: Nicotinamin-guanin-dinucleótido

B-CLL: Leucemia linfocítica crónica de células B

PBMCs: Células mononucleares de sangre periférica.

DC: Células dendríticas

GM-CSF: Granulocyte macrophage colony stimulating factor

FRET: Fluorescence resonance energy transfer

fMLF: formyl-metionil peptide

$InsP_3$: Inositoles tri-fosfato

CsA: Ciclosporina A

ITAM: Motivos de activación del receptor basados en tirosina

DRM: Dominios de membrana resistentes a detergente

SI: Sinapsis inmunológica

MC: Microcluster

PI: Fosfatidil inositol

Resumen

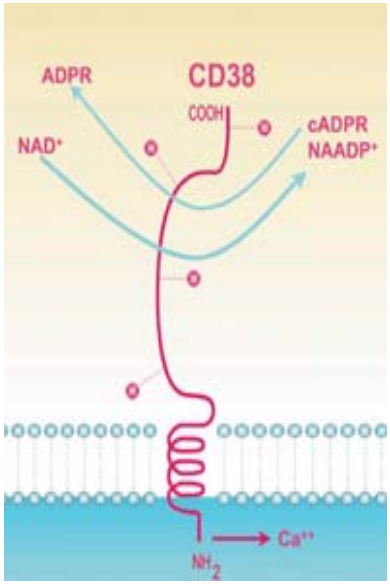

CD38 es una glicoproteína transmembrana de tipo II. Está ampliamente expresada en diferentes tipos celulares incluyendo timocitos, células T activadas, y células B diferenciadas (células plasmáticas) y en tejidos como cerebro, hígado, páncreas, tejido cardíaco... Otras células en las que se expresa son monocitos, macrófagos, células dendríticas, algunas células epiteliales y células NK.

Czura, A.W., et al. *Mol. Med*. (2006) **12**(11-12);309-311

Su dominio extracelular tiene actividad enzimática (puede convertir NAD^+ en ADPRc, que es un agente movilizante de Ca^{2+}). A pesar de tener un corto dominio intracelular sin motivos de activación, CD38 es capaz de señalizar, por lo que en su papel como receptor promuevo proliferación celular, rescate de apoptosis, fosforilación en tirosina de proteínas, movilización de calcio intracelular...Para la señalización celular CD38 necesita de la presencia del complejo TCR/CD3 y de Lck. ZAP-70 y LAT son algunos de los sustratos que se fosforilan tras la estimulación a través de CD38.

Está descrito que CD38 controla la quimiotaxis de neutrófilos hacia quimioatrayentes bacterianos a través de su producción de ADPRc y que actúa como regulador de inflamación y respuesta inmune innata. Además, CD38 se requiere para la migración de granulocitos, monocitos y células dendríticas a los sitios de inflamación en la piel y pulmón.

CD38 está presente en los microdominios de membrana o *"rafts",* que son zonas de la membrana enriquecidas en glicoesfingolípidos y colesterol. Además en células T, el complejo TCR/CD3 también aparece en *rafts* y proteínas como Lck y LAT.

Por todo esto, en nuestro laboratorio nos planteamos cómo podía estar todo esto acoplado en los microdominios de membrana. Para ello, mediante técnicas de inmunoprecipitación, analizamos la composición proteica de los *rafts* en los que estaba presente CD38 y además nos planteamos el estudio de la cascada de señalización en el linfocito T cuando es estimulado a través de CD38 mediante anticuerpos monoclonales anti-CD38.

Otro marco de estudio en el que nos centramos fue el de la sinapsis inmunológica. En este contexto, la célula presentadora (APC) "presenta" el antígeno a la célula T dando así lugar al desencadenamiento de toda una cascada de reacciones: liberación de Ca^{2+}, producción de citoquinas... Dada la dependencia de CD38 por el complejo TCR/CD3 nos preguntamos si CD38 se localizaría en la sinapsis inmunológica y que función podría desempeñar en este contexto. En nuestros experimentos vimos que CD38 se redistribuía en toda la zona de contacto célula T-célula B de una manera antígeno-dependiente. Mediante diferentes técnicas y experimentos de transfección con la molécula CD38-GFP, microscopía confocal, western-blot, cuantificación de calcio, citometría de flujo, cultivos celulares, formación de conjugados, fluorimetría… llevamos a cabo el estudio del papel funcional de CD38 en la sinapsis inmunológica.

Comenzamos…

Introducción

El ADP-ribosa cíclico (ADPRc) es un importante metabolito movilizador de calcio producido por la familia de las enzimas ADP-ribosil ciclasa (ciclasas). Se han identificado 3 miembros de esta superfamilia (evolucionalmente conservados), uno del invertebrado *Aplisia californica* y dos de tejidos de mamíferos, CD38 y CD157. En esta tesis nos centramos en el estudio de CD38.

1. CD38

1.1 Descripción

El antígeno humano **CD38** (primeramente denominado T10 [1]) es una glicoproteína transmembrana de tipo II de 45-kDa (300 aminoácidos), con un corto dominio N-terminal citoplasmático (20 aminoácidos), un largo dominio C-terminal extracelular (256 aa), donde reside su capacidad enzimática [1, 2] y cuatro sitios de glicosilación. Ésta molécula puede también existir en una forma soluble presente en fluidos biológicos en condiciones normales y patológicas [3]. CD38 puede estar glicosilado [1] y el dominio intracelular no contiene motivos de activación. Sin embargo hay estudios que demuestran, al menos en linfocitos T, una asociación directa entre el dominio intracelular de CD38 y el dominio SH2 de la cinasa Lck [4]

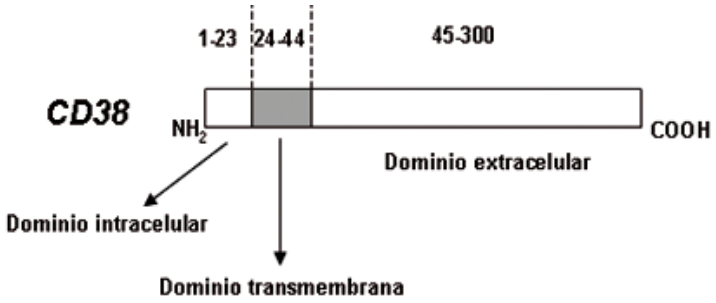

Fig. 1 Esquema de los dominios que componen CD38

CD38 se expresa en diferentes tipos celulares incluyendo timocitos, linfocitos T activados y células B terminalmente diferenciadas (células plasmáticas) [5] [6], células NK, monocitos, macrófagos, células dendríticas y algunas células epiteliales. CD38 no sólo está presente en la superficie celular sino que también se ha detectado en diferentes orgánulos intracelulares [7, 8], incluyendo el núcleo [9-11].

CD38 es un importante regulador en la reabsorción de hueso (osteoclastos) a través de su producción de ADPRc [12]. Además se ha demostrado que el CD38 localizado en el interior de la membrana nuclear es crítico en la regulación del Ca^{+} nuclear vía ADPRc/RyR

Mediante el uso de anticuerpos anti-CD38 se demostró que, através de CD38, se inducía activación, proliferación [13] y movilización de Ca^{2+} en células T, B y NK humanas. [14].

La estimulación de los linfocitos T con anticuerpos monoclonales específicos contra CD38 induce la secreción de numerosas citocinas como IL-6, IL-10, IFN-γ y GMCSF (granulocyte-macrophage colony stimulating factor) [15]. En el modelo murino se ha descrito que CD38 se expresa selectivamente durante la activación de un conjunto de linfocitos T periféricos maduros, con una proliferación reducida, pero con un mejor potencial de producción de citoquinas (IL-2 e IFN-γ), lo que sugiere un papel de CD38 durante la activación de la célula T y diferenciación [16].

En células B, los efectos de la estimulación a través de CD38 son diferentes: en células B inmaduras humanas se induce apoptosis [17] y en células B maduras humanas y murinas se inhibe la apoptosis [18, 19]

La estimulación a través de CD38 de diversas poblaciones de células linfoides y mieloides implica a numerosos sustratos intracelulares [20] tales como c-*cbl*, ZAP-70 [21], fosfolipasa C-γ [21, 22], *syk* [22] y la tirosina cinasa de Bruton [23, 24]. Además se ha descrito el papel de CD38 en la adhesión linfocito-célula endotelial [25] y la unión a hialurónico [26]

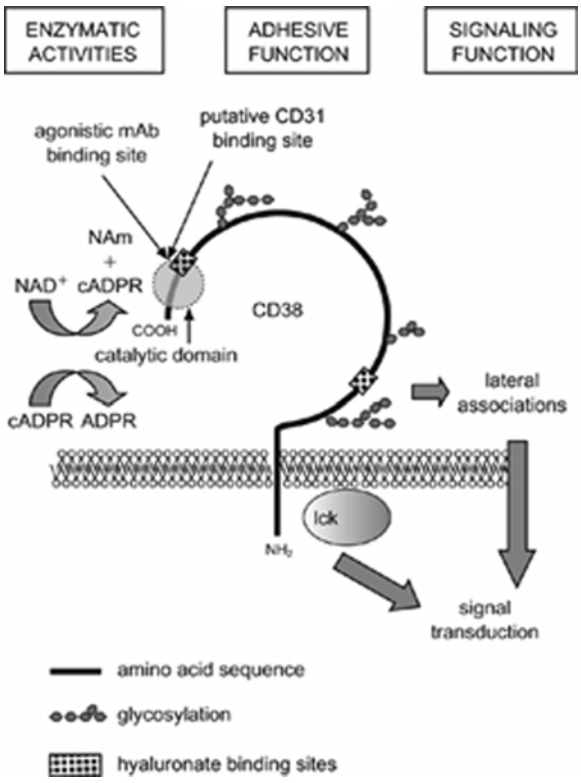

Fig.2

Modelo hipotético del CD38h de superficie basado en la información conocida. En la figura se muestran las regiones de unión a hialurónico y posiblemente a CD31, zona de actividad enzimática, sitios de glicosilación e interacciones moleculares laterales [27].

Savarino, A., et al. *AIDS* (2000), **14** : 1079-1089

1.2 Gen *CD38*

El gen que codifica CD38 está localizado en el cromosoma 4 [28] humano en la región p15 [29] y en el cromosoma 5 en ratón [30].

El CD38 humano está codificado por un gen de copia única de más de 62 kb y que consiste en ocho exones y siete intrones, incluyendo un gran intrón que interrumpe la región 5´ codificante. La región 5´ "aguas arriba" del gen está caracterizada por la ausencia de las cajas TATA y CAAT, la presencia de una región rica en GC inmediatamente aguas arriba del codón, de inicio, algunos sitios de inicio de la transcripción y potenciales sitios de unión para factores de transcripción [31].

CD38 tiene un polimorfismo bien caracterizado (SNP= single-nucleotide polymorphism) localizado en el extremo 5´ del primer intrón (182C>G), el cual resulta en la presencia o (ausencia) de un sitio de restricción *PvuII* [32]. Además este intrón contiene la isla CpG el cual contiene contiene *RARE* (elemento de respuesta al ácido retinoico) responsable de la expresión de CD38 inducida por ácido retinoico (ATRA) [33]. Otra mutación puntual es C/T localizado en el exon 3, en la posición 418, resultando el cambio de la Arg418 por Trp [34]. Un trabajo reciente

[35] investiga la posible asociación de polimorfismos localizados en la posición 182 del intrón 1 (C/G) y 418 (C/T, localizado en el exon 3) en el gen que codifica CD38 con la susceptibilidad y manifestaciones clínicas del lupus eritematoso sistémico (SLE). La frecuencia del genotipo en 194 controles sanos era de 53,1% CC, 40,2% CG y 6,7% GG. Según sus datos, el genotipo CC confiere susceptibilidad y el genotipo CG confiere protección al desarrollo de lupus discoide, por lo que sugieren una ligera influencia en el polimorfismo localizado en el exón 1 al desarrollo del lupus discoide en pacientes con SLE [35].

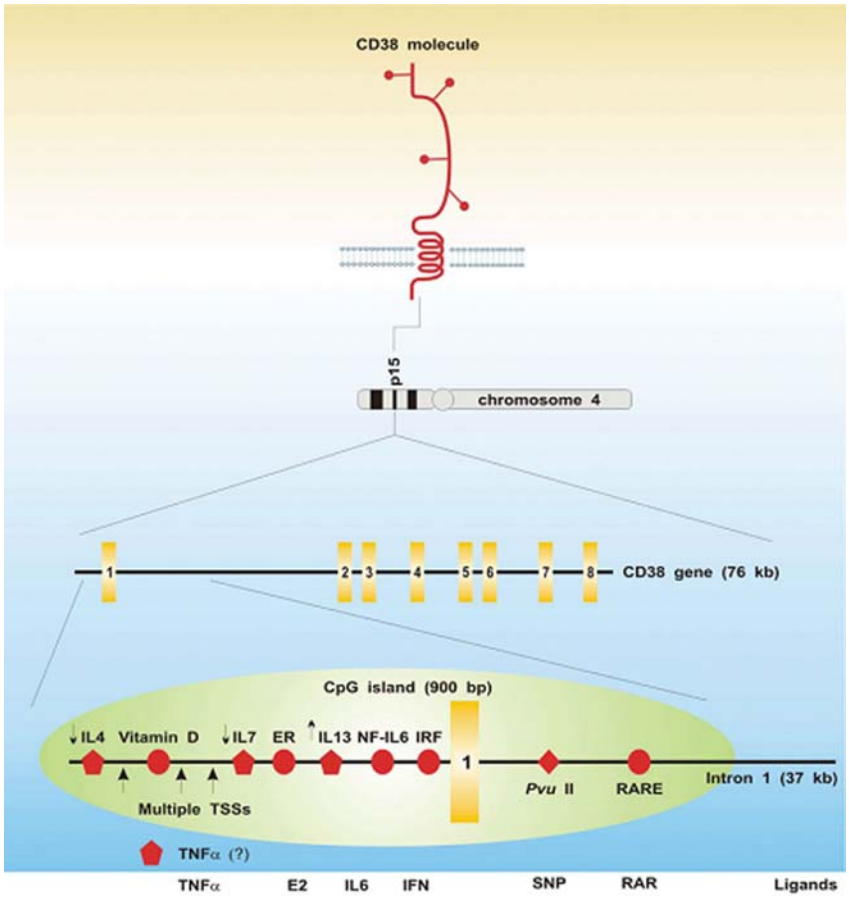

Deaglio S. et al. *Blood* 2006 (**108**); 1135-1144

Fig.3 Gen *CD38*

En 1998, Yagui et al. [34] estudiaron mutaciones de CD38 en 31 pacientes japoneses con diabetes mellitus tipo II. Identificaron 2 patrones variantes en el exón 3 y 4 del gen *CD38*. La variante en el exón 3 resultaba en la sustitución de la Arg^{140} (CGG) por Trp (TGG). Esta mutación la observaron en 4 de estos 31 pacientes y las frecuencias alélicas eran significativamente diferentes en pacientes y en controles. Estudios enzimáticos usando las células COS-7 que expresan esta mutación mostraban una reducción del 50% en la actividad ADP-ribosil ciclasa y cADPR hidrolasa. Esta reducción de ambas actividades causada por la mutación Arg^{140}Trp en CD38 muestra que esta mutación puede contribuir al impedimento de la secreción de insulina *in vivo* en pacientes con diabetes mellitus tipo II. Se sabe que el ADPRc tiene un papel de segundo mensajero en la secreción de insulina a través de la movilización de Ca^{2+} [36-38]. Como CD38 tiene ambas actividades, ADP-ribosil-ciclasa y ADPRc hidrolasa y el ATP inhibe la actividad ADPRc hidrolasa [37, 39], CD38 puede regular la secreción de insulina inducida por glucosa en los islotes pancreáticos [37, 40-42]. Según este estudio, esta mutación estaría implicada en el desarrollo de la diabetes mellitus tipo II vía impedimento de la secreción de insulina inducida por glucosa. El efecto biológico exacto de esta mutación no se conoce, pero la introducción de un anillo aromático podría afectar a la estabilidad de CD38, resultando así la reducción de su actividad enzimática, o incluso a la unión a su ligando [43].

Esta mutación Arg^{140}Trp descrita en pacientes japoneses con diabetes mellitus tipo II fue estudiada en 84 pacientes caucásicos por Mallone et al. [44]. No encontraron esta mutación en ningún paciente y tan sólo la vieron en un sujeto control. Esta discrepancia puede deberse a la heterogeneidad del background genético en estos 2 grupos étnicos [45]. Además, no observaron diferencias en los análisis genéticos del alelo CD38*A (recientemente identificado en la población caucásica [46]) entre individuos sanos y pacientes con diabetes mellitus tipo I y II.

Pupilli, et al [47] demostraron la presencia, en exceso, de anticuerpos anti-CD38 en sueros de pacientes diabéticos (tipo 1 y 2) caucásicos y que estos anticuerpos ejercen un efecto estimulatorio en la secreción de insulina en los islotes pancreáticos humanos. Cuando incubaban estos islotes con suero $CD38^{+}$ generalmente potenciaba el aumento de la producción de insulina de una forma dosis-dependiente. Éste aumento de la secreción era independiente de la cantidad de glucosa porque ocurría a concentraciones bajas y altas de glucosa, mientras que el anticuerpo monoclonal anti-CD38 T16 sólo potenciaba el aumento de insulina en respuesta a altas concentraciones de glucosa.

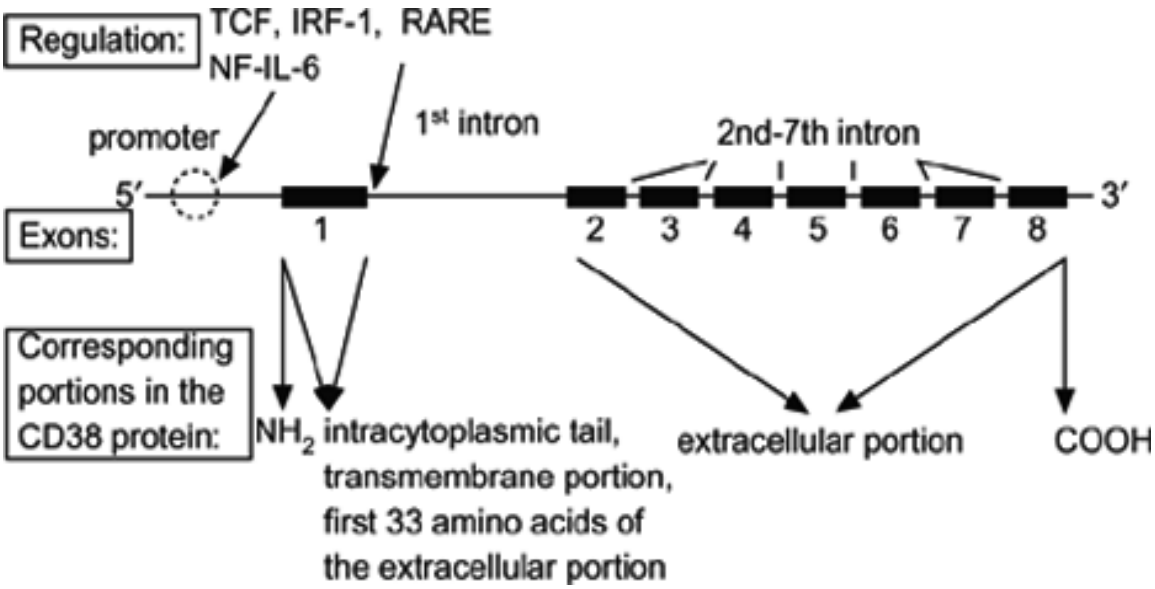

Savarino, A., et al. *AIDS* (2000), **14** ; 1079-1089

Fig. 4

Representación esquemática del gen humano para CD38 (*CD38*) y sus correspondientes porciones en CD38. Además están representados los potenciales sitios de unión a TCF, IRF-1, ácido retinoico y NF-IL-6 [27].

Dentro de la superfamilia de genes que codifican ADP-ribosil ciclasas se conocen, además de *CD38*, otros dos genes estructuralmente relacionados, el que codifica para CD157 y el que codifica para la ADP-ribosil ciclasa del molusco *Aplysia* [48, 49]. Los genes muestran una marcada conservación en la estructura del exón así como la estructura de las proteínas que codifican. Las proteínas además comparten la actividad ciclasa responsable de la conversión catalítica del NAD^+ en ADPRc [32] mediada por su extremo C-terminal. Algunos motivos de unión a ácido hialurónico en su dominio catalítico se piensan que son los responsables de la unión a sustrato. El dominio intracitoplasmático no contiene motivos de activación para permitir por su directa interacción, la señalización intracelular [50].

CD157 y CD38 son ambos productos de un gen duplicado localizado en el brazo corto del cromosoma 4 humano. Sin embargo hay una mayor diferencia en tipología. Mientras que CD38 tiene un dominio transmembrana cerca de su extremo N-terminal, CD157 está unido a membrana mediante GPI. Esto significa que las 2 moléculas pueden posiblemente interaccionar. Por ejemplo, CD157, expresado abundantemente en células endoteliales, podría ser un receptor para CD38, el

cuál es principalmente expresado en linfocitos y plaquetas [32, 48]. Éstas diferentes funciones son consistentes con la baja similaridad (~28%) entre las secuencias de aminoácidos de CD38 y CD157, así como la baja actividad ciclasa de CD157 [51]

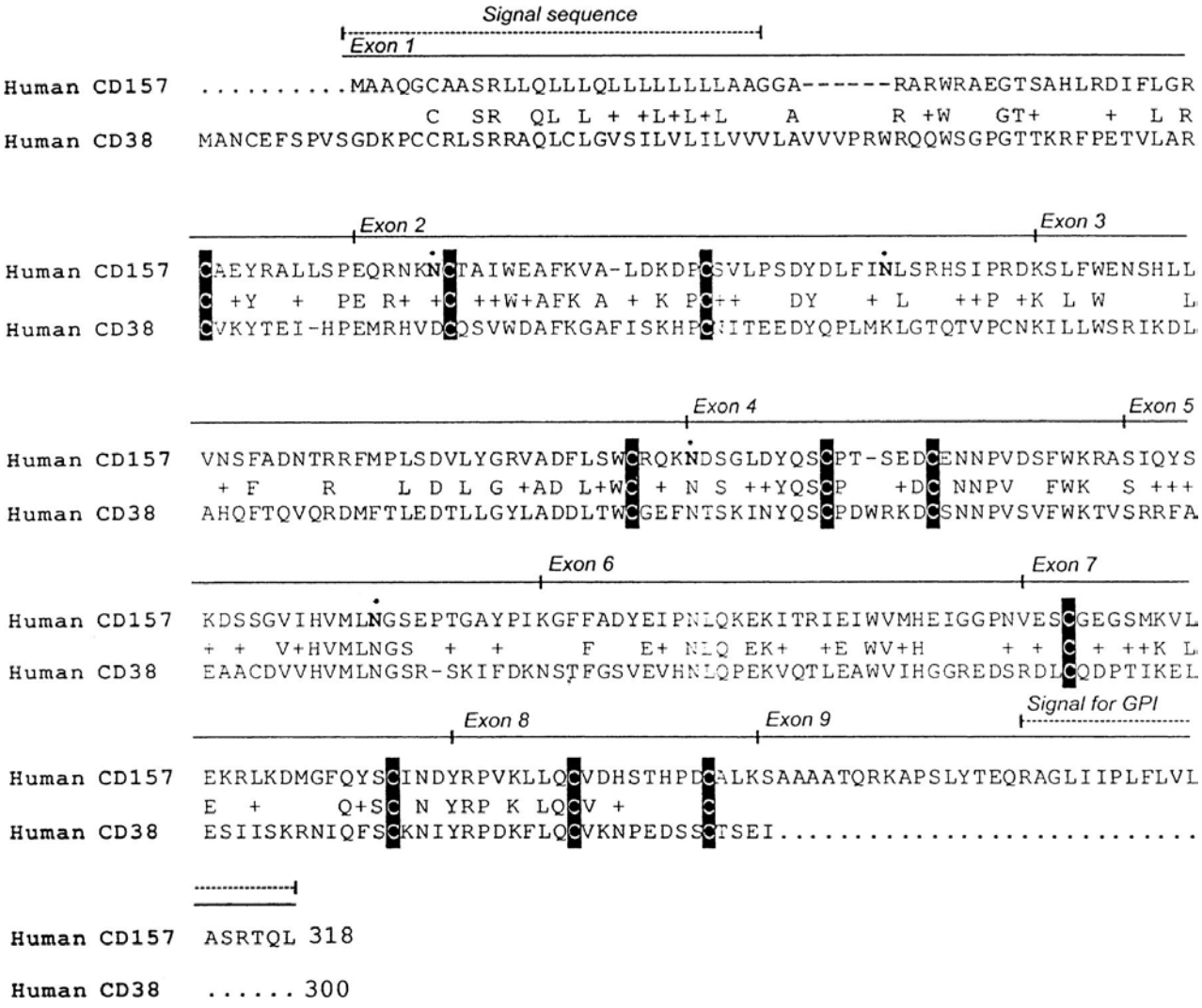

Ortolan E. e al. *Cell. Biochem. Funct* 2002; **20**: 309-322

Fig. 5 Comparación de las secuencias de aminoácidos de CD38 y CD157 (humano)

C- Cisteínas conservadas.

•N- Posibles sitios de glicosilación

Un estudio reciente sugiere que hay un cuarto miembro de la familia ciclasa, otra proteína anclada a membrana mediante GPI encontrada en *Schistosoma mansoni*, un parásito humano [52]. Ésta proteína tiene un 21% de homología de secuencia con el CD8 humano, posee el motivo

conservado TLEDTL y sus cisteínas también alinean con las de los otros miembros de la familia. Es además un ectoenzima, catalizando la producción de NADP a partir de NADP y la hidrólisis de NAD a ADPR. Sin embargo, su actividad ciclasa (síntesis de ADPRc a partir de NAD) es muy baja, más baja incluso que la de CD157 [52].

A pesar de algunas diferencias entre las proteínas de esta familia, un hecho común es que todos los miembros de la familia ciclasa son capaces de ciclar NGD^+, un análogo del NAD^+, a GDPRc, un análogo fluorescente del ADPRc que es mucho más estable a la hidrólisis [53]. Ésta reacción ha sido usada como un ensayo simple fluorimétrico para identificar homólogos de ciclasa y poder distinguir las NADasas (por ejemplo de *Neurospora*) que no tienen del todo actividad ciclasa [54, 55].

1.3 Estructura cristalina del dominio extracelular del CD38 humano (CD38hs).

Se ha desarrollado un eficiente sistema de expresión en levadura para facilitar los estudios de la estructura y función y para así poder purificar suficiente cantidad de ciclasa para cristalografía [56].

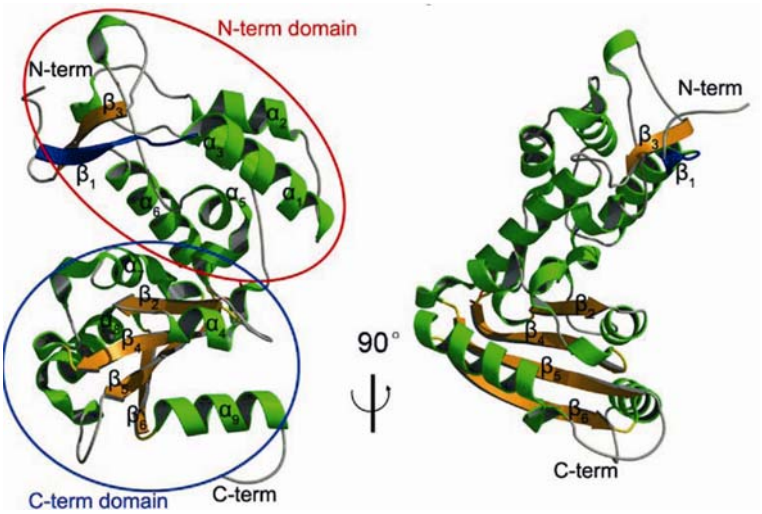

Qun Liu et al. *Structure* 2005, Vol 13, 1331-1339

Fig. 6 Estructura del CD38 humano soluble (expresado en la levadura *Pichia pastoris*).

El modelo estructural final contiene dos moléculas de CD38hs en la unidad asimétrica cristalográfica, cada cual consistente en 252 residuos.El péptido GPGTTK implicado en la inhibición de la infección del HIV-1 está coloreado en azul.

La molécula CD38hs puede dividirse en 2 dominios separados. El dominio N-terminal (residuos 45-118 y 144-200) está formada por 5 α-hélices (α1, α2, α3, α5, α6) y 2 cortas cadenas β (β1, β3); y un dominio C-terminal (residuos 119-143 y 201-300) que consiste de 4 láminas β paralelas (β2, β4, β5, y β6) rodeadas de 2 largas hélices (α8 y α9) y 2 cortas hélices (α4 y α7). Hay un único puente disulfuro en CD38 (Cys119-Cys201).

Aunque la estructura cristalina de *Aplisia cyclase* [57, 58] y CD157 [59] revelan homodímeros cabeza-cabeza y tallo-tallo, las 2 moléculas de CD38hs no forman dímero en el cristal. Además hay evidencias que sugieren que la estructura enzimática funcional de CD38hs en solución podría ser un monómero [3, 60] Por otra parte, hay artículos que describen que CD38 puede formar homodímeros en la superficie de la célula [60, 61] los cuáles parece que requieren contribuciones estructurales de la porción intracelular [61]. Así, la ausencia de dominio transmembrana y la parte intracelular, CD38hs podría no formar un dímero funcional en solución o en cristales.

También fue considerada la posibilidad de que la deglicosilación de CD38hs pudiera alterar su dimerización, sin embargo, la mutación de estos sitios no debería afectar a la dimerización de CD38hs puesto que los alineamientos estructurales de CD38 con CD157 y la ciclasa de *Aplysia* revelan que los sitios de glicosilación en CD38 y CD157 no toman parte en la formación de dímeros [62]

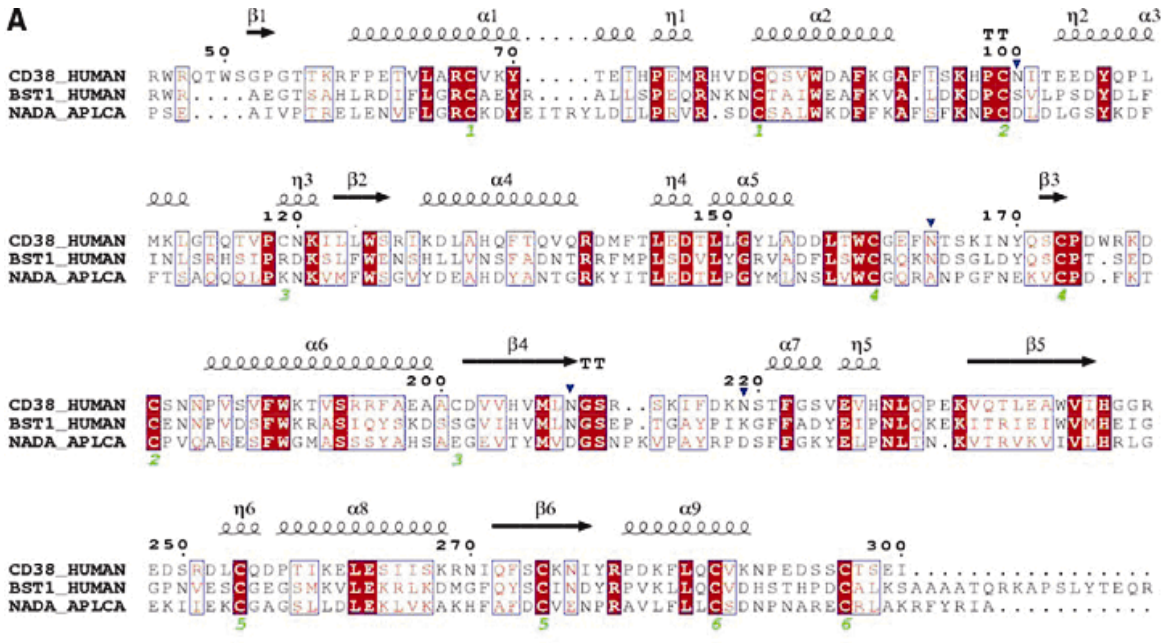

Fig. 7.A Alineamiento de secuencias de CD38hs, CD157/BST-1 y la ciclasa de *Aplysia*

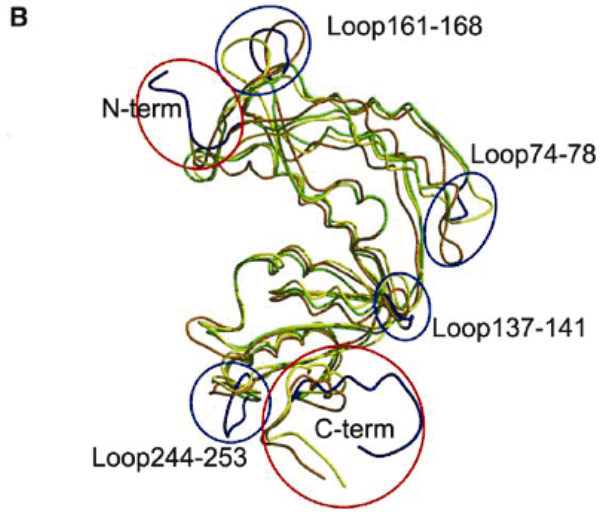

Fig.7.B Comparación estructural de los miembros de la familia de la ADP-ribosil ciclasa (CD38hs, verde; CD157/BST-1, amarillo; Ciclasa de *Aplysia* , marrón). Las áreas de mayores diferencias estructurales están marcadas mediante círculos. CD38hs está de azul en estas áreas).

Los residuos RWRQTW del extremo N-terminal tienen cadenas cargadas positivamente y residen en la región próxima a la membrana por lo que tendría capacidad de interaccionar con las cargas hidrofílicas de los lípidos de los *rafts* (balsas lipídicas) [63].

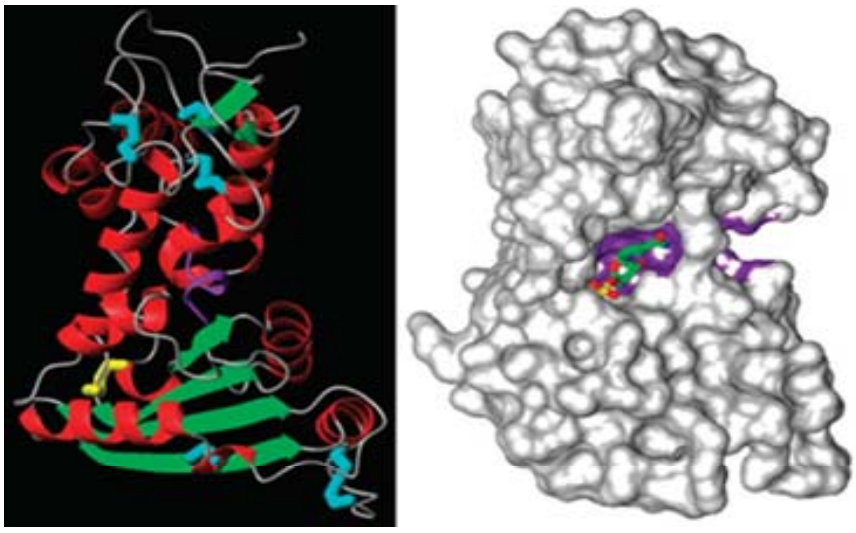

Hong Cheung Lee. *Mol Med* (2006) 12; 317-323

Fig. 8 Estructura cristalina de CD38

Panel izquierdo: verde, estructuras β; rojo, α-hélice; azul, puentes disulfuro conservados; amarillo, puente disulfuro único; morado, motivo conservado TLEDTL (presente en CD3, CD157 y la ciclasa de *Aplysia Californica*).

Panel derecho: Superficie de van der Waal. La molécula unida al sitio activo es nicotinamida mononucleótido (NMN). En morado está representado el motivo conservado TLEDTL.

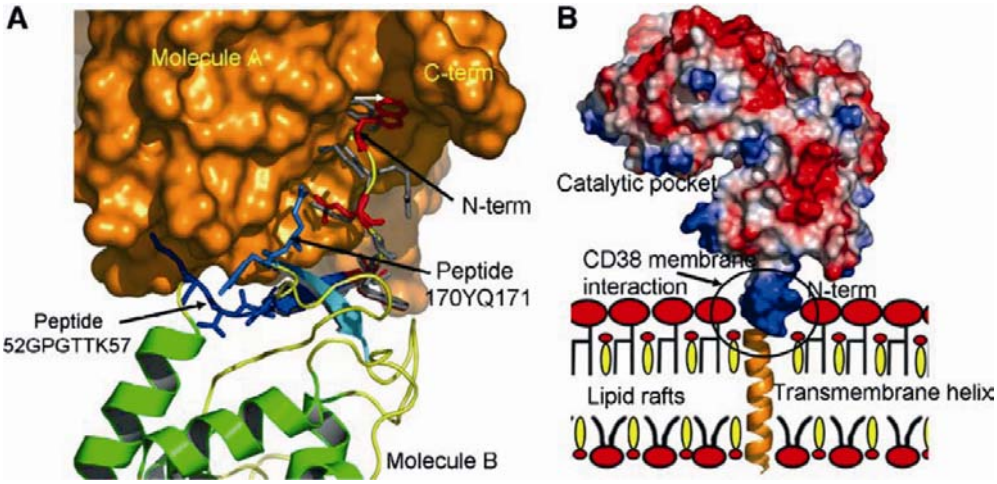

Hong Cheung Lee. *Mol Med* (2006) 12; 317-323

Fig. 9

A- Asociaciones laterales de 2 moléculas CD38hs. Los residuos de la molécula B implicados en las interacciones polares hidrofóbicas están marcados con flechas.

B- Posible orientación de CD38hs en la superficie de la célula e interacciones entre CD38 y las balsas lipídicas (*rafts*). Las elipses rojas representan los grupos polares de los glicerofosfolípidos, esfingolípidos y colesterol. El dominio extracelular de CD38hs se muestra representado con las cargas electrostáticas (rojo = negativo, blanco = neutro, azul = positivo). La hélice transmembrana está propuesta como una extensión del extremo N-terminal de CD38hs.

La síntesis de ADPRc requiere 2 pasos: corte de la nicotinamida-ribosa unida al NAD seguido de la entrada de adenina y ciclación [59]. El residuo Glu146, conservado en la ciclasa de *Aplysia,* pero no en CD157, tiene un importante papel en la regulación de la ratio de las actividades ciclasa y NADasa de CD38 [64]. CD38 *wild-type* tiene alta actividad NADasa pero sólo una mínima actividad ciclasa. Interesantemente, el mutante E146A de CD38 sin embargo, tiene muy incrementada la actividad ciclasa y disminuida la actividad NADasa [64]. NMN es un sustrato que imita al NAD y que puede ser hidrolizado por CD38 [65]

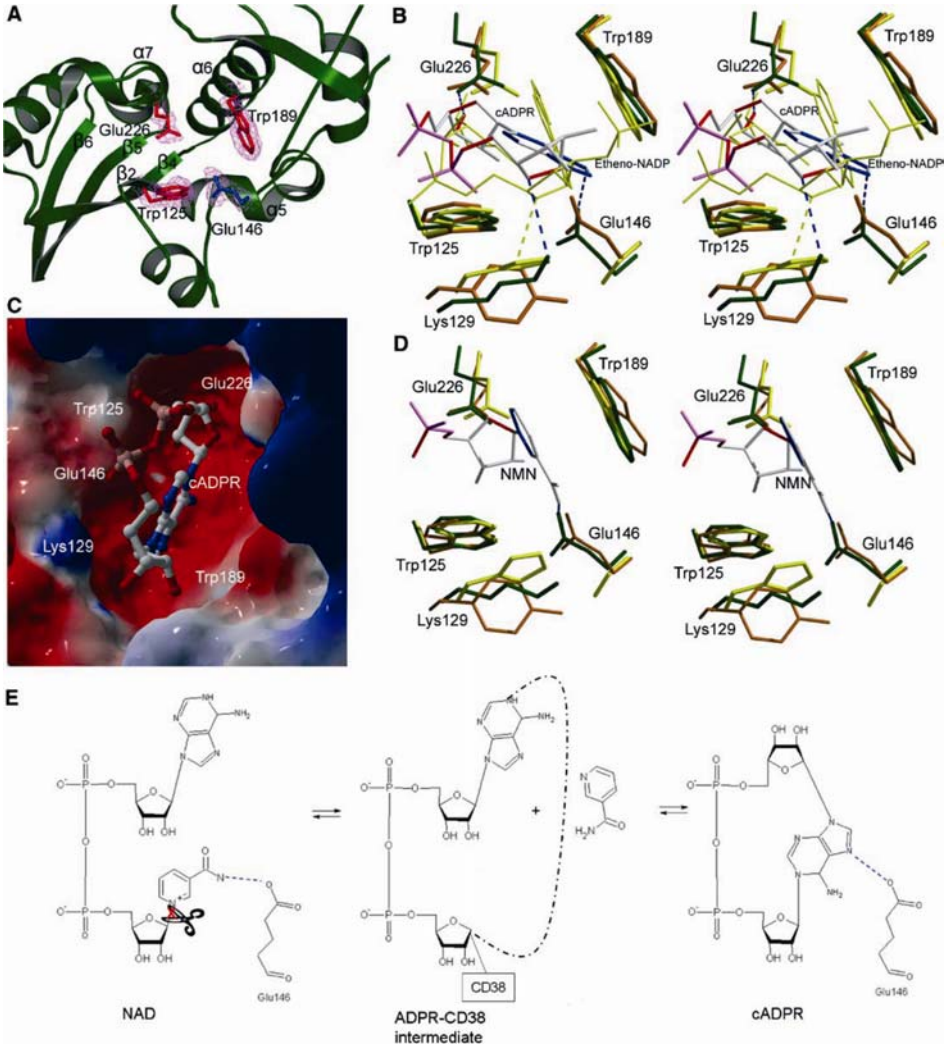

Fig. 10

A- Estructura del centro activo. Residuos implicados en el sitio activo: Glu226,Trp125, Trp189 y Glu146.

B- Modelo de unión de CD38-ADPRc. Verde = CD38hs, amarillo = CD157, rosa = ciclasa de *Aplysia.*

C- Modelo de ADPRc en el sitio activo de CD38hs. Los residuos funcionalmente esenciales están marcados. El potencial positivo está coloreado en azul y el negativo está en rojo.

D- Modelo de unión de NMN a CD38 (NMN es un sustrato de CD38).

E- Diagrama esquemático del papel de Glu146 durante la síntesis de ADPRc a partir de NAD.

1.4 CD38 como marcador de pronóstico en enfermedades

CD38 es marcador de pronóstico negativo en B-CLL (leucemia linfocítica crónica de células B) [66-68].

Está reconocido que alta proporción de células T $CD8^+CD38^+$ tienen valor pronóstico para el seguimiento del desarrollo del SIDA, aunque además se utilizan las células $CD4^+$. Esto se atribuye a la capacidad de CD38 de marcar activación en el sistema inmune. Algunos de los linfocitos $CD8^+CD38^+$ tienen actividad citotóxica contra las células CD4 que expresan los antígenos virales, contribuyendo posiblemente a la depleción de células T $CD4^+$ [69].

El incremento de la expresión es un indicador de la progresión de la enfermedad y la bajada de la expresión es un buen indicador de la efectividad de la terapia anti-retroviral (HAART) [70-72]. Es curioso que aunque CD38 es un marcador de pronóstico de la progresión del HIV-1, en las fases tempranas del desarrollo de la infección por HIV-1, la expresión de CD38 podría prevenir la infección de los linfocitos por HIV-1 [73]. La relación molecular entre CD38 y HIV-1 fue primero identificada mediante la interacción entre CD38 y CD4, el principal receptor para HIV-1 [74].

El valor pronóstico de la expresión de CD38 en células CD8 debe completarse con la evaluación de la expresión de las células T $CD45RO^+CD8^+$: proporciones relativas de células T $CD45RO^+CD8^+CD38^+$ correlacionan mejor con el declive de linfocitos T $CD4^+$ que sólo la proporción de células $CD8^+CD38^+$ [75]. Esto podría explicarse por el hecho de que las células T $CD45RA^+CD8^+$ (principalmente células *naive*) expresan constitutivamente CD38 incluso en controles normales y no ofrece una contribución significativa. Por el contrario, las células T $CD45RO^+CD8^+$ (principalmente células memoria) no expresan normalmente CD38, por lo que hacen que CD38 sea un buen marcador de linfocitos T sólo en el tipo $CD45RO^+$. Además, los valores de intensidad son sensibles a la cantidad relativa de CD38 expresado en linfocitos $CD45RO^+$ o $CD45RA^+$ dado que los linfocitos $CD45RA^+$ expresan CD38 a baja intensidad ($CD38^{low}$) mientras que las células activadas $CD45RO^+$ lo expresan con alta intensidad ($CD38^{bright}$)

Nuestro laboratorio está trabajando con pacientes de lupus eritematoso sistémico (SLE). Ésta es una enfermedad autoinmune sistémica y estudios de Pavón et al. demuestran que la expresión

de CD38 en estos pacientes está aumentada en linfocitos T $CD3^+$, $CD4^+$, $CD8^+$, y $CD25^+$, lo cual correlaciona con un incremento en la insolubilidad de CD38 en el detergente Brij 98 y una mayor proporción de CD38 en los *rafts* [76]. Además, las células de estos pacientes muestran una alteración en la ratio CD4:CD8 (lo normal es 2:1), lo cual es debido a un descenso de la proporción de linfocitos T $CD4^+$ y un aumento en la proporción de linfocitos T $CD8^+$. Estos datos son consistentes con el incremento de la expression de CD38 y la formación de *rafts,* y la significativa reducción en la ratio CD4:CD8 observada en linfocitos T normales estimulados con mitógeno si se compara con células T normales sin tratar.

1.5 Anticuerpos anti-CD38

1.5.1 Para investigación

Para el análisis de las funciones de CD38 se han utilizado diversos anticuerpos monoclonales, que reconocen diferentes epitopos de CD38. Mediante ensayos de competición se han identificado 2 familias de anticuerpos monoclonales: por un lado IB4, IB6 y AT2 y por otro lado OKT10, SUN-4B7 y AT1 [77]. Cada familia reconoce epítopos que son completa o parcialmente comunes. Sin embargo, las actividades funcionales de CD38 no pueden ser simplemente atribuidas a los epítopos que reconocen. Por ejemplo, IB4 y OKT10, los cuáles se unen a diferentes epítopos, inducen proliferación de PBMCs y la secreción de IFN-γ.

Anticuerpo	***Isotipo***	***Secuencia que reconoce***
IB4	IgG_{2a}	220-241
IB6	IgG_{2b}	¿?
SUN-4B7	IgG_1	¿?
OKT10	IgG_1	280-298
AT1	IgG_1	¿?
AT2	IgG_1	¿?
HB136	IgG_1	C-terminal

Adaptado de Ausiello C. et al. *Tissue Antigens* (2000) **56**; 539-547

Fig. 11 Tabla de anticuerpos anti-CD38

La estimulación a través del CD38 humano mediante anticuerpos monoclonales lleva consigo:

1. Expresión de RNAm de IL-1β, TNF-α, IL-6, GM-CSF, IL-2, IFN-γ, IL-10 y de IL-12 [78] (en PBMCs).
2. En células T purificadas inducen secreción de IL-2 e IFN-γ (tipo 1), IL-6 e IL-10 (tipo 2) [79].
3. La producción de citoquinas no está asociada con la proliferación de los linfocitos T (indicando una dicotomía de los 2 sucesos) y no se requieren células presentadoras de antígeno [79].
4. La secreción de citoquinas tipo 1 y 2 sugiere un reclutamiento de moléculas de la maquinaria de activación de las células T, un rasgo compartido con CD3 [79].

1.5.2 Anticuerpos para tratamiento en clínica

Existen anticuerpos comerciales para el tratamiento en clínica, creados frente a CD38, para el tratamiento del mieloma múltiple (MM). El MM es un cáncer de las células plasmáticas en la médula ósea que ocurre cuando estas células crecen fuera de control. Las células plasmáticas excesivas pueden formar un tumor en la médula ósea llamado mieloma y la presencia de muchos tumores se denomina MM.

HuMax-CD38™ (GenMab) es un anticuerpo totalmente humano que se dirige a la molécula CD38 que está altamente presente en la superficie de las células tumorales del mieloma múltiple. En estudios preclínicos previos, HuMax-CD38 fue más efectivo en poner en funcionamiento el sistema inmunitario destruyendo los mecanismos de citotoxicidad celular dependiente de anticuerpos (ADCC) y la citotoxicidad dependiente del complemento (CDC) que cualquier otro anticuerpo humano CD38 al probarlo en tumores de mieloma múltiple. HuMax-CD38 también destruyó eficazmente células tumorales de un paciente con leucemia de célula plasmática positiva CD38/138 que fue refractaria a la quimioterapia en el momento del análisis. Además, el tratamiento con HuMax-CD38 ralentizó el crecimiento tumoral en marcos preventivos y terapéuticos en ratones con severas deficiencias inmunológicas combinadas (SCID) en modelos animales. http://www.genmab.com

MOR202™ (Morphosys) es un anticuerpo HuCAL dirigido contra CD38 humano, una diana terapeútica para el tratamiento del mieloma múltiple y ciertas leucemias. En estudios pre-clínicos, MOR202 eliminaba efectivamente células cancerosas de tumor primario de pacientes y específicas líneas de células cancerosas. La eficacia preclinica fué demostrada por la fuerte inhibición del crecimiento de tumor en un modelo de ratón con SCID.
http://www.morphosys.com

1.6 CD31 como ligando de CD38

La proteína **CD31** (PECAM-1) es una glicoproteína transmembrana y ha sido identificada como ligando de CD38 [80] [81]. Se expresa principalmente en células endoteliales, plaquetas, macrófagos y en algunas células T. Interviene en el tráfico de leucocitos a través del endotelio [82]. La interacción entre CD38 y su ligando CD31 podría ser un paso importante en la regulación de la vida celular y en la migración de leucocitos a través de las células endoteliales [27].

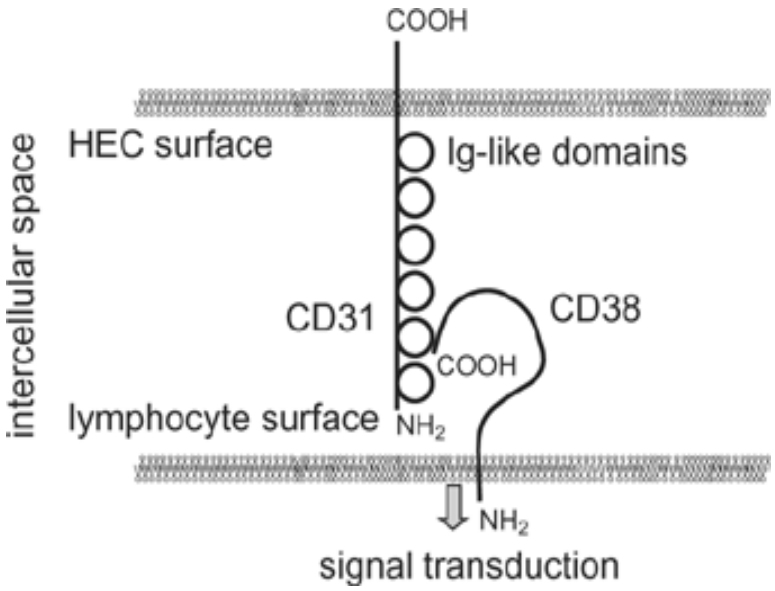

Savarino, A., et al. *AIDS* (2000), **14** : 1079-1089

Fig. 12 Posible modelo de interacción CD38-CD31 en endotelio, en el cual interaccionarían la secuencia adyacente al C-terminal y el segundo loop respectivamente.

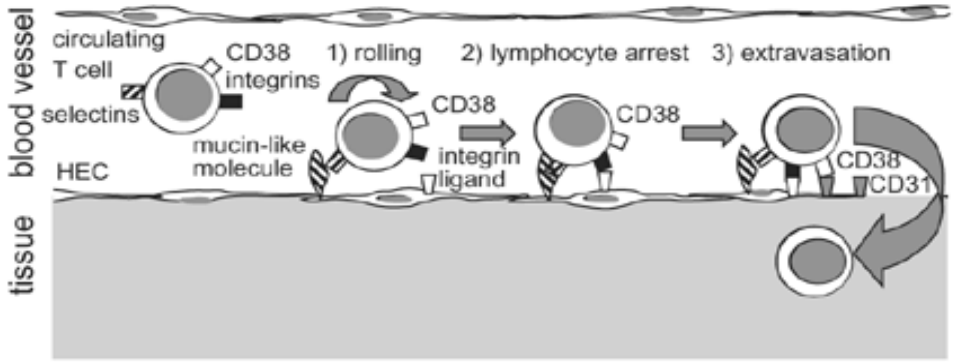

Savarino, A., et al. *AIDS* (2000), **14** : 1079-1089

Fig. 13

CD38 y CD31 podrían estar implicados en la interacción del linfocito con el endotelio. Este modelo constaría de 3 pasos: 1) rodamiento del linfocito sobre el endotelio mediado por receptores de adhesión tales como selectinas y moléculas *mucin-like*; 2) activación de integrinas por moléculas tales como chemoquinas presentes en las células endoteliales resultan en la "parada" del linfocito; 3) extravasación mediada por moléculas tales como CD31 e integrinas, los cuales dirigen al linfocito hacia el tejido.

1.7 CD38 en:

Esta tesis se centra en el estudio de CD38 en linfocitos T pero no hay que olvidar que CD38 también se expresa en otras células:

1.7.1 Linfocitos B

Durante la ontogénesis de las células B, CD38 está fuertemente regulado y está presente en altos niveles en los precursores de médula ósea, baja su expresión en células B sin estimular y de nuevo se expresa en células plasmáticas diferenciadas [83]. CD38 es usado para clasificar subtipos de células B funcionales maduras.

Estimulando células B humanas purificadas y líneas B celulares, a través de CD38, mediante el uso de anticuerpos monoclonales anti-CD38, se identifican las rutas de señalización de CD38. Hay fosforilación de la tirosina cinasa Syk, PLC-γ y c-Cbl [84].

CD38 no tiene motivos de activación por lo que, para poder señalizar, está localizado cerca de receptores "profesionales" de señalización como es el BCR en linfocitos B [85, 86] . Usando

líneas de linfocitos B humanos, se ha demostrado que, tras estimulación a través de CD38 hay una marcada fosforilación en tirosina de CD19 y asociación con Lyn y PI-3K. CD19 es el mayor componente de la cascada de señalización de CD38 en precursores de linfocitos B, sirviendo como sitio de anclaje de la superficie de la célula para las cinasas citoplasmáticas [87]. Usando líneas celulares linfoblastoides, Deaglio et al. [88] comprobaron que la estimulación a través de CD38 induce un número significativo de moléculas CD38 que se asocian a CD19 y que se localizan en los microdominios de membrana (*rafts*). La asociación física entre CD19 y CD38 fue confirmada mediante experimentos de *cocapping* y coinmunoprecipitación y además esta asociación es funcional, ya que el flujo de Ca^{2+} mediado por CD38 no se activa si se silencia la expresión de CD19 [88].

Estudios funcionales sobre la función de CD38 en células B maduras confirman que la estimulación de CD38 mediante anticuerpos monoclonales agonistas, protege de la apoptosis a través de la up-regulación de la proteína Bcl-2. Estos efectos son similares a los mediados por la ruta CD40-CD40L, aunque estos 2 sistemas parecen que trabajan independientemente [89]. La estimulación de linfocitos B maduros circulantes a través de CD38 induce la síntesis de novo de citocinas tales como IL-6, GM-CSF e IFN-γ [90].

1.7.2 Monocitos

CD38 está implicado en actividades funcionales reguladas por IFN-γ, tales como la interacción del monocito con el endotelio. Estudios previos demostraron que el "rodamiento" (*rolling*) del monocito sobre el endotelio es, en parte, mediado por interacción de CD38 con su ligando, CD31, expresado en la superficie de las células endoteliales [91]. IFN-γ, aumenta la expresión constitutiva de CD38 en monocitos de sangre periférica y en líneas monolíticas. IL-2 también aumenta la expresión de CD38, aunque en menor medida. Este aumento de expresión va en paralelo con el aumento de las actividades hidrolasa y ciclasa, sugiriendo que IFN-γ está induciendo la expresión de una molécula totalmente funcional. Otros activadores de monocitos como son LPS no afectan a la expresión de CD38, ni tampoco IL-4, IL-13 o IL-10 [92]. El papel específico del IFN-γ en la inducción de CD38 es apoyada por la identificación de tres elementos de respuesta a interferón (IRF-1) en el promotor de CD38 [93].

1.7.3 Células dendríticas

Las células dendríticas (DC) immaduras capturan el antígeno en el sitio de infección [94]. La maduracion es el resultado de una reorganización de genes que regulan la producción de diferentes citoquinas y que conlleva a la migración de la DC a los nódulos linfáticos donde presentan los antígenos a las células T [95].

CD38 es un marcador de transición de monocitos a células dendríticas inducida por procesos inflamatorios [96]. Las DC inmaduras van perdiendo progresivamente la expresión de CD38 y CD14 de la superficie y simultáneamente van adquiriendo CD1a.

CD38 podría actuar como molécula de superficie que modula la adhesión y señalización entre DC y linfocito T, ya que CD83, que es un marcador de DC madura humana y juega un papel importante en la activación del linfocito T mediada por DC, está constantemente asociado al CD38 en la membrana. En esta asociación puede estar CD31 (expresado en los linfocitos T *naive*) y además, otras moléculas implicadas en migración como son CD11b y CCR7, están asociadas a CD38. Finalmente, el papel de CD38 en señalización ha sido indirectamente confirmado por su localización en los *rafts* [97].

DC inmaduras ($CCR7^{+}$) migran desde la piel y el epitelio de la mucosa a los tejidos linfoides, donde interaccionan con linfocitos T *naive*. Los conocimientos sobre el papel de CD38 en el rodamiento y adherencia de los linfocitos, a través de su interacción con el CD31 que expresan las células endoteliales, fueron aplicados al análisis de las propiedades de migración de las DC. La quimiotaxis y el transporte a través del endotelio en respuesta a CCL21 indican que la migración de DC maduras a LPS era inhibida significativamente en presencia de anticuerpo anti-CD38 bloqueante y CD38 recombinante soluble. También se observaron inhibiciones significativas en presencia de anticuerpo anti-CD31. La actividad enzimática de CD38 no estaba implicada en este contexto porque la adición de 8-Br-ADPRc (antagonista del ADPRc) no influía en la quimiotaxis o en la migración a través del endotelio.

1.7.4 Neutrófilos

Ratones CD38 KO infectados con *S. pneumoniae* sufren una rápida diseminación desde el sitio de infección (pulmón) a la sangre. Esta rápida diseminación hace que estos ratones sean 10 veces más susceptibles a la infección por *S. pneumoniae.* Además, los neutrófilos de estos ratones

knockout para CD38 son incapaces de migrar eficientemente al sitio de infección en el pulmón [98].

Los neutrófilos de ratones CD38 KO pueden ser activados por fMLP e IL-8 por lo que tienen capacidad para migrar no-direccionalmente (quimioquinesis). Sin embargo no son capaces de migrar direccionalmente hacia gradientes de fMLP o IL-8 (quimiotaxis) [98]. Este es un defecto selectivo porque si eran capaces de migrar hacia gradiente de IL-8. Además, la quimiotaxis de neutrófilos hacia fMLP es dependiente de la producción de ADPRc por CD38.

1.7.5 Células *Natural Killer* (NK)

La estimulación a través de CD38 conlleva un aumento significativo del nivel de Ca^{2+} intracelular, aumento de la expresión de HLA-II y CD25 y la fosforilación en tirosina de diversos sustratos citoplasmáticos: CD3-ζ, FcεRIγ, ZAP-70 y c-Cbl y ligero aumento del mRNA de IFN-γ y GM-CSF (*"granulocyte macrophage colony stimulating factor")* [99]. Además, la estimulación a través de CD38 mediante anticuerpos monoclonales agonistas induce señales que permiten la activación de la maquinaria de lisis de las células NK de adulto. Esto no puede reproducirse en las líneas NK humanas YT, NKL, y 2 $CD16^-$. Se había hipotetizado que CD38 pudiera establecer una cooperación funcional con moléculas de señalización de la membrana de la célula NK. Estos efectos son similares a los que se observan con CD16 por lo que podrían tener rutas de señalización comunes. De hecho, Deaglio et al. [100] confirmaron en un trabajo posterior, que CD38 y CD16 son funcionalmente dependientes y están físicamente asociados en las células NK humanas. La molécula CD16 es un requisito necesario y suficiente para que a través de CD38 pueda haber flujo de calcio, fosforilación en tirosina de ZAP-70 y MAPK, secreción de IFN-γ y respuesta citotóxica. Mediante microscopía FRET y experimentos de *"co-capping"* demostraron que CD38 y CD16 estaban próximos. Resumen su trabajo confirmando que CD38 no puede señalizar por sí mismo pero su función como receptor es rescatada mediante la asociación física y funcional con estructuras de señalización profesionales que varían según la línea y el ambiente, siendo CD16 en el caso de las células NK [100].

2. ADP-ribosilación de CD38

La mono-ADP-ribosilación es una reacción de modificación post-traduccional en proteína. La mono-ADP-ribosilación de proteínas de superficie de células T por mono-ADP ribosiltransferasa (ADPRT) anclada a membrana por GPI, resulta en la inhibición de las funciones citotóxicas de la célula T, tales como proliferación, citotoxicidad y secreción de citoquinas [101]. Está descrito que la ADP-ribosilación de CD38 por ADPRT en células T activadas resulta en apoptosis, así como la inactivación de CD38, sugiriendo que la ADP-ribosilación de CD38 juega un papel importante en la regulación inmune [102].

Durante la exposición de las células T al NAD^+, el CD38 es modificado por ecto-mono-ADP-ribosiltransferasas (ecto-mono-ADPRTs) específicas para residuos de cisteína y arginina [103]. La ADP-ribosilación en arginina resulta en la inactivación de las actividades ciclasa e hidrolasa de CD38, en cambio, la ADP-ribosilación en cisteína resulta sólo en la inhibición de la actividad hidrolasa. La ADP-ribosilación en arginina causa un descenso en el ADPRc intracelular con lo que hay una bajada del flujo de Ca^{2+}, resultando en la apoptosis de las células T activadas [103]. Además se ha visto que la ADP-ribosilación en células B sólo ocurre en el residuo de cisteína y no se ha detectado apoptosis o inhibición de la proliferación cuando son incubadas con NAD^+.

Todo esto sugiere que la ADP-ribosilación de CD38 juega un importante papel en la regulación inmune y que la señalización mediada por ADPRc es esencial para la supervivencia de las células T activadas.

3. Mutaciones en residuos de CD38

Mediante mutagénesis dirigida de CD38 se han identificado 3 residuos críticos en el sitio activo: Glu-226, Trp-125 y Trp-189 . El reemplazamiento del residuo Glu-226 resulta en la completa pérdida de todas las actividades enzimáticas. Los 2 residuos de Trp parecen ser responsables del posicionamiento del sustrato

Cuando se incuba CD38 con NAD^+, CD38 predominantemente lo hidroliza a ADPR (NAD-glicohidrolasa), pero también se produce una pequeña cantidad de ADPRc mediante la ciclación del sustrato. Se han hecho mutagénesis dirigidas para investigar los aminoácidos importantes para el control de las reacciones de ciclación e hidrólisis. El residuo Glu-146 es un residuo conservado presente en el sitio activo de CD38. Su reemplazamiento por Phe aumenta fuertemente la actividad ciclasa a un nivel similar al de la actividad NAD^+ hidrolasa [104]

4. Internalización de CD38

Debido a la existencia de la paradoja del sistema CD38-ADPRc, se han usado anticuerpos monoclonales frente a CD38 marcados con I^{125} para el estudio del proceso de internalización de CD38 [105] en células T Jurkat y células B Raji. Los resultados mostraron que la internalización de CD38 es un fenómeno reproducible tras la unión de anticuerpos específicos para CD38 (agonista (IB4) y no-agonista (IB6)). Éste proceso sería independiente de la transducción de señales porque ambos tipos de anticuerpos son efectivos y la dinámica de internalización es mucho más lenta que la de señalización celular. Es plausible que la endocitosis mediada por anticuerpos simularía lo que ocurre *in vivo* tras la interacción con su ligando fisiológico [105].

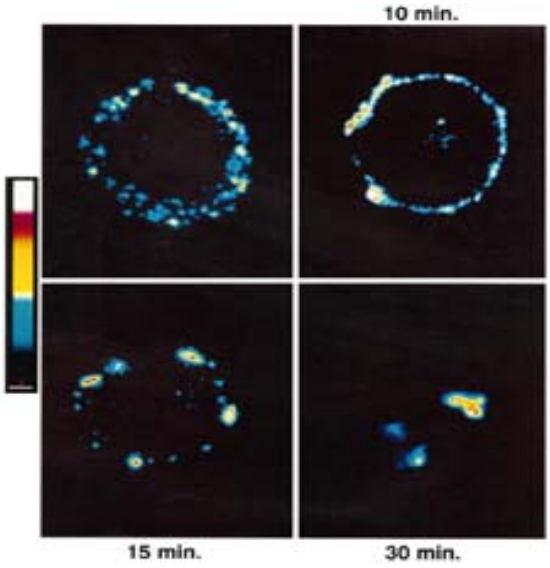

Fig. 14

Microscopía confocal para el análisis de la internalización de CD38 en blastos humanos. Las células son marcadas a 4º C con IB4 más 2º anticuerpo *("crosslinking")* y luego incubadas a 37º C a diferentes tiempos. La escala del azul al rojo representa el incremento en la señal de fluorescencia.

Funaro, A. et al. *The Journal of Immunology* 1998 (**160**): 2238-2247

So-Young Rah et al. [106] han demostrado que el tratamiento de células LAK con IL8 induce la asociación de MHCIIA (nonmuscle myosin heavy chain IIA) con CD38 y que MHCIIA fosforilado por PKG está asociado a CD38 via dominio SH3 de Lck, siendo éste un paso crítico en la internalización y activación de CD38 [106].

5. Funciones de CD38h

5.1 Ectoenzima

CD38 es una ectoenzima multifuncional que actúa como $NAD(P)^+$ glicohidrolasa [107] y juega un papel importante en la activación del linfocito [32, 108]. Sin embargo, CD38 puede también actuar como una ectociclasa que convierte NAD^+ en el ADPRc [109]. Además, el CD38 intracelular puede catalizar la conversión de NAD^+ a ADPRc, el cual también está implicado en la regulación del Ca^{2+} citosólico [8] y puede controlar la quimiotaxis de neutrófilos hacia quimioatrayentes bacterianos a través de su producción de ADPRc [98]. Sin embargo, CD38 es más eficiente NAD^+ glicohidrolasa que ADP-ribosil ciclasa porque más del 97% del producto total producido por CD38 es ADPR [110].

La actividad enzimática de CD38 es altamente dependiente del pH, por lo que esto sugiere que la actividad *in vivo* de esta enzima puede cambiar en acorde al ambiente [111].

El NAADP es estructuralmente diferente del ADPRc y movilizan Ca^{2+} de diferentes compartimentos de la célula: NAADP lo hace de orgánulos acídicos (lisosomas) [112, 113] y el ADPRc moviliza Ca^{2+} del retículo endoplásmico modulando los receptores de rianodina [114, 115]. Ambos, ADPRc y $NAADP^+$ son fuertes mobilizantes de Ca^{2+} en diferentes tipos celulares [116, 117], aunque las reacciones que implican al NAADP ocurren sólo a pH ácido.

Hay numerosas evidencias que indican que la síntesis de ADPRc por ADP-ribosil-ciclasas es estimulada a través de proteína G heterotrimérica acoplada a receptor de señalización . Los receptores implicados en la activación de ADP-ribosil-ciclasa incluyen a los receptores β-adrenérgicos [118, 119], angiotensina II [120] y muscarínicos [121]. Se ha descrito la activación de la ADP-ribosil-ciclasa CD38 por cGMP [122, 123] y la activación dependiente de AMPc en células musculares lisas arteriales [119] y cardiomiocitos [124].

Aunque la secuencia de aminoácidos de la ADP-ribosil ciclasa de *Aplisia Californica* exhibe un alto grado de identidad con la secuencia de CD38, la enzima de *Aplisia* sólo tiene actividad ADP-ribosil ciclasa y no ADPRc hidrolasa. Las cisteínas 119 y 201 de CD38 tienen un papel crucial en la síntesis e hidrólisis de ADPRc [125]. Cuando se incuba con NAD^+, CD38 predominantemente lo hidroliza a ADP-ribosa (NAD glicohidrolasa), pero una cantidad de ADPRc es también producida a través de la ciclación del sustrato. Se han hecho mutagénesis dirigidas para investigar la importancia de los aminoácidos en el control de las

reacciones de hidrólisis y ciclación. El Glu-146 es un residuo conservado presente en el sitio activo de CD38 y su cambio por Phe aumenta la actividad ciclasa a un nivel similar al de la hidrólisis del NAD^+ [64].

CD38 cataliza, no solo la formación de ADPRc a partir de NAD^+, sino además la hidrólisis del ADPRc a ADPR y es el ATP quien inhibe esta hidrólisis [40]. La actividad ADPRc hidrolasa de CD38 es inhibida por ATP de una forma competitiva con el ADPRc. La Lys-129 de CD38 la participa en la unión del ADPRc y el ATP compite con el ADPRc por el sitio de unión, resultando en la inhibición de la actividad ADPRc hidrolasa de CD38 [39].

Mediante mutagénesis dirigida se ha comprobado la importancia de la Ser^{193}. La actividad enzimática es fuertemente reducida y además, este residuo es altamente conservado en diferentes especies (desde invertebrados a humanos), apoyando así su importante papel en el sitio activo de CD38 [126].

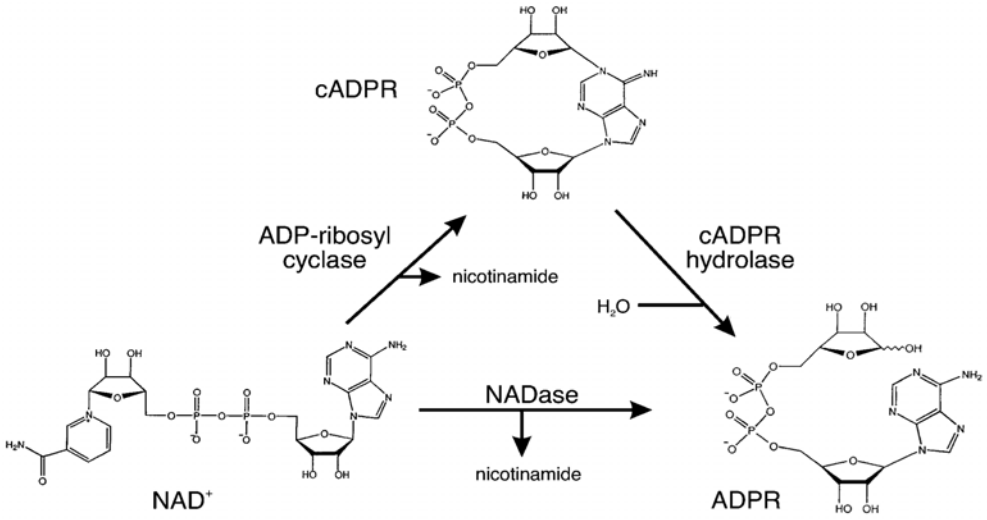

Guse A.H. *J. Mol. Med.* (2000) **78**:26-35

Fig. 15 Actividades enzimáticas de CD38

El ADPRc producido por CD38 controla la quimiotaxis de neutrófilos murinos respondiendo a fMLF, un péptido agonista para 2 subtipos de receptores quimioatrayentes: FPR y FPR-like 1.

Un componente sintético que se puede usar para alterar el producto formado por las ADP-ribosil ciclasas es el análogo al NAD^+ $N(8\text{-Br-A})D^+$ [127]. Las ADP-ribosil ciclasas, como CD38, utilizan este análogo del NAD^+ como sustrato, pero en lugar de producir ADPRc, las

células producen 8-Br-ADPRc, el antagonista del ADPRc. Usando este antagonista de ADPRc se bloquea la quimiotaxis de monocitos humanos a ligandos de CXCR4, CCR1 y CCR5 [128].

Se sabe que es ADPRc generado por CD38 juega un papel importante en la liberación de insulina inducida por Ca^{2+} en las células β-pancreáticas [129, 130]. Los ratones deficientes en CD38 manifiestan daño en la tolerancia a la glucosa[131].

5.1.1 Paradoja del sistema CD38-ADPRc

Puesto que el producto de la actividad de CD38 se produce en el exterior de la célula y su acción la realiza en el interior ¿Cómo se puede explicar esta paradoja?

Muchos autores han intentado explicar el mecanismo de acción pero aún hoy sigue el debate. Existen variedad de hipótesis:

Una es que el NAD^+ unido a CD38 causa su internalización y que por tanto el ADPRc es generado en el citosol (en células Namalwa (linfoma de células B) [132, 133]. Además, el CD38 internalizado podría tener acceso al NAD^+ [133] e incluso se ha descrito la localización nuclear de CD38 [134]. Otra hipótesis es que el ADPRc es generado extracelularmente y sería traslocado al interior por su enzima [109]. En cambio, otro grupo de investigación no observa internalización de CD38 tras la incubación de células Jurkat con NAD^+ y afirman que la actividad ADP-ribosil ciclasa de CD38 no está implicada en la síntesis de ADPRc intracelular en células Jurkat y HPB.ALL [135]. De esta forma, en células Jurkat, no jugaría un papel importante en la señalización mediada por Ca^{2+} regulada por ADPRc.

Sin embargo, CD38 puede jugar un papel en la regulación de los niveles basales de ADPRc a largo término. De hecho, Zocchi y colaboradores [136] muestran que la transfección de CD38 cDNA seguido de la expresión de CD38 en células Hela y 3T3 $CD38^-$ resulta en un incremento del ADPRc intracelular, acompañado de un modesto incremento basal del Ca^{2+} intracelular. Takahashi y colaboradores [137] además muestran que la diferenciación de las células HL-60 con ácido retinoico estaba acompañada por un aumento en la expresión de CD38 y un incremento basal del ADPRc intracelular.

Otras investigaciones han identificado unos hemicanales de conexina 43 [138] que permiten el paso del NAD^+ del interior de la célula al exterior.

Se ha demostrado que CD38 es un transportador unidireccional activo de ADPRc a través de la membrana, el cual entonces podría operar en los reservorios de calcio intracelular [133]. El NAD^+ intracelular se encuentra el concentraciones micromolares (comparado con las concentraciones nanomolares que se encuentran en el exterior) y pueden bajar su gradiente de concentración a través de los canales de conexina 43 hacia el sitio activo (extracelular) de CD38. CD38 puede entonces catalizar la formación de ADPRc, el cuál pasa a través del canal central formado por la estructura homodimérica de la proteína [139]

Además, está descrito que CD38 se internaliza mediante vesículas endocíticas (derivadas de la membrana plasmática) rodeadas de clatrina tras la incubación de células CD38+ con NAD+ o componentes del thiol: estas vesículas endocíticas pueden convertir el NAD+ citosólico en ADPRc a pesar de la desfavorable orientación asimétrica que hace intravesicular el centro activo de CD38 [133]. De modo que hay un aumento del [Ca2+]i dependiente de la internalización de CD38 [133].

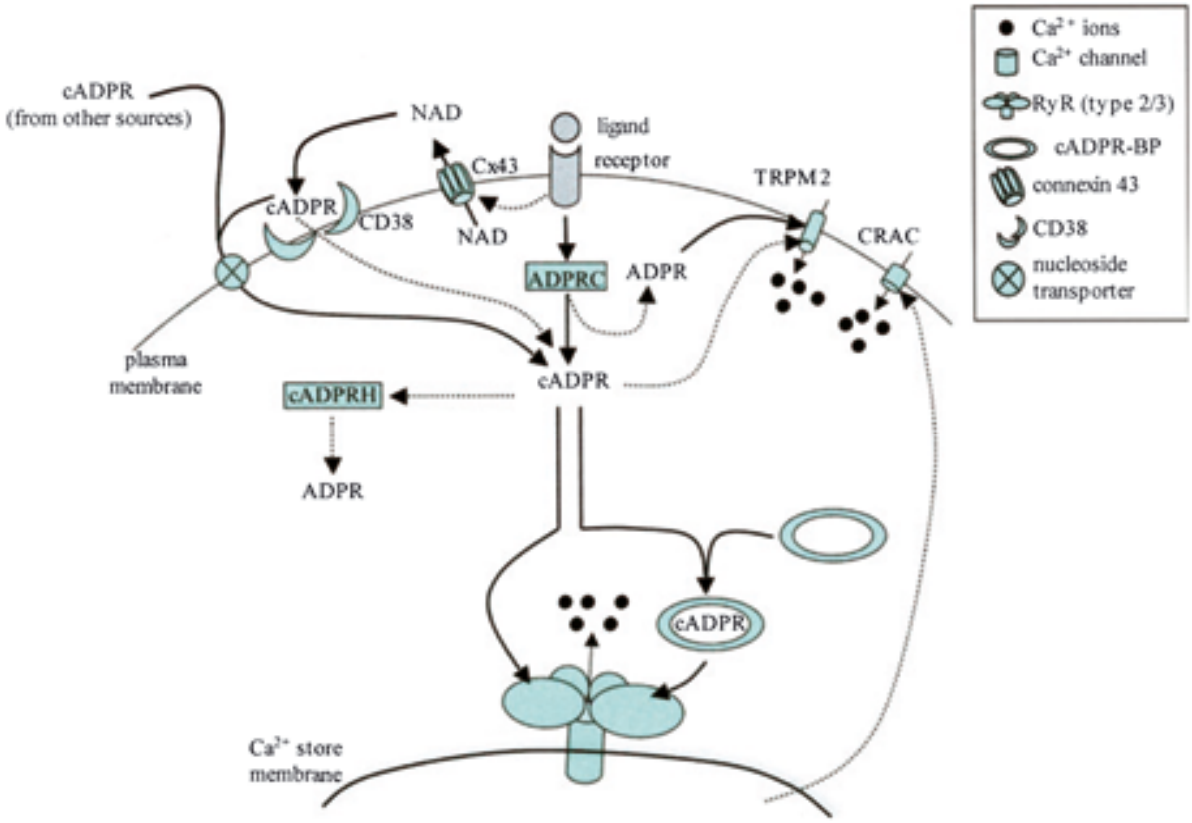

Guse et al. FEBS J. (2005) 272, 4590-4597

Fig. 16 Rutas de transporte del ADPRc en la célula

5.1.2 Movilización de calcio

En linfocitos T humanos se ha demostrado la implicación de los inositoles tri-fosfato ($InsP_3$) y el ADPRc en el aumento de Ca^{2+} mediante la señalización a través del complejo TCR/CD3. Jayaraman et al. [140] comprobaron que el knockout funcional del $InsP_3$ tipo 1 resulta en la completa inhibición de la señalización de Ca^{2+} y de la producción de IL-2. En células T, los $InsP_3$ y el ADPRc parecen actuar temporalmente coordinados: los $InsP_3$ en la fase inicial y el ADPRc en una segunda fase de señalización de Ca^{2+} en linfocitos T [141].

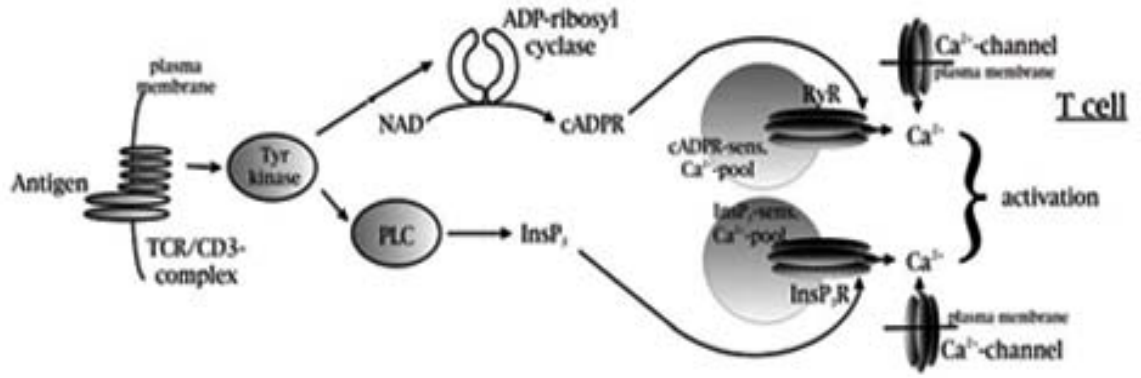

Guse A.H. *J. Mol. Med.* (2000) 78:26-35

Fig. 17 Rutas de movilización de calcio en el linfocito T

Este modelo está además en concordancia con la cinética de la formación de los $InsP_3$ y del ADPRc: los $InsP_3$ están elevados principalmente en los primeros minutos [142, 143], mientras que la concentración de ADPRc aumenta despacio en los primeros minutos, pero entonces permanece elevado durante unos 10 minutos [144].

5.2 Receptor [145]

CD38 está localizado en áreas críticas de la membrana plasmática, cercano a receptores "profesionales" de señalización [146] tales como el receptor de células T (TCR) en linfocitos T [147], el complejo receptor de células B (BCR) [148, 149], CD16 en células NK [150],

complejo principal de histocompatibilidad (MHC) de clase II y CD9 en monocitos [151, 152], CD83 (receptor para la quimioquina CCR7) y CD11b en células dendríticas maduras [153].

Gran parte de esta tesis está centrada en el papel de CD38 como receptor por lo que desarrollaré este apartado para profundizar en lo que se conocía hasta la fecha en la que se inició esta tesis.

CD38 tiene efectos estimuladores en linfocitos T y B [89, 108, 154, 155], pero inhibe el crecimiento e induce apoptosis en células precursoras de linfocitos B[156] . Anticuerpos anti-CD38 además inducen fosforilación de algunas proteínas intracelulares de linfocitos B [84], células B de bazo [157] y células HL-60 humanas que han sido diferenciadas con ácido retinoico [158], incluyendo PLC-γ1, c-Cbl, p85-PI3K, Btk y Syk. En el trabajo de Zubiaur et al. [159] se demuestra que la activación a través de CD38 resulta en la activación de las rutas Raf-1/MAP cinasa y CD3-ζ/ZAP-70/PLC-γ1, ambas dependientes de Lck. La estimulación a través de CD38 induce la fosforilación en tirosina de diversos sustratos y la fosforilación de las proteínas citoplasmáticas PLC-γ1, c-Cbl, ZAP-70, Shc, Erk-2 y la cadena ζ del CD3 [159]. Está descrito que, tras estimulación del TCR, hay un reclutamiento a través de Ras, de Raf-1 a la membrana plasmática, permitiendo así la activación de MAPK. La MAP cinasa predominante en linfocitos T es Erk-2 [160]. Además, este trabajo [159] concluye diciendo que TCR y CD38 comparten algunas propiedades para señalizar como son las rutas de señalización Raf-1/Erk-2 y CD3-ζ/ZAP-70 y que la fosforilación en tirosina de CD3-ζ mediada por CD38 y el reclutamiento de ZAP-70 en la proximidad del complejo TCR/CD3 sugiere una relación funcional entre las señales producidas a través de CD38 y el TCR.

Continuando con la posible relación CD38-TCR/CD3, Morra et al. [147] analiza si la señalización mediada por CD38 ocurre a través de una ruta independiente o está unida a la ruta de señalización del TCR/CD3. La estrategia que adoptaron fué el estudio de la capacidad de CD38 de modular los niveles de Ca^{2+} e interferir en la vía del TCR/CD3 y su coreceptor CD28. Utilizan diferentes anticuerpos monoclonales anti-CD38 pero solo IB4 era capaz de inducir aumento de los niveles de Ca^{2+} citoplasmático. Además inducía la fosforilación de PLC-γ1 y el aumento de expresión de CD69. Tras estimular con anti-CD38 o anti-CD3 hay un incremento en el nivel de Ca^{2+} intracelular. Cuando hay EGTA en el medio hay un rápido descenso en los niveles de Ca^{2+}. La respuesta inicial de Ca^{2+} tras la estimulación a través de CD38 derivaría inicialmente de compartimentos intracelulares mientras que el aumento más tardío y sostenido de Ca^{2+} vendría de un flujo de compartimentos extracelulares [147]. Los

primeros indicios de la posible vinculación entre la señalización de CD38 y el complejo TCR/CD3 se estudiaron mediante el uso de un clon de la línea celular Jurkat que no expresaba CD3 en superficie porque no expresaba la cadena β del TCR. Cuando se trataban estas células con anticuerpos anti-CD38 o anti-CD3 no había inducción de la expresión de CD69 ni movilización de Ca^{2+}. Por el contrario, cuando se restauraba el complejo TCR/CD3 en estas células Jurkat (reconstituyendo la cadena β del TCR) se restauraba la movilización de Ca^{2+} y la expresión de CD69 en superficie inducida por CD38.

Estaba demostrado que, cuando se cultivaban linfocitos T Jurkat en presencia de IB4 durante 48h se inducía el aumento de expresión de CD28, similar al que se observaba tras la estimulación a través de CD3. La estimulación a través de CD38 en linfocitos T Jurkat era seguida de una muerte por apoptosis, la cual era específicamente inhibida mediante ciclosporina A (CsA) y, paralelamente, había un aumento de la expresión de la molécula CD95 (Fas). Además observaron que había un mayor número de células muertas cuando se estimulaban simultáneamente CD38 y CD28. Dado que CD38 tiene un corto dominio citoplasmático sin motivos de activación surgió la hipótesis de la posible existencia de interacciones laterales con alguna de las cadenas del CD3 para explicar la capacidad de señalización de CD38 [147].

Antes de seguir profundizando en la relación CD38-complejo TCR/CD3 haré una breve descripción de los componentes de dicho complejo.

5.2.1 Componentes del complejo TCR/CD3

Inmunologiaonline. Universidad de Córdoba y Sweden Diagnostics (Spain). www.uco.es/grupos/inmunologia-molecular/inmunologia/.

L. M. Allende, A. Corell, A. Pacheco, J. R. Regueiro y A. Arnaiz-Villena.

El complejo TCR/CD3 consta de dos partes bien diferenciadas:

- ***TCR***

  Es un heterodímero con dos subunidades protéicas, denominadas alfa (α) y beta (β), unidas covalentemente por puentes disulfuro. Es la porción específica del receptor, por lo

tanto polimórfica, y en ella se dá la variación clonotípica que va a permitir el reconocimiento de los más de 10^8 antígenos diferentes.

Existe una variante del TCR que se encuentra en unas pocas células T, y está formada por cadenas gamma (γ) y delta (δ) en lugar de las cadenas α y β. Este heterodímero no se asocia covalentemente.

- ***CD3***

Es la porción invariante del complejo y está formado por al menos 3 monómeros unidos no covalentemente, denominados gamma (γ), delta (δ) y epsilon (ε). Es el encargado de transmitir la señal del reconocimiento antigénico al interior celular. Al complejo CD3 se le asocia un gran homodímero intracitoplasmatico ζζ.

Todos los componentes del receptor de la célula T son proteínas de membrana, y están formadas por una secuencia, dominio N-terminal extracelular, dominio transmembrana y dominio citoplásmico C-terminal.

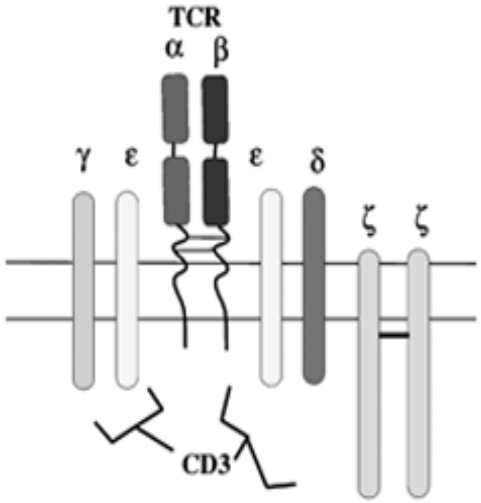

Fig. 18 Estructura del complejo TCR/CD3

CD3 y TCRζ son responsables de transmitir la señal al interior celular mediante unos motivos aminoacídicos conservados que están presentes en sus dominios citoplasmáticos. Estos motivos contienen residuos de tirosina y se denominan ITAM (motivos de activación basados en tirosina) [161-163]. Otros inmunoreceptores, tales como el receptor de células B (BCR) y el receptor para inmunoglobulinas Fcγ también usan ITAMs para señalizar [164]. La

secuencia consenso de aminoácidos de este motivo es YXX(L/I)X_{6-8}YXX(L/I) (donde Y es tirosina, L leucina y X es cualquier aminoácido). La cadena ζ del TCR contiene 3 motivos ITAMs en tándem mientras que cada cadena del CD3 tiene 1, resultando 10 ITAMs por cada complejo receptor.

La señalización a través del TCR también facilitada por los coreceptores CD4 y CD8, los cuales interaccionan con moléculas MHC expresadas en las células APC durante la presentación antigénica [165].

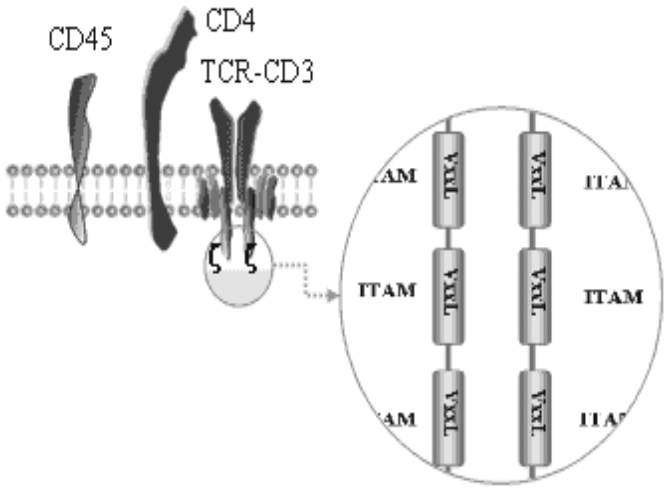

Fig.19 Motivos de activación en tirosina del complejo TCR/CD3

La fosforilación en tirosina de estos ITAMs proporciona la interacción de las proteínas Syk y ZAP-70. Éstas a su vez permiten el reclutamiento y la activación de proteínas tales como LAT, Vav y Slp-76. Esto permite la formación de complejos multimoleculares que activan algunas cascadas de señalización como la de PLC-γ1, la ruta de las MAP cinasas y la del PI3-K [166-168]. Estas rutas de señalización convergen en el núcleo resultando en la expresión de genes que caracterizan la activación del linfocito T.

A continuación del trabajo de Morra et al. [147], Zubiaur et al. [169] investigaron la participación de varios de los componentes del complejo TCR/CD3 en la señalización mediada por CD38. Con sus experimentos demostraron que en células TCR^+ que expresan todas las subunidades del CD3, la estimulación a través de CD38 producía la completa fosforilación en tirosina de CD3-ζ y CD3-ε. Ésta fosforilación en tirosina, inducida por CD38, de CD3-ζ y CD3-ε sugería una relación funcional entre las señales derivadas a través

de CD38 y TCR/CD3. Utilizaron la línea de linfocitos T Jurkat 31-13 [170] ($CD38^{+}TCR^{-}/CD3^{-}$), la cual no expresa el complejo TCR/CD3 porque tiene defecto en la expresión del gen para la cadena β del TCR. En estas células, cuando se estimulaba a través de CD38 mediante el anticuerpo anti-CD38 IB4, no había incremento de proteínas fosforiladas en tirosina. Cuando estas células eran transfectadas con el cDNA que codificaba para la cadena β del TCR, se recuperaba la expresión del TCR/CD3 en superficie, así como la fosforilación en tirosina de Erk-2, Cbl, PLC-γ1, ZAP-70 y Slp-76 mediada por CD38 [169].

Para averiguar cual de los componentes del complejo TCR/CD3 era el que requería CD38 para señalizar, utilizaron una línea Jurkat 31-13 que tenía reconstituido TCR-β pero que tenía mutación puntual de una tirosina por una leucina en el dominio transmembrana (Y11L) impidiendo así la asociación de CD3-ζ al TCR [171]. No obstante, TCR se expresaba en superficie y estaba fuertemente unido al complejo CD3-γδε y cuando eran estimuladas con anticuerpos anti-CD3 había aumento en la fosforilación en tirosina. En estas células, cuando se activaba a través de CD38, seguía produciéndose la activación de Erk-2 probando así que CD38 no requiere de la asociación de CD3-ζ al TCR. No obstante, no excluyen el papel funcional que puede desarrollar CD3-ζ, ya que la estimulación a través de CD38 en linfocitos T Jurkat conlleva a la fosforilación en tirosina de CD3-ζ y la asociación de ZAP-70 a CD3-ζ [159], lo que puede reflejar un papel de CD3-ζ en la ruta de señalización de CD38.

Para estudiar el papel de CD3-ζ en la transducción de señales mediada por CD38, Zubiaur et al. [172] utilizaron células de ratón deficientes en CD3-ζ a las que reconstituyeron con la cadena ζ total o con la cadena ζ pero con los ITAMs delecionados y transfectaron el cDNA que codifica para CD38 humano. Sus resultados mostraron que en ambas situaciones, la estimulación a través de CD38 da como resultado la fosforilación en tirosina de diversos sustratos, incluyendo CD3-ε, ZAP-70 y Shc y la activación de las rutas de señalización PI3-K/Akt y Ras/Erk. Además demostraron que CD38 estaba constitutivamente asociado a los *rafts*. Cuando deplecionaban el colesterol de la membrana (50-60% según los trabajos de otros grupos [173]) mediante la preincubación de las células con metil-β-ciclodextrina (MβCD) (desorganización de los *rafts*) y a continuación eran estimuladas con anti-CD3 o anti-CD38, observaron que el tratamiento con MβCD causaba una sustancial inhibición de la estimulación de Akt mediada por CD3 o por CD38, mientras que Erk se activaba incluso más. Está descrito [174] que el pretratamiento de linfocitos T con MβCD inhibe la movilización de Ca^{2+} y la fosforilación en tirosina mediada por el TCR, por lo que estos datos evidencian el

importante papel del colesterol en la función del complejo TCR/CD3. Por el contrario, el aumento de la fosforilación de Erk anteriormente comentado sugiere que los niveles normales de colesterol pueden regular negativamente algunas rutas de señalización por debajo de ella. Hay resultados de otros grupos que demuestran que el tratamiento de linfocitos T con MβCD estimula la ruta Ras/Erk mediada por CD3 [175].

Dado que LAT es importante en la activación la ruta Ras/Erk mediada por el TCR y que la activación a través de CD38 induce la fosforilación en tirosina de LAT, estudiaron que ocurría en estas células. Cuando estimulaban a través de CD38 apenas había fosforilación de LAT, mientras que cuando estimulaban a través de CD3, las células con la cadena ζ reconstituida presentaban LAT fosforilado pero no las que tenían esta cadena mutada (aunque en ambas se detectaba Sos). Puesto que LAT fosforilado une Grb2 directamente [176] y no contiene dominio SH3 para interaccionar con la región rica en prolinas de Sos, la interacción Grb2/Sos puede mediar la asociación de LAT fosforilado-Sos.

Estaba demostrado que la estimulación a través de CD38 conlleva a la fosforilación en tirosina de ZAP-70 [177] y en este trabajo comprobaron que la cadena CD3-ζ no ejercía ningún efecto de amplificación de la fosforilación de ZAP-70 mediada por CD38. Además demostraron que había activación de Erk cuando estimulaban a través de CD38 en células T Jurkat LAT-deficientes y en células T Jurkat ZAP-70 negativas.

Debido al papel crucial que tienen los ITAMs dentro de las cadenas del CD3 para el reclutamiento de proteín tirosín cinasas y moléculas efectoras al TCR, Guirado et al [178] llevaron a cabo el estudio de las tirosinas de los ITAMs del CD3. Para ello construyeron moléculas quiméricas que contenían el dominio extracelular y el dominio transmembrana del CD8α humano y el dominios citoplasmático del CD3-ε de ratón (llamado CD8-ε). Además realizaron estas construcciones pero haciendo mutaciones de una o dos tirosinas), Y170F, Y181F y Y170F/Y181F. En su trabajo concluyen diciendo que, en células T humanas, la fosforilación de las tirosinas N-terminal y C-terminal del ITAM del CD3-ε de ratón está diferencialmente regulada: la sustitución por phenilalanina de la tirosina N-terminal del ITAM de CD3-ε elimina las funciones de transducción de la señal de éste ITAM, incluyendo la fosforilación en la tirosina del ITAM C-terminal y su asociación con ZAP-70. Por el contrario, la mutación en la tirosina C-terminal del ITAM de CD3-ε no previene la fosforilación en la tirosina N-terminal, ni su asociación con Lck o la subunidad reguladora

p85 PI3-K [178]. La interacción Lck/CD3-ε es sensible al octil-glucósido, un detergente que rompe a asociación de Lck con los *rafts* de membrana [179]. La acumulación de Lck y CD3-ε en *rafts* puede aumentar la concentración de ambas proteínas y estabilizar su asociación. Guirado et al. postulan que la Y^{170} tiene la ventaja adicional sobre la Y^{181} de ser fosforilada por Lck ya que está próxima a una región rica en prolinas, la cual puede interaccionar con el dominio SH3 de Lck. Esta interacción puede ayudar a Lck de la regulación negativa de su propio dominio SH3 [180, 181]. Para la formación de un complejo estable y una extensiva fosforilación de CD3-ε se requiere una segunda interacción más fuerte con el dominio SH2 de Lck.

5.2.2 Reconocimiento del antígeno por el receptor del linfocito T

Una vez en la periferia, el linfocito T tiene la capacidad de migrar a través del cuerpo, adheriéndose tanto funcional como no funcionalmente a distintos tipos celulares, sobre los que reconoce antígenos exógenos. Por otro lado, una célula presentadora de antígeno que ha procesado una proteína antigénica determinada expresará en su superficie celular un largo número de diferentes complejos MHC/antígeno. Los péptidos que son reconocidos por las células T deben tener una estructura secundaria en α-hélice. Se ha visto que todos los péptidos antigénicos son anfipáticos, con una cara hidrofílica y otra hidrofóbica, pudiendo interaccionar una de las caras con el complejo TCR/CD3 y la otra con la molécula de MHC, respectivamente. Por esta razón, el reconocimiento de la asociación MHC/péptido antigénico es un proceso dinámico que incluye un primer paso de complejas interacciones célula-célula, antes de que se produzca un contacto productivo que dé lugar a la activación celular.

5.2.3 Reconocimiento de superantígenos bacterianos

Se denominan superantígenos a aquellos antígenos capaces de reaccionar con distintas moléculas MHC de clase II y TCR de un mismo individuo. Pueden ser exógenos (como las toxinas de ciertos estafilococos (SEE, SEB…), si provienen del exterior, o endógenos (como el retrovirus MMTV), si se reproducen en la línea germinal.

El reconocimiento del superantígeno se distingue del reconocimiento del péptido antigénico convencional por tres características fundamentales: la especificidad de la célula T a los superantígenos está determinada por la región variable de la cadena β, siendo independiente de otros componentes del receptor de la célula T; el superantígeno tiene dos sitios de unión, uno para la molécula MHC de clase II, fuera de la hendidura de reconocimiento peptídico, y otro para el TCR, situado en la región V_β fuera del sitio clásico de unión al complejo MHC-antígeno (esta característica hace posible que un mismo superantígeno pueda interaccionar con distintas células del repertorio T).

Como consecuencia del reconocimiento de superantígenos exógenos en periferia, se produce la activación celular y fuerte expansión de las células T implicadas en el reconocimiento.

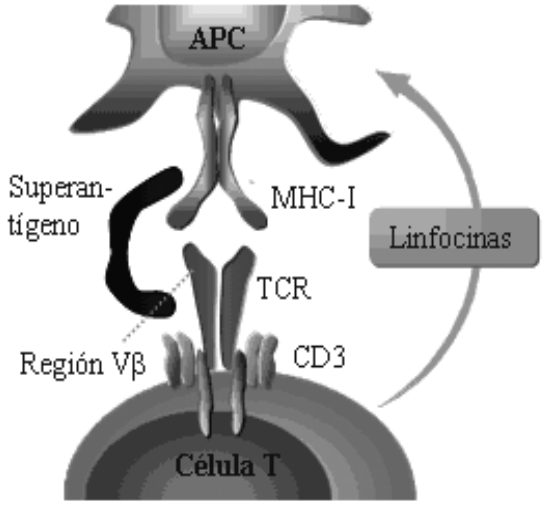

Fig.20 Interacción del superantígeno bacteriano presentado por la APC con el TCR

Hay descrita la existencia de complejos supramoleculares. Estos complejos residen en áreas de la membrana plasmática enriquecidas en colesterol, los llamados microdominios de membrana o *rafts* [21, 182].

6. Microdominios de membrana (*Rafts*)

6.1 Descripción

En la membrana plasmática de las células eucariotas podemos encontrar microdominios de membrana (también llamadas balsas lipídicas, *rafts* o dominios de membrana resistentes a

detergente (DRM). Estas zonas de la membrana están enriquecidas en glicoesfingolípidos y colesterol. Aparecen proteínas, las cuales están miristoiladas o palmitoiladas para así poder estar asociadas a la membrana. Un ejemplo de proteínas que sufren estas modificaciones son las quinasas de la familia Src. Hay proteínas que están ancladas a la membrana mediante GPI (en células T por ejemplo están CD48, CD52, CD55, CD59, CD90 (Thy-1), CD108, CD230 y Ly-6).

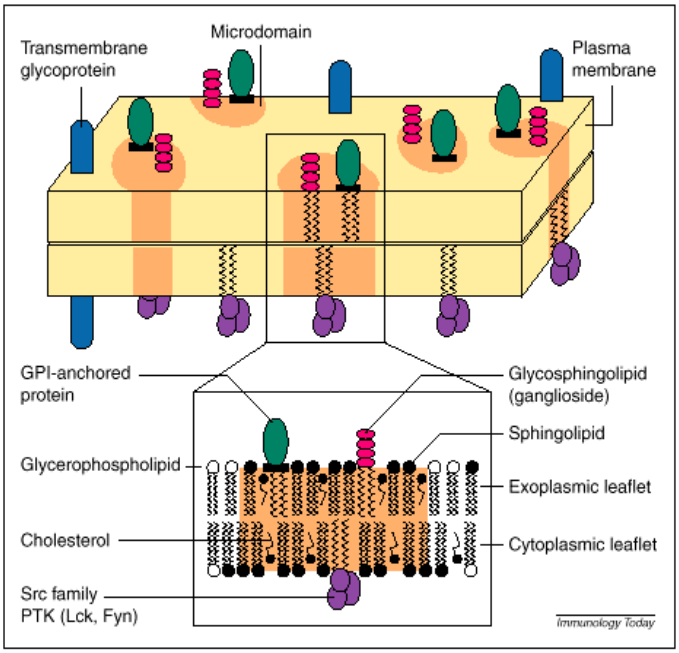

Ilangumaran, S., et al. *2000.Immunology Today 21: 2-7*

Fig.21 Composición de los microdominios de membrana (*rafts*)

Hay receptores y moléculas de señalización implicadas en la activación de la célula T que están localizadas en las balsas lipídicas incluyendo CD8 [183], CD4 [184], Lck, Fyn [185], LAT [186, 187], Cbl/PAG [188], Syk, Ras [185] y PKC-θ [189]. Otras moléculas son traslocadas a los *rafts* sólo tras la estimulación del TCR, incluyendo el TCR fosforilado [174, 185, 190], ZAP-70 [185, 190], PLCγ1, Vav, Grb2 y PI3K [185, 186]. La deplección del colesterol disocia estas proteínas de los DRM e inactiva la cascada de señalización, previniendo la completa activación del linfocito T [175, 185].

Se ha propuesto que los *rafts* actúan como compartimentos de señalización en membranas celulares [191]. Esta hipótesis ha sido corroborada por estudios que muestran que la señalización del linfocito es inhibida cuando se elimina el colesterol de los *rafts* [185]. Estos

dominios tienen también un papel muy importante en endocitosis de moléculas y patógenos, e incluso hay trabajos que han demostrado que estos microdominios de membrana están involucrados en el funcionamiento de algunos canales iónicos.

Son complejas estructuras cuyo tamaño va desde pocos nanómetros hasta macrodominios que tienen micrómetros de diámetro [192-196]. Un ejemplo importante de macrodominios de *rafts* es la sinapsis inmunológica que se forma cuando linfocitos estimulados entran en contacto con una célula adyacente [195, 197, 198] así como entre un linfocito T y una célula presentadora de antígeno (APC) [199]. El hecho de que los *rafts* de membrana están ensamblados para formar una sinapsis inmunológica es importante para los inmunólogos porque se requiere una sinapsis estable para una eficiente activación de la célula inmune [200].

Fig.22 Funciones de los *rafts*

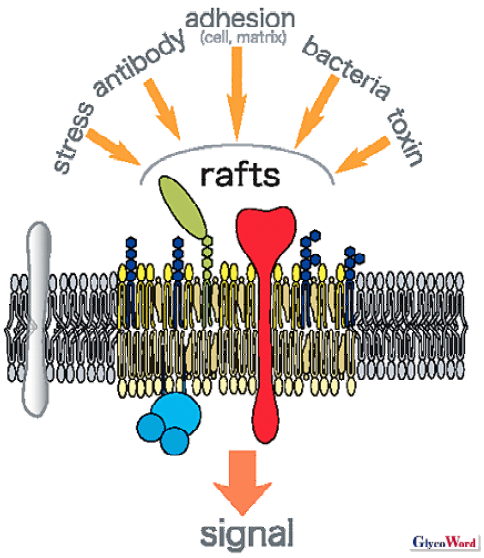

6.2 Propiedades básicas de los *rafts*

Debido a su composición lipídica, los *lipid-rafts* son relativamente resistentes a la solubilización en determinados detergentes a bajas temperaturas, tales como Triton X-100, detergentes de la serie Brij, NP-40 o CHAPS [201]. Estas propiedades hacen posible separarlos, mediante ultracentrifugación de gradiente de densidad, de otros componentes de membranas completamente solubilizados.

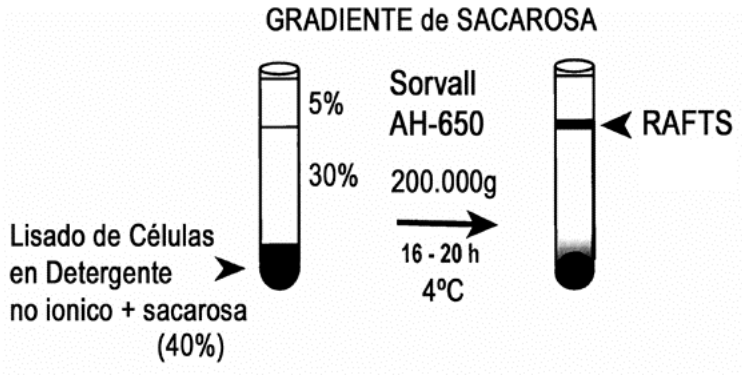

Fig. 23 Método para el aislamiento de microdominios de membrana mediante gradiente de sacarosa. El lisado de células (con inhibidores de fosfatasas y proteasas) se mezcla con sacarosa al 80% y a continuación se añade sacarosa al 30% y 5%. Tras la centrifugación los rafts se localizan en las primeras fracciones del gradiente [172].

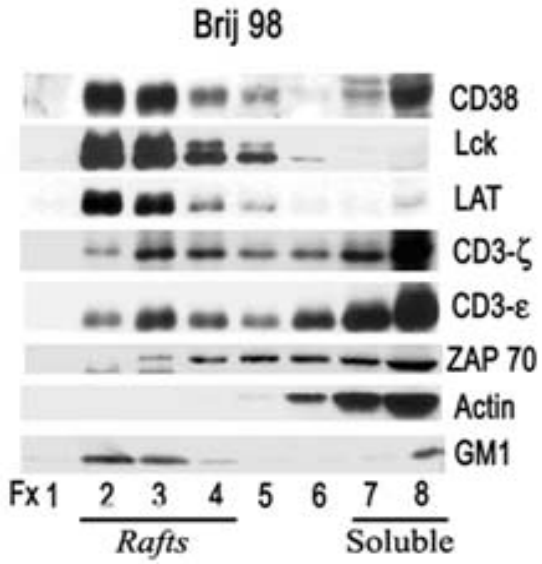

Fig. 24 Distribución de las proteínas en el gradiente de sacarosa

6.2 Aspectos problemáticos de los *rafts [201].*

Mediante técnicas de microscopía es difícil detectarlos debido a su pequeño tamaño, por lo que la mayoría de los datos que se obtienen acerca de las balsas lipídicas es a partir del análisis de preparaciones obtenidas mediante la ultracentrifugación, en gradiente de densidad, de lisados en detergentes a bajas temperaturas. Esto por supuesto es un problema: no está claro hasta que punto la composición y las propiedades de los rafts originales de la membrana corresponden con aquellos obtenidos mediante la extracción a baja temperatura. Sería posible que algunos componentes presentes en los *rafts* lipídicos "in vivo" se pierdan por la extracción mediante el detergente, mientras que la presencia de un detergente a baja temperatura puede inducir artificialmente asociaciones, e incluso transiciones entre fases lipídicas. Este problema es aún más complicado ya que la composición de los *rafts* aislados depende de la naturaleza y la concentración del detergente utilizado. Detergentes suaves como el Brij-98 o el Brij-58 producen rafts flotantes que contienen la mayoría de las proteínas totales ancladas a GPI, adaptadores transmembrana como LAT o PAG/Cbp y quinasas de la familia Src.

Los rafts lipídicos pueden ser aislados a 37º C usando el detergente Brij-98, el cual excluye la objeción de que la solubilización a baja temperatura induce transiciones de fase lipídica, creando artificialmente los complejos lípido-proteína resistentes a detergente. De hecho, fragmentos de membrana muy similares a los *rafts* lipídicos pueden obtenerse mediante desintegración de la membrana en ausencia de detergente (aunque a baja temperatura).

6.3 Los *rafts* en la señalización a través del TCR

Estudios bioquímicos en mastocitos, células T y B revelan que la activación a través de sus respectivos inmunoreceptores (FcεRI, TCR y BCR) resulta en una agregación de receptores con los *rafts*-lipídicos resistentes a detergente. Como resultado, los motivos ITAM (motivos de activación en tirosina) de las cadenas citoplasmáticas de los complejos inmunoreceptores (CD3, cadena ζ, Igα/β, cadena γ del receptor Fc) están expuestos a las

quinasas de la familia Src presentes en los *rafts*. Los ITAMs fosforilados sirven de sitios de unión a dominios SH2 de quinasas de la familia Syk (ZAP70 o Syk). ZAP70 activado en células T fosforila otro componente de los *rafts,* el adaptador transmembrana LAT. Aunque Lck está constitutivamente presente en los *rafts* cambia su interacción con los microdominios de membrana dependiendo de la activación del TCR. Se ha visto que esta quinasa está presente en las balsas lipídicas enana estructura cerrada (o inactiva) y que LAT es esencial para el mantenimiento de esta conformación [202].

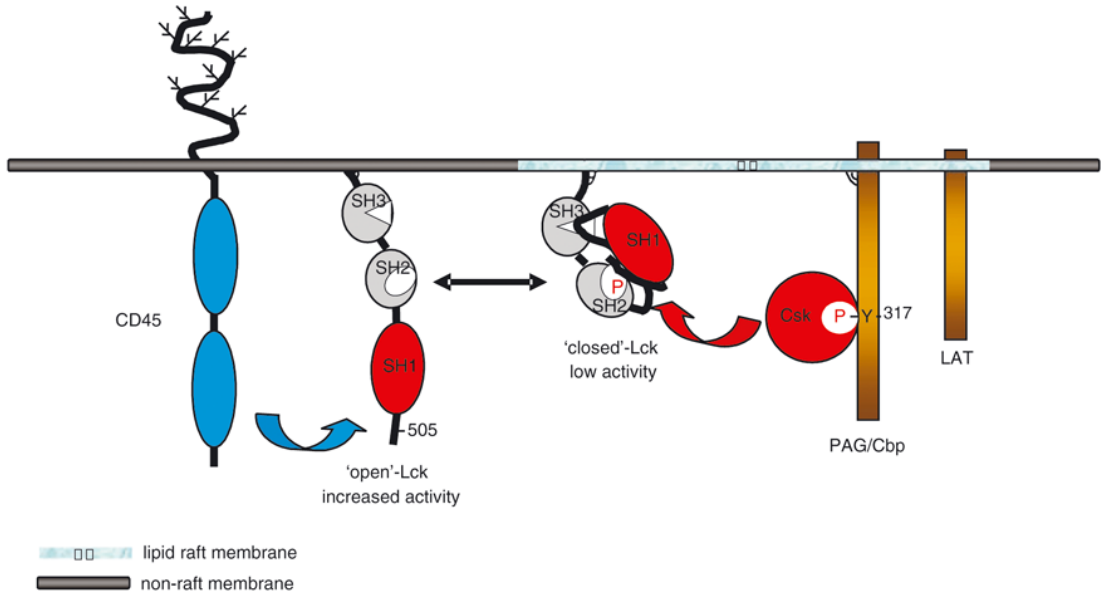

Tahir M. Razzaq. et al. *Immunology* 2004 **113**, 413-426

Fig. 25 Regulación de Lck en la membrana plasmática.

En células T, Lck se localiza principalmente en las fracciones *rafts* de la membrana. Lck asociado a los *rafts* es fosforilado en la tirosina reguladora C-terminal, la cuál interacciona con el domino SH2 promoviendo una estructura de baja actividad. Esta fosforilación está mediada por el complejo proteico PAG/Cbp-Csk y puede mantenerse en las balsas lipídicas porque hay una exclusión de la fosfatasa CD45. Por el contrario, el pool de Lck presente en la membrana plasmática preferencialmente adopta una

conformación “abierta” con alta actividad catalítica debido a la acción positiva de CD45, la cuál desfosforila la tirosina inhibidora C-terminal.

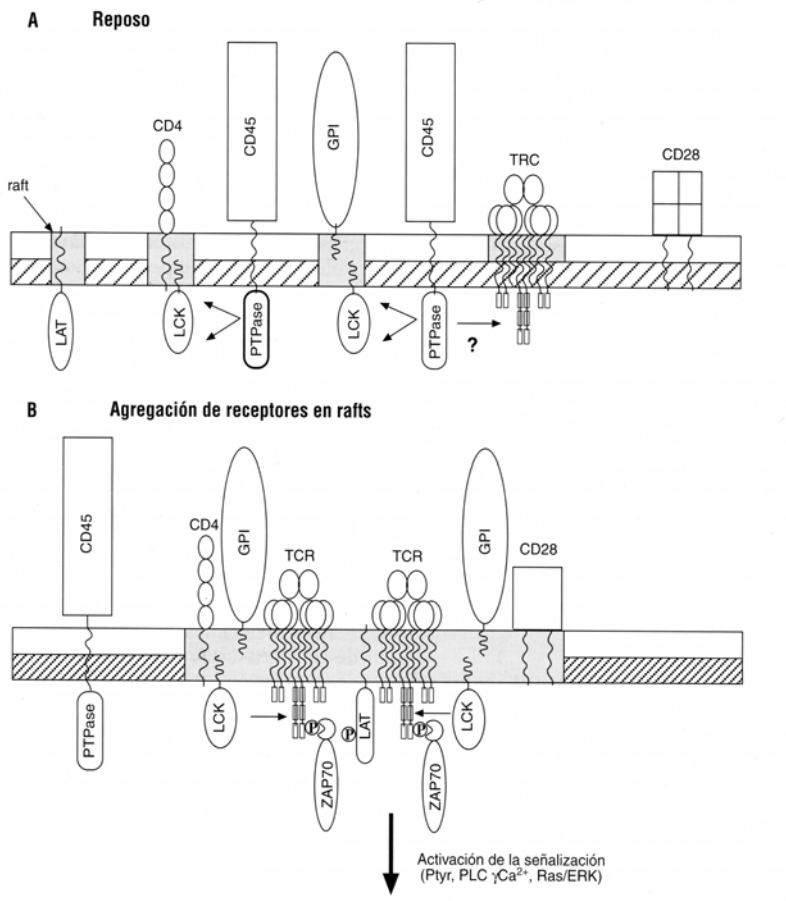

F. Martín-Belmonte, J. Millán. *Inmunología.* Vol 120 Núm 4 2001

Fig. 26 Modelo de agregación de microdominios de membrana en la señalización a través del TCR

Bajo la activación fisiológica de la célula T, la forma activa de Lck se acumula en los DRM [203], sugiriendo que el signalosoma del TCR está organizado en *rafts* lipídicos. Por el contrario, después de la estimulación de los linfocitos T mediante anticuerpos anti-CD3, Lck activo y proteínas fosforiladas en tirosina aparecen en la fracción soluble (no *raft*) [203].

LAT es una proteína transmembrana de tipo II que se localiza en la membrana plasmática por adición de grupos palmíticos a sus 2 residuos de cisteína. LAT fosforilado une moléculas citoplasmáticas que contienen SH2, tales como los adaptadores Grb2 y Gads (y a través de ellos, indirectamente, otras moléculas de señalización como Sos1, SLP-76, Vav y Itk), así

como la enzima fosfolipasa Cγ. SLP-76 y Vav permiten la activación de la serín-treonín-quinasa PKC-θ (isoforma de la PKC presente selectivamente en células T e independiente de Ca^{2+}) y el reclutamiento de esta cinasa a los lipid-*rafts* de la membrana plasmática. De acuerdo con el modelo [204], PKC-θ activaría a IKK a través de proteínas adicionales incluyendo CARMA1 (también llamada CARD11), BCL10 y MALT1, lo cual forma un complejo. Cada componente de este complejo es esencial para la activación de NF-κB en células T [205]. La importancia de PKC-θ en la activación del linfocito T fue confirmada por estudios en ratones PKC-θ knockout, los cuales muestran un defecto selectivo en la activación del linfocito T a nivel de la inducción de AP-1, NF-κB e IL2 [206].

La interacción TCR-*raft* parece estar regulada negativamente por una proteína adaptadora citoplasmática, Cbl-b. La proteína CD45 quedaría excluida de los rafts para permitir así la activación de Lck, aunque una pequeña cantidad de CD45 aparentemente está presente en los rafts y activa las Src quinasas por desfosforilación de la fosfotirosina reguladora del C-terminal [207, 208]. Hay interpretaciones que dicen que el papel de CD45 es el de mantener el balance de la activación de Lck por la interacción con la quinasa Csk [207, 208].

- ✓ CD28 no está basalmente presente en los *rafts* después de la estimulación se redistribuye a las balsas lipídicas, pudiendo ser esto importante para su actividad co-estimuladora [209].
- ✓ PKCθ, después de ser fosforilado en tirosina, se asocia físicamente con Lck y se trasloca a los *rafts* lipídicos asociados con la sinapsis inmunológica [210].
- ✓ Los microdominios de membrana están implicados en el funcionamiento de algunos receptores para quimioquinas, tales como los receptores para IL-2 e IFNγ [211, 212].
- ✓ Ambos tipos de receptores para HIV (CD4 y receptores de quimioquinas) residen en las balsas lipídicas y el particular ambiente lipídico es necesario para la infectividad del HIV así como para la liberación de partículas víricas [213].
- ✓ Una fracción importante funcionalmente de las proteínas del MHC-II se encuentran en los *rafts* lipídicos de la superficie de la célula APC [214]. Este ambiente lipídico específico puede ayudar a mantener las uniones entre antígeno y molécula presentadora en unas condiciones óptimas para el reconocimiento por el TCR. Así, las balsas lipídicas son importantes en ambos lados de la zona de contacto célula T- APC.

- ✓ Alteraciones en la composición de los *rafts* lipídicos y dinámica aparentemente pueden contribuir a respuestas anormales de las células T en el lupus eritematoso sistémico (LES). Además, la localización de CD45 (regulador positivo de la actividad de Lck) en las balsas lipídicas está aumentada en las células T de pacientes con LES [215].

CD3-ζ fosforilado es reclutado a las balsas lipídicas y debido a la localización de Lck en los rafts, se supone que la fosforilación de CD3 ocurre sólo dentro de los *rafts,* aunque aún están por saber qué mecanismos pueden mediar la inducción de la traslocación de los componentes del TCR a los *rafts*. Una posible solución para este problema puede ser el hecho de que pueden recuperarse constitutivamente de los *rafts* componentes del TCR e independientemente de la actividad de las cinasas de la familia Src donde los rafts fueron aislados a temperatura fisiológica usando Brij-98 como detergente [216]. CD38 está presente en los rafts y, tras su estimulación, permite la activación de Akt/PKB y Erk en ausencia de los motivos ITAM del CD3-ζ [172].

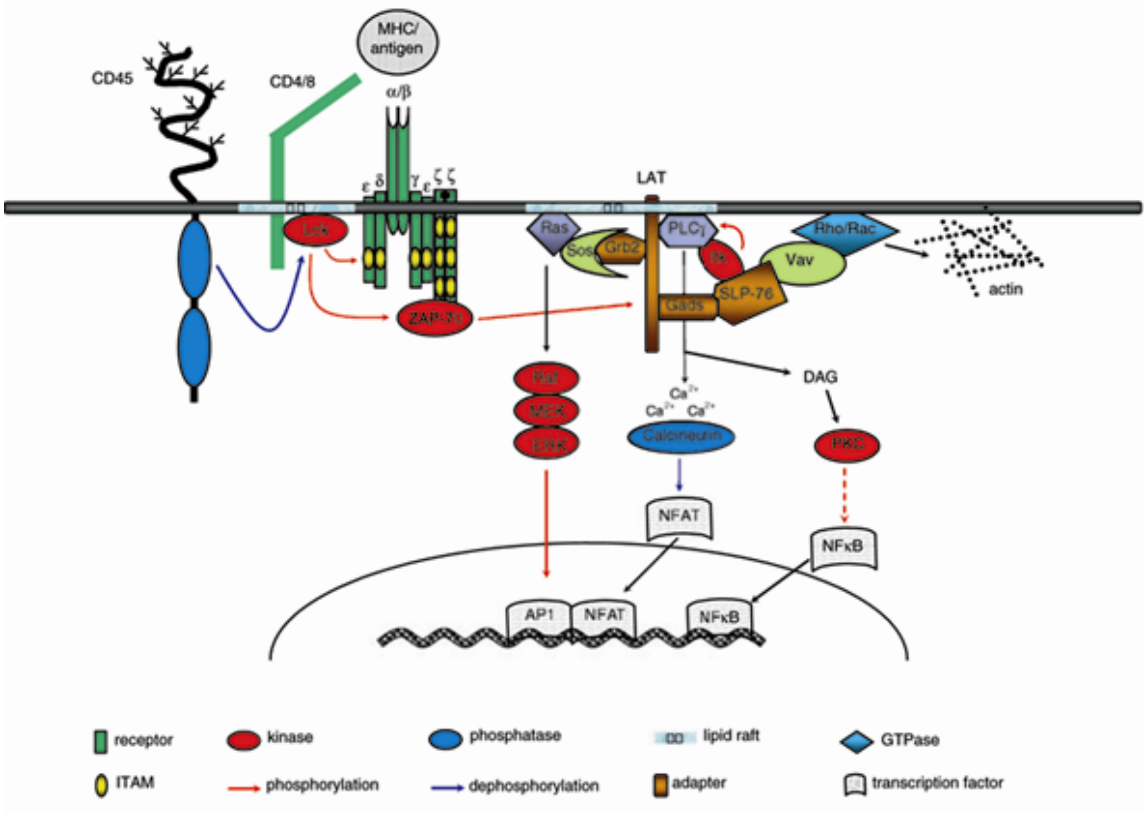

Tahir M. Razzaq et al. *Immunology* 2004 **113**, 413-426

Fig. 27 Cascadas de señalización estimuladas por TCR.

Otra función de los *rafts* es la amplificación y estabilización de señales permitido por la agregación de *rafts* en grandes complejos acompañados por el reclutamiento de mediadores de señales tales como LAT y moléculas asociadas [217] así como componentes de TCR [218]. Estos complejos de *rafts* se denominaron con el término "plataformas de señalización" [219]. Se encontró que las balsas lipídicas y los filamentos de actina (F-actina) están co-localizando [220] y el citoesqueleto de actina conduce la agregación de *rafts* lipídicos [194, 218, 221]. Además, el movimiento dirigido por la actina de las moléculas de membrana permite un incremento de la duración de la señalización de la célula T [222].

Estos movimientos inducen a la acumulación de moléculas en la interfaz de la célula T y la célula presentadora del antígeno (APC) [222] (sinapsis inmunológica).

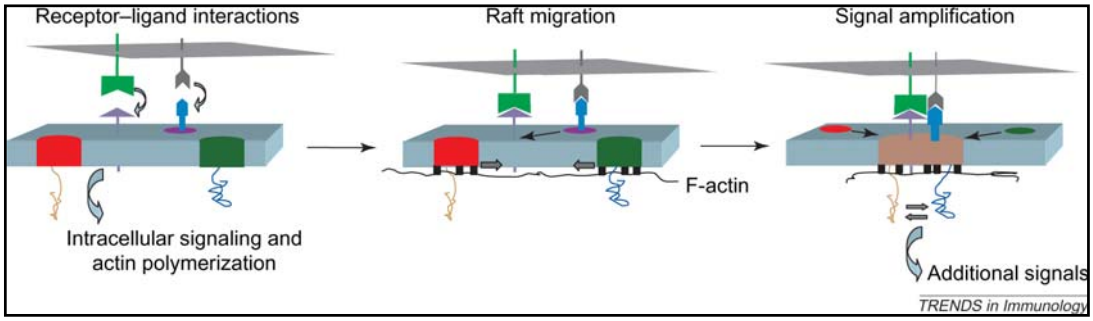

Rodgers,W. et al. *Trends in Immunology* Vol. 26 Nº2 February 2005

Fig. 28 Modelo de ensamblaje de macrodominos *rafts* mediada por citoesqueleto: Unión de los receptores con sus ligandos, cascada de señalización intracelular que permitiría la polimerización de actina y la aproximación de los dominios discretos que conducen a una amplificación de la señal. La cascada continuaría hasta la aparición de señales de stop, lo cuál incluiría a proteín tirosín fosfatasas. El cese de la acumulación de *rafts* probablemente coincida con la formación de la sinapsis inmunológica madura en células T y B.

7. Sinapsis inmunológica

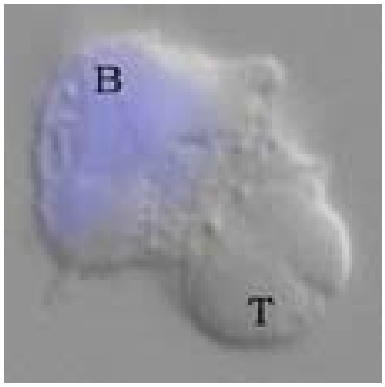

Fig. 29 Conjugado células T:B

La interacción antígeno-específica de las células T con las células presentadoras del antígeno (APC) es lo que se denomina *sinapsis inmunológica* (SI).
En la SI madura hay una agregación de receptores de superficie y componentes de señalización [223].
En esta interacción célula T- APC hay una movilización de Ca^{2+}, lo cuál es requerido para la activación de la producción de citoquinas y proliferación [224, 225].

En un primer paso, la célula T migra hacia la célula APC y el contacto de adhesión inicial permite la redistribución de la molécula de adhesión intercelular ICAM-3 sobre la célula T [226]. La interacción de ICAM-3 con el antígeno asociado a la función del leucocito (LFA)-1 y DC-SIGN parece proveer de la fuerza adhesiva necesaria para el reconocimiento de la superficie de la APC por el linfocito T [227]. Este paso es presumiblemente seguido de la unión de CD-2 y LFA-3 (CD58), lo cual permite el acercamiento necesario para que el TCR de la célula T interaccione con el péptido unido al MHC en la célula presentadora. La unión TCR/CD3, ICAM-3 y CD2 aumenta la adhesión LFA-1/ICAM-1 [228-230], lo que incrementa la fuerza de la unión célula T-APC. Tras la unión del TCR con el péptido antigénico, otros mecanismos adicionales parecen contribuir a la estabilización del conjugado linfocito T-APC, con lo que ambas células estarían cercanas durante su activación. Un elemento importante durante la interacción es el citoesqueleto, el cual juega un papel crucial en la segregación de la membrana y de proteínas señalizadoras intracelulares.

A continuación de la señalización inicial a través del TCR se forma un área central de unión de integrinas en la zona de contacto de la célula T, rodeado de una región cercana con el TCR [231]. Pocos minutos más tarde, el TCR unido al péptido se mueve al centro del área de contacto, formando un complejo central supramolecular de activación (cSMAC) y las integrinas son forzadas a ir a un anillo que rodea a este cSMAC (pSMAC) [199, 231] . Los correceptores de la célula T como CD4 o CD8 [199, 231, 232], moléculas coestimuladoras como CD28 (el cuál interacciona con CD80/86 expresado en la APC) [233] y moléculas de señalización intracelular como PKC-θ, Lck, Fyn y ZAP-70 [199, 231, 232] son también localizados en el cSMAC, en la cara interna de la membrana plasmática de la célula T.

Moléculas como LFA-1 e ICAM-1 se acumulan en una región periférica al cSMAC, denominado pSMAC.

Muchos autores describen la presencia de una región aún más periférica llamada dSMAC. La proteína CD43 se ha visto que es excluida del cSMAC y que se trasloca al dSMAC tras la estimulación a través del TCR [234, 235]. La proteína CD45 es tempranamente reclutada al cSMAC pero después se mueve al dSMAC probablemente debido a su función de activar Lck en la SI en estado temprano de activación [236, 237]. Otras moléculas que se acumulan en la SI son PAK1 [238], Akt [239], HIP-55 [240], CD26 [241] y el receptor de transferrina [242].

La activación del linfocito T antígeno-dependiente también implica la traslocación del centro organizador de microtúbulos (MTOC) y la asociación del aparato de Golgi a la zona de contacto con la célula APC [243].

Ésta es una estructura dinámica cuya función exacta aunque aún es desconocida, no hay duda que es el sitio de reconocimiento del antígeno y señalización. Se piensa que está asociada con el mantenimiento de la activación del linfocito T, promoviendo señales positivas o negativas en la proliferación celular [244, 245].

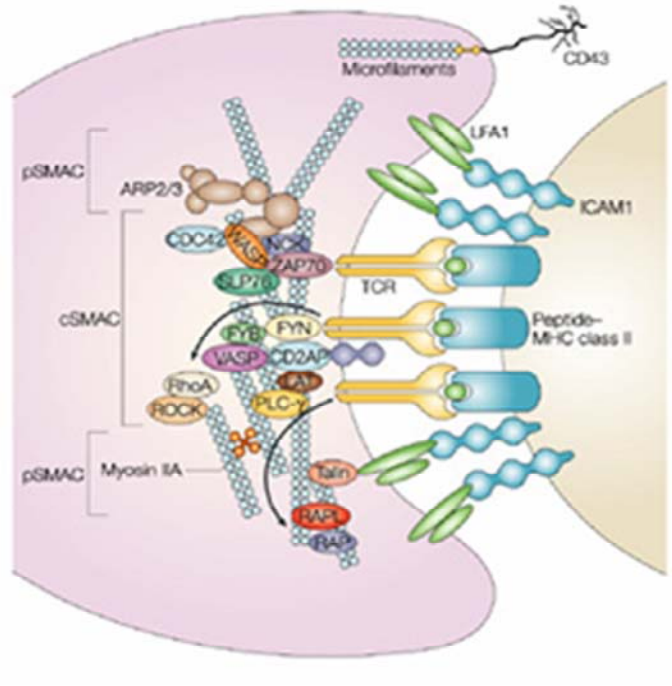

Vicente-Manzanares M., et al. M. *Nature Reviews.* (2004) Vol. 4

Fig. 30 Sinapsis inmunológica entre una célula T célula presentadora de antígeno (APC).

Se ha descrito la formación de pequeños "cúmulos" de TCR ("*clusters*") previos a la formación de la SI [246]. Krummel et [247] al fueron los primeros en observar pequeños cúmulos dispersos de CD3-ζ y CD4 usando proteínas fusionadas a GFP, los cuales aparecían al mismo tiempo que la respuesta inicial de Ca^{2+} tras el contacto célula-célula entre clones de células T y células presentadoras del antígeno (APC). Microclusters similares fueron observados y estudiados usando células T Jurkat estimuladas con anticuerpo anti-CD3 unido a placa [248, 249] y mediante microscopía de fluorescencia de reflección total interna (TIRF). Segundos después del contacto con la placa, las células T desarrollaban clusters, los cuales eran dinámicamente regulados. Estos microclusters (MC) contenían TCR, ZAP-70, LAT, Grb2, Gads, SLP-76, y fosfotirosina. Mientras que LAT y Gads eran temporalmente traslocados a los clusters con TCR, los clusters que contenían ZAP-70 eran más estables. Por el contrario, SLP-76 era dinámicamente traslocado a la región perinuclear tras la formación del cluster. Además, estos MC estaban asociados a WASP y fueron unidos a regulación por citoesqueleto de actina [250]. Estos análisis indican que la estimulación a través del TCR induce cambios dinámicos en los clusters de receptores y moléculas de señalización y sugiere que los clusters inician las señales de activación.

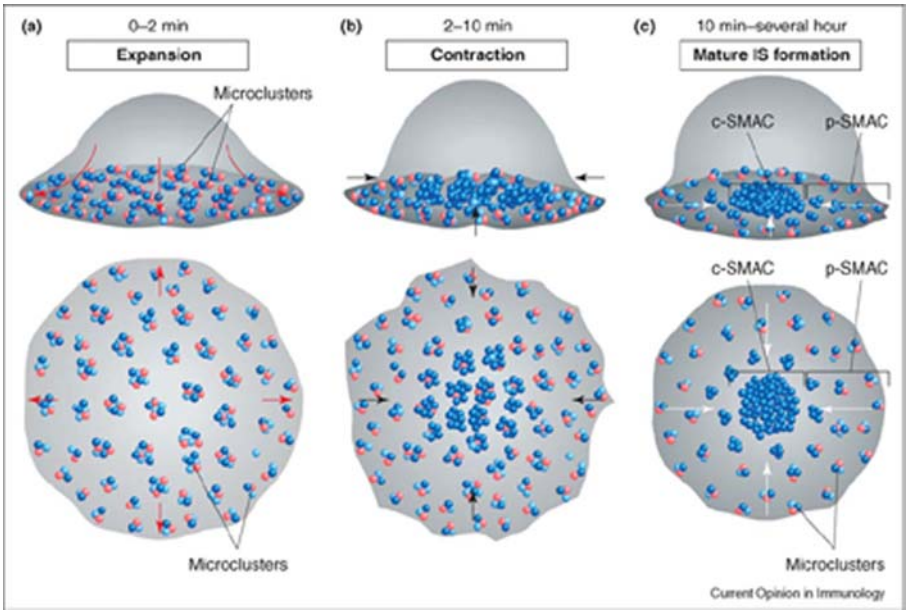

Saito, T. and Yokosuda, T. *Current Opinión in Immunology* (2006), **18**:305-313

Fig. 31 Proceso dinámico de reconocimiento del antígeno y activación de la célula T por formación de microclusters y sinapsis inmunológica. En rojo está representada la cinasa, en azul oscuro el receptor y en azul claro el adaptador.

Aunque la activación inicial de las señales en linfocitos T incluyendo fosforilación en tirosina, flujo de Ca^{2+} y movimiento de PI son inducidos en unos minutos, las células T requieren la estimulación continua durante al menos algunas horas para la final inducción de la activación, tal como la producción de citoquinas y proliferación [246].

Justificación y objetivos

Dada la gran implicación de CD38 en enfermedades tales como la leucemia linfocítica crónica, SIDA, LES… nos planteamos el estudio de la localización de la proteína CD38 en microdominios de membrana del linfocito T y su función en la sinapsis inmunológica.

Los objetivos que nos planteamos para esta tesis son los siguientes:

1. Estudiar la distribución de CD38 en la membrana plasmática del linfocito T.
2. Analizar la composición proteica de los microdominios de membrana (*rafts*) en los que se localiza CD38 y su posible asociación a otras proteínas señalizadotas.
3. Identificar las proteínas que son fosforiladas y traslocadas a los *rafts* cuando se estimula el linfocito T a través de CD38.
4. Estudiar donde se localiza CD38 en la sinapsis inmunológica (linfocito T:APC).
5. Papel funcional de CD38 en la sinapsis inmunológica.

Discusión

En trabajos anteriores de nuestro laboratorio hemos demostrado que CD38 está asociado a los *rafts* en células T. Sin embargo se conoce poco sobre la composición en proteínas de estas balsas lipídicas que contienen CD38 y si existen interacciones específicas entre CD38 y las proteínas señalizadoras asociadas a los *rafts*. Mediante el uso de anticuerpos específicos unidos a proteína G y bolitas magnéticas (μMACS), hemos analizado el patrón de distribución de CD38, Lck, LAT, CD3-ζ y CD3-ε en *rafts* de células T Jurkat. En este estudio demostramos que CD38 está concentrado en un tipo de *raft* con relativos altos niveles de Lck y CD3-ζ, mientras que CD3-ε y LAT son débilmente detectados. Además, las subunidades CD3-ζ y CD3-ε parecen estar concentradas en un tipo de *rafts* enriquecido en Lck y menor contenido de LAT. Así, el patrón de distribución de estas moléculas en los CD3-ε *rafts* es muy similar al de los inmunoaislados realizados en una línea T murina [251].

Por otra parte, los Lck *rafts* recuperan todas las moléculas analizadas, mientras que los LAT *rafts* están altamente enriquecidos en Lck, mostrando niveles intermedios de CD3-ζ y CD3-ε y bajos niveles de CD38.

Datos recientes sugieren que LAT y Lck pueden residir en *rafts* separados en linfoblastos T humanos [252]. En este artículo se describe que la estimulación a través del TCR induce la colocalización de LAT y Lck en microdominios de 50-100 nm lo cual sugiere que en estas células, la coalescencia de rafts que contienen Lck y LAT requiere de la activación de la célula T. En cambio, los resultados presentados en esta tesis demuestran que, en células T Jurkat sin estimular, existen tipos de rafts que contienen Lck, LAT y el complejo TCR-CD3. Además, otros estudios [202] muestran la selectiva interacción de LAT con la forma activa (abierta) de Lck en los *rafts* lipídicos de las células T Jurkat, mientras que tal interacción en la fracción soluble es mínima. Todos estos datos juntos sugieren que en células T normales, la asociación de LAT con los *rafts* que contienen Lck está regulada por la señalización del TCR, mientras que en células T Jurkat hay una asociación constitutiva de estas proteínas en el mismo tipo de *rafts*, lo cual puede explicar por qué en estas células, las señales generadas por el TCR son amplificadas más rápidamente que en células T en reposo.

Dentro de estas unidades, algunos de estos complejos proteicos son muy sensibles a la disgregación de los *rafts*, lo cual sugiere unas interacciones débiles y muy dinámicas,

implicando interacciones proteína-proteína y proteína-lípido. Así el tratamiento de las vesículas de rafts de membrana con octil-glucósido (ODG) causa la disociación de LAT de los inmunoprecipitados de CD3-ζ y CD3-ε. Además el ODG causa la disociación de Lck de los inmunoprecipitados de CD38 y la completa pérdida de CD38 de los inmunoprecipitados de Lck. Estos resultados pueden explicar la disociación selectiva de LAT y CD38 de las vesículas de *rafts* de membrana por el ODG, mientras que Lck, CD3-ζ, y CD3-ε permanecen asociadas a ellas. En este sentido se ha publicado un artículo en células T de ratón en el que CD38 y Lck pueden interaccionar directamente a través del dominio citoplasmático de CD38 y el dominio SH2 de Lck [253]. Interesantemente, tal interacción tiene lugar en células solubilizadas en un buffer de lisis que contiene 1% de digitonina, el cual es un detergente que preserva las interacciones proteína-lipid *raft* [254].

Otros complejos proteicos se mantienen bien, incluso utilizando el ODG para solubilizar los *rafts*, lo cual sugiere que primeramente ocurre una interacción vía proteína-proteína. Así, las asociaciones de Lck con CD3-ζ o CD3-ε son relativamente mantenidas en presencia de ODG y se detectan independientemente del anticuerpo usado para la inmunoprecipitación (por ejemplo: anti-Lck, anti-CD3-ζ, anti-CD3-ε).

Otras proteínas ensambladas, lo cual probablemente tenga lugar vía interacciones proteína-proteína, es la asociación de CD38 con CD3-ζ. Así, en los inmunoprecipitados con anti-CD38 de fracciones *rafts* hay una proporción similar de CD3-ζ que permanece asociado a CD38 independientemente de la presencia o ausencia de ODG. Además, la asociación de CD38 con CD3-ζ es encontrada en ambas fracciones rafts y soluble de células deficientes en Lck, lo cual demuestra que las interacciones CD38-CD3-ζ pueden ocurrir independientemente de otros componentes que haya en los *rafts*. Sin embargo, en células T Jurkat hay claras diferencias en la expresión en superficie de CD38 y de las subunidades CD3, además de diferencias en la proporción de cada molécula que participa en los rafts, lo cual influye en la estequiometría de los complejos CD38-CD3-ζ dentro de los *rafts* o fuera de ellos. El resultado indica que los cambios de expresión en superficie de CD38, CD3-ζ o ambas pueden afectar al número de complejos CD38-CD3-ζ, lo cual puede afectar al umbral que es requerido para iniciar la señalización transmembrana a través de CD38.

La estimulación a través de CD38 induce la fosforilación de Lck, LAT, ZAP-70 y p55PI3K dentro de los *rafts*. Además, la completa fosforilación de CD3-ζ y CD3-ε ocurre sólo en los rafts de membrana, a juzgar por el aparente peso molecular de las diferentes formas de CD3-ζ

fosforilado (23 y 21 kDa) y las formas de CD3-ε detectadas en inmunoprecipitados con anti-fosfotirosina (pTyr). Las formas de 21 y 23 kDa de CD3-ζ pueden contribuir a la supervivencia de la célula T y a la respuesta de la célula T frente a patógenos tales como bacterias y virus [255]. Estos datos sugieren que la activación de la señalización iniciada en los CD38 *rafts* es rápidamente propagada a otros compartimentos *rafts*, donde la maquinaria de amplificación de la señal está presente (por ejemplo *rafts* enriquecidos en LAT).

La fosforilación en tirosina mediada por CD38 de CD3-ζ, CD3-ε, ZAP-70 y LAT puede relacionarse funcionalmente con la traslocación de Sos y la subsiguiente activación de N-Ras en los rafts. En la señalización a través del TCR, la fosforilación en tirosina de LAT (asociada a *raft*) por ZAP-70 puede resultar en un intercambio de Sos entre los complejos ZAP-70-Grb2-Sos y LAT-Grb2-Sos [256]. Un modelo similar es compatible con nuestras observaciones en células T Jurkat, donde la estimulación a través de CD38 induce la fosforilación en tirosina de ZAP-70 y LAT, el reclutamiento de Sos por fosfo-LAT (Fig. 6A, Paper JBC 2003) y la unión de Sos a los rafts (Fig. 5 Paper JBC 2003). De esta forma, la ruta que conduce desde CD38 (a través de Ras) hasta Erk requiere de la formación de un complejo de señalización formado por TCR-CD3 [169], Lck [177], ZAP-70 [172, 177] y LAT. En este modelo, la fosforilación en tirosina de ZAP-70 y LAT parece ser esencial para la traslocación de Sos a los rafts que contienen Ras, tras la estimulación a través de CD38. Así, la formación de complejos señalizadores funcionales es estabilizada por interacciones proteína-lipid *raft* pero también requiere interacciones dependientes de fosforilación en tirosina [178, 249, 257].

En células T de ratón, donde la fosforilación en tirosina de LAT mediada por CD38 es más débil que en células T Jurkat, pensamos que el adaptador Shc puede jugar un papel crucial [172]. En este sentido, Shc aparece en los rafts tras la activación a través de TCR [185], y la unión de Shc a los *rafts* permite una activación constitutiva de la ruta de señalización Ras/Erk y un aumento en la señalización del TCR [258].

La diferente microlocalización de las distintas isoformas de Ras tiene importantes consecuencias en las interacciones y activación de rutas por debajo de Ras [259]. En membranas de células preparadas bajo condiciones libres de detergente, H-Ras doblemente palmitoilado se localiza en ambos microdominios (*rafts* y soluble), mientras que K-Ras está presente predominantemente en la fracción soluble [259-261]. La estimulación a través de CD38 con un

anticuerpo anti-CD38 causa la activación de N-Ras dentro de los *rafts* resistentes a Brij 98 (Fig. 7 Paper JBC 2003) y no en las fracciones solubles. Sin embargo, la mayor parte de la activación de Erk ocurre en las fracciones no-raft (Fig. 4 Paper JBC 2003) y la disrupción de las interacciones mediante tratamiento con metil-β-ciclodextrina estimula fuertemente la activación de Erk mediada por CD38 [172]. Así, la asociación con *rafts* de membrana puede estar implicada en los primeros pasos que permiten la activación de Ras/Erk, pero los *rafts* no constituyen el sitio final de activación de esta ruta de señalización.

En células T Jurkat, la subunidad reguladora p85α de la PI3K es traslocada a los *rafts* después de la estimulación a través de CD38, mientras que la isoforma p85β está presente en los *rafts* constitutivamente. Además, la fosforilación en tirosina de la isoforma p55α estaba presente en los *rafts* y llegaba a incrementarse la fosforilación en tirosina bajo la ligación de CD38. Como CD3-ζ y CD3-ε son fosforilados en tirosina tras la estimulación a través de CD38 [169, 172] y estas proteínas pueden interaccionar de forma fosforilación-dependiente con p85α PI3K [172, 262, 263], pueden unir PI3K a los *rafts*. Incluso, la unión de PI3K al TCR/CD3 *per se* puede *up* regular la actividad PI3K [262, 263], probablemente por cambio conformacional como se describió previamente para otras proteínas que se unen a p85 [264, 265].

Otras moléculas candidatas son LAT, Shc y Cbl. Estas moléculas se unen a p85 [266] y son fosforiladas en tirosina tras la estimulación a través de CD38 (Figs. 4 y 6) [169, 172, 177]. Un proceso inicial puede ocurrir con moléculas tales como CD3-ζ y CD3-ε, mientras que LAT o Shc pueden ser responsables de mantener o amplificar la activación de PI3K. Ambos eventos son muy importantes para la generación de $PI(3,4,5)P_3$ después de la ligación de CD38. Estas interacciones con los *rafts* lipídicos parecen ser funcionalmente significativos, porque en un estudio previo demostramos que la disrupción de los dominios rafts con metil-β-ciclodextrina previene la activación de PI3K/Akt mediada por CD38 [172].

Por el contrario, c-Cbl, el cual en células B está relacionado con la inhibición del crecimiento celular mediado por CD38 [267], llega a ser fosforilado en tirosina exclusivamente en los compartimentos no-*raft.* La parcial fosforilación de CD3-ζ, el cual ha sido correlacionado con una parcial señalización del TCR [268], es además encontrada en la fracción no-*raft* de la membrana plasmática. En la fracción no-*raft*, la pequeña cantidad de Lck detectada no está asociada a CD38, lo cual puede explicar por qué la completa fosforilación de CD3-ζ no puede ocurrir tras la estimulación a través de CD38.

De esta forma, el CD38 presente en la fracción soluble (no-*raft*) puede estar implicado en la iniciación de señales inhibidoras como la fosforilación en tirosina de c-Cbl y la parcial

fosforilación en tirosina de CD3-ζ, aunque no podemos descartar que la ligación de CD38 dentro de los rafts pueda regular la segregación lateral de moléculas inhibidoras de la señalización desde los rafts a los compartimentos no-*raft*. De cualquier forma, la segregación lateral de moléculas activadoras de la señalización desde los *rafts* a sitios no-*raft* parece que ocurre más tarde, porque la activación de Erk es detectada en cualquier sitio fuera de los *rafts* lipídicos.

En resumen, este estudio nos da nuevos conocimientos sobre los mecanismos a través de los cuales CD38 puede transducir señales dentro de la célula, demostrando que hay 2 *pooles* de CD38, los cuales difieren en su localización en microdominios, proteínas asociadas y diferente rendimiento.

Dentro del trabajo realizado para estudiar CD38 en la sinapsis inmunológica observamos que, en células T, CD38 aparece en 2 pooles celulares diferentes, uno en la membrana plasmática y otro en compartimentos intracelulares y que ambos se redistribuyen hacia la sinapsis inmunológica (SI) tras la estimulación del TCR. CD38-GFP intracelular tiene una distribución similar al de CD3-ζ, o CD71 endógeno intracelular, los cuales están presentes en endosomas de reciclamiento y son reclutados hacia la SI formada entre la célula B y la célula presentadora del antígeno (APC) (SEE). Está descrito el reclutamiento a la SI madura de los endosomas de reciclamiento que contienen CD3-ζ, Lck, LAT, y el receptor de transferrina [269-272].

El reclutamiento del contenido de endosomas de reciclamiento hacia la SI madura ha sido previamente descrito [269-272]. En este sentido, en células T humanas estimuladas con anticuerpos anti-CD38 se induce la internalización de CD38 y por tanto su localización en endosomas tempranos y tardíos [105], procesos que pueden ser ligados al incremento de la fosforilación en tirosina de c-Cbl tras la estimulación a través de CD38 [177, 273]. Además, está descrito, en monocitos humanos, que anticuerpos monoclonales anti-CD38 inducen la internalización, shedding y nueva expresión de CD38 en la superficie de la célula [274]. Éste CD38 nuevo deriva del CD38 preformado en el pool intracelular o del CD38 de superficie que ha sido internalizado y devuelto de nuevo a la membrana de la célula [274]. Así, al igual que ocurre con CD3-ζ [270], es como si el CD38 intracelular debiera reciclarse de nuevo a la membrana plasmática, suministrando una fuente adicional de esta proteína a la sinapsis madura.

La presencia de vesículas intracelulares que contienen CD38 cerca de la SI puede tener consecuencias funcionales debido a la intrínseca actividad enzimática de CD38, el cual cataliza la formación de ADPRc a partir de NAD^+. El ADPRc abre canales de Ca^{2+}, activando receptores de ryanodina tipo 2 y 3 y además induce la entrada de Ca^{2+} extracelular vía activación de la capacidad de entrada del Ca^{2+} y/o la activación de un canal catiónico TRPM2 en conjunción con ADPRc [275]. TRPM2 es un canal permeable a cationes Ca^{2+} expresado en la membrana plasmática de diferentes tipos celulares tales como linfocitos T, neutrófilos, granulocitos, monocitos y células microgliales. TRPM2 es activado por la unión de ADPR redistribución de CD38 de membrana en la SI, con el dominio extracelular hacia la APC, abre la posibilidad de la producción de ADPRc (mediada por CD38) fuera de la célula y que pueda concentrarse en una pequeña área en la superficie de la célula T. La liberación de NAD^+ del citosol al espacio extracelular (revisado en [139]) y la siguiente producción de ADPRc catalizado por el CD38 acumulado en la SI podría establecer una relativa alta concentración de este metabolito en el espacio sináptico. La traslocación del ADPRc (generado in situ) al interior de la célula, vía CD38 o por transportadores de nucleósidos [139] puede permitir la estimulación preferencial de la APC o de la propia célula T. Sin embargo, nuestros resultados sugieren que hay un aumento de la actividad de CD38 tras el contacto célula T:APC, independiente de antígeno. Así, este efecto fue solamente estabilizado cuando las células T expresaban altos niveles de CD38 en su superficie (por ejemplo J77 CD38-GFP^+, $CD38^{high}$) y no en células T con baja expresión de CD38 (J77 pEGFP-C1, $CD38^{normal}$), a pesar de que el número de moléculas expresado en la superficie de las células B (Raji) era claramente superior a las expresadas en las células T transfectadas. Además, la introducción del paso de centrifugación a favor de la formación de los conjugados, parecía ser crucial para ver las diferencias en la actividad enzimática de CD38, sugiriendo que el contacto célula-célula era requerido para este proceso.

Está sin demostrar si el incremento de la actividad ectoenzimática tiene algún efecto en la activación de la célula T, sin embargo, la sobreexpresión de CD38 ($CD38^{high}$) tenía mayor nivel basal de Ca^{2+} citosólico que su homólogo $CD38^{normal}$, lo cual parecía deberse al incremento del ADPRc intracelular como ocurre en fibroblastos 3T3 murinos transfectados con CD38 [136]. Además, en células T $CD38^{high}$ había un incremento más potente y mantenido de Ca^{2+} citosólico

en respuesta a estimulación por superantígeno que en células T Jurkat $CD38^{normal}$. También observamos un incremento en la fosforilación en tirosina de PLC-γ1. Así, hay una relación entre el incremento de la expresión de CD38 y la señalización mantenida de calcio de células T estimuladas con antígeno. Sin embargo, la sobreexpresión de CD38 tenía un poco efecto en la producción de IL-2 tras estimulación con superantígeno, al menos a las concentraciones de SEE usadas en este estudio. Es importante destacar que Bueno y colaboradores [276] han descrito recientemente que los superantígenos de bacterias pueden activar células T por rutas alternativas, evitando así los eventos de fosforilación dependientes de la tirosina quinasa Lck, activando en su lugar una ruta mediada por PLC-β dependiente de Gα11, la cual no ha sido estudiada en nuestro laboratorio.

Otro punto estudiado fue si la sobreexpresión de CD38 podía modular otros procesos en células T como son proliferación, apoptosis o supervivencia celular. En este sentido, se ha observado, en otros tipos celulares, un incremento potencial en la supervivencia de las células $CD38^+$ comparadas con sus homólogas $CD38^-$ [83, 97]. Además, el ADPRc añadido exógenamente o producido por células $CD38^+$, inducen movilización intracelular de calcio, proliferación de progenitores hematopoyéticos humanos [277], y la expansión *in vivo* de células stem hematopoyéticas [277]. Es importante señalizar que, además de la actividad ciclasa de membrana debida a CD38, se ha descrito una ADP-ribosil ciclasa citosólica (aún sin identificar) en células T Jurkat y linfocitos T de sangre periférica [144, 278]. Esta ciclasa citosólica, o el CD38 intracelular localizado en endosomas de reciclamiento, el cual se acumula en la SI, podrían ser también candidatos de inducir el aumento de la cantidad de ADPRc en respuesta de las células T a la interacción con el antígeno presentado por las APC. En este último caso, los mecanismos para el transporte del NAD^+ hacia el interior de los endosomas y la consiguiente liberación de ADPRc al citosol debería estar completamente en funcionamiento [139]. En este sentido, se ha descrito la producción polarizada de NO en la SI, con un papel modulador basado en la señalización dirigida por TCR [279]. La liberación de NO en la SI requiere del aumento de Ca^{2+} intracelular [279] y aunque no ha sido objeto de este estudio, es muy probable que este incremento del Ca^{2+} intracelular dirigido por antígeno y la siguiente respuesta del NO, esté principalmente mediada por ADPRc como así ocurre en otros tipos de células [280].

Para resolver la cuestión de cómo CD38 puede contribuir a la señalización en la célula T en células T estimuladas con antígeno, investigamos el impacto de bloquear CD38 con un anticuerpo monoclonal anti-CD38, IB6, el cual actúa como un no-agonista en la mayoría de los ensayos funcionales probados [77]. Nuestro datos muestran que el bloqueo de CD38 afecta a la cinética de fosforilación, inducida por antígeno, de LAT en el residuo Tyr^{191}, resulta en la inhibición de la fosforilación de PKCθ en la Thr^{538} a niveles basales y parcial aunque significativa inhibición de la producción de IFN-γ. Sin embargo, la fosforilación de Erk en la Thr^{202} y Tyr^{204} no se afectaba. Usando otro anticuerpo monoclonal no-agonista anti-CD38, HB136, también se afectaba la producción de IFN-γ inducida por antígeno. Puesto que las células APC usadas en estos experimentos (Raji) eran CD31 prácticamente negativas, es improbable que el anticuerpo anti-CD38 usado pudiera afectar la interacción CD38/CD31, aunque podrían afectar a la interacción de CD38 con otro ligando, aún no conocido, expresado por las APC.

CD38 se acumula primeramente en toda la zona de contacto entre la célula T y la APC y más tarde se sitúa en la zona mas periférica, colocalizando con moléculas de adhesión como ICAM-3 (Fig.1 Paper J. Immunol.) [226]. Éste patrón de acumulación es también parecido al de Lck, el cual aparece también en la periferia de la sinapsis (pSMAC) tras una acumulación inicial en el cSMAC [272]. En este sentido, usando la línea celular JCaM 1.6, la cual tiene Lck no funcional, hemos visto que la proporción de conjugados que muestran sinapsis madura y/o CD38 traslocado a la interfaz entre la célula T y la APC, es muy reducido si se compara con las células T Jurkat. Otra característica de las células JCaM 1.6 es que la señalización mediada por CD38 es defectuosa [177]. Comprobamos que las tirosin-quinasas de la familia Src eran requeridas para la relocalización de CD38 ya que células T Jurkat tratadas con el inhibidor de la familia Src PP2 mostraban menor acumulación de CD38 en la SI. Estos resultado están en acuerdo con trabajos previos [281] que muestran defectos en la formación de conjugados de las células JCaM1.6, o células T Jurkat tratadas con PP2 y fallo en el reclutamiento de F-actina y LFA-1 al sitio de contacto célula T:APC. Además, las células T Jurkat presentan alta cantidad de ezrina, un miembro de la familia ezrina-radixina-moesina, en las protusiones de membrana (altamente enriquecidas en F-actina) en el pSMAC, mientras que las células JCaM 1.6 muestran

poca acumulación [282]. Por lo tanto, nuestros resultados sugieren que la redistribución de CD38 hacia la SI depende fuertemente de los eventos tempranos de señalización mediados por Lck que permiten la polimerización de actina y remodelación.

La formación de dominios de membrana condensados, lo cual biofísicamente refleja acumulación de *rafts* de membrana, es detectado primero en la región central y más tarde en la periferia de la SI productiva [283]. Así, la redistribución de CD38 y Lck, los cuales son proteínas asociadas a *rafts*, a sitios periféricos de la SI puede además estar unido a la dinámica de condensación de la membrana plasmática que muestra la célula T en el sitio de activación, mientras que CD3-ζ permanece en el cSMAC. Está estudiado [272] que diferentes patrones de acumulación de CD3-ζ y Lck no reflejan necesariamente una absoluta segregación molecular, más bien cambios en la distribución relativa de estas moléculas, lo cual podría tener un efecto sustancial en las señales transducidas por ellas. En apoyo a este concepto, nuestros datos muestran que, en células T Jurkat , donde CD38, Lck y CD3-ζ están asociados en un tipo de *rafts*, la estimulación a través de CD38 resulta en la activación de señales tales como la completa fosforilación de los ITAM de CD3-ζ y CD3-ε, activación de Ras y traslocación a los *rafts* de los componentes de señalización Sos y p85 PI-3 quinasa (1ª parte de esta tesis). Por el contrario, en los microdominios no-*raft* (fracción soluble), donde CD38 está asociado con CD3-ζ pero no con Lck, la estimulación a través de CD38 resulta en señales inhibidoras tales como la parcial fosforilación de CD3-ζ y CD3-ε y una fuerte fosforilación de c-Cbl. Es como si la reorganización de CD38 y Lck a sitios más periféricos de la sinapsis madura, lejos de CD3-ζ, pudiera generar diferentes o reducidas señales que aquellas que se observan inmediatamente después de la unión del linfocito T con la APC, justo cuando las tres moléculas están asociadas en el mismo tipo de *raft* y los eventos de señalización temprana están tomando lugar [272] por la formación activa de microclusters que contienen TCR [284, 285]. Interesantemente, las señales próximas al TCR son mantenidas en microclusters periféricos y terminadas en el cSMAC [286], así la localización de CD38 en la periferia de la SI podría estar relacionada con estas capacidades de señalización. Además, el efecto del bloqueo con anticuerpos anti-CD38 estaría ejerciendo en contra de eventos de señalización que ocurren antes de la maduración de la sinapsis. Así mismo, la principal función observada en células T en las que CD38 está

sobreexpresado tiene que ver con la movilización de calcio que es iniciada inmediatamente después de la formación del conjugado linfocito T:APC.

En una pequeña, pero significativa, proporción de conjugados célula T/APC formados con células B Raji transfectadas con CD38-GFP y preincubadas con SEE, el CD38-GFP de las células Raji se acumula a lo largo de la zona de contacto entre la célula T/APC. En muchos de estos conjugados se observó también la traslocación de CD31, sugiriendo un reclutamiento activo causado por la interacción ligando-receptor. CD31 contiene ITIMs funcionales dentro de su dominio citoplasmático y la co-ligación de CD31 con el TCR resulta en una fosforilación en las tirosinas de los ITIMs dependiente de Lck, reclutamiento de SHP-2 (proteín-tirosín-fosfatasa que contiene dominio SH2) y atenuación de la señalización celular mediada por TCR [287]. Nuestros datos son la primera evidencia fisiológica de que CD31 podría estar en la proximidad del TCR tras activación del linfocito T mediada por antígeno sin forzar artificialmente tal interacción con anticuerpos monoclonales específicos.

La regulación negativa que ejerce Lck en la activación de la célula T inducida por SEE [276] es consistente con el requerimiento de Lck para la fosforilación en tirosina de CD31 en respuesta a la activación del TCR [287]. Esto parece probable ya que la proximidad de CD31 al TCR y Lck en la SI podría favorecer la función inhibitoria que CD31 juega en la activación del linfocito T. Si CD38 en las APCs está implicado en el reclutamiento de CD31 a la SI requiere más investigación.

La relocalización, en las APCs, de las moléculas MHC-II en balsas lipídicas o en microdominios que contienen tetraspaninas hacia la SI ha sido implicada en una óptima presentación del péptido y en activación del linfocito T [288, 289]. Cambios dinámicos en estas asociaciones moleculares, tales como el reclutamiento de otras moléculas de superficie y/o de señalización, pueden ocurrir durante la formación y establecimiento de sinapsis. Así, la unión de ICAM-3, e ICAM-1 en menor grado, a LFA-1 expresado por células dendríticas (DCs) maduras, induce relocalización de MHC-II hacia la SI [290].

Se ha descrito, en monocitos, la asociación de CD38 con moléculas MHC de clase II y la tetraspanina CD9 en *rafts* lipídicos [291], así como con la tetraspanina CD81 en DCs maduras [97]. CD81 está presente en células B Raji y es activamente reclutado a la SI tras la

estimulación con antígeno [223]. Por otro lado, en células B Raji hay una gran proporción de CD38 localizado en *rafts* (datos del laboratorio). La presencia simultánea de los complejos MHC clase II con antígeno, tetraspaninas y moléculas moduladoras así como CD38, en microdominios físicamente distinguibles en la superficie de la APC es probable que influya en la capacidad de las APCs de estimular células T antígeno específicas.

En este sentido, CD38 expresado en monocitos parece tener un papel en la transducción de señales implicadas en la activación del linfocito T inducida por antígeno, operando en sinergia con MHC clase II [292]. Además, la señalización mediada por CD38 y su localización en *rafts* lipídicos es requerida para la migración, supervivencia y polarización hacia respuestas Th1 de las DCs maduras [97]. De esta forma, la relocalización de CD38 a la SI y la contribución de ambas, célula T y APC, a este fenómeno suguiere que CD38 puede jugar un papel importante durante la presentación antigénica.

Conclusiones

1. El aislamiento y caracterización de los microdominios de membrana insolubles en Brij-98 que contienen CD38 de linfocitos T Jurkat nos ha llevado a distinguir 3 tipos de rafts:
   Rafts CD38: enriquecidos en CD38, CD3-ζ y Lck.
   Rafts TCR/CD3: enriquecidos en CD3-ζ, CD3-ε y Lck.
   Rafts LAT: enriquecidos principalmente en Lck.
   CD38 en los rafts es capaz de iniciar y propagar algunas rutas de señalización activadoras, posiblemente para facilitar las asociaciones críticas dentro de otros tipos de rafts, por ejemplo, los LAT raft a través de su capacidad de interaccionar con Lck y CD3-ζ.

2. La estimulación de linfocitos T Jurkat a través de CD38 conlleva a la fosforilación en tirosina de Lck, LAT y la completa fosforilación de CD3-ζ y CD3-ε y esto ocurre exclusivamente en los rafts. Además también se induce la activación de Ras en los microdominios de membrana. Por el contrario, la fosforilación en tirosina de c-Cbl ocurre exclusivamente en la fracción soluble.

3. Tras la estimulación de linfocitos T a través de CD38 hay un reclutamiento de Sos y la subunidad reguladora p85α de la PI3K a los rafts de membrana. La proteína Sos es reclutada para la fosforilación en tirosina de LAT y la proteína SLP-76 también es reclutada para dicho fin.

4. CD38 se localiza en la sinapsis inmunológica madura en conjugados célula T:célula B. En estos conjugados, CD38 se distribuye en toda la zona de contacto T:B, lo cual difiere claramente de la distribución de CD3-ζ, el cual típicamente se localiza en el cSMAC de la sinapsis. En linfocitos T y B transfectados con la construcción CD38-GFP hemos observado que, son los linfocitos T las células que más contribuyen a que CD38 se localice en la sinapsis inmunológica madura. Además, para el reclutamiento de CD38 en la sinapsis serían necesarios eventos de señalización en los que estaría implicado Lck.

5. En células T y B transfectadas con la construcción CD38-GFP, CD38 se distribuye en la membrana plasmática del linfocito y en compartimentos intracelulares, comportándose como CD3-ζ. El CD38 que se localiza en estos compartimentos intracelulares (endosomas de reciclamiento y aparato de Golgi) se redistribuye hacia la zona de contacto célula T:célulaB.

6. Al sobreexpresar CD38 en linfocitos T Jurkat y ponerlos en presencia de linfocitos B (mediante un spin se favorece este contacto T:B), se observa un aumento en la actividad ciclasa en los primeros 20 minutos de contacto. A partir de este tiempo no se observan cambios notables.

7. Al sobreexpresar CD38 en linfocitos T Jurkat no se observa movilización intracelular de calcio. La sobreexpresion de CD38 en linfocitos T Jurkat aumenta la movilización de calcio dependiente de TCR de una forma dependiente de célula presentadora y de antígeno si la formación de los conjugados entre célula T y célula B está favorecida por una breve centrifugación.

8. El bloqueo de CD38 mediante el uso del anticuerpo monoclonal anti-CD38, IB6, modifica la cinética de fosforilación de sustratos como LAT y PKC-θ, mientras que Erk apenas se altera. Además, hay una parcial, pero significativa, inhibición de la producción de IFN-γ.

Perspectivas

Este trabajo resuelve algunos aspectos muy interesantes de CD38 pero como suele suceder, cuanto más se conoce algo, más puertas a nuevas cuestiones se abren. Ya sabemos que CD38 se localiza en *rafts* de la membrana plasmática del linfocito T y que está asociado a diversas proteínas por lo que es posible estimular a través de CD38, pero aún desconocemos qué mecanismos están implicados en la movilización de las proteínas a los rafts, cómo son los mecanismos de regulación... Ensamblar todas las piezas para conocer cómo es la ruta de señalización de CD38 como receptor es el objetivo final.

Además, esta tesis abre camino a la investigación de CD38 en la sinapsis inmunológica. La tarea no es fácil porque esta proteína tiene doble función: como enzima y como receptor, ambas independientes una de la otra, por lo que su función en la sinapsis debe investigarse en profundidad.

"No basta dar pasos que puedan conducir hasta la meta, sino que cada paso sea una meta, sin dejar de ser un paso"

Johann Meter Eckerman

Referencias

1. Jackson, D.G., and Bell, J. I., *Isolation of a cDNA encoding the human CD38 (T10) molecule, a cell surface glycoprotein with an inusual discontinuous pattern of expresion during lymphocyte differentiation.* J. Immunol., 1990. **144**: p. 2811.
2. Terhorst, C., van Agthoven, A., Le Clair, K., Snow, P., Reinherz, E. L., and Schlossman, S. F., Cell, 1981. **23**: p. 771-780.
3. Funaro A., H.A.L., Calosso L., et al., *Identification and characterization of an active soluble form of human CD38 in normal and pathological fluids.* Int. Immunol., 1996. **8**: p. 1643-1650.
4. Cho Y. S., H.M.K., Choi Y. B., Yun Y., Shin J., and Kim U. H., *Direct interaction of the CD38 cytoplasmic tail and the Lck SH2 domain: CD38 transduces T cell activation signals through associated Lck.* J. Biol. Chem, 2000. **275**: p. 1685-1690.
5. Funaro, A., Ferrero, E., Mehta, K., and Malavasi, F., Chem. Immunol., 2000. **75**: p. 256-273.
6. Malavasi, F., Funaro, A., Roggero, S., Horenstein, A., Calosso, L., and Mehta, K., Immunology Today, 1994. **15**: p. 95-97.
7. Yamada, M., Mizuguchi, M., Otsuka, N., Ikeda, K. and Takahashi, H., *Ultrastructural localization of CD38 immunoreactivity in rat brain.* Brain Res., 1997. **756**: p. 52-60.
8. Sun, L., Adebanjo, O. A., Koval, A., Anandatheerthavarada, H. K., Iqbal, J., Wu, X. Y., Moonga, B. S., Wu, X. B., Biswas, G., Bevis, P. J., Kumegawa, M., Epstein, S., Huang, C. L., Avadhani, N. G., Abe, E., and Zaidi, M., *A novel mechanism for coupling cellular intermediary metabolism to cytosolic Ca^{2+} signaling via CD38/ADP-ribosyl cyclase, a putative intracellular NAD^{+} sensor.* FASEB J., 2002. **16**: p. 302-314.
9. Adebanjo, O.A., et al., *A new function for CD38/ADP-ribosyl cyclase in nuclear Ca^{2+} homeostasis.* Nature Cell Biol., 1999. **1**: p. 409-414.
10. Khoo, K.M., et al., *Localization of the cyclic ADP-ribose-dependent calcium signaling pathway in hepatocyte nucleus.* J. Biol. Chem., 2000. **275**: p. 24807-24817.
11. Yalcintepe, L., et al., *Nuclear CD38 in retinoic acid-induced HL-60 cells.* Exper. Cell. Res., 2005. **303**: p. 14-21.
12. Sun, L., Adebanjo, O. A., Moonga, B. S., Corisdeo, S., Anandatheerthavarada, H. K., Biswas, G., Arakawa, T., Hakeda, Y., Koval, A., Sodam, B., Bevis, P. J., Moser, A. J., Lai, F. A., Epstein, S., Troen, B. R., Kumegawa, M., and Zaidi, M., *CD38/ADP-ribosyl cyclase. A new role in the regulation of osteoclastic bone resorption.* J. Cell. Biol., 1999. **146**: p. 1161-1172.
13. Funaro A., S.G.C., Ausiello C. M., Alessio M., Roggero S., Delia D., Zaccolo M., and Malavasi F. , *Involvement of the multilineage CD38 molecule in a unique pathway of cell activation and proliferation.* . J. Immunol., 1990. **145**: p. 2390.
14. Malavasi F., F.A., Alessio M., De Monte L. B., Ausiello C. M., Dianzani U., Lanza F., Magrini M., Momo M., and Roggero S., *CD38: a multilineage cell activation molecule with a split personality.* Int. J. Clin. Lab. Res., 1992. **22**: p. 73.
15. Ausiello, C.M., la Sala A., Ramoni C., Urbani F., Funaro A., and Malavasi F., *Secretion of IFN-γ, IL-6, granulocyte-macrophage colony-stimulating factor and IL-10 citokynes after activation of human purified T lymphocytes upon CD38 ligation.* Cell. Immunol., 1996. **173**: p. 192.
16. Sandoval-Montes, C., and Santos-Argumedo, L., *CD38 is expressed selectively during the activation of a subset of mature T cells with reduced proliferation but improved potential to produce cytokines.* J. Leukoc. Biol., 2005. **77**(4): p. 513-521.

17. Kumagai M., C.-S.E., Murray D. J., Silvennoinen O., Murti K. G., Evans W. E., Malavasi F., and Campana D., *Ligation of CD38 supresses human B lymphopoiesis.* J. Exp. Med., 1995. **181**: p. 1101.
18. Zupo S., R.E., Dono M., Tamborelli G., Malavasi F., and Ferrarini M., *CD38 signaling by agonistic monoclonal antibody prevents apoptosis of human germinal center B cells.* Eur. J. Immunol., 1994. **24**: p. 1218.
19. Santos-Argumedo L., T.C., Preece G., Kirkham P. A., and Parkhouse R. M. E., *A molecule on the surface of murine B lymphocites mediating activation and protection from apoptosis via calcium channels.* J. Immunol., 1993. **151**: p. 3119.
20. Kirkham P. A., S.-A.L., Harnett M. M. and Parkhouse R. M. E., *Murine B cell activation via CD38 and protein tyrosine phosphorylation* . Immunology, 1994. **83**: p. 513.
21. Zubiaur M., I.M., Terhorst C., Malavasi F., and Sancho J., *CD38 ligation results in activation of the Raf-1/MAP kinase and the CD3-ζ/ZAP-70 signaling pathways in Jurkat T lymphocytes.* J. Immunol., 1997. **159**: p. 193-205.
22. Silvennoinen O., N.H., Kitanaka A., Kumagai M., Ito C., Malavasi F., Lin Q., Conley M. E., and Campana D., *CD38 signal transduction in human B cell precursors: rapid induction of tyrosine phosphorylation, activation of syk tyrosine kinase and phosphorylation of phospholipase C-γ and phosphatidylinositol 3-kinase.* J. Immunol., 1996. **156**: p. 100.
23. Santos-Argumedo L., L.F.E., Heath A. W., Solvason N., Wu W. W., Grimaldi J. C., Parkhouse R. M. E., and Howard M., *CD38 unresponsiveness of xid B cells implicates Bruton´s tyrosine kinase (btk) as a regulator of CD38 induced signal transduction.* Int. Immunol., 1995. **7**: p. 163.
24. Kikuchi Y., Y.T., Miyake K., Kimoto M., and Takatsu K., *CD38 ligation induces tyrosine phosphorilation of Bruton tyrosine kinase and enhanced expression of interleukin-5 receptor on α chain: synergistic effects with interleukin 5.* Proc. Natl. Acad. Sci. USA, 1995. **92**: p. 11814.
25. Dianzani U., F.A., DiFranco D., Garbarino G., Bragardo M., Redoglia V., Buonfiglio D., De Monte L. B., Pileri A., and Malavasi F., *Interaction between endothelium and $CD4^+$/$CD45RA^+$ lymphocytes: role of the human CD38 molecule.* J. Immunol., 1994. **153**: p. 952.
26. Nishina H., I.K., Takahashi K., Hoshino S., Ikeda K., and Katada T., *Cell surface antigen CD38 identified as ecto-enzyme of NAD glycohydrolase has hyaluronate-binding activity.* Biochem. Biophys. Res. Commun., 1994. **203**: p. 1318.
27. Savarino, A., Bottarel, F., Malavasi, F., and Dianzani, U., *Role of CD38 in HIV-1 infection: an epiphenomenon of T-cell activation or an active player in virus/host interactions?* . AIDS, 2000. **14**: p. 1079-1089.
28. Katz F., P.S., Parkar M., Schneider C., Sutherland R., Stanley K., Solomon E., and Greaves M., *Chromosome assignment of monoclonal antibody-defined determinants on human leukemic cells.* Eur. J. Immunol., 1983. **13**: p. 1008.
29. Nakagawara K., M.M., Takasawa S., Nata K., Takamura T., Berlova A., Tohgo A., Karasawa T., Yonekura H., Takeuchi T., and Okamoto H., *Assignment of CD38, the gene encoding human leukocyte antigen CD38 (ADP-ribosyl cyclas/cyclic ADP-ribose hydrolase), to chromosome 4p15.* Cytogenet. Cell. Genet., 1995. **69**: p. 38.
30. Harada N., S.-A.L., Chang R., Grimaldi J. C., Lund F. E., Brannan C. I., Copeland N. G., Jenkins N. A., Heath A. W., Parkhouse R. M. E., and Howard M., *Expression cloning of a cDNA encoding a novel murine B cell activation marker: homology to human CD38.* J. Immunol., 1993. **151**: p. 3111.

31. Malavasi, E.F.a.F., *Human CD38, a leukocyte receptor and ectoezyme, is a member of a novel eukariotic gene family of nicotinamide adenine dinucleotide^{+}-converting enzymes.* The Journal of Immunology, 1997. **159**: p. 3858-3865.
32. Ferrero E., S.F., and Malavasi F., *The human CD38 gene: polymorphism, CpG island and linkage to the CD157 (BST-1) gene.* Immunogenetics., 1999. **49**: p. 597-604.
33. Deaglio S., V.T., Aydin S., Ferrero E., and Malavasi F., *In-tandem insight from basic science combined with clinical research: CD38 as both marker and key component of the pathogenetic network underlying chronic lymphocytic leukemia.* Blood, 2006. **108**: p. 1135-1144.
34. Yagui, K., Shimada F, Mimura N, Hashimoto N, Suzuki, T.Y. Y, Nata K, Tohgo A, Ikehata I, Takasawa S,, and M.H. Okamoto H, Saito Y, Kanatsuka A: , *A missense mutation in the CD38 gene, a novel factor for insulin secretion: association with type II diabetes mellitus in Japanese subjects and evidence of abnormal function when expressed in vitro.* . Diabetologia, 1998. **41**: p. 1024.
35. González-Escribano, M.F., Aguilar, F., Torres, B., Sánchez-Román, J., and Núñez-Roldán, A., *CD38 polymorphisms in Spanish patients with systemic lupus erythematosus.* Hum. Immunol., 2004. **65**(6): p. 660-664.
36. Takasawa, S., Nata, K., Yonekura, H., and Okamoto, H., *Cyclic ADP-ribose in insulin secretion from pancreatic beta cells.* Science, 1993. **259**: p. 370-373.
37. Okamoto, H., Takasawa, S., and Nata, K. , *The CD38-cyclic ADP-ribose signalling system in insulin secretion: molecular basis and clinical implications.* Diabetologia, 1997. **40**: p. 1485-1491.
38. Takasawa, S., Akiyama, T., Nata, K., et al., *Cyclic ADP-ribose and inositol 1, 4, 5-triphosphate as alternate second messengers for intracellular Ca^{2+} mobilization in normal and diabetic β-cells* J Biol Chem, 1998. **273**: p. 2497-2500.
39. Tohgo, A., Munakata, H., Takasawa, S., Nata, K., Akiyama, T., Hayashi, N., y Okamoto, H., *Lysine 129 of CD38 (ADP-ribosyl cyclase/cyclic ADP-ribose hydrolase) participates in the binding of ATP to inhibit the cyclic ADP-ribose hydrolase.* J. Biol. Chem, 1997. **272**(7): p. 3879-3882.
40. Takasawa, S., Tohgo, A., Noguchi, N., Koguma, T., Nata, K., Sugimoto, T., Yonekura, H., and Okamoto, H., *Synthesis and hydrolisis of cyclic ADP-ribose by human leukocyte antigen CD38 and inhibition of the hydrolisis by ATP.* J. Biol. Chem, 1993. **268**: p. 26052-26054.
41. Koguma, T., Takasawa, S., Tohgo, A., et al., *Clonning and characterization of cDNA encoding rat ADP-ribosyl cyclase/cyclic ADP-ribose hydrolase (homologue to human CD38) from islets of Langerhans.* Biochim. Biophys. Acta, 1994. **1223**: p. 160-162.
42. Kato, I., Takasawa S., Akabane A., Tanaka O., Abe H., Takamura T., Suzuki Y., Nata K., Yonekura H., and Yoshimoto T., *Regulatory role of CD38 (ADP-ribosyl cyclase/cyclic ADP-ribose hydrolase) in insulin secretion by glucose in pancreatic beta cells. Enhanced insulin secretion in CD38-expressing transgenic mice.* J. Biol. Chem, 1995. **270**: p. 30045-30050.
43. Prasad, G.S., McRee, D. E., Stura, E. A., Levitt, D. G., Lee, H. C., and Stout, C. D., *Crystal structure of aplysia ADP ribosyl cyclase, a homologue of the bifunctional ectoenzyme CD38.* Nat. Struct. Biol. , 1996. **3**: p. 957-964.
44. Mallone, R., Ortolan, E., Baj, G., Funaro, A., Giunti, S., Lillaz, E., Saccucci, F., Cassader, M., Cavallo-Perin, P., and Malavasi, F., *Autoantibody response to CD38 in caucasian patients with type 1 and type 2 diabetes. Immunological and genetic characterization.* Diabetes, 2001. **50**: p. 752-762.
45. Fujimoto, W.Y., *Overview of noninsulin-dependent diabetes mellitus (NIDDM) in different population groups.* Diabet. Med., 1996. **13**(Suppl. 6): p. S7-S10.

46. Ferrero, E., Saccucci, F., and Malavasi, F., *The human CD38 gene: polymorphism, CpG island and linkage to the CD157 (BST-1) gene.* Immunogenetics., 1999. **49**: p. 597-604.
47. Pupilli, C., Giannini, S., Marchetti, P., Lupi, R., Antonelli, A., Malavasi, F., Takasawa, S., Okamoto, H., and Ferrannini. E., *Autoantibodies to CD38 (ADP-Ribosyl Cyclase/Cyclic ADP-Ribose Hydrolase) in caucasian patients with diabetes. Effects on insulin release from human islets.* Diabetes, 1999. **48**: p. 2309-2315.
48. Kaisho T., I.J., Oritani K., Inazawa J., Tomizawa H., Muraoka O, Ochi T., and Hirano T., *BST-1, a surface molecule of bone marrow stromal cell lines that facilitates pre-B-cell growth.* Proc. Natl. Acad. Sci USA, 1994. **91**: p. 5325-5329.
49. Prasad G. S., M.D.E., Stura E. A. Levitt D.G., Lee H. C., and Stout C. D., *Crystal structure of Aplysia ADP ribosyl cyclase, a homologue of the bifunctional ectoenzyme CD38.* Nat. Struct. Biol., 1996. **3**: p. 957-964.
50. Alessio M., R.S., Funaro A., De Monte L. B., Peruzzi L., Geuna M., and Malavasi F., *CD38 molecule: Structural and biochemical analysis of human T lymphocytes, thymocytes and plasma cells.* J. Immunol., 1990. **145**: p. 878-884.
51. Olugbenga A. Adebanjo, A.K., Baljit S. Moonga, Xue B. Wu, Shen Yao, Peter J.R. Bevis, Mayaoshi Kumegawa, Mone Zaidi and Li Sun., *Molecular cloning, expression and functional characterization of a novel member of the CD38 family of ADP-ribosyl cyclases.* Biochemical and Biophysycal Research Communications, 2000. **273**: p. 884-889.
52. Goodrich, S.P.e.a., *Production of calcium mobilizing metabolites by a novel member of the ADP-ribosyl cyclase family expressed in Schistosoma mansoni.* Biochemistry, 2005. **44**: p. 11082-11097.
53. Graeff, R.M., Mehta, K., Lee, H. C., *GDP-ribosyl cyclase activity as a measure of CD38 induction by retinoic acid in HL-60 cells.* Biochem. Biophys. Res. Commun., 1994. **205**: p. 722-727.
54. Graeff, R.M., Walseth, T. F., Hill, H. K., Lee, H. C., *Fluorescent analogs of cyclic ADP-rybose: synthesis, spetral characterization and use.* Biochemistry, 1996. **35**: p. 379-386.
55. Lee, H.C., Graeff R. M., and Walseth T. F., *Cyclic ADP-ribose and its metabolic enzymes.* Biochemie, 1995. **77**: p. 345-355.
56. Munshi, C., and Lee, H. C., *High-level expression of recombinant Aplysia ADP-ribosyl cyclase in Pichia Pastoris by fermentation.* . Prot. Express. Purif. , 1997. **11**: p. 104-110.
57. Prasad G. S., M.D.E., Stura E. A., Levitt D. G., Lee H. C., and Stout C. D., *Crystal structure of aplysia ADP ribosyl cyclase, a homologue of the bifunctional ectoenzyme CD38.* Nat. Struct. Biol. , 1996. **3**: p. 957-964.
58. Love M. L., S.D.M., Kriksunov I. A., Thiel D. J., Munshi C., Graeff R., Lee H. C., and Hao Q., *ADP-ribosyl cyclase; crystal structures reveal a covalent intermediate.* . Structure, 2004. **12**: p. 477-486.
59. Yamamoto-Katayama S., A.M., Ishihara K., Hirano T., Jingami H., and Morikawa K. , *Crystallographic studies on human BST-1/CD157 with ADP-ribosyl cyclase and NAD glycohydrolase activities.* J. Mol. Biol., 2002. **316**: p. 711-723.
60. Bruzzone S., G.L., Franco L., Zocchi E., Corte G., and De Flora A. , *Dimeric and tetrameric forms of catalytically active transmembrana CD38 in transfected HeLa cells.* . FEBS Lett., 1998. **433**: p. 275-278.
61. Moreno-García M. E., P.-S.S., Primack J., Sumoza-Toledo A., Muller-Steffner H., Schuber F., Oppenheimer N., Lund F. E., and Santos-Argumedo L. , *CD38 is expressed as noncovalently associated homodímeros on the surface of murine B lymphocytes.* Eur. J. Biochem. , 2004. **271**: p. 1025-1034.
62. Qun Liu, I., A. Kriksunov, Richard Graeff, Cyrus Munshi, Hon Cheung Lee, and Quan Hao. , Structure, 2005. **13**: p. 1331-1339.

63. Zubiaur M., F.O., Ferrero E., et al., *CD38 is associated with lipid rafts and upon receptor stimulation leads to Akt/protein kinase B and Erk activation in the absence of CD3-zeta immune receptor tyrosine-based activation motifs.* J. Biol. Chem, 2002. **277**: p. 13-22.
64. Graeff R., M.C., Aarhus R., Johns M., and Lee H. C., *A single residue at the active site of CD38 determines its NAD cyclizing and hydrolyzing activities.* The Journal of Biological Chemistry, 2001. **276**(15 Issue of April 13): p. 12169-12173.
65. Sauve A. A., D.H.T., Angeletti R. H., and Scharamm V. L. , *A covalent intermediate in CD38 is responsible for ADP-ribosylation and cyclation reactions.* . J. Am. Chem. Soc., 2000 **122**: p. 7855-7859.
66. Ghia P., G.G., Scielzo C., Geuna M., and Caligaris-Cappio F., *CD38 modifications in chronic lymphocytic leukemia: are they relevant?* Leukemia, 2004. **18**: p. 1733-1735.
67. During J., N.M., Schmucker U., Renzing-Kohler K., Holter T., Huttmann A., and Durhsen U., *CD38 expression is an important prognostic marker in chronic lymphocytic leukemia.* Leukemia, 2002. **16**: p. 30-35.
68. Thornton P. D., F.C., Giustolisi G. M., Morilla R., Atkinson S., A´Hern R. P., Matutes E., and Catovsky D., *CD38 expression as a prognostic indicator in chronic lymphocytic leukemia.* Hemato. J., 2004. **5**: p. 145-151.
69. Ho, H.N., Hultin, L.E., Mitsuyasu, R.T., et al., *Circulating HIV-specific $CD8^+$ cytotoxic T cells express CD38 and HLA-DR antigens.* J. Immunol., 1993. **150**: p. 3070-3079.
70. Autran B., C.G., Li T. S., Blanc C., Mathez D., Tubiana R., Katlama C., Debre p., and Leibowitch J., *Positive effects of combined antiretroviral therapy on CD4+ T cell homeostasis and function in advanced HIV disease.* Science, 1997. **277**: p. 112-116.
71. Roussanov B. V., T.J.M., and Giorgi J. V., *Calculation and use of an HIV-1 disease progression score.* AIDS, 2000. **14**: p. 2715-2722.
72. Vigano A., S.M., Rusconi S. Ferrante P. and Clerici M., *Expression of CD38 on CD8 T cells predicts maintenance of high viraemia in HAART-treated HIV-1-infected children.* Lancet, 1998. **352**: p. 1905-1906.
73. Savarino A., B.F., Calosso L., Feito M. J. Bensi T., Bragardo M., Rojo J. M., Pugliese A., Abbate I., Capobianchini M. R., et al., *Effects of the human CD38 glycoprotein on the early stages of the HIV-1 replication cycle.* FASEB J., 1999. **13**: p. 2265-2276.
74. Dianzani U., B.M., Buonfiglio D., Redoglia V., Funaro A., Portoles P., Rojo J., Malavasi F., and Pileri A., *Modulation of CD4 lateral interaction with lymphocyte surface molecules induced by HIV-1 gp120.* Eur. J. Immunol., 1995. **25**: p. 1306-1311.
75. Bofill, M., Mocroft, A., Lipman, M., et al., *Increased numbers of primed activated $CD8^+CD45RO^+$ T cells predict the decline of $CD4^+$ T cells in HIV-1-infected patients.* AIDS, 1996. **10**: p. 827-834.
76. Pavón, E.J., Muñoz, P., Navarro, M. C., Raya-Álvarez, E., Callejas-Rubio, J. L., Navarro-Pelayo, F., Ortego-Centeno, N., Sancho, J., and Zubiaur, M., *Increased association of CD38 with lipid rafts in T cells from patients with systemic lupus erythematosus and in activated normal T cells.* Mol. Immunol., 2006. **43(7)**: p. 1029-1039.
77. Ausiello, C.M., *Functional topography of discrete domains of human CD38.* Tissue Antigens, 2000. **56**: p. 539-547.
78. Ausiello, C.M., Urbani, F., de la Sala, A., Funaro, A., and Malavasi, F., *CD38 ligation induces discrete cytokine mRNA expression in human cultured lymphocytes.* Eur. J. Immunol., 1995. **25**: p. 1477-1480.
79. Ausiello, C.M., la Sala, A., Ramoni, C., Urbani, F., Funaro, A., and Malavasi, F., *Secretion of IFN-gamma granulocyte-macrophage colony-stimulating factor and IL-10*

cytokines after activation of human purified T lymphocytes upon CD38 ligation. Cell. Immunol., 1996. **173**: p. 192-197.
80. Deaglio, S., Mallone, R., Baj, G., Arnulfo, A., Surico, N., Dianzani, U., Mehta, K., y Malavasi, F., Chem. Immunol., 2000. **75**: p. 99-120.
81. Deaglio, S., Morra, M., Mallote, R., Ausiello, C.M., Prager, E., Garbarino, G., Dianzani, U., Stockinger, H., y Malavasi, F.,, Journal Immunology, 1998. **160**: p. 395-402.
82. Newman., P., *The biology of PECAM-1.* J. Clin. Invest., 1997. **99**: p. 3-8.
83. Deaglio, S., Vaisitti, T., Aydin, S., Ferrero, E., and Malavasi, F., *In-tandem insight from basic science combined with clinical research: CD38 as both marker and key component of the pathogenetic network underlying chronic lymphocytic leukemia.* Blood, 2006. **108**: p. 1135-1144.
84. Silvennoinen, O., Nishigaki, H., Kitanaka, A., Kumagai, M., Ito, C., Malavasi, F., Lin, Q., Conley, M. E., and Campana, D., *CD38 signal transduction in human B cell precursors: rapid induction of tyrosine phosphorylation, activation of syk tyrosine kinase and phosphorylation of phospholipase C-γ and phosphatidylinositol 3-kinase.* J. Immunol., 1996. **156**: p. 100.
85. Lund, F.E., Yu N., Kim K. N., Reth M., and Howard M. C., *Signaling through CD38 augments B cell antigen receptor (BCR) responses and is dependent on BCR expression.* J. Immunol., 1996. **157**: p. 1455-1467.
86. Deaglio, S., Capobianco, A., Bergui, L., et al., *CD38 is a signaling molecule in B-cell chronic lymphocytic leukemia cells.* Blood, 2003. **102**: p. 2146-2155.
87. Kitanaka, A., Ito, C., Coustan-Smith, E., and Campana, D., *CD38 ligation in human B cell progenitors triggers tyrosine phosphorylation of CD19 with Lyn and phosphatidylinositol-3-kinase.* J. Immunol., 1997. **159**: p. 184-192.
88. Deaglio, S., Vaisitti, T., and Malavasi, F., *Role of human CD38 in B cell signaling.* VIII HLDA Meeting Adelaide, Australia., 2004.
89. Zupo, S., Rugari, E., Dono, M., Tamborelli, G., Malavasi, F., and Ferrarini, M., *CD38 signaling by agonistic monoclonal antibody prevents apoptosis of human germinal center B cells.* Eur. J. Immunol., 1994. **24**: p. 1218.
90. Funaro, A., Morra, M., Calosso, L., Zini, M.G., Ausiello, C.M., and Malavasi, F., *Role of the human CD38 molecule in B cell activation and proliferation.* Tissue Antigens, 1997. **49**: p. 7-15.
91. Dianzani, U., Funaro, A., DiFranco, D., Garbarino, G., Bragardo, M., Redoglia, V., Buonfiglio, D., De Monte, L. B., Pileri, A., and Malavasi, F., *Interaction between endothelium and $CD4^+/CD45RA^+$ lymphocytes: role of the human CD38 molecule.* J. Immunol., 1994. **153**: p. 952.
92. Musso, T., Deaglio, S. Franco, L., Calosso, L., Badolato, R., Garbarino, G., Dianzani, U., and Malavasi, F., *CD38 expression and functional activities are up-regulated by IFN-γ on human monocytes and monocytic cell lines.* Journal of Leukocyte Biology, 2001. **69**: p. 605-612.
93. Weinberg, J.B., Larrick, J.W., *Receptor-mediated monocytoid differentiation of human promyelocytic cells by tumor necrosis factor: synergistic actions with interferon-gamma and 1,25-dihydroxyvitamin D3.* Blood, 1987. **70**: p. 994-1002.
94. Malavasi, F., et al., *CD38 and CD157 as receptors of the immune system: a bridge between innate and adaptive immunity.* Mol Med, 2006. **12**(11-12): p. 334-41.
95. Randolph, G.J., Sánchez-Schmitz, G., Angeli, V., *Factors and signals that govern the migration of dendritic cells via lymphatics: recent advances.* Springer Semin. Immunopathol., 2005. **26**: p. 273-287.
96. Fedele, G., Frasca, L., Palazzo, R., Ferrero, E., Malavasi, F. and Ausiello, C.M., *CD38 is expressed on human mature monocyte-derived dendritic cells and is functionally*

involved in CD83 expression and IL-12 induction. Eur. J. Immunol., 2004. **34**: p. 1342-1350.
97. Frasca, L., Fedele, G., Deaglio, S., et al., *CD38 orchestrates migration, survival and Th1-immune response of human mature dendritic cells.* Blood, 2006. **107**: p. 2392-2399.
98. Partida-Sanchez, S., Cockayne, D. A., Monard, S., Jacobson, E. L., Oppenheimer, N., Garvy, B., Kusser, K., Goodrich, S., Howard, M., Harmsen, A., Randall, T. D., and Lund, F. E., *Cyclic ADP-ribose production by CD38 regulates intracellular calcium release, extracellular calcium influx and chemotaxis in neutrophils and is required for bacterial tolerance in vivo.* Nature Med., 2001. **7**: p. 1209-1216.
99. Mallone, R., Funaro A., Zubiaur M., et al., *Signaling through CD38 induces NK cell activation.* Int. Immunol., 2001. **13**: p. 397-409.
100. Deaglio, S., Zubiaur, M., Gregorini, A., et al., *Human CD38 and CD16 are functionally dependent and physically associated in natural killer cells.* Blood, 2002. **99(7)**: p. 2490-2498.
101. Wang, J., Nemoto, E., Kots, A.Y., Kaslow, H.R., and Dennert, G., *Regulation of cytotoxic T cells by ecto-nicotinamide adenine dinucleotide (NAD) correlates with cell surface GPI-anchored/arginine ADP-ribosyltransferase.* J. Immunol., 1994. **153**: p. 4048-4058.
102. Han, M., Lee, JY., Cho, YS., Song, YM., An, NH., Kim, HR., and Kim, UH. , *Regulation of NAD^+ glycohydrolase activity by NAD^+-dependent auto-ADP-ribosylation.* Biochem. J., 1996. **318**: p. 903-908.
103. Han, M., Cho, YS., Kim, YS., Yim, CY., and Kim, U.H., *Interaction of two classes of ADP-ribose transfer reactions in immune signaling.* The Journal of Biological Chemistry, 2000. **275 (27)**(July 7): p. 20799-20805.
104. Graeff, R., Munshi, C., Aarhus, R., Johns, M., and Lee, H. C., *A single residue at the active site of CD38 determines its NAD cyclizing and hydrolyzing activities.* The Journal of Biological Chemistry, 2001. **276**(15 Issue of April 13): p. 12169-12173.
105. Funaro, A., Reinis, M., Trubiani, O., Santi, S., Di Primio, R., and Malavasi, F., *CD38 functions are regulated through an internalization step.* The Journal of Immunology, 1998. **160**: p. 2238-2247.
106. Rah, S.-Y., Park, K-H., Nam, T-S., Kim, S-J., Kim, H., Im, M-J., and Kim, U-H., *Association of CD38 with nonmuscle Myosin Heavy Chain IIA and Lck is essential for the internalization and activation of CD38.* J. Biol. Chem., 2007. **282**(8): p. 5653-5660.
107. Berthelier, V., Tixier, J. M., Muller-Steffner, H., Schuber, F., and Deterre, P., Biochem. J., 1998. **330**: p. 1383-1390.
108. Mehta, K., Shahid, U., and Malavasi, F., *Human CD38, a cell-surface protein with multiple functions.* FASEB J., 1996. **10**: p. 1408-1417.
109. Franco, L., Guida, L., Bruzzone, S., Zocchi, E., Usai, C., and De Flora, A., *The transmembrane glycoprotein CD38 is a catalytically active transporter responsible for generation and influx of the second messenger cyclic ADP-ribose across membranes.* FASEB J., 1998. **12**: p. 1507-1520.
110. Howard M., G.J.C., Bazan J. F., Lund F. E., Santos-Argumedo L., Parkhouse R. M. E., Walseth T. F., and Lee H. C., *Formation and hydrolysis of cyclic ADP-ribose catalyzed by lymphocyte antigen CD38.* Science, 1993. **262**: p. 1056.
111. Lee, H.C., *Structure and enzymatic functions of human CD38.* Mol. Med., 2006. **12**(11-12): p. 317-323.
112. Churchill, G.C., et al., *NAADP mobilizes Ca^{2+} from reserve granules, lysosome-related organelles, in sea urchin eggs.* Cell, 2002. **111**: p. 703-708.
113. Yamasaki, M., et al., *Organelle selection determines agonist-specific Ca^{2+} signals in pancreatic acinar and beta cells.* J. Biol. Chem., 2004. **279**: p. 7234-7240.

114. Lee, H.C., et al., *Mechanisms of calcium signaling by cyclic ADP-ribose and NAADP.* Physiol. Rev., 1997. **77**: p. 1133-1164.
115. Lee, H.C., et al., *Physiological functions of cyclic ADP-ribose and NAADP as calcium messengers.* Annu. Rev. Pharmacol. Toxicol., 2001. **43**: p. 317-345.
116. Aarhus R., G.R.M., Dickey D. M., Walseth T. F., and Lee H. C., *ADP-ribosyl cyclase and CD38 catalyze the synthesis of a calcium mobilizing metabolite from NADP.* J. Biol. Chem, 1995. **270**: p. 30327-30334.
117. Lee H. C., G.R.M., and Walseth T. F., *ADP-ribosyl cyclase and CD38. Multi-functional enzymes in Ca^{2+} signaling. In: ADP-ribosylation in animal tissues (Haag F., and Koch-Nolte F., eds).* Plenum Press, New York, 1997: p. 411-419.
118. Higashida, H., Egorova, A., Higashida, C., Zhong, Z.G., Yokoyama, S., Noda, M., and Zhang, J.S., J. Biol. Chem., 1999. **274**: p. 33348-33354.
119. Boittin, F.X., Dipp, M., Kinnear, N.P., Galione, A., and Evans, A.M., J. Biol. Chem., 2003. **278**: p. 9602-9608.
120. Higashida, H., Zhang, J.S., Hashii, M., Shintaku, M., Higashida, C., and Takeda, Y., Biochem. J., 2000. **352**: p. 197-202.
121. Higashida, H., Yokoyama, S., Hashii, M., Taketo, M., Higashida, M., Takayasu, T., Ohshima, T., Takasawa, S., Okamoto, H., and Noda, M., J. Biol. Chem., 1997. **272**: p. 31272-31277.
122. Graeff, R.M., Franco, L., De Flora, A., and Lee, H.C., J. Biol. Chem., 1998. **273**: p. 118-125.
123. Rah, S.-Y., *Activation of CD38 by interleukin-8 signaling regulates intracellular calcium level and motility of Lymphokine-activated killer cells.* The Journal of Biological Chemistry, 2005. **280**(No 4 Issue of January 28): p. 2888-2895.
124. Xie, G.H., Rah, S.Y., Kim, S.J., Nam, T.S., Ha, K.C., Chae, S.W., Im, M.J., and Kim, U.H., Biochem. Biophys. Res. Commun., 2005. **330**: p. 1290-1298.
125. Tohgo, A., Takasawa, S., Noguchi, N., Koguma, T., Nata, K., Sugimoto, T., Furuya, Y., Yonekura, H., y Okamoto, H., J. Biol. Chem, 1994. **46**: p. 28555-28557.
126. Liu, Q., Kriksunov, I. A., Graeff, R., Munshi, C., Lee, H. C., and Hao, Q., *Structural basis for the mechanistic understanding human CD38 controlled multiple catalysis.* J. Biol. Chem, 2006. **281(43)**: p. 32861-32869.
127. Abdallah M. A., B.J.F., Nordström B., and Brändén C. I., *The conformation of adenosine diphosphoribose and 8-bromoadenosine diphosphoribose when bound to liver alcohol dehydrogenase.* Eur. J. Biochem., 1975. **50**: p. 475.
128. Partida-Sánchez S., I., P., Moreno-García, M. E., Ji-Liang Gao, Murphy, P. M., Oppenheimer, N., Ji Ming Wang, and Lund, F., *Chemotaxis and calcium responses of phagocytes to formyl peptide receptor ligands is differentially regulated by cyclic ADP ribose.* The Journal of Immunology, 2004. **172**: p. 1896-1906.
129. Takasawa S., N.K., Yonekura H., and Okamoto H., *ADP-ribose in insulin secretion from pancreatic beta cells.* Science, 1993. **259**: p. 370-373.
130. Kato I., T.S., Akabane A., Tanaka O., Abe H., Takamura T., Suzuki Y., Nata K., Yonekura H., and Yoshimoto T., *Regulatory role of CD38 (ADP-ribosyl cyclase/cyclic ADP-ribose hydrolase) in insulin secretion by glucose in pancreatic beta cells. Enhanced insulin secretion in CD38-expressing transgenic mice.* J. Biol. Chem, 1995. **270**: p. 30045-30050.
131. Kato I., Y.Y., Fujimura M., Noguchi N., Takasawa S., and Okamoto H., *CD38 disruption impairs glucose-induced increases in cyclic ADP-ribose, $[Ca^{2+}]_i$, and insulin secretion.* J. Biol. Chem, 1999. **274**: p. 1869-1872.

132. Zocchi E., F.L., Guida L., Piccini D., Tachetti C., and De Flora A., *NAD^+ -dependent internalization of the transmembrane glycoprotein CD38 in human Namalwa B cells.* FEBS Lett., 1996. **396**: p. 327-332.
133. Zocchi E., U.C., Guida L., Franco L., Bruzzone S., Passalacqua M., and De Flora A., *Ligand-induced internalization of CD38 results in intracellular Ca^{2+} mobilization: role of NAD^+ transport across cell membranes.* FASEB J., 1999. **13**: p. 273-283.
134. Sun L., A.O.A., Moonga B. S., Corisdeo S., Anandatheerthavarada H. K., Biswas G., Arakawa T., Hakeda Y., Koval A., Sodam B., Bevis P. J., Moser A. J., Lai F. A., Epstein S., Troen B. R., Kumegawa M., and Zaidi M., *CD38/ADP-ribosyl cyclase. A new role in the regulation of osteoclastic bone resorption.* J. Cell. Biol., 1999. **146**: p. 1161-1172.
135. da Silva, C.P., Schweitzer, K., Heyer, P., Malavasi, F., Mayr, G. W., and Guse, A. H., *Ectocellular CD38-catalyzed synthesis and intracellular Ca^{2+} signalling activity of cyclic ADP-ribose in T-lymphocytes are not functionally related.* FEBS Lett., 1998. **439**: p. 291-296.
136. Zocchi, E., Daga, A., Usai, C., Franco, L., Guida, L., Bruzzone, S., Costa, A., Marchetti, C., and De Flora, A., *Expression of CD38 increases intracellular calcium concentration and reduces doubling time in HeLa and 3T3 cells.* J. Biol. Chem., 1998. **273**: p. 8017-8024.
137. Takahashi, K., Kukimoto, I., Tokita, K., Inageda, K., Inoue, S., Kontani, K., Hoshino, S., Nishina, H., Kanaho, Y., and Katada, T., FEBS Lett., 1995. **371**: p. 204-208.
138. Bruzzone, S., Guida, L., Zocchi, E., Franco, L., De Flora, A. , *Connexin 43 hemi channels mediate Ca^{2+}-regulated transmembrane NAD^+ fluxes in intact cells.* FASEB J., 2001. **15**: p. 10-12.
139. De Flora, A., Zocchi, E., Guida, L., Franco, L., Bruzzone, S., *Autocrine and paracrine calcium signaling by the CD38/NAD^+/cyclic ADP-ribose system.* Ann. N. Y. Acad. Sci., 2004. **1028**: p. 176-191.
140. Jayaraman, T., Ondriasova, E., Ondrias, K., Harnick, D.J., Marks, A.R., *The inositol 1,4,5-triphosphate receptor is essential for T-cell receptor signaling.* Proc. Natl. Acad. Sci. USA, 1995. **92**: p. 6007-6011.
141. Guse, A.H., *Cyclic ADP-ribose.* J. Mol. Med., 2000. **78**: p. 26-35.
142. Ng, J., Gustavsson, J., Jondal, M. Anderson, T., *Regulation of calcium influx across the plasma membrane of the human T-leukemic cell line, JURKAT: dependence on a rise in cytosolic free calcium can be dissociated from formation of inositol phosphates.* Biochim. Biophys. Acta, 1990. **1053**: p. 97-105.
143. Brattsand, G., Cantrell, D.A., Ward, S. Ivars, F., Gullberg, M., *Signal transduction through the T cell receptor-CD3 complex. Evidence for heterogeneity in receptor coupling.* J. Immunol., 1990. **144**: p. 3651-3658.
144. Guse, A.H., da Silva, C.P., Berg, I., Weber, K., Heyer, P., Hohenegger, M., Ashamu, G.A., Skapenko, A.L., Schulze-Koops, H., Potter, B.V.L., Mayr, G.W., *Regulation of Ca^{2+}-signaling in T-lymphocytes by the second messenger cyclic ADP-ribose.* Nature, 1999. **398**: p. 70-73.
145. Deaglio S., T.V., Aydin S., Ferrero E., and Malavasi F., *In-tandem insight from basic science combined with clinical research: CD38 as both marker and key component of the pathogenetic network underlying chronic lymphocytic leukemia.* Blood, 2006. **108**(number 4): p. 1135-1144.
146. Funaro A., D.M.L.B., Dianzani U., Forni M., and Malavasi F., *Human CD38 is associated to distinct molecules which mediate transmembrane signaling in different lineages.* Eur. J. Immunol., 1993. **23**: p. 2407-2411.
147. Morra, M., Zubiaur M., Terhorst C., Sancho J., and Malavasi F., *CD38 is functionally dependent on the TCR/CD3 complex in human T cells.* FASEB J., 1998. **12**: p. 581-592.

148. Lund F. E., Y.N., Kim K. N., Reth M., and Howard M. C., *Signaling through CD38 augments B cell antigen receptor (BCR) responses and is dependent on BCR expression.* J. Immunol., 1996. **157**: p. 1455-1467.
149. Deaglio S., C.A., Bergui L., et al., *CD38 is a signaling molecule in B-cell chronic lymphocytic leukemia cells.* Blood, 2003. **102**: p. 2146-2155.
150. Deaglio S., Z.M., Gregorini A., et al., *CD38 and CD16 are functionally dependent and physically associated in natural killer cells.* Blood, 2002. **99**: p. 2490-2498.
151. Zilber M. T., G.S., Mallone R., et al., *CD38 expressed on human monocytes: a coaccessory molecule in the superantigen-induced proliferation.* Proc. Natl. Acad. Sci. USA, 2000. **97**: p. 2840-2845.
152. Zilber M. T., S.N., Vasselon T., et al., *MHC class II/CD38/CD9: a lipid-raft-dependent signaling complex in human monocytes.* Blood, 2005. **106**: p. 3074-3081.
153. Frasca L., F.G., Deaglio S., et al., *CD38 orchestrates migration, survival and Th1-immune response of human mature dendritic cells.* Blood, 2006. **107**: p. 2392-2399.
154. Lund, F.E., Solvason, N., Grimaldi, J.C., Parkhouse, R.M.E., and Howard, M, *Murine CD38: an immunoregulatoy ectoenzyme.* Immunol. Today, 1995. **16**: p. 469.
155. Funaro, A., Spagnoli, G.C., Ausiello, C.M., Alessio, M., Roggero, S., Delia, D., Zaccolo, M., and Malavasi, F. , *Involvement of the multilineage CD38 molecule in a unique pathway of cell activation and proliferation.* J. Immunol., 1990. **145**: p. 2390.
156. Kumagai, M., Coustan-Smith E., Murray D. J., Silvennoinen O., Murti K. G., Evans W. E., Malavasi F., and Campana D., *Ligation of CD38 supresses human B lymphopoiesis.* J. Exp. Med., 1995. **181**: p. 1101.
157. Kikuchi, Y., Yasue, T., Miyake, K., Kimoto, M., and Takatsu, K., *CD38 ligation induces tyrosine phosphorilation of Bruton tyrosine kinase and enhanced expression of interleukin-5 receptor on α chain: synergistic effects with interleukin 5.* Proc. Natl. Acad. Sci. USA, 1995. **92**: p. 11814.
158. Kontani, K., Kukimoto, I., Nishina, H., et al., *Tyrosine phosphorilation of the c-cbl proto-oncogene product mediated by cell surface antigen CD38 in HL-60 cells.* J. Biol. Chem, 1996. **271**: p. 1531-1537.
159. Zubiaur, M., et al., *CD38 ligation results in activation of the Raf-1/mitogen-activated protein kinase and the CD3-zeta/zeta-associated protein-70 signaling pathways in Jurkat T lymphocytes.* J Immunol, 1997. **159**(1): p. 193-205.
160. Whitehurst, C.E., Boulton, T.G., Cobb, M.H., and Geppert, T.D., *Extracelullar signal-related kinases in T cells: anti-CD3 and 4β-phorbol 12-myristate 13-acetate-induced phosphorilation and activation.* J. Immunol., 1992. **148**: p. 3230.
161. Reth, M., *Antigen receptor tail clue.* Nature, 1989. **338**: p. 383-384.
162. Irving, B.A., Weiss, A., *The cytoplasmic domain of the T cell receptor zeta chain is sufficient to couple to receptor-associated signal transduction pathways.* Cell, 1991. **64**: p. 891-901.
163. Irving, B.A., Chan, A. C., Weis, A., *Functional characterization of a signal transducing motif present in the T cell antigen receptor zeta chain.* J. Exp. Med., 1993. **177**: p. 1093-1103.
164. Cambier, J.C., *Antigen and Fc receptor signaling. The awesome power of the immunoreceptor tyrosine-based activation motif (ITAM).*
. J. Immunol., 1995. **155**: p. 3281-3285.
165. Germain, R.N., Stefanova, I., *The dynamics of T cell receptor signaling: complex orchestration and the key roles of tempo and cooperation.* Annu. Rev. Immunol., 1999. **17**: p. 467-522.
166. Weiss, A., and Littman, D.R., Cell, 1994. **76**: p. 263-274.

167. Izquierdo, M., Leevers, S.J., Marshall, C.J., and Cantrell, D., J. Exp. Med., 1993. **178**: p. 1199-1208.
168. Chan, A.C., and Shaw, A.S., Curr. Opin. Immunol., 1995. **8**: p. 394-401.
169. Zubiaur, M., Guirado, M., Terhorst, C., Malavasi, F., and Sancho, J., *The CD3-gamma delta epsilon transducing module mediates CD38-induced protein-tyrosine kinase and mitogen-activated protein kinase activation in Jurkat T cells.* J. Biol. Chem, 1999. **274(29)**: p. 20633-20642.
170. Alcover, A., Alberini, C., Acuto, O., Transy, C., Spagnoli, C.G., Moingeon, P., López, P., and Reinherz, E.L., Embo J., 1988. **7**: p. 1973-1977.
171. Rodríguez-Tarduchy, G., Sahuquillo, A.G., Alarcón, B., and Bragado, R., J Biol Chem, 1996. **271**: p. 30417-30425.
172. Zubiaur, M., Fernández, O., Ferrero, E., et al., *CD38 is associated with lipid rafts and upon receptor stimulation leads to Akt/protein kinase B and Erk activation in the absence of CD3-zeta immune receptor tyrosine-based activation motifs.* J. Biol. Chem, 2002. **277**: p. 13-22.
173. Yancey, P.G., Rodrigueza, W.V., Kilsdonk, E.P., Stoudt, G.W., Johnson, W.J., Phillips, M.C., and Rothblat, G.H., J Biol Chem, 1996. **271**: p. 16026-16034.
174. Moran, M., Miceli, M. C., *Engagement of GPI-linked CD48 contributes to TCR signals and cytoskeletal reorganization: a role for lipid rafts in T cell activation.* Immunity, 1998. **9**: p. 787-796.
175. Kabouridis, P.S., Janzen, J., Magee, A. L., Ley, S. C., *Cholesterol depletion disrupts lipid rafts and modulates the activity of multiple signaling pathways in T lymphocytes.* Eur. J. Immunol., 2000. **30**: p. 954-963.
176. Zhang, W., Sloan-Lancaster, J., Kitchen, J., Trible, R.P., and Samelson, L.E., Cell, 1998. **92**: p. 83-92.
177. Zubiaur, M., Izquierdo, M., Terhorst, C., Malavasi, F., and Sancho, J., *CD38 ligation results in activation of the Raf-1/MAP kinase and the CD3-ζ/ZAP-70 signaling pathways in Jurkat T lymphocytes.* J. Immunol., 1997. **159**: p. 193-205.
178. Guirado, M., de Aos, I., Orta, T., Rivas, L., Terhorst, C., Zubiaur, M., and Sancho, J., *Phosphorylation of the N-terminal and C-terminal CD3-epsilon-ITAM tyrosines is differentially regulated in T cells.* Biochem. Biophys. Res. Commun., 2002. **291(3)**: p. 574-581.
179. Millán, J., Cerny, J., Horejsi, V., and Alonso, M.A., *CD4 segregates into specific detergent-resistant T-cell membrane microdomains.* Tissue Antigens, 1999. **53**: p. 33-40.
180. Sicheri, F., and Kuriyan, J., *Structures of Src-family tyrosine kinases.* Curr. Opin. Struct. Biol., 1997. **7**: p. 777-785.
181. Young, M.A., Gonfloni, S., Superti-Furga, G., Roux, B., and Kuriyan, J., *Dynamic coupling between the SH2 and SH3 domains of c-Src and Hck underlies their inactivation by C-terminal tyrosine phosphorilation.* Cell, 2001. **105**: p. 115-126.
182. Muñoz P., N.C.P.E.e.a., *CD38 signaling in T cells is iniciated within a subset of membrane rafts containing Lck and the CD3-zeta subunit of the T cell antigen receptor.* J. Biol. Chem, 2003. **278**: p. 50791-50802.
183. Arcaro, A.e.a., *Essential role of CD8 palmitoylation in CD8 coreceptor function.* J. Immunol., 2000. **165(4)** p. 2068-2076.
184. Rodgers, W., Rose, J. K., *Exclusion of CD45 inhibits activity of p56Lck associated with glycolipid-enriched membrane domains.* J. Cell. Biol., 1996. **135**: p. 1515-1523.
185. Xavier, R., et al., *Membrane compartmentalization is required for efficient T cell activation.* Immunity, 1998. **8**: p. 723-732.

186. Zhang, W., Trible, R. P., Samelson, L. E., *LAT palmitoylation: its essential role in membrane microdomain targeting and tyrosine phosphorilation during T cell activation.* Immunity, 1998. **9**: p. 239-246.
187. Brdicka, T., Cerny, J., Horejsi, V., *T cell receptor signaling results in rapid tyrosine phosphorylation of the linker protein LAT present in detergent-resistant membrane microdomains.* . Biochem. Biophys. Res. Commun., 1998. **248**: p. 356-360.
188. Kawabuchi, M., et al., *Transmembrane phophoprotein Cbp regulates the activities of Src-family tyrosine kinases.* Nature, 2000. **404**: p. 999-1003.
189. Bi, K.e.a., *Antigen-induced translocation of PKC-theta to membrane rafts is required for T cell activation.* Nat. Immunol., 2001. **2**: p. 556-563.
190. Montixi, C., et al., *Engagement of T cell receptor triggers its recruitment to low density detergent-insoluble membrane microdomains.* Embo J., 1998. **17**: p. 5334-5348.
191. Simons, K., and Toomre, D., *Lipid raft and signal transduction.* Nature Mol. Cell Biol. Rev., 2000. **1**: p. 31-39.
192. Sharma, P.e.a., *Nanoscale organization of multiple GPI-anchored proteins in living cell membranes.* Cell, 2004. **116**: p. 577-589.
193. Wilson, B.S.e.a., *Markers for detergent-resistant lipid rafts occupy distinct and dynamic domains in native membranes.* Mol. Bio. Cell., 2004. **15**: p. 2580-2592.
194. Rodgers W., Z.J., *Glycolipid-enriched membrane domain are assembled into membrane patches by associating with the actin cytoskeleton.* J. Exp. Cell. Res., 2001. **267**: p. 173-183.
195. Jordan, S.a.R., W., *T cell glycolipid-enriched membrane domains are constitutively assembled as membrane patches that translocate to immune synapses.* J. Immunol., 2003. **171**: p. 78-87.
196. Prior, I.A.e.a., *Direct visualization of Ras protein in spatially distinct cell surface microdomains.* J. Cell. Biol., 2003. **160**: p. 165-170.
197. Viola, A.e.a., *T lymphocyte costimulation mediated by reorganization of membrane microdomains.* Science, 1999. **283**: p. 680-682.
198. Gordy, C.e.a., *Visualization of antigen presentation by actin-mediated targeting of glycolipid-enriched membrane domains to the immune synapse by B cell APCs.* J. Immunol., 2004. **172**: p. 2030-2038.
199. Monks, C.R.F., Freiberg, B. A., Kupfer, H., Sciaky, N., and Kupfer, A., *Three-dimensional segregation of supramolecular activation clusters in T cells.* Nature, 1998. **395**: p. 82-86.
200. Lee, K.H.e.a., *T cell receptor signaling precedes immunological synapse formation.* Science, 2002. **295**: p. 1539-1542.
201. Horejsi, V., *Lipid rafts and their roles in T-cell activation.* Microbes Infect. , 2005. **7**: p. 310-316.
202. Kabouridis, P.S.e.a., *Selective interaction of LAT (linker of activated T cells) with the open-active form of Lck in lipid rafts reveals a new mechanism for the regulation of Lck in T cells.* Biochem. J., 2003. **371**: p. 907-915.
203. Pizzo, P., Giurisato, E., Bigsten, A., Tassi, M., Tavano, R., Shaw, A., Viola, A., *Physiological T cell activation starts and propagates in lipid rafts.* . Immunol. Lett., 2004. **91/1**: p. 3-9.
204. van Oers, N.S.C.a.C., Zhijian. J., *Kinasing and clipping down the NF-κB trail.* Science, 2005. **308**: p. 65-66.
205. Lin, X., Wang, D., Semin. Immunol. , 2004. **16**: p. 429.
206. Sun, Z.e.a., *PKC-θ is required for TCR-induced NF-κB activation in mature but not immature T lymphocytes.* Nature, 2000. **404**: p. 402-407.

207. Irles C., S.A., Michel F., Bakker T. R., Van der Merwe P. A., and Acuto O., *CD45 ectodomain controls interactin with GEMS and Lck activity for optimal TCR signaling.* Nat. Immunol., 2003. **4**: p. 189-197.
208. Davidson D., B.M., Thomas M. L., Horejsi V., and Veillette A., Mol. Cell. Biol., 2003. **23**: p. 2017-2028.
209. Sadra A., C.T., and Imboden J. B., *Translocation of CD28 to lipid rafts and coestimulation of IL-2.* Proc. Natl. Acad. Sci. USA, 2004. **101**: p. 11422-11427.
210. Bi K., a.A.A., *Membrane lipid microdomains and the role of PKCtheta in T cell activation.* Semin. Immunol., 2001. **13**: p. 136-146.
211. Sehgal P. B., G.G.G., Shah M., Kumar V., and Patel K. , *Cytokine signaling: STATs in plasma membrane rafts.* J. Biol. Chem, 2002. **277**: p. 12067-12074.
212. Goebel J., F.K., Morford L., and Roszman T. L., *Differential localization of IL-2 and IL-15 receptor chains in membrane rafts of human T cells.* J. Leukoc. Bio., 2002. **72**: p. 199-206.
213. Ono A., a.F.E.O., *Plasma membrane rafts play a critical role in HIV-1 assembly and release.* Proc. Natl. Acad. Sci. USA, 2001. **98**: p. 13925-13930.
214. Poloso N. J., R.P.A., *Association of MHC-class II-peptide complexes with plasma membrane lipid microdomains.* Curr. Opin. Immunol., 2004. **16**: p. 103-107.
215. Jury E. C., K.P.S., Flores-Borja F., Mageed R. A., and Isenberg D. A., *Altered lipid raft-associated signaling and ganglioside expression in T lymphocytes from patients with systemic lupus erythematosus.* J. Clin. Invest., 2004. **113**: p. 1176-1187.
216. Drevot P., L.C., Guo X. J., Bernard A. M., Colard O., Chauvin J. P., et al., Embo J., 2002. **21**: p. 1899-1908.
217. Janes P. W., L.S.C., Magee A. I., J. Cell. Biol., 1999. **147**: p. 447-461.
218. Valensin S., P.S.R., Ulivieri C., Mercati D., Pacini S., Patrussi L., et al., Eur. J. Immunol., 2002. **32**: p. 435-446.
219. Hoessli D. C., I.S., Soltermann A., Robinson P. J., Borisch B., Nasir U. D., Glycoconj. J., 2000. **17**: p. 191-197.
220. Harder T., S.K., Eur. J. Immunol., 1999. **29**: p. 556-562.
221. Villalba M., B.K., Rodriguez F., Tanaka Y., Schoenberguer S., Altman A., J. Cell. Biol., 2001. **155**: p. 331-338.
222. Wulfing C., D.M.M., Science, 1998. **282**: p. 2266-2269.
223. Sancho, D., Vicente, M., Mittelbrunn, M., Montoya, M. C., Gordón, M., Serrador, J. M., and Sánchez-Madrid, F., *Regulation of microtubule-organizing center orientation and actomyosin cytoskeleton rearrangement during immune interactions.* Immunological Reviews, 2002. **189**: p. 84-97.
224. Goldsmith, M.A., and Weiss, A., *Early signal transduction by the antigen receptor without commitment to T cell activation.* Science, 1988. **240**: p. 1029.
225. Wacholtz, M.C., and Lipsky, P. E., *Anti-CD3-stimulated Ca^{2+}signal in individual human peripheral T cells. Activation correlates with a sustained increase in intracellular Ca^{2+}.* J. Immunol., 1993. **150**: p. 5338.
226. Montoya, M.C., et al., *Role of ICAM-3 in the initial interaction of T lymphocytes and APCs.* Nat. Immunol., 2002. **3**: p. 159-168.
227. Geijtenbeek, T.B., Torensma, R., van-Vliet, S. J., van-Duijinhoven, G. C. F., van-Kooyk, Y., *Identification of DC-SIGN, a novel dendritic cell-specific ICAM-3 receptor that supports immune responses.* Cell, 2000. **100**: p. 575-585.
228. van-Kooyk, Y., van-der-Wiel, P., van-Kemenade, I., Weder, P., Kuijpers, T. W., Figdor, C. G., *Enhancement of LFA-1 mediated cell adhesion by triggering through CD2 or CD3 on T lymphocytes. .* Nature, 1989. **342**: p. 811-813.

229. Dustin, M.L., Springer, T. A., *T cell receptor cross-linking transiently stimulates adhesiveness through LFA-1.* Nature, 1989. **341**: p. 619-624.
230. Campanero, M.R., et al., *ICAM-3 interacts with LFA-1 and regulates the LFA-1/ICAM-1 cell adhesion pathway.* J. Cell. Biol., 1993. **123**: p. 1007-1016.
231. Grakoui, A., et al., *The immunological synapse: a molecular machine controlling T cell activation.* Science, 1999. **285**: p. 221-227.
232. Krummel, M.F., Sjaastad, M. D., Wülfing, C., Davis, M. M., *Differential clustering of CD4 and CD3 during T cell recognition.* Science, 2000. **289**: p. 1349-1352.
233. van-der-Merwe, P.A., Davis, S. J., Shaw, A. S., Dustin, M. L., *Cytoskeletal polarization and redistribution of cell-surface molecules during T cell antigen recognition.* Semin. Immunol., 2000. **12**: p. 5-21.
234. Delon, J., Kaibuchi, K., and Germain, R.N., *Exclusion of CD43 from the immunological synapse is mediated by phosphorylation-regulated relocation of the cytoskeletal adaptor moesin.* . Immunity, 2001. **15**: p. 691-701.
235. Allenspach, E.J., Cullinan, P., Tong, J., Tang, Q., Tesciuba, A.G., Cannon, J.L., Takahashi, S.M., Morgan, R., Burkhardt, J.K., and Sperling, A.I., *ERM-dependent movement of CD43 defines a novel protein complex distal to the immunological synapse.* Immunity, 2001. **15**: p. 739-750.
236. Johnson, K.G., Bromley, S.K., Dustin, M.L., and Thomas, M.L., *A supramolecular basis for CD45 tyrosine phosphatase regulation in sustained T cell activation.* Proc. Natl. Acad. Sci. USA, 2000. **97**: p. 10138-10143.
237. Freiberg, B.A., Kupfer, H., Maslanik, W., Delli, J., Kappler, J., Zaller, D.M., and Kupfer, A., *Staging and resetting T cell activation in SMACs.* Nat. Immunol., 2002. **3**: p. 911-917.
238. Phee, H., Abraham, R.T., and Weiss, A., *Dynamic recruitment of PAK1 to the immunological synapse is mediated by PIX independently of SLP-76 and Vav1.* . Nat. Immunol., 2005. **6**: p. 608-617.
239. Kane, L.P., Mollenauer, M.N., and Weiss, A., *A proline-rich motif in the C-terminus of Akt contributes to its localization in the immunological synapse.* . J. Immunol., 2004. **172**: p. 5441-5449.
240. Le Bras, S., Foucault, I., Foussat, A., Brignone, C., Acuto, O., and Deckert, M. , *Recruitment of the actin-bindin protein HIP-55 to the immunological synapse regulates T cell receptor signaling and endocytosis.* J. Biol. Chem., 2004. **279**: p. 15550-15560.
241. Pacheco, R., Martínez-Navio, J.M., Lejeune, M., Climent, N., Oliva, H., Gatell, J.M., Gallart, T., Mallol, J., LLuis, C., and Franco, R., *CD26, adenosine deaminase and adenosine receptors mediate costimulatory signals in the immunological synapse.* Proc. Natl. Acad. Sci. USA, 2005. **102**: p. 9583-9588.
242. Batista, A., Millan, J., Mittelbrunn, M., Sanchez-Madrid, F., and Alonso, M.A., *Recruitment of transferrin receptor to immunological synapse in response to TCR engagement.* J. Immunol., 2004. **172**: p. 6709-6714.
243. Kupfer, A., Swain, S. L., Janeway, C. A., Jr., and Singer, S. J., *The specific direct interaction of helper T cells and the antigen-presenting B cells.* Proc. Natl. Acad. Sci. USA, 1986. **83**: p. 6080-6083.
244. Huppa, J.B., Gleimer, M., Sumen, C., and Davis, M. M., *Continuous T cell receptor signaling required for synapse maintenance and full effector potencial.* Nat. Immunol., 2003. **4**: p. 749-755.
245. Lee, K.H., Dinner, A. R., Tu, C., Campi, G., Raychaudhuri, S., Varma, R., Sims, T. N., Burack, W. R., Wu, H., Wang, J. et al., *The immunological synapse balances T cell receptor signaling and degradation.* Science, 2003. **302**: p. 1218-1222.

246. Saito, T., and Yokosuda, T., *Immunological synapse and microclusters: the site for recognition and activation of T cells.* Current Opinion in Immunology 2006. **18**: p. 305-313.
247. Krummel, M.F., Sjaastad, M.D., Wulfing, C., and Davis, M.M., *Differential clustering of CD4 and CD3ζ during T cell recognition.* Science, 2000. **289**: p. 1349-1352.
248. Brunnell, S.C., Kapoor, V., Trible, R.P., Zhang, W., Samelson, L.E., *Dynamic actin polymerization drives T cell receptor-induced spreading: a role for the signal transduction adaptor LAT.* Immunity, 2001. **14**: p. 315-329.
249. Bunnell, S.C., Hong, D.I., Kardon, J.R., Yamazaki, T., McGlade, C.J., Barr, V.A., Samelson, L.E., *T cell receptor ligation induces the formation of dynamically regulated signaling assemblies.* J. Cell. Biol., 2002. **158**: p. 1263-1275.
250. Vicente-Manzanares, M., Sánchez-Madrid, F., *Role of the cytoskeleton during leukocyte responses.* Nat. Rev. Immunol., 2004. **4**: p. 110-122.
251. Drevot, P., Langlet, C., Guo, X. J., Bernard, A. M., Colard, O., Chauvin, J. P., et al., Embo J., 2002. **21**: p. 1899-1908.
252. Schade, A.E., and Levine, A.D., J. Immunol., 2002. **168**: p. 2233-2239.
253. Cho, Y.S., Han, M. K., Choi, Y. B., Yun, Y., Shin, J., and Kim, U. H., *Direct interaction of the CD38 cytoplasmic tail and the Lck SH2 domain: CD38 transduces T cell activation signals through associated Lck.* J. Biol. Chem, 2000. **275**: p. 1685-1690.
254. Van´t Hof, W., and Resh, M.D., J. Cell. Biol., 1999. **145**: p. 377-389.
255. Pitcher, L.A., Young, J.A, Mathis, M.A., Wrage, P.C., Bartok, B., and Van Oers, N.S., Immunol. Rev., 2003. **191**: p. 47-61.
256. Salojin, K.V., Zhang, J., Meagher, C., and Delovitch, T.L., J. Biol. Chem., 2000. **275**: p. 5966-5975.
257. Hartgroves, L.C., Lin, J., Langen, H., Zech, T., Weiss, A., and Harder, T., J. Biol. Chem., 2003. **278**: p. 20389-20394.
258. Plyte, S., Majolini, M.B., Pacini, S., Scarpini, F., Bianchini, C., Lanfrancone, L., Pelicci, P., and Baldari, C.T., Oncogene, 2000. **19**: p. 1529-1537.
259. Prior, I.A., Harding, A., Yan, J., Sluimer, J., Parton, R.G., and Hancock, J.F., Nat. Cell Biol., 2001. **3**: p. 368-375.
260. Song, K.S., Li, S., Okamoto, T., Quilliam, L.A., Sargiacomo, M., and Lisanti, M., J. Biol. Chem., 1996. **271**: p. 9690-9697.
261. Roy, S., Luetterforst, R., Harding, A., Apolloni, A., Etheridge, M., Stang, E., Rolls,B., Hancock, J.F., and Parton, R.G., Nat. Cell Biol., 1999. **1**: p. 98-105.
262. Exley, M., Varticovski, L., Markus, P., Sancho, J., and Terhorst, C., J. Biol. Chem., 1994. **269**: p. 15140-15146.
263. de Aós, I., Metzger, M.H., Exley, M., Dahl, C.E., Misra, S., Zheng, D., Varticovski, L., Terhorst, C., and Sancho, J., J. Biol. Chem., 1997. **272**: p. 25310-25318.
264. Shoelson, S.E., Sivaraja, M., Williams, K.P., HU, P., Schlessinger, J., and Weiss, M.A., Embo J., 1993. **12**: p. 795-802.
265. Buhl, A.M., and Cambier, J.C., Immunol. Rev., 1997. **160**: p. 127-138.
266. Wange, R.L., Sci. STKE, 2000. **RE1**.
267. Kitanaka, A., Ito, C., Nishigaki, H., and Campana, D., Blood, 1996. **88**: p. 590-598.
268. Sloan-Lancaster, J., Shaw, A.S., Rothbard, J.B., and Allen, P.M., Cell, 1994. **79**: p. 913-922.
269. Blanchard, N., Di Bartolo, V., and Hivroz, C., *In the immune synapse, ZAP-70 controls T cell polarization and recruitment of signaling proteins but not formation of the synaptic pattern.* Immunity, 2002. **17**: p. 389-399.
270. Das, V., Nal, B., Dujeancourt, A., Thoulouze, M.I., Galli, T., Roux, P., Dautry-Varsat, A., and Alcover, A., *Activation-induced polarized recycling targets T cell antigen*

receptors to the immunological synapse; involvement of SNARE complexes. Immunity, 2004. **20**: p. 577-588.
271. Bonello, G., Blanchard, N., Montoya, M.C., Aguado, E., Langlet, C., He, H.T., Nuñez-Cruz, S., Malissen, M., Sanchez-Madrid, F., Olive, D., Hivroz, C., and Collette, Y., *Dynamic recruitment of the adaptor protein LAT: LAT exits in two distinct intracellular pools and controls its own recruitment.* J. Cell Sci., 2004. **117**: p. 1009-1016.
272. Ehrlich, L.I., Ebert, P.J., Krummel, M.F., Weiss, A., and Davis M.M. , *Dynamics of p56lck translocation to the T cell immunological synapse following agonist and antagonist stimulation.* Immunity, 2002. **17**: p. 809-822.
273. Muñoz, P., Navarro, M. C., Pavón, E. J., Salmerón, J., Malavasi, F., Sancho, J., and Zubiaur, M. , *CD38 signaling in T cells is iniciated within a subset of membrane rafts containing Lck and the CD3-zeta subunit of the T cell antigen receptor.* J. Biol. Chem, 2003. **278**: p. 50791-50802.
274. Pfister, M., Ogilvie, A., da Silva, C.P., Grahnert, A., Guse, A.H., and Hauschildt, S., *NAD degradation and regulation of CD38 expression by human monocytes/macrophages.* Eur. J. Biochem., 2001. **268**: p. 5601-5608.
275. Guse, A.H., *Second messenger function and the structure-activity relationship of cyclic adenosine diphosphoribose (cADPR).* FEBS J., 2005. **272**: p. 4590-4597.
276. Bueno, C., Lemke, C.D., Criado, G., Baroja, M.L., Ferguson, S.S., Rahman, A.K., Tsoukas, C.D.., McCormick, J.K., and Madrenas, J., *Bacterial superantigens bypass Lck-dependent T cell receptor signaling by activating a Galpha11-dependent, PLC-beta-mediated pathway.* Immunity, 2006. **25**: p. 67-78.
277. Podesta, M., Pitto, A., Figari, O., Bacigalupo, A., Bruzzone, S., Guida, L., Franco, L., De Flora, A., and Zocchi, E., *Cyclic ADP-ribose generation by CD38 improves human hemopoietic stem cell engraftment into NOD/SCID mice.* FASEB J., 2003. **17**: p. 310-312.
278. Bruzzone, S., De Flora, A., Usai, C., Graeff, R., and Lee, H.C., *Cyclic ADP-ribose is a second messenger in the lipopolysaccharide-stimulated proliferation of human peripheral blood mononuclear cells.* Biochem. J., 2003. **375**: p. 395-403.
279. Ibiza, S., Victor, V.M., Bosca, I., Ortega, A., Urzainqui, A., O´Connor, J.E., Sánchez-Madrid, F., Esplugues, J.V., and Serrador, J.M., *Endothelial nitric oxide synthase regulates T cell receptor signaling at the immunological synapse.* Immunity, 2006. **24**: p. 753-765.
280. Zhang, A.Y., and Li, P.L., *Vascular physiology of a Ca^{2+} mobilizing second messenger-cyclic ADP-ribose.* J. Cell Mol. Med., 2006. **10**: p. 407-422.
281. Morgan, M.M., Labno, C.M., Van Seventer, G.A., Denny, M.F., Straus, D.B., and Burkhardt, J.K., *Superantigen-induced T cell:B cell conjugation is mediated by LFA-1 and requires signaling throught Lck, but not ZAP-70.* J. Immunol., 2001. **167**: p. 5708-5718.
282. Roumier, A., Olivo-Marin, J.C., Arpin, M., Michel, F., Martin, M., Mangeat, P., Acuto, O., Dautry-Varsat, A., and Alcover, A., *The membrane-microfilament linker ezrin is involved in the formation of the immunological synapse and in T cell activation.* Immunity, 2001. **15**: p. 715-728.
283. Gaus, K., Chklovskaia, E., Fazekas de St Groth, B., Jessup, W., and Harder, T., *Condensation of the plasma membrane at the site of T lymphocyte activation.* J. Cell Biol., 2005. **171**: p. 121-131.
284. Yokosuka, T., Sakata-Sogawa, K., Kobayashi, W., Hiroshima, M., Hashimoto-Tane, A., Tokunaga, M., Dustin, M.L., and Saito, T., *Newly generated T cell receptor microclusters iniciate and sustain T cell activation by recruitment of ZAP-70 and SLP-76.* Nat. Immunol., 2005. **6**: p. 1253-1262.

285. Campi, G., Varma, R., and Dustin, M.L., *Actin and agonist MHC-peptide complex-dependent T cell receptor microcluster as scaffolds for signaling.* J. Exp. Med., 2005. **202**: p. 1031-1036.
286. Varma, R., Campi, G., Yokosuka, T., Saito, T., and Dustin, M.L. , *T cell receptor-proximal signals are sustained in peripheral microclusters and terminated in the central supramolecular activation cluster.* Immunity, 2006. **25**: p. 117-127.
287. Newman, P.J., *The biology of PECAM-1.* J. Clin. Invest., 1997. **99**: p. 3-8.
288. Hiltbold, E.M., Poloso, N.J., and Roche, P.A., *MHC class II-peptide complexes and APC lipid rafts accumulate at the immunological synapse.* J. Immunol., 2003. **170**: p. 1329-1338.
289. Kropshofer, H., Spindeldreher, S., Rohn, T.A., Platania, N., Grygar, C., Daniel, N., Wolpl, A., Langen, H., Horejsi, V., and Vogt, A.B., *Tetraspan microdomains distinct from lipid rafts enrich select peptide-MHC class II complexes.* Nat. Immunol., 2002. **3**: p. 61-68.
290. de la Fuente, H., Mittelbrunn, M., Sánchez-Martín, L., Vicente-Manzanares, M., Lamana, A., Pardi, R., Cabanas, C., and Sánchez-Madrid, F., *Synaptic clusters of MHC class II molecules induced on DCs by adhesion molecule-mediated initial T-cell scanning.* Mol. Biol. Cell, 2005. **16**: p. 3314-3322.
291. Zilber, M.T., Setterblad, N., Vasselon, T., et al., *MHC class II/CD38/CD9: a lipid-raft-dependent signaling complex in human monocytes.* Blood, 2005. **106**: p. 3074-3081.
292. Zilber, M.T., Gregory, S., Mallone, R., et al., *CD38 expressed on human monocytes: a coaccessory molecule in the superantigen-induced proliferation.* Proc. Natl. Acad. Sci. USA, 2000. **97**: p. 2840-2845.

Anexo I

Artículos publicados

THE JOURNAL OF BIOLOGICAL CHEMISTRY
Vol. 279, No. 50, Issue of December 12, pp. 50791–50802, 2003
Printed in U.S.A.

CD38 Signaling in T Cells Is Initiated within a Subset of Membrane Rafts Containing Lck and the CD3-ζ Subunit of the T Cell Antigen Receptor*

Received for publication, July 23, 2003, and in revised form, September 22, 2003
Published, JBC Papers in Press, September 30, 2003, DOI 10.1074/jbc.M308034200

Pilar Muñoz‡§, María-del-Carmen Navarro‡¶, Esther J. Pavón‡‖, Javier Salmerón, Fabio Malavasi‡‡, Jaime Sancho‡, and Mercedes Zubiaur‡§§**

*From the ‡Instituto de Parasitología y Biomedicina, Consejo Superior de Investigaciones Científicas, 18001 Granada, the **Hospital Universitario San Cecilio, 18012 Granada, Spain, and the ‡‡Laboratory of Immunogenetics, University of Torino Medical School, 10126 Torino, Italy*

In this study we present data supporting that most CD38 is pre-assembled in a subset of Brij 98-resistant raft vesicles, which were stable at 37 °C, and have relatively high levels of Lck and the CD3-ζ subunit of T cell antigen receptor-CD3 complex in contrast with a Brij 98-soluble pool, where CD38 is associated with CD3-ζ, and Lck is not detected. Our data further indicate that following CD38 engagement, LAT and Lck are tyrosine-phosphorylated exclusively in Brij 98-resistant rafts, and some key signaling components translocate into rafts (*i.e.* Sos and p85-phosphatidylinositol 3-kinase). Moreover, N-Ras results activated within rafts immediately upon CD38 ligation, whereas activated Erk was mainly found in soluble fractions with delayed kinetics respective to Ras activation. Furthermore, full phosphorylation of CD3-ζ and CD3-ε only occurs in rafts, whereas partial CD3-ζ tyrosine phosphorylation occurs exclusively in the soluble pool, which correlated with increased levels of c-Cbl tyrosine phosphorylation in the non-raft fractions. Taken together, these results suggest that, unlike the non-raft pool, CD38 in rafts is able to initiate and propagate several activating signaling pathways, possibly by facilitating critical associations within other raft subsets, for example, LAT rafts via its capacity to interact with Lck and CD3-ζ. Overall, these findings provide the first evidence that CD38 operates in two functionally distinct microdomains of the plasma membrane.

Human CD38 antigen is a 45-kDa type II transmembrane glycoprotein with a short N-terminal cytoplasmic domain and a long C-terminal extracellular domain (1, 2). It is widely expressed in different cell types including thymocytes, activated T cells, and terminally differentiated B cells (plasma cells) (3–6). Other reactive cells include NK cells, monocytes, macrophages, dendritic cells, and some epithelial cells. The CD38 antigen acts mainly as a $NAD(P)^+$ glycohydrolase (7) and plays a role in lymphocyte activation (3, 8). However, CD38 may also act as an ectocyclase that converts NAD^+ to the Ca^{2+}-releasing second messenger cyclic ADP-ribose (9). Moreover, intracellularly expressed CD38 may catalyze NAD^+/cyclic ADP-ribose conversion to cause cytosolic Ca^{2+} release (10), and CD38 may control neutrophil chemotaxis to bacterial chemoattractants through its production of cyclic ADP-ribose (11).

Plasma membranes of many cell types, including T cells, contain specialized microdomains, or lipid rafts, enriched in sphingolipids, cholesterol, sphingomyelin, and glycosylphosphatidylinositol-anchored proteins. These membrane domains are characterized by detergent insolubility at low temperatures and low buoyant density. Based on these biochemical properties, they are often referred to as glycosphingolipid-enriched membranes or detergent-insoluble glycolipid fractions (12, 13). Several signaling proteins are enriched in lipid rafts. Src family kinases and the adaptor protein LAT,[1] both of which require acylation for raft targeting, are constitutively present in rafts. The densely packed, liquid-ordered environment of rafts excludes most integral membrane proteins. However, antibody-mediated clustering can recruit receptors on several cell types to rafts. These include some components of the TCR-CD3 complex (14–17), BCR (18–20), FcεRI (21), CD20 (22), and human CD2 (23). Other transmembrane proteins seem to be constitutively associated with rafts as CD44, CD5, CD9, and murine CD2 (24–26).

Recent data, however, demonstrate that in resting T cells 10–20% of the TCR-CD3 complex partitions into rafts that are resistant to solubilization in 1% Brij 98 at 37 °C (27), which suggests that part of the TCR-CD3 complex is constitutively associated with lipid rafts. Our previous data led to the proposition that in T cells CD38 requires the TCR-CD3 complex for signaling (28, 29). In addition, we have demonstrated that Lck,

* This work was supported in part by Instituto Carlos III-FIS, Ministerio de Sanidad y Consumo Grant 01/1073, Consejería de Salud de la Junta de Andalucía Grant 209/02 (to M. Z.), CICYT Grants SAF99-0024 and SAF2002-00721 (to J. Sancho), AIRC (Milano, Italy), TELETHON (Roma, Italy), Biotecnologia (CNR, Roma, Italy), and by the AIDS and TB projects (ISS, Rome, Italy) (to F. M.). The costs of publication of this article were defrayed in part by the payment of page charges. This article must therefore be hereby marked "*advertisement*" in accordance with 18 U.S.C. Section 1734 solely to indicate this fact.

§ Supported by Fellowship I3P from Fondo Social Europeo and Fellowship FPI from the Ministerio de Ciencia y Tecnología, Spain.

¶ Supported by Contract I3P from Fondo Social Europeo.

‖ Supported by Fellowship from CICYT Grant SAF2002-00721.

§§ Supported by a Contrato de Investigadores del Plan Nacional de Salud from the Ministerio de Sanidad y Consumo, and a contract of the program "Ramón y Cajal" from the Ministerio de Ciencia y Tecnología, Spain. To whom correspondence should be addressed: Instituto de Parasitología y Biomedicina, Consejo Superior de Investigaciones Científicas, Ventanilla, 11, 18001 Granada, Spain. Tel.: 34-958805182; Fax: 34-958203911; E-mail: mzubiaur@ipb.csic.es.

[1] The abbreviations used are: LAT, linker for activation of T cells; TCR, T cell antigen receptor; PI, phosphatidylinositol; ZAP-70, ζ-associated protein-70; Erk, extracellular signal-regulated protein kinase; Tyr(P), phosphotyrosine; mAb, monoclonal antibody; PVDF, polyvinylidene difluoride; ODG, octyl D-glucoside or *n*-octyl β-D-glucopyranoside; ECL, enhanced chemiluminescence; HRP, horseradish peroxidase; FITC, fluorescein isothiocyanate-conjugated; αmo, $F(ab')_2$ Goat anti-mouse IgG; GM1, Galβ1–3GalNacβ1–4Gal(3–2αNeuAc)β1–4Glcβ1–1-Cer; Sos, Son of Sevenless; RBD, Ras-binding domain; GST, glutathione *S*-transferase.

which partitions into rafts, is required for CD38-mediated signaling (30), and CD38 itself is constitutively associated with lipid rafts resistant to solubilization in 1% Nonidet P-40 at 4 °C (31). Moreover, upon CD38 cross-linking, a number of proteins are tyrosine-phosphorylated including ZAP-70 and LAT (30, 31). These studies suggested that rafts and the proteins associated or targeted to them as the TCR-CD3, Lck, ZAP-70, and LAT could be involved in CD38 signaling. However, a key issue remained unclear: how is CD38 ligation coupled to activation events in rafts? Does CD38 ligation induce coalescence of membrane rafts, and does such aggregation facilitate the transactivation of the raft-associated Lck, thereby initiating the intracellular cascades, or is CD38 and a fraction of the TCR-CD3 complex constitutively present in a subset of rafts where they co-localize and physically interact?

A major concern about rafts isolated by 1% Triton X-100 or 1% Nonidet P-40 at 4 °C is that they are large vesicles of 0.5 and 1 μm in diameter, which probably results from the coalescence of segregated raft units (32). Therefore, it is difficult to interpret data on protein composition of raft subsets. However, the size of 1% Brij 98-resistant vesicles isolated at 37 °C is rather small (67 ± 39 nm) (27), which is quite close to the size (~50 nm in diameter) of circular raft patches estimated by photonic force microscopy in living fibroblasts (33) or to the size of glycosylphosphatidylinositol-anchored protein domains (less than 70 nm in diameter) measured by fluorescence resonance energy transfer microscopy in living Chinese hamster ovary cells (34). Moreover, Brij 98 vesicles are very stable, and once isolated from different cell membranes they do not coalesce (27). If a circular raft patch has a radius of about 30 nm and thus occupies 2827 nm^2, it follows that a Brij 98 vesicle on average should harbor about 1 separate raft unit, which theoretically would allow it to immunoisolate homogeneous raft subsets. Indeed, raft subsets with different protein compositions from the same membrane could actually be isolated (27).

In the present study, using 1% Brij 98 at 37 °C to isolate raft from Jurkat T cells, we have demonstrated the existence of at least three types of Brij 98-resistant raft subsets: CD38 rafts, which are enriched in CD38, CD3-ζ, and Lck; TCR/CD3 rafts, which are enriched in CD3-ζ, CD3-ϵ, and Lck; and LAT rafts, which are primarily enriched in Lck. Indeed, immunoisolated Lck rafts retrieve all the above proteins, which is in agreement with its presence in all raft subsets studied so far. Our results further indicated that following stimulation of CD38, LAT and Lck are tyrosine-phosphorylated exclusively in Brij 98-resistant rafts, and many key components of signaling pathways that are regulated by CD38 translocate into rafts (*i.e.* Sos and p85 PI 3-kinase). Moreover, N-Ras is found in its activated state within rafts upon CD38 stimulation. Furthermore, full phosphorylation of CD3-ζ and CD3-ϵ only occurs in rafts, whereas c-Cbl tyrosine phosphorylation occurs exclusively in non-raft fractions. Taken together, these data provide new insights in how rafts take part in CD38 signal transduction.

EXPERIMENTAL PROCEDURES

Cell Lines—Jurkat D8 cells, which constitutively express CD38, were obtained from wild-type Jurkat cells (subclone E6-1, American Tissue Culture Collection (ATCC), Manassas, VA) by the limiting dilution technique (35). The Lck-deficient Jurkat T cell variant JCaM1.6 (36) was kindly provided by Dr. Arthur Weiss (University of California, San Francisco).

Antibodies and Reagents—Anti-human CD3-ϵ mAb OKT3 (IgG2a) or the CD38 mAbs HB136 (IgG1) and OKT10 (IgG1) were prepared and purified by affinity chromatography on HiTrap protein A or HiTrap protein G HP column, respectively, using the ÄKTA explorer system (Amersham Biosciences) as described (28). Anti-human CD38 mAb IB4 (IgG2a) was prepared and purified by affinity chromatography on protein A-Sepharose and high pressure liquid chromatography on hydroxyapatite columns, as described (37). Anti-human CD3-ζ mAb 1D4.1 is directed against the C-terminal portion of CD3-ζ, and it has been described previously (38). Affinity-purified, fluorescein isothiocyanate-conjugated (FITC) $F(ab')_2$ fraction of rabbit antibody to mouse immunoglobulins ($F(ab')_2$ FITC-RαmIg) was purchased from Dako (Glostrup, Denmark). Affinity-purified $F(ab')_2$ fraction of goat antibody to mouse IgG (whole molecule) ($F(ab')_2$ GαmIg) was purchased from Cappel (ICN Pharmaceuticals, Inc., Costa Mesa, CA). Recombinant anti-Tyr(P) antibody coupled to horseradish peroxidase (RC20-HRP), anti-Sos1 mAb, and anti-p85 PI 3-kinase mAb were obtained from BD Biosciences. The anti-phospho-p44/42 mitogen-activated protein kinase (Thr-202/Tyr-204) E10 mouse mAb was purchased from Cell Signaling Technology (New England Biolabs, Beverly, MA). The following affinity-purified rabbit polyclonal antibodies were purchased from Santa Cruz Biotechnology (Santa Cruz, CA): anti-Erk-2, anti-ZAP-70, anti-Vav, anti-Sos, anti-Cbl, anti-p85α PI 3-kinase, and the affinity-purified mouse monoclonal antibody anti-Lck 3A5 mAb. An affinity-purified rabbit antibody to CD3-ϵ was purchased from Dako (Denmark). Polyclonal antibodies anti-LAT and anti-Lck (N-terminal) were from Upstate Biotechnology, Inc. Anti-Zap-70 (Zap-4) rabbit antiserum was a kind gift from Dr. S. C. Ley (Medical Research Council, London, UK) (30). Anti-CD3-ζ antiserum 448 was a gift from Dr. B. Alarcón (Centro de Biología Molecular, CSIC, Madrid, Spain). Affinity-purified goat anti-rabbit IgG (Fc) HRP conjugate and goat anti-mouse IgG (H+L) HRP conjugate were from Promega (Madison, WI). Prestained SDS-PAGE standards (broad and precision range), and ImmunoStart reagents were from Bio-Rad. The cholera toxin HRP-conjugated and the anti-actin mAb, AC40, were purchased from Sigma. Protein G-Sepharose 4 Fast Flow and ECL reagents were from Amersham Biosciences. Raf-1 Ras-binding domain agarose conjugate, anti-Ras (clone RAS 10, mouse monoclonal IgG2a-κ), was purchased from Upstate Biotechnology, Inc. μMACS protein G Microbeads, μMACS Separator, and μColumns were purchased from Miltenyi Biotec (Germany).

Fluorescence-activated Cell Sorter Analysis—Cells were analyzed for surface expression of CD3 and CD38 by flow cytometry as described previously by using saturating concentrations of the unlabeled primary mouse mAbs and of the $F(ab')_2$ FITC-RαmIg secondary antibody (30). Samples were analyzed in a FACScan flow cytometer (BD Biosciences), using the CellQuest Software. Under these conditions the primary antibody binds to the cell surface antigen monovalently; therefore, the number of bound antibody molecules corresponds to the number of antigenic sites (39). In experiments on peripheral blood binding of anti-CD38 mAbs tend to be exclusively monovalent when CD38 antigen density is low but partially bivalent at higher CD38 densities (40). Therefore, these estimates may be incorrect by as much as a factor of 2. However, the ratio between the median fluorescence intensities of CD3 and CD38 was constant from experiment to experiment, because the same Jurkat line was used throughout the study, and because saturating concentrations of the mAbs were used.

Detergent Solubilization of Cells at 37 °C—Cells (7–9 × 10^7) were washed twice in ice-cold RPMI/HEPES, resuspended in 0.45 ml of ice-cold 1× lysis buffer (20 mM HEPES, pH 7.6, 150 mM NaCl, 1 mM EGTA, 50 mM sodium fluoride, 1 mM sodium orthovanadate, 20 μM phenylarsine oxide, 1 mM phenylmethylsulfonyl fluoride, 10 mM iodoacetamide, and a mixture of small peptide protease inhibitors at 1 μg/ml each) without detergent to disrupt the cells (30), quick-frozen on dry ice, and then thawed on ice. Broken cells were homogenized by shearing through a 25-gauge needle with a 1-ml syringe, 10 times, on ice (41). The particulate suspension was preincubated for 4 min at 37 °C. 50 μl of a 10% Brij 98 (Sigma) stock solution in 20 mM HEPES, pH 7.4, was then added to bring a final concentration of 1% Brij 98. After 5 min of solubilization at 37 °C, the lysate was quick-frozen on dry ice and kept at −80 °C until use. Before the sucrose gradient centrifugation, lysates were thawed on ice and then diluted with 0.5 ml of lysis buffer containing 80% sucrose (final sucrose concentration 40%; final Brij 98 concentration 0.5%) and incubated on ice for 50 min (27). Samples were then placed at the bottom of a discontinuous sucrose gradient and fractionated as described below.

Fractionation of Detergent-insoluble and -soluble Fractions by Sucrose Gradient Ultracentrifugation—Detergent-insoluble and -soluble fractions were separated as described (31) with some modifications. Cell lysates were mixed with an equal volume of 80% sucrose and transferred to Sorvall ultracentrifuge tubes. Two ml of 30% sucrose, followed by 1 ml of 5% sucrose in 1× lysis buffer without detergent, were overlaid. All the sucrose solutions were prepared in 1× lysis buffer without detergent and in the presence of small peptide protease inhibitors at 1 μg/ml each, (30). Samples were centrifuged for 18–20 h at 200,000 × *g* in a Sorvall AH-650 rotor. Eight fractions of 0.5 ml each were collected on ice, from the top to the bottom of the gradients. 18-μl

aliquots of each fraction of the gradient was diluted with 9 μl of 3× Laemmli sample buffer and resolved on 12.5% SDS-PAGE under non-reducing conditions, transferred to PVDF, and immunoblotted with specific antibodies. Ganglioside GM1, which migrated with the dye front on a 12.5% SDS-PAGE gel, was detected by blotting with cholera toxin-HRP conjugated following by the ECL system.

In indicated experiments two pools of the sucrose gradient fractions were then collected. First was the low density fractions corresponding to the 5/30% interface (fractions 2 and 3, along fraction 4) and referred to as rafts. Second was the high density soluble material corresponding to fractions 7 and 8 of the gradient and referred to as soluble. Except where otherwise indicated, 18 μl of each pool were diluted with 9 μl of 3× Laemmli sample buffer and loaded onto gels. In indicated experiments proteins of each fraction of the gradient were concentrated by methanol/chloroform precipitation as described (31).

Immunoisolation of Raft Subsets under Non-solubilizing Conditions—Pooled sucrose gradient fractions 2–4 (rafts) or fractions 7–8 (soluble) were diluted with lysis buffer containing 1% Brij 98 to less than 20% sucrose. To avoid variability inherent to each sucrose gradient centrifugation, the rafts or soluble fractions from six different sucrose gradients were pooled and then divided into 6 aliquots for the immunoisolation experiments with anti-CD38, anti-Lck, anti-CD3-ζ, anti-CD3-ϵ, anti-LAT, or isotype-matching antibodies. After 1 h of incubation on ice with specific mAbs, 50–100 μl of protein G superparamagnetic microbeads (Miltenyi Biotec S. L. (Spain)) were added and mixed well, and the mixture was incubated for an additional 45 min on ice. Subsequently, the magnetically labeled raft subsets were passed over μColumns placed in the magnetic field of the μMACS separator following the manufacturer's specifications. The columns were then rinsed twice with 200 μl of 1% Brij 98 lysis buffer, followed 2 times by 200 μl of Solution A (0.5% Brij 98 lysis buffer), 1 time by 200 μl of Solution B (0.01% Brij 98 lysis buffer), and 1 time by 200 μl of low salt wash buffer (20 mM Tris-HCl, pH 7.5). The immunoisolated raft subsets were then eluted with 20 + 50 μl of pre-heated 95 °C hot 1× SDS gel sample buffer and the collected second eluate (50 μl) was analyzed by SDS-PAGE and Western blotting. The data shown are representative of three independent experiments.

Immunoprecipitation under Solubilizing Conditions—Pooled rafts and soluble sucrose gradient fractions were diluted with lysis buffer containing 1% Brij 98 + 60 mM ODG to less than 20% sucrose. ODG is a gentle non-ionic detergent that is very efficient in solubilizing proteins associated with rafts (42–45). Immunoprecipitation of protein assemblies was performed by incubation of these fractions with specific antibodies followed by capture of the immune complexes on protein G superparamagnetic microbeads as described above or on protein G-Sepharose 4 Fast Flow beads (Amersham Biosciences) as described elsewhere (30).

Cell Stimulation and Western Blotting—Cells were grown up to a density of 0.5–1 × 10^6/ml, centrifuged, and serum-starved in RPMI/HEPES + 0.1% fetal bovine serum 15–20 h. The cells were then washed twice in RPMI/HEPES without serum and resuspended at 4–9 × 10^7 cells per sample, or as otherwise indicated, in serum-free RPMI/HEPES medium at 4 °C. Stimulation with anti-CD38 mAbs, lysis, and Western blotting analyses were performed as described in detail elsewhere (30). Densitometric analysis was performed on a MacIntosh computer using the public domain NIH Image program version 1.62 (developed at the National Institutes of Health and available at rsb.info.nih.gov/nih-image/) or on a personal computer using the Quantity One–dimensional Analysis Software version 4.4 (Bio-Rad).

Affinity Assay for Ras Activation in Postnuclear Supernatants—D8 Jurkat T cells were grown and stimulated as described. Cells were then lysed in ice-cold 2× Mg^{2+} lysis buffer (50 mM HEPES, pH 7.5, 300 mM NaCl, 2% Igepal CA-630, 20 mM $MgCl_2$, 2 mM EDTA, 4% glycerol, 20 μg/ml aprotinin, 20 μg/ml leupeptin, 50 mM sodium fluoride, and 2 mM sodium orthovanadate) for 30 min. Postnuclear supernatants were obtained by centrifugation at 13,000 × *g* for 15 min at 4 °C. Activated Ras was assayed on equivalent amounts of lysates from unstimulated or anti-CD38-stimulated cells. The lysates were incubated with GST-Raf1-RBD (Ras-binding domain) as specified by the manufacturer (Upstate Biotechnology, Lake Placid, NY). Proteins were eluted with 3× Laemmli reduced sample buffer and applied to either a 12.5 or a 15% SDS-PAGE under reducing conditions. Proteins were transferred to a PVDF membrane, blocked at room temperature for 1 h in 5% milk, and probed with anti-Ras antibody overnight at 4 °C (clone RAS 10) (46). Total Ras was measured by anti-Ras immunoblot analysis of an aliquot of the postnuclear lysate followed by an HRP-conjugated anti-mouse secondary. Proteins were detected using enhanced chemiluminescence (ECL System, Amersham Biosciences, or ImmunoStart System from Bio-Rad).

Affinity Assay for Ras Activation in Raft and Soluble Fractions—Pooled raft and soluble fractions from 4 to 5 × 10^6 unstimulated or anti-CD38-stimulated Jurkat T cells were diluted with 1× Mg^{2+} lysis buffer to bring the sucrose concentration to less than 20%. Samples were then incubated with GST-RBD and processed as above.

Statistical Analysis—Statistical analysis were performed using the Student's *t* test parametric) to compare sample groups. *p* values less than 0.05 were considered significant.

RESULTS

Isolation and Characterization of CD38-containing Brij 98-insoluble Raft Microdomains—In this study we used Jurkat T cells, which constitutively express CD38 (30) (Fig. 1*A*), to test whether CD38-mediated signaling is initiated within rafts. We first investigated whether CD38 is associated with the membrane raft vesicles that are recovered as detergent-insoluble complexes upon solubilization of cells in Brij 98 at 37 °C. This detergent has a hydrophilic-lipophilic balance of 15.3 mM, and it has been successfully used to selectively isolate detergent-insoluble microdomains at 37 °C exhibiting the expected biochemical characteristics of rafts (27). Jurkat T cells were lysed in 1% Brij 98 at 37 °C as described under "Experimental Procedures," and the lysates were fractionated into supernatant and pellet after centrifugation at 13,000 × *g* for 15 min. As shown in Fig. 1*B*, only about 42% of CD38 was found in the supernatant (*lane 1*), and therefore, most CD38 was found precipitated in the pellet (*lane 3*). These results demonstrated that a large fraction of CD38 was insoluble in Brij 98 at 37 °C and strongly suggested that CD38 was associated with Brij 98-resistant lipid rafts. However, insolubility of a membrane protein in a non-ionic detergent could be due to its association with detergent-resistant lipid rafts and/or its anchoring to cytoskeletal elements. To distinguish between these two possibilities, we used ODG, which is a gentle non-ionic detergent that is very efficient in solubilizing proteins associated with glycolipid-enriched membranes, and it does not disrupt the cytoskeleton (42–45). As shown in Fig. 1*B, lane 2*, in cells lysed in 1% Brij 98 in the presence of 60 mM ODG about 98% of CD38 was recovered in the supernatant upon centrifugation at 13,000 × *g* for 15 min, which indicated that CD38 was almost entirely solubilized by ODG. Therefore, the efficiency of ODG to solubilize CD38 supports the conclusion that its insolubility in Brij 98 is due to raft association and not to cytoskeleton interactions.

To confirm this, raft membranes were isolated from Jurkat T cells by using a flotation assay based on resistance to solubilization by Brij 98 at 37 °C (27), and buoyancy at low density fractions of a bottom-loaded discontinuous sucrose gradient, with steps of 5, 30, and 40% sucrose (31). As shown in Fig. 1*C*, most of the transmembrane proteins CD38 and LAT, the intracellular membrane-bound Lck, and the ganglioside GM1 partitioned into low density fractions 2–4, which is consistent with its residency in floating lipid rafts or glycolipid-enriched membranes. Thus, densitometric analysis showed that the CD38 present in rafts was composed of 62.2 ± 3.7% of the total CD38, whereas the CD38 present in soluble fractions 7–8 was 35.0 ± 3.9% of total CD38 ($p < 0.006$, $n = 10$, Table I). Likewise, 73.9 ± 4.7% of total GM1 localized to rafts, whereas only 13.1 ± 2.5% was in soluble fractions ($p < 0.00001$, $n = 10$, Table I). Moreover, about 84% of Lck, 75% of LAT, and less than 30% of CD3-ζ and CD3-ϵ were enriched in floating rafts. In contrast, about 10% of ZAP-70 and none of actin or Cbl were detected in those fractions (Fig. 1*C*, and data not shown). These low density fractions contained only about 2% of total proteins found in the whole sucrose gradient (Fig. 1*D*); therefore they were highly enriched in proteins associated with lipid rafts.

We next examined how ODG affected the recovery of CD38, CD3-ζ, CD3-ϵ, LAT, Lck, and the ganglioside GM1 in floating

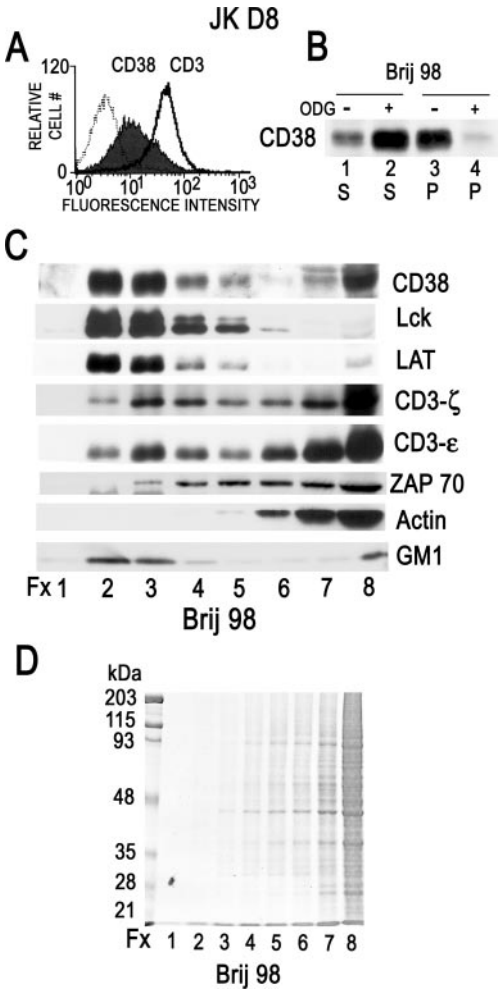

FIG. 1. **Isolation and characterization of CD38-containing detergent-insoluble membrane microdomains using Brij 98 at 37 °C.** *A*, the surface expression of CD3 and CD38 was analyzed by indirect immunofluorescence staining with saturating concentrations of both primary and secondary antibodies. Thus, Jurkat D8 cells were incubated with the anti-human CD3-ϵ mAb OKT3 (*open histogram*, *continuous line*) or with the anti-human CD38 mAb HB136 mAb (*filled histogram*), followed by incubation with $F(ab')_2$ FITC-anti-mouse IgG secondary antibody. Representative flow cytometric profiles are shown. Negative controls were obtained after staining with an isotype-matching unrelated mAb plus a secondary antibody (*open histogram*, *dotted line*). Flow cytometric data are presented as the logarithm of fluorescence intensity. Median fluorescence intensity after subtraction of the fluorescence detected with an isotype-matched control was 38.02 and 7.74 for CD3 and CD38, respectively. The data shown are representative of more than 20 independent experiments. *B*, Jurkat T cells were lysed in 1% Brij 98-containing lysis buffer at 37 °C for 5 min (−) or with 1% Brij 98 in the presence of 60 mM ODG (+). Cell lysates were fractionated into a supernatant of soluble proteins (*S*) and a pellet (*P*) of insoluble proteins by centrifugation at 13,000 × *g* for 15 min at 4 °C, as described under "Experimental Procedures." Proteins were separated on 11% SDS-PAGE under non-reducing conditions, and upon transference to PVDF membranes were immunoblotted with the anti-CD38 mAb HB136. Blot in *B* was scanned, and CD38 bands were quantified using the NIH Image program 1.62 version. CD38 in either the supernatant or in the pellet was expressed as percentage of total (sum of supernatant plus pellet). The numbers are as follows: 42% (*lane 1*), 98% (*lane 2*), 58% (*lane 3*), and 2% (*lane 4*). The data shown are representative of three independent experiments. *C*, Jurkat T cells were lysed in 1% Brij 98-containing lysis buffer at 37 °C for 5 min and fractionated on a sucrose gradient as described under "Experimental Procedures." Eight fractions of 0.5 ml were collected from the top to the bottom of the gradient. 18-μl aliquots of each fraction of the gradient were diluted with 9 μl of 3× Laemmli non-reducing sample buffer, and the resulting 27 μl were resolved on 12.5% SDS-PAGE under non-reducing conditions, transferred to PVDF, and blotted with specific antibodies against the indicated proteins to the *right of each panel*. Ganglioside GM1, which migrated with the dye front of the 12.5% SDS-PAGE gel, was detected by blotting with cholera toxin-HRP conjugated by following the ECL system. A representative experiment is shown from more than 10 independent experiments. Blots in *C* were scanned, and protein bands were quantified using the NIH Image program 1.62 version. The percentage of each protein that migrated to low and high density fractions is shown in Table I. *D*, an 18-μl aliquot of each gradient fraction was resolved on SDS-PAGE as above and stained with Coomassie Blue. The gel was scanned and protein bands were quantified using the NIH Image version 1.62 software system. A representative experiment is shown from five independent experiments. The results were confirmed by analyzing the same fractions in solution with the Bio-Rad colorimetric protein assay (data not shown).

rafts by treating the Brij 98 lysates with 60 mM ODG before gradient centrifugation. As shown in Table I, ODG dissociated >50% of CD38, LAT, and GM1 from the top fractions, whereas Lck was less affected (about 28% of Lck moved out of the raft fractions). Note, however, that only 43% of CD38 migrated to high density fractions 7–8 upon ODG treatment, despite the fact that same treatment yielded little pelletable CD38 upon centrifugation at 13,000 × *g* (Fig. 1*B*). Likewise, ODG seemed not to affect the recovery of CD3-ζ or CD3-ϵ in the low density fractions, although there was a small but highly reproducible reduction in the percentage of these proteins found in the high density fractions 7–8 (Table I). These apparent contradictions were caused by the appearance in fractions 5–6 of CD38, CD3-ζ, and CD3-ϵ forms of greater buoyant density than those floating to fractions 2–4 but with lower densities than those remaining in fractions 7–8 (data not shown). These data suggest that ODG caused partial solubilization with the appearance of less buoyant CD38, CD3-ζ, and CD3-ϵ complexed with sphingolipid and other lipids in non-vesicular form (47), or forming vesicles of smaller size (nanovesicles) with a distinct cholesterol/lipid environment than that in fractions 2–4 (48). Therefore, ODG altered the buoyant properties of CD38, CD3-ζ, and CD3-ϵ shifting to intermediate densities.

Lck and the TCR-CD3 Complexes Are Specifically Concentrated in Anti-CD38 Immunoisolated Rafts—We next examined whether the CD3 subunits and Lck are located within the same raft subset as CD38. To this end, CD38-containing rafts were immunoisolated from the total pool of Brij 98-resistant raft fractions with μMACS protein G Microbeads as described under "Experimental Procedures." Then the immunoisolated rafts bound to the anti-CD38-coated magnetic beads were analyzed biochemically. Western blot analysis showed that nonspecific binding of CD38 to an irrelevant isotype-matching mouse mAb (IgG1) was about 1% of the total amount of CD38 in the pooled raft fractions 2–4, whereas its specific binding to the anti-CD38 mAb OKT10 was about 38%, which suggested a substantial enrichment over the amount in the pooled raft fraction (data not shown), despite the fact that these experiments were done in antigen excess according to the manufacturer's specifications. Similar analysis showed that Lck, CD3-ζ, CD3-ϵ, and LAT were also detected in rafts immunoisolated with the anti-CD38 mAb, OKT10 (Fig. 2*A*, *lane 1*), although there was a hierarchy of binding, Lck > CD3-ζ ≫ CD3-ϵ ≥ LAT. Binding of CD3-ϵ and LAT to OKT10 was considered nonspecific because it was in the range of that bound to the irrelevant isotype-matching mAb (0.2–0.8%). Then, we examined the protein composition of the rafts immunoisolated with anti-Lck, anti-CD3-ζ, anti-CD3-ϵ, or anti-LAT antibodies. The data showed that Lck, CD38, and CD3-ζ were readily detected in rafts immunoisolated with the anti-Lck mAb 3A5 (Fig. 2*A*, *lane 2*). Likewise, CD3-ζ, CD38, and Lck were clearly present in rafts immunoisolated with the anti-CD3-ζ mAb 1D4.1 (Fig. 2*A*, *lane 3*). Moreover, significantly higher amounts of LAT were detected in Lck- than in CD3-ζ-immunoisolated rafts (Fig. 2*A*, *lanes 2* and *3*, respectively). Regarding CD3-ϵ rafts immunoiso-

TABLE I

Effects of detergents Brij 98 or ODG on the floatability of cell surface and intracellular membrane-associated molecules

Jurkat T cells were lysed in 1% Brij 98 or in 1% Brij 98 + 60 mM ODG before sucrose gradient centrifugation as described under "Experimental Procedures." 0.5-ml fractions were collected, and aliquots of each fraction were analyzed by Western blot for the indicated proteins or ganglioside GM1. Densitometric data on rafts (fractions 2–4) and soluble (fractions 7–8) pools are presented as percentage of the sum of all sucrose gradient fractions (fractions 1–8).

	Rafts		Soluble	
	Brij 98	Brij 98 + ODG	Brij 98	Brij 98 + ODG
CD38	62.2 ± 3.7[a]	28.7 ± 0.2[b]	35.0 ± 3.9[a]	43.2 ± 1.7[b]
Lck	83.7 ± 4.0[c]	59.8 ± 9.4[b]	6.2 ± 3.2[c]	20.7 ± 14.4[b]
LAT	75.1 ± 13.6[c]	25.5 ± 5.0[b]	20.3 ± 11.4[c]	54.3 ± 2.0[b]
CD3-ζ	22.6 ± 2.0[c]	23.4 ± 2.4[b]	61.9 ± 1.4[c]	49.9 ± 2.1[b]
CD3-ε	26.8 ± 6.5[c]	31.3 ± 6.4[b]	54.6 ± 7.8[c]	40.5 ± 6.1[b]
GM1	73.9 ± 4.7[a]	36.6 ± 3.2[b]	13.1 ± 2.5[a]	37.3 ± 5.7[b]

[a] The data are the means ± S.E. of 10 independent experiments.
[b] The data are the means ± S.E. of 2 independent experiments.
[c] The data are the means ± S.E. of 3 independent experiments.

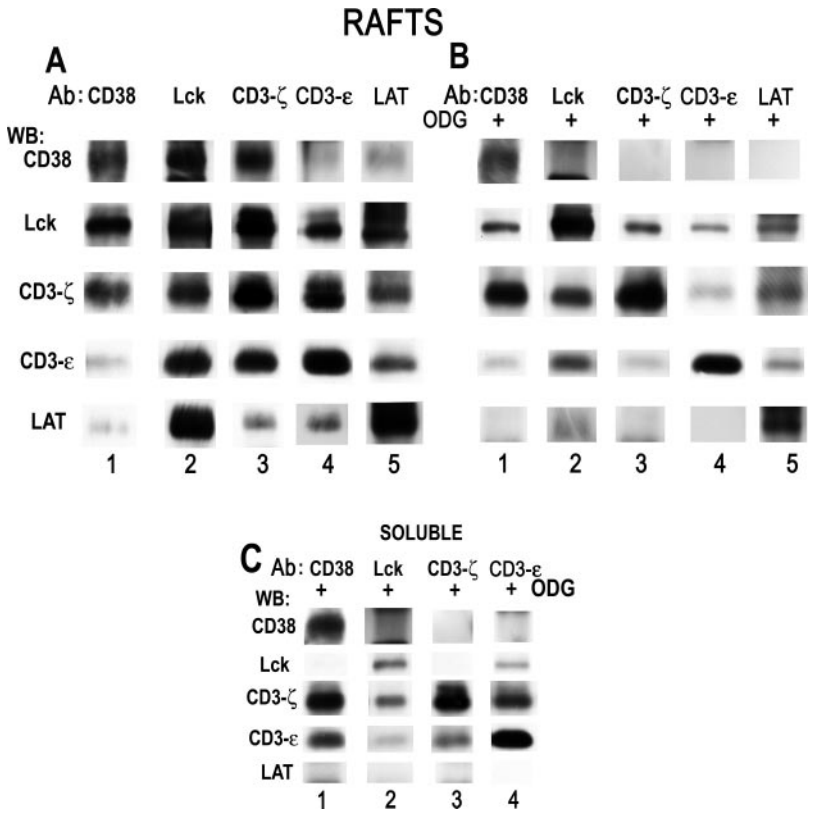

FIG. 2. **Lck and CD3-ζ are associated with CD38 in membrane rafts.** *A*, Jurkat T cells were lysed in 1% Brij 98 at 37 °C for 5 min. Rafts were isolated by sucrose gradient ultracentrifugation, and pooled fractions 2–4 were resuspended in 1% Brij 98 lysis buffer. The raft subsets enriched in CD38 (*lane 1*), Lck (*lane 2*), CD3-ζ (*lane 3*), CD3-ϵ (*lane 4*), or LAT (*lane 5*) were immunoisolated with specific antibodies (*Ab*) and μMACS protein G microbeads as described under "Experimental Procedures." Immunoisolates were separated on 11% SDS-PAGE gels under non-reducing conditions and blotted with the indicated antibodies. The amount of CD38, Lck, CD3-ζ, CD3-ϵ, or LAT in the corresponding immunoisolates was estimated by comparison with the total amount of each protein recovered in the pooled raft fractions 2–3, and ranged from 22% for Lck up to 51% for CD3-ϵ. Nonspecific binding to an isotype-matched mouse immunoglobulin (IgG1) ranged from 0.1 to 1%. *WB*, Western blot. *B*, pooled raft fractions isolated as in *A* were prepared and treated for raft solubilization with 1% Brij 98 + 60 mM ODG lysis buffer before being subjected to immunoprecipitation with anti-CD38 (*lane 1*), anti-Lck (*lane 2*), anti-CD3-ζ (*lane 3*), anti-CD3-ϵ (*lane 4*), or anti-LAT (*lane 5*) mAbs bound to μMACS protein G microbeads. Immunoprecipitates were blotted with the indicated antibodies. *C*, soluble fractions were prepared and treated as in *B* with 1% Brij 98 + 60 mM ODG before being subjected to immunoprecipitation with anti-CD38 (*lane 1*), anti-Lck (*lane 2*), anti-CD3-ζ (*lane 3*), or anti-CD3-ϵ (*lane 4*) mAbs bound to μMACS protein G microbeads. Immunoprecipitates were blotted with the indicated antibodies. The data shown are representative of at least three independent experiments.

lated with the anti-CD3-ϵ mAb OKT3, CD3-ζ was the major protein co-isolated, following by Lck, with relatively weaker detection of LAT and CD38 (Fig. 2*A*, *lane 4*). This correlated with the fact that CD3-ϵ was readily detected in both Lck- and CD3-ζ-immunoisolated rafts (Fig. 2*A*, *lanes 2* and *3*) showed intermediate levels in LAT rafts and was weakly detected in CD38-immunoisolated ones (Fig. 2*A*, *lanes 1* and *5*, respectively).

The higher level of Lck relative to LAT in CD3-ζ- and CD3-ϵ-immunoisolated rafts indicated that TCR-CD3 raft distribution in Jurkat T cells was very similar to that in the murine T cell line 3A9 lysed in Brij 98 (27). Of note is that LAT was readily detected in Lck rafts and vice versa Lck was clearly present in LAT rafts, whereas the amount of the other proteins was significantly higher in Lck rafts than in LAT rafts (Fig. 2*A*, *lanes 2* and *5*), which is in agreement with the strong presence of Lck in all raft subsets studied so far and suggesting that Lck is the linker that keeps most of these proteins together.

ODG Extraction Reveals Distinct Protein Assemblies within Rafts, Which Differ in Their Requirements for Stable Association—To examine whether the protein assemblies detected in immunoisolated rafts correspond to protein-protein interactions or whether they are dependent on the raft integrity, pooled low density Brij 98-resistant raft vesicles were resuspended in a buffer containing 1% Brij 98 + 60 mM ODG, which efficiently disrupts many lipid raft-protein associations (see Table I). Then either CD38, Lck, CD3-ζ, CD3-ϵ, or LAT was immunoprecipitated with specific antibodies bound to μMACS protein G microbeads as described above, and the retrieved proteins were detected by Western blot analysis (Fig. 2*B*). Because ODG did not affect much the interaction of Lck with lipid rafts, although greatly affecting the CD38-raft interaction (Table I), it was expected that in ODG-treated raft vesicles the ratio Lck/CD38 would be significantly higher than that in Brij 98-resistant ones. In this sense, CD38 was no longer detectable in the Lck immunoprecipitates from ODG-treated raft vesicles (Fig. 2*B*, *lane 2*), whereas Lck was still detectable in the CD38 immunoprecipitates (Fig. 2*B*, *lane 1*). Note, however, that the relative amount of Lck co-immunoprecipitated with CD38 was significantly reduced as compared with that in the intact raft vesicles (Fig. 2, *B* and *A*, *lane 1*). These data were in accordance with the reduced amount of CD38 that still remained associated with raft fractions upon ODG treatment (Table I) and therefore susceptible to interact with Lck, or being part of the same raft subset. Likewise, in the presence of ODG LAT was no longer detected in CD3-ζ or CD3-ϵ immunoprecipitates (Fig. 2*B*, *lanes 3* and *4*, respectively), and vice versa, low amounts of CD3-ζ and CD3-ϵ were co-immunoprecipitated with LAT (Fig. 2*B*, *lane 5*). Again, these data correlated with the ability of ODG to selectively disrupt raft-LAT association, whereas the association of either CD3-ζ or CD3-ϵ with lipid rafts was less affected (Table I).

Other protein assemblies were affected by the presence of ODG but not completely disrupted. Thus, lower amounts of LAT was co-immunoprecipitated with Lck as compared with that in Brij 98 alone (Fig. 2, *B versus A*, *lane 2*), and vice versa a lower amount of Lck was detected in LAT immunoprecipitates than that in Brij 98 (Fig. 2, *B versus A*, *lane 5*), which is in agreement with a recent report (49) showing that in Jurkat cells solubilized in 1% Triton X-100 LAT preferentially interacts with the open active form of Lck and weakly with the closed non-active Lck in lipid rafts, the latter being the predominant form in unstimulated Jurkat cells.

On the other hand, in the presence of ODG the associations of Lck with CD3-ζ or with CD3-ϵ were readily detectable, although the relative amounts of CD3-ζ and CD3-ϵ co-immunoprecipitated with Lck were significantly reduced (Fig. 2*B*, *lane 2*) as compared with that in Brij 98 alone (Fig. 2*A, lane 2*). Moreover, CD3-ζ-Lck and CD3-ϵ-Lck interactions were detectable despite much less Lck was co-immunoprecipitated with both CD3 subunits (Fig. 2, *B versus A*, *lanes 3* and *4*).

CD38 Associates with CD3-ζ in Both Raft and Soluble Fractions—Because both the TCR-CD3 complex and CD38 were present in raft and soluble fractions, it was of interest to know whether they could interact in both compartments. The data clearly showed that the presence of ODG did not significantly affect the amount of CD3-ζ co-immunoprecipitated with CD38 in low density fractions (Fig. 2*B*, *lane 1*) as compared with that retrieved in Brij 98-resistant CD38-containing raft vesicles (Fig. 2*A*, *lane 1*). Moreover, CD3-ζ was readily detected in CD38 immunoprecipitates from the non-raft fraction either in the presence of ODG (Fig. 2*C*, *lane 1*) or in Brij 98 alone (data not shown). It is worth noting that although CD3-ϵ was also detected in the CD38 immunoprecipitates from soluble fractions

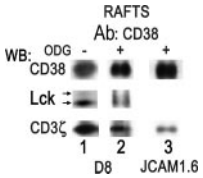

FIG. 3. **CD38 is associated with CD3-ζ in the absence of Lck.** Pooled raft fractions from sucrose gradient from Brij 98 lysates from Jurkat D8 (*lanes 1 and 2*) or JCaM 1.6 cells (*lane 3*) were immunoprecipitated with the anti-CD38 mAb OKT10 in the presence of 1% Brij 98 alone (*lane 1*) or in the presence of 1% Brij 98 + 60 mM ODG (*lanes 2* and *3*) using protein G-bound-Sepharose beads as described previously (30). Immunoprecipitates were separated on 11% SDS-PAGE gels under non-reducing conditions and blotted with the indicated antibodies to the *left of each panel*. The data shown are representative of at least three independent experiments. *WB*, Western blot.

(Fig. 2*C, lane 1*), its concentration in CD38 raft fractions was significantly lower than that of CD3-ζ (Fig. 2, *A* and *B*, *lane 1*), which suggested that, at least in rafts, CD38-CD3-ζ interaction could occur independently of the presence of the other subunits of the TCR-CD3 complex or at other CD3-ζ/CD3-ϵ ratios than that of the TCR-CD3 complex. Moreover, CD38-CD3-ζ association also occurred in soluble fractions were Lck did not co-immunoprecipitate with CD38 (Fig. 2*C*, *lane 1*), and in ODG-solubilized rafts from the Lck-deficient Jurkat variant JCaM 1.6 (Fig. 3, *lane 3*), which strongly suggests that Lck is not required for CD38-CD3-ζ interaction. Together, these results emphasize that the association of CD38 with CD3-ζ can occur outside of raft membrane vesicles and that CD38-CD3-ζ complexes are not artifacts of incomplete solubilization but instead represent discrete units that are capable of being fully solubilized.

However, CD38 was not detected in CD3-ζ immunoprecipitates from either ODG-solubilized rafts or non-raft compartments (Fig. 2, *B* and *C*, *lane 3*), which was a clear discrepancy from the data in intact raft vesicles where CD38 is readily retrieved by CD3-ζ immunoisolates (Fig. 2*A*, *lane 3*), and suggested an interaction of either low affinity or low stoichiometry. Against the low affinity of the CD38-CD3-ζ interaction is the fact that upon extraction with ODG, CD3-ζ is still readily detectable in CD38 immunoprecipitates (Fig. 2*B*, *lane 1*, and Fig. 3, *lane 2*), while almost undetectable in the CD3-ϵ immunoprecipitates (Fig. 2*B*, *lane 4*). Likewise, relatively lower amounts of CD3-ϵ were co-immunoprecipitated with CD3-ζ in the ODG-treated raft compartment (Fig. 2*B*, *lane 3*), as compared with those in Brij 98 alone (Fig. 2*A*, *lane 3*), which suggests that CD38-CD3-ζ interaction has a relatively higher affinity than that of the well established CD3-ϵ-CD3-ζ association (50).

Moreover, it is worth noting that in Jurkat T cells TCR-CD3 surface expression was significantly higher than that of CD38, with a CD3/CD38 ratio of about 5:1 at saturating concentrations of both the anti-CD3-ϵ and anti-CD38 mAbs (Fig. 1*A*), which is indicative of a higher number of surface CD3 molecules than that of CD38. However, because these proteins are not equally distributed in the different cell surface microdomains, the real number of CD3 and CD38 molecules in each microdomain may vary significantly. One might expect that in Brij 98-resistant rafts CD38 and CD3-ζ will be constrained to be close together at a more balanced concentration, and hence they were readily co-isolated independently of the antibody used for immunoisolation (Fig. 2*A*, *lanes 1* and *3*). In contrast, in Brij 98- or ODG-soluble fractions the number of CD3 molecules clearly exceeds those of CD38; therefore, it is expected that a large proportion of CD3-ζ will be associated with receptors other than CD38 (*i.e.* the TCR-CD3 complex), or it will be remain free. Under conditions of large antigen excess, as occurs

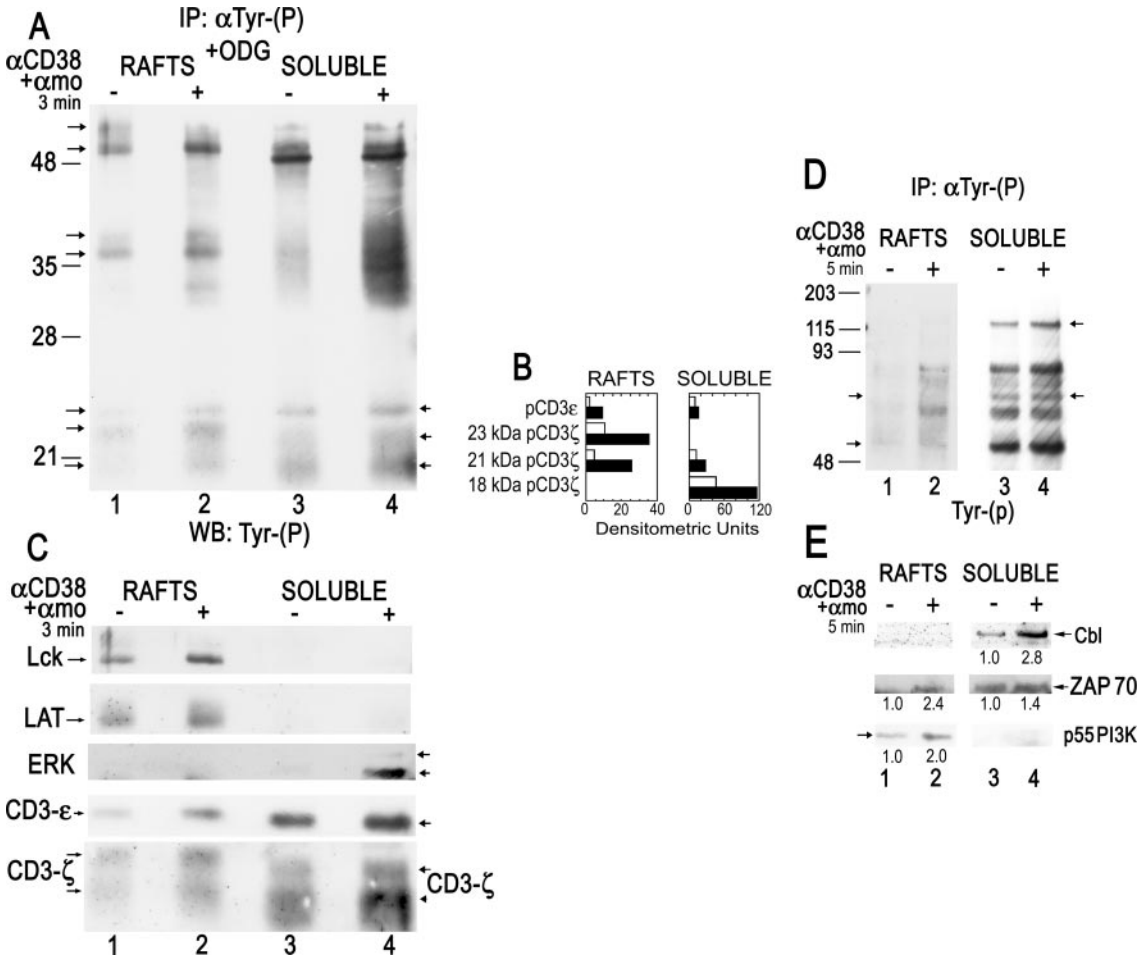

FIG. 4. **Upon CD38 engagement LAT, Lck, CD3-ζ, and CD3-ε tyrosine phosphorylation occurs in rafts, whereas c-Cbl tyrosine phosphorylation occurs in non-raft soluble fractions.** *A*, serum-starved Jurkat D8 T cells were stimulated (+) or not (−) with the anti-CD38 mAb IB4 at 5 μg/10^7 cells, followed by cross-linking with the F(ab′)$_2$ fragment of a secondary antibody for 3 min at 37 °C. Cells were then lysed in 1% Brij 98 at 37 °C, and rafts and soluble fractions were isolated by sucrose gradient centrifugation as described under "Experimental Procedures." 60 mM ODG + 1% Brij 98-containing lysis buffer was then added to these fractions, and they were subjected to immunoprecipitation (*IP*) with an anti-Tyr-(P) mAb bound to agarose beads. Tyrosine-phosphorylated proteins were eluted from the beads with 40 mM phenyl phosphate. Proteins were separated on 11% SDS-PAGE under reducing conditions and blotted with the anti-Tyr(P) mAb RC20-HRP. The position of molecular mass markers is indicated to the *left*. *B*, blots in *A* were scanned, and tyrosine-phosphorylated CD3-ε and CD3-ζ bands were quantified using the NIH Image program 1.62 version. *Open bars* represent the amount of each phosphoprotein expressed in densitometric units before stimulation. *Closed bars* represent that upon IB4 stimulation. *C*, filter from *A* was subsequently stripped and reprobed with specific antibodies against the indicated proteins. The data shown are representative of three independent experiments. *D*, Jurkat T cells were stimulated (+) or not (−) with IB4+αmo for 5 min at 37 °C. Then rafts and soluble fractions were isolated. Tyrosine-phosphorylated proteins were immunoprecipitated and immunoblotted with anti-Tyr(P) mAb as above, except that 1% Brij 98-containing lysis buffer without ODG was added before the immunoprecipitation. The position of molecular mass markers is indicated to the *left*. *E*, filter from *D* was stripped and reprobed with antibodies against the indicated proteins. Fold increase in the densitometric units (corrected by area) relative to unstimulated cells is indicated at the *bottom of each lane*. The data are representative of three independent experiments.

in our immunoprecipitation experiments, it is likely that the anti-CD3-ζ mAb would bind much more the CD3-ζ molecules that remain free or associated with other receptors (Fig. 2, *B* and *C*, *lane 3*), rather than associated with CD38, which would be preferentially captured by the anti-CD38 mAb (Fig. 2, *B* and *C*, *lane 1*). Therefore, these findings support the idea that the CD38 raft subset represents a significant fraction of CD3-ζ-containing rafts, whereas CD38 in the disordered plasma membrane represents a very minor fraction of CD3-ζ-associated complexes.

Tyrosine Phosphorylation of Lck, LAT, and Fully Phosphorylation of CD3-ζ and CD3-ε Occurs Exclusively in Rafts upon CD38 Engagement—The first signaling events following CD38 engagement involve increased tyrosine phosphorylation of a number of cellular proteins, including ZAP-70, Lck, LAT, and the CD3 subunits, CD3-ζ and CD3-ε (28, 30, 31). To analyze whether these events occur in rafts, pooled Brij 98-resistant raft and soluble fractions from unstimulated or IB4-stimulated cells were treated with 1% Brij 98 + 60 mM ODG before immunoprecipitation with an anti-Tyr(P) mAb bound to agarose beads. This was followed by elution of tyrosine-phosphorylated proteins with 40 mM phenyl phosphate, Western blot with anti-Tyr(P) mAb, and subsequent re-blotting with specific antibodies as described (30). As shown in Fig. 4, *A* and *C*, Lck and LAT were readily detected in the anti-Tyr(P) immunoprecipitates from rafts with a significant increase upon CD38 ligation for 3 min (in Fig. 4*C*, compare *lane 1* with *lane 2*). Neither Lck nor LAT was detected in the anti-Tyr(P) immunoprecipitates from the soluble fraction (Fig. 4, *A*, and *C*, *lanes 3* and *4*). In contrast, tyrosine-phosphorylated Erk was mainly detected in the soluble fraction (*lane 4*). Tyrosine phosphorylation of Erk correlates with increased Erk catalytic activity (30).

Tyrosine phosphorylation of CD3-ε and CD3-ζ occurred in both raft and soluble fractions upon CD38 ligation (Fig. 4, *A* and *C*). However, in rafts CD3-ε tyrosine phosphorylation increased 4-fold relative to that in unstimulated cells, whereas in

the soluble fraction such an increase was only 1.7-fold (for quantification see Fig. 4*B*). Likewise, the increases in CD3-ζ tyrosine phosphorylation were more prominent in rafts than in soluble fractions (3–5-fold in rafts *versus* 2-fold in soluble fractions, Fig. 4*B*). It is worth noting that in the raft fraction tyrosine-phosphorylated CD3-ϵ exhibited a slower migration on SDS-PAGE than its counterpart in the soluble fraction (Fig. 4, *A* and *C*, *lanes 1* and *2 versus lanes 3* and *4*). Its apparent molecular weight coincided with that of the upper band of the fully tyrosine-phosphorylated CD3-ϵ, which runs as a 24–25-kDa doublet on high resolution SDS-PAGE (38). Likewise, the 23-kDa form of tyrosine-phosphorylated CD3-ζ, which corresponds to that of fully phosphorylated CD3-ζ species (51), was only detected in rafts and not in the soluble fraction. In contrast, in the soluble fraction from IB4-stimulated cells 81% of tyrosine-phosphorylated CD3-ζ migrated with an apparent molecular mass of 18 kDa (Fig. 4, *A*, *lane 4*, and *B*). Moreover, in rafts from IB4-stimulated cells the 23-kDa form was predominant over the 21-kDa form (Fig. 4, *A*, *lane 2*, and *B*). Both the 21- and 18-kDa forms correspond to partially phosphorylated CD3-ζ species (51). The appearance of fully phosphorylated CD3-ζ and a 23:21-kDa ratio near 1 has been correlated with the activation of ZAP-70 and T cell activation, whereas altered CD3-ζ phosphorylation and a 23:21 ratio of much less than 1 has been associated with partial TCR signaling (51–54).

c-Cbl Tyrosine Phosphorylation Occurs Exclusively in the Soluble Fraction upon CD38 Engagement—c-Cbl is a cytosolic protein that becomes tyrosine-phosphorylated upon CD38 engagement although with slower kinetics than those of LAT, CD3-ϵ, and CD3-ζ (28, 30). Because in Jurkat T cells anti-CD3 stimulation induces the association of a highly tyrosine-phosphorylated pool of c-Cbl with lymphocyte membranes and with a detergent-insoluble particulate fraction (55), it was of interest to examine whether this phenomenon occurred upon CD38 ligation. To this end, cells were stimulated for 5 min with the anti-CD38 mAb IB4 followed by cross-linking with the $F(ab')_2$ fraction of a secondary antibody. Then pooled Brij 98-resistant raft and soluble sucrose gradient fractions from unstimulated or IB4-stimulated cells were immunoprecipitated with an anti-Tyr(P) mAb bound to agarose beads as described above. As shown in Fig. 4*E*, c-Cbl was exclusively detected in the anti-Tyr(P) immunoprecipitates from the soluble fraction, with a significant increase upon CD38 engagement (Fig. 4*E*, *upper panel*, *lanes 3* and *4*). In contrast, tyrosine phosphorylation of p55 PI 3-kinase was exclusively detected in raft fractions (Fig. 4*E*, *lower panel*, *lanes 1* and *2*), whereas phospho-ZAP-70 was detected in both raft and soluble fractions, although after CD38 stimulation the increase in ZAP-70 tyrosine phosphorylation was seen better in the raft fraction (Fig. 4*E*, *middle panel*). Increased ZAP-70 tyrosine phosphorylation has been correlated with augmentation of its catalytic activity (56), whereas c-Cbl has been associated with the negative regulation of immune receptor signaling (57). Note that in both raft and soluble fraction from cells stimulated with anti-CD38 mAb for 5 min, several tyrosine-phosphorylated proteins were detected, with apparent molecular masses above 50 kDa. However, in the soluble fraction the relative abundance of tyrosine-phosphorylated proteins was higher than in rafts, which correlated with its higher protein content. Overall, these findings strongly corroborate our initial suggestion that raft microdomains play an important role in the activation of the earliest CD38 signaling events (31), in which Lck, CD3-ζ, CD3-ϵ, ZAP-70, and LAT become tyrosine-phosphorylated. In contrast, potentially inhibitory signals involving altered CD3-ζ tyrosine phosphorylation and fully c-Cbl tyrosine phosphorylation could be initiated simultaneously, or a few minutes later in the bulk of non-raft plasma membrane and/or the cytosol.

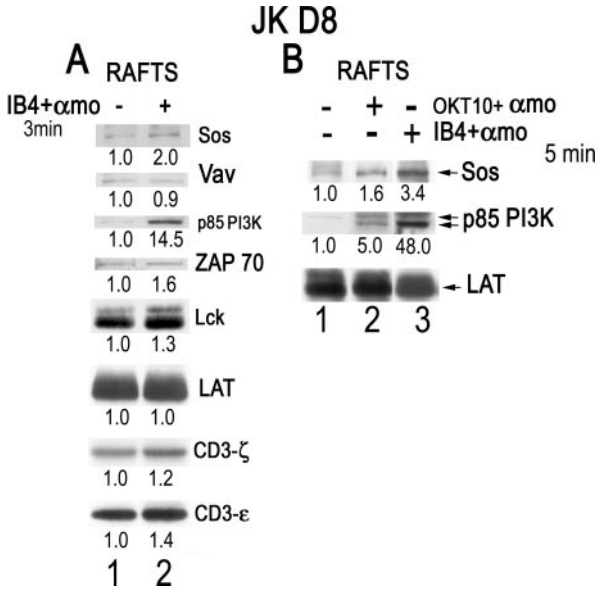

FIG. 5. **Recruitment of Sos and p85 PI 3-kinase to membrane rafts upon CD38 ligation.** *A*, overnight serum-starved Jurkat T cells (*JK D8*) were left unstimulated (−) or they were stimulated (+) with the anti-CD38 mAb antibody IB4 (5 μg/10^7 cells), followed by cross-linking with the $F(ab')_2$ fragment of a secondary antibody (*αmo*) for 3 min at 37 °C. Cells were then lysed in 1% Brij 98-containing lysis buffer at 37 °C for 5 min. Rafts were isolated and concentrated as described under "Experimental Procedures." 25-μl aliquots (in sample buffer) of rafts fractions were resolved on 11% SDS-PAGE under non-reducing conditions and transferred to PVDF. The membranes were then immunoblotted with the indicated specific antibodies. *B*, serum-starved Jurkat T cells were left unstimulated (*lane 1*) or stimulated either with the anti-CD38 mAb antibody, OKT10 (*lane 2*), or with IB4 (*lane 3*), followed by cross-linking with the αmo for 5 min at 37 °C. Rafts were isolated as in *A*. 25-μl aliquots (in sample buffer) of rafts fractions were resolved on 11% SDS-PAGE under non-reducing conditions and transferred to PVDF. Separated proteins were immunoblotted with anti-Sos (*upper panel*), anti-p85α subunit of the PI 3-kinase (*middle panel*), or anti-LAT (*lower panel*) antibodies. Blots from *A* and *B* were scanned, and protein bands were quantified using the NIH Image program 1.62 version. Fold increase in the densitometric units (corrected by area) relative to unstimulated cells is indicated at the *bottom of each lane*. The data are representative of three independent experiments.

Recruitment of Sos and the p85α Regulatory Subunit of the PI 3-Kinase to Membrane Rafts upon CD38 Ligation—To examine whether additional signaling molecules were recruited to rafts upon CD38 engagement, despite the fact that they do not become tyrosine-phosphorylated, Jurkat T cells were stimulated with the anti-CD38 mAb, IB4, followed by cross-linking with the $F(ab')_2$ fraction of a secondary antibody for 3 min. Cells were then lysed in 1% Brij 98 at 37 °C and subjected to sucrose gradient fractionation. The low density raft fractions 2–4 were pooled and concentrated, and proteins were separated by SDS-PAGE under non-reducing conditions and analyzed by Western blot with various specific antibodies. As shown in Fig. 5*A*, we observed that upon CD38 ligation for 3 min the amount of Sos and p85 PI 3-kinase in rafts increased 2- and 14-fold, respectively (Fig. 5*A*, *lane 2 versus lane 1*). These increments appeared to be specific because the relative amounts of Vav and LAT remained unchanged following CD38 engagement, whereas ZAP-70, Lck, CD3-ζ, and CD3-ϵ increments ranged from 1.2- to 1.6-fold over unstimulated cells. Furthermore, a more patent translocation of Sos, and particularly of p85 PI 3-kinase, to rafts was observed at 5 min following CD38 ligation with IB4 (Fig. 5*B*, *lane 3*, *upper* and *middle panels*, respectively). When another anti-CD38 mAb, OKT10, was used to stimulate cells, the translocation of Sos and p85α to rafts also occurred but less efficiently (Fig. 5*B*, *upper* and

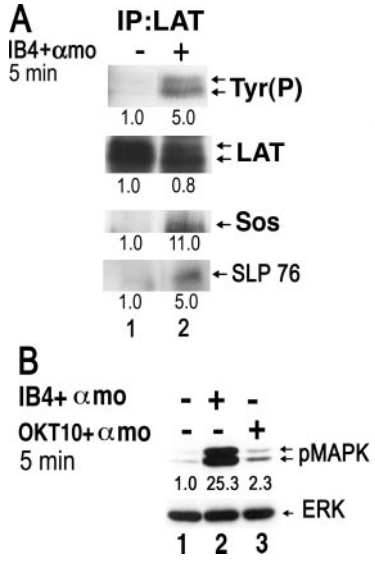

FIG. 6. *A*, recruitment of Sos and SLP-76 by tyrosine-phosphorylated LAT upon CD38 ligation. Jurkat T cells serum-starved overnight (4×10^7 per point) were prepared and stimulated with the anti-CD38 mAb IB4 + αmo for 5 min at 37 °C as described above. Cells were lysed in 1% Nonidet P-40 lysis buffer on ice. Post-nuclear supernatants were subjected to immunoprecipitation (*IP*) of LAT as described under "Experimental Procedures." Immunoprecipitates were separated on 11% SDS-PAGE under reducing conditions and subjected to immunoblotting with an anti-Tyr(P) mAb (*upper panel*). Membrane was then striped and reblotted with antibodies to the indicated proteins (to the *right* of each panel). Fold increase in the densitometric units (corrected by area) relative to unstimulated cells is indicated at the *bottom of each lane*. *B*, CD38-mediated Erk activation. Jurkat cells were left unstimulated (*lane 1*), stimulated with the anti-CD38 mAb antibodies IB4 (*lane 2*), or OKT10 (*lane 3*), followed by cross-linking with the αmo for 5 min at 37 °C. After stimulation cells were immediately lysed in ice-cold 1% Nonidet P-40 lysis buffer. Post-nuclear supernatants were separated on 10% SDS-PAGE under reducing conditions and subjected to immunoblotting with an anti-diphospho-Erk mAb (*upper panel*). Then the filter was stripped and reprobed with an anti-Erk polyclonal antibody (*lower panel*). Fold increase in the densitometric units (corrected by area) relative to unstimulated cells is indicated at the *bottom* of the *upper panel*. The data are representative of three independent experiments.

middle panels, *lane 2*), which correlated with its relatively lower capability of inducing Erk activation (Fig. 6*B*). Note that the anti-p85α mAb used for immunoblotting detected a doublet in CD38-stimulated cells (Fig. 5*B*, *middle panel*, *lanes 2* and *3*). The upper band, which is also present in unstimulated cells (*lane 1*), may correspond to the p85β isoform, which is constitutively associated with lipid rafts in Jurkat T cells (14). Because neither Sos nor p85 PI 3-kinase become tyrosine-phosphorylated upon CD38 engagement (Ref. 30 and data not shown), the data suggested that the recruitment of Sos and p85 PI 3-kinase to raft membranes may reflect the specific interaction of these proteins with raft components, which in turn may facilitate the CD38-mediated activation of the Raf-Erk and PI 3-kinase/Akt signaling pathways.

Recruitment of Sos and SLP-76 to Tyrosine-phosphorylated LAT upon CD38 Engagement—LAT tyrosine phosphorylation and recruitment of Grb2-Sos are important steps for TCR-mediated Ras activation (58). Given that LAT is located in rafts, and Sos is translocated to rafts upon CD38 cross-linking, we addressed the question whether cross-linking of CD38 leads to LAT tyrosine phosphorylation and subsequent recruitment of Sos in Jurkat T cells. To this end, anti-LAT immunoprecipitates from unstimulated or anti-CD38-stimulated cells lysed in 1% Nonidet P-40 were immunoblotted with an anti-Tyr(P) mAb. As shown in Fig. 6*A*, CD38 ligation induced a significant increase in LAT tyrosine phosphorylation (*upper panel*, *lane 2 versus lane 1*). Sos was readily detected in LAT immunoprecipitates from CD38-stimulated cells, and not from unstimulated cells (Fig. 6*A*, *3rd panel*, *lanes 2* and *1*, respectively). Therefore, this result suggests that CD38-mediated tyrosine phosphorylation of LAT promotes the recruitment of Grb2-Sos complexes to rafts. Because another critical role of LAT is to bring SLP-76-Gads complexes, and its associated proteins, to the membrane in a tyrosine phosphorylation manner (59), we next tested whether SLP-76 was recruited to LAT upon CD38 ligation. As shown in Fig. 6*A*, SLP-76 was detected in LAT immunoprecipitates from CD38-stimulated cells (*lower panel*, *lane 2*) and not from unstimulated cells (*lower panel*, *lane 1*), which is in agreement with an active recruitment of SLP-76-Gads to tyrosine-phosphorylated LAT.

Because translocation of Sos to rafts was better induced by the anti-CD38 mAb IB4 than with OKT10, the relative potency of these mAbs to induce Erk activation was studied. As shown in Fig. 6*B*, IB4 mAb induced a higher increase in Erk phosphorylation than OKT10, as expected.

CD38 Ligation Induces Ras Activation Within Rafts—Although translocation of Grb2-Sos complexes into rafts leads to Ras activation upon TCR stimulation (60), and we have demonstrated that CD38 ligation leads to Raf/Erk activation (28, 30, 31), it is not known whether Ras is activated upon CD38 engagement. To determine this possibility, serum-starved Jurkat T cells were stimulated with the anti-CD38 mAb IB4 for 2 and 5 min. Activated GTP-bound Ras was extracted from lysates with a GST fusion protein containing the N-terminal Ras binding domain of Raf (see "Experimental Procedures"). The amount of activated Ras in the pull-outs was determined by immunoblotting with an anti-Ras antibody that recognizes the three main Ras isoforms (H-Ras, N-Ras, and K-Ras). As shown in Fig. 7*A*, CD38 ligation induced a time-dependent activation of Ras, which was stronger at 2 min following stimulation than at 5 min.

In Jurkat T cells the only Ras isoform expressed is N-Ras (61), which potentially could be targeted to lipid rafts via palmitoylation at cysteine 181 (62). To examine whether N-Ras present within rafts become activated upon CD38 engagement, the GTP-Ras pull-down assay was performed in pooled raft fractions from either unstimulated or CD38-stimulated Jurkat T cells. As shown in Fig. 7*B*, CD38 ligation induced activation of Ras within rafts at 2 min following stimulation, as judged by the increase in the amount of GTP-bound Ras recovered in the pull-outs (*lane 2 versus lane 1*). In contrast, not such increase was observed in the non-raft-soluble fraction at this time point (data not shown).

DISCUSSION

In a previous paper (31), we have demonstrated that in T cells CD38 is associated with lipid rafts. However, little is known about the protein composition of CD38-containing rafts and whether specific interactions exist between CD38 and other well characterized raft-associated signaling proteins. By using specific antibodies bound to protein G superparamagnetic microbeads, we have analyzed the distribution pattern of CD38, Lck, CD3-ζ, CD3-ϵ, and LAT in immunoisolated rafts from Jurkat T cells. This study indicates that CD38 is concentrated in a subset of rafts that have relatively high levels of Lck and CD3-ζ, whereas CD3-ϵ and LAT are weakly detected. Moreover, the CD3-ζ and CD3-ϵ subunits seem to be concentrated in a subset highly enriched in Lck and to a lesser extent with LAT. Thus, the distribution pattern of these molecules in CD3-ϵ rafts is very similar to that in Brij 98-resistant immunoisolated CD3-ϵ rafts from a murine T cell line (27). On the other hand, Lck rafts retrieve all the molecules analyzed, whereas LAT rafts are highly enriched in Lck, show intermediate levels of CD3-ζ and CD3-ϵ, and low levels of CD38. There-

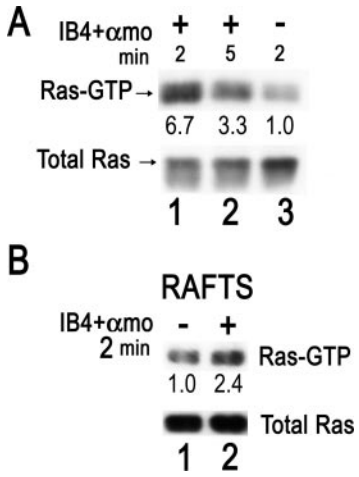

FIG. 7. **CD38 ligation induces Ras activation within rafts.** *A*, $2–4 \times 10^7$ Jurkat T cells, which were starved overnight in 0.1% serum RPMI/HEPES, were left unstimulated (−) or stimulated with the anti-CD38 mAb antibody, IB4, at 5 $\mu g/10^7$ cells, followed by cross-linking with the $F(ab')_2$ fragment of a secondary antibody (*αmo*), for the indicated periods of time, at 37 °C. After stimulation cells were immediately lysed in ice-cold Mg^{2+} lysis buffer (see "Experimental Procedures"). Active GTP-bound Ras was extracted from post-nuclear supernatants with the GST-Raf-Ras-binding domain (*RBD*), coupled to glutathione-agarose, and analyzed by immunoblotting with anti-Ras antibody (clone RAS 10) (*upper panel*). Total Ras was measured by anti-Ras immunoblot analysis of the post-nuclear supernatants (400,000 cell equivalents per lane) (*lower panel*). Fold increase in the GTP-bound Ras relative to unstimulated cells is indicated at the *bottom* of the *upper panel*. The data were previously corrected by dividing the amount of GTP-bound Ras by the amount of total Ras protein detected in the immunoblots. *B*, pooled Brij 98-resistant raft sucrose gradient fractions from unstimulated (*lane 1*) or IB4-stimulated (*lane 2*) Jurkat cells were solubilized in ice-cold Mg^{2+} lysis buffer and processed as above. Fold increase in the GTP-bound Ras (corrected by total Ras content) relative to unstimulated cells is indicated at the *bottom* of the *upper panel*. The data are representative of at least three independent experiments.

fore, there are quantitative and qualitative differences in the protein content of the raft subsets so far studied, although there is also some degree of overlapping, presumably because most of these molecules are part of pre-formed signaling complexes**.**

Recent evidence suggests that LAT and Lck could reside in separate raft domains in human T lymphoblasts (63). Interestingly, in the same report TCR stimulation induced the co-localization of LAT and Lck to 50–100 nm microdomains, which suggested that in these cells the coalescence of LAT- and Lck-containing rafts requires T cell activation. In contrast, the results presented in this report demonstrate that in unstimulated Jurkat T cells raft subsets exist containing Lck, LAT, and the TCR-CD3 complex. Moreover, recent data by Kabouridis (49) show the selective interaction of LAT with the open active form of Lck in lipid rafts from Jurkat T cells, whereas such interaction in the soluble non-raft fraction is minimal. Altogether, these data suggest that in normal T cells the association of LAT with Lck-containing rafts is regulated by TCR signaling, whereas in Jurkat T cells there is a constitutive association of these proteins in the same raft subsets, which may explain why in these cells the TCR-generated signals are amplified more rapidly than in resting T cells.

Within these pre-assembled signaling units, some of these protein complexes are very sensitive to raft disruption, which suggest weak and very likely dynamic interactions, involving protein-protein and protein-lipid interactions. Thus, treatment of the raft membrane vesicles with ODG causes the dissociation of LAT from CD3-ζ and CD3-ϵ immunoprecipitates. Likewise, ODG causes a significant dissociation of Lck from CD38 immunoprecipitates and the complete lost of CD38 from Lck immunoprecipitates. These results could be explained by the selective dissociation of LAT and CD38 from raft membrane vesicles by ODG, whereas Lck, CD3-ζ, and CD3-ϵ remain associated to them (Table I). In this sense, it has been reported in murine T cells that CD38 and Lck could interact directly through the CD38 cytoplasmic tail and the Lck Src homology 2 domain (64). Interestingly, such interaction takes place in cells solubilized in a lysis buffer containing 1% digitonin, which is a mild detergent known to preserve lipid raft-protein interactions (65).

In contrast, other protein complexes are well maintained regardless of using ODG detergent to solubilize rafts, which suggest that they occur primarily via protein-protein interactions. Thus, the associations of Lck with either CD3-ζ or CD3-ϵ are relatively well maintained in the presence of ODG and are detected independently of the antibody used for immunoprecipitation (*i.e.* anti-Lck, anti-CD3-ζ, or anti-CD3-ϵ). These data further support that Lck and the TCR-CD3 complex are tightly associated within the Lck and/or the TCR raft subsets. Since in rafts a small fraction of both CD3-ζ and CD3-ϵ seems to be constitutively phosphorylated (Fig. 4), it is likely that Lck-CD3 association takes place through phosphotyrosine-dependent interactions.

Another protein ensemble, which probably takes place via protein-protein interactions, is the association of CD38 with CD3-ζ. Thus, in the anti-CD38 immunoprecipitates from raft fractions a similar proportion of CD3-ζ remains associated with CD38 independently of the presence or absence of ODG. Moreover, the association of CD38 with CD3-ζ is found in both raft and soluble fractions and in rafts from Lck-deficient cells, which demonstrates that CD38-CD3-ζ interactions can occur independently of raft partitioning of their components, do not require Lck, and are not artifacts of incomplete solubilization. However, in Jurkat T cells there are clear differences in the surface expression of the CD3 subunits and CD38, along with differences in the proportion of each molecule partitioning into rafts, which may dramatically influence the stoichiometry of CD38-CD3-ζ complexes within rafts, or outside them. The results indicate that changes in the surface expression of CD38, CD3-ζ, or both may greatly affect the number of available CD38-CD3-ζ complexes, which in turn may affect the threshold level required to initiate transmembrane signaling through CD38.

Other protein associations, which are stable in 1% Brij 98 but not in 60 mM ODG, are direct, however. Perhaps the best example is the CD3-ζ-CD3-ϵ complexes, which are detected in both raft and soluble fractions. Our data are consistent with the evidence that CD3-ζ is loosely associated to the other TCR-CD3 subunits (66), and therefore its interaction with the other CD3 polypeptide chains is more sensitive to non-ionic detergents than the more tightly associated TCR-αβ·CD3-γϵ or TCR-αβ·CD3-δϵ subcomplexes (50, 67, 68).

CD38 clustering induces tyrosine phosphorylation of Lck, LAT, ZAP-70, and p55 PI 3-kinase within rafts. Moreover, full phosphorylation of CD3-ζ and CD3-ϵ only occurs in raft membranes, as judged by the apparent molecular weight of the different tyrosine-phosphorylated CD3-ζ (23- and 21-kDa forms with a ratio 23:21 higher than 1) and CD3-ϵ forms detected in the anti-Tyr(P) immunoprecipitates. The 21- and/or 23-kDa forms of CD3-ζ may contribute to T cell survival and to T cell responses against pathogens such as bacteria and viruses (69). These data suggest that activation signals initiated in CD38 rafts are rapidly propagated to other raft compartments, where the amplification signaling machinery is present (*i.e.* LAT-enriched rafts, etc.).

CD38-mediated tyrosine phosphorylation of CD3-ζ, CD3-ϵ, ZAP-70, and LAT may be functionally related to the recruit-

ment of Sos and subsequent activation of N-Ras within rafts. In TCR-mediated signaling tyrosine phosphorylation of raft-associated LAT by ZAP-70 may result in an exchange of Sos between the ZAP-70-Grb2-Sos and LAT-Grb2-Sos complexes (60). A similar model is compatible with our observations in Jurkat T cells, where CD38 ligation induces tyrosine phosphorylation of both ZAP-70 and LAT, recruitment of Sos to phospho-LAT (Fig. 6*A*), and targeting of Sos into rafts as well (Fig. 5). Therefore, a pathway leading from CD38 through Ras to Erk requires the formation of a signaling complex made up of the TCR-CD3 (28), Lck (30), ZAP-70 (30, 31), and its downstream effector LAT. In this model, tyrosine phosphorylation of ZAP-70 and LAT are likely to be essential for CD38-induced targeting of Sos into rafts containing Ras. Therefore, as it is pointed out elsewhere, the formation of functional signaling complexes is unlikely to be stabilized solely through interactions with lipid rafts but does require phosphotyrosine-dependent interactions (70–72). In murine T cells, where CD38-mediated LAT tyrosine phosphorylation is weaker than in Jurkat T cells, we favor a model in which the adaptor Shc might have a crucial role (31). In this sense, Shc partitions into rafts following TCR engagement (14), and targeting of Shc to rafts leads to constitutive activation of the Ras/Erk signaling pathway and enhanced TCR signaling (73).

The distinct membrane microlocalization of the different Ras isoforms clearly has important potential consequences for effector interactions and activation of downstream pathways (74). In cell membranes prepared under detergent-free conditions, doubly palmitoylated H-Ras localizes in both lipid raft microdomains and bulk plasma membrane, whereas K-Ras is predominantly present in the bulk disordered membrane (74–76). On the other hand, 75–80% of unipalmitoylated N-Ras is found in non-caveolar lipid raft fractions from N-Ras-transfected COS-7 cells lysed in 0.25% Triton X-100 (77), and in unstimulated Jurkat T cells extracted with 1% Brij 98 at 37 °C, about 13% of N-Ras migrates with lipid rafts (data not shown). Because Ras interaction with lipid rafts is highly sensitive to detergent extraction (74, 75), it is likely that we are underestimating the amount of N-Ras present in lipid rafts. In any case, CD38 ligation with an agonist anti-CD38 mAb causes N-Ras activation within Brij 98-resistant rafts (Fig. 7) and not in soluble fractions. However, the bulk of the Erk activation occurs in the non-raft fractions (Fig. 4), and disruption of raft interactions by treatment with methyl-β-cyclodextrin strongly stimulates CD38-mediated Erk activation (31). Thus, association with raft domains may be involved in the first steps leading to Ras/Erk activation, but rafts do not constitute the final site of activation of this signaling pathway. These data are consistent with the concept that N-Ras may exist in a dynamic equilibrium between lipid rafts and the disordered plasma membrane, as has been demonstrated for doubly palmitoylated H-Ras (74, 76, 78).

In Jurkat T cells the regulatory p85α subunit of the PI 3-kinase is recruited to rafts after CD38 cross-linking, whereas the p85β isoform is constitutively present in rafts. Moreover, a tyrosine-phosphorylated p55α isoform was also present in rafts and became increasingly tyrosine-phosphorylated upon CD38 ligation. Because CD3-ζ and CD3-ϵ are tyrosine-phosphorylated upon CD38 cross-linking (Zubiaur *et al.* (28, 31) and this paper), and these proteins could interact in a phosphorylation-dependent manner with the p85α PI 3-kinase (31, 79, 80), they could target PI 3-kinase to rafts. In addition, binding of PI 3-kinase to the TCR-CD3 *per se* could up-regulate the PI 3-kinase activity (79, 80), presumably by a conformational change as reported previously for other p85-binding proteins (81, 82). Other candidate molecules are LAT, Shc, and Cbl, as these molecules bind p85 (83), and are tyrosine-phosphorylated upon CD38 stimulation (Figs. 4 and 6) (28, 30, 31). An initiating process could occur with molecules such as CD3-ζ and CD3-ϵ, whereas LAT or Shc may responsible for maintaining or amplifying PI 3-kinase activation. Both events are likely important for PI(3,4,5)P_3 generation after CD38 cross-linking. These interactions with lipid rafts are likely to be functionally significant, because in one earlier study we demonstrated that disruption of raft domains by treatment with methyl-β-cyclodextrin prevents the PI 3-kinase/Akt activation mediated by CD38 (31).

In contrast, c-Cbl, which in B cells is related to inhibition of CD38-mediated cell growth (84), becomes tyrosine-phosphorylated exclusively in the non-raft compartment with delayed kinetics in respect to other signaling molecules. Partial tyrosine phosphorylation of CD3-ζ, which has been correlated with partial TCR signaling (52), is also found in the non-raft plasma membrane. Note that in the non-raft fraction the small amount of Lck detected is not associated with CD38, which could explain why full phosphorylation of CD3-ζ does not occur upon CD38 ligation. Therefore, the CD38 present in the disordered, non-raft plasma membrane might be involved in the initiation of inhibitory signals as c-Cbl tyrosine phosphorylation and partial CD3-ζ tyrosine phosphorylation, although we cannot rule out that CD38 ligation within rafts may regulate lateral segregation of inhibitory signaling molecules from rafts to the non-raft compartment. Likewise, lateral segregation of activating signaling molecules from raft to non-raft sites is likely to occur later on, because the bulk of Erk activation is detected somewhere outside the lipid rafts. In summary, this study provides new insights into the mechanisms by which CD38 transduces signals inside the cell, demonstrating that there are two pools of CD38, which differ in their microdomain localization, associated proteins, and distinct signaling outputs.

Acknowledgments—We gratefully acknowledge Dr. José-Manuel Palma from the Estación Experimental del Zaidín (CSIC), Granada, Spain, for sharing knowledge and the invaluable help in sucrose gradient ultracentrifugation experiments. We thank Dr. Balbino Alarcón for the gift of the anti-CD3-ζ antibody 448, Dr. Stephen C. Ley for kindly supplying the anti-ZAP-70 antibody Zap-4, and Dr. Arthur Weiss for providing the JCaM1.6 cells. We also thank Antonio Mérida for expert mAb purification.

REFERENCES

1. Terhorst, C., van Agthoven, A., Le Clair, K., Snow, P., Reinherz, E. L., and Schlossman, S. F. (1981) *Cell* **23,** 771–780
2. Jackson, D. G., and Bell, J. I. (1990) *J. Immunol.* **144,** 2811–2815
3. Malavasi, F., Funaro, A., Roggero, S., Horenstein, A., Calosso, L., and Mehta, K. (1994) *Immunol. Today* **15,** 95–97
4. Deaglio, S., Mallone, R., Baj, G., Arnulfo, A., Surico, N., Dianzani, U., Mehta, K., and Malavasi, F. (2000) *Chem. Immunol.* **75,** 99–120
5. Ferrero, E., Saccucci, F., and Malavasi, F. (2000) *Chem. Immunol.* **75,** 1–19
6. Funaro, A., Ferrero, E., Mehta, K., and Malavasi, F. (2000) *Chem. Immunol.* **75,** 256–273
7. Berthelier, V., Tixier, J. M., Muller-Steffner, H., Schuber, F., and Deterre, P. (1998) *Biochem. J.* **330,** 1383–1390
8. Mehta, K., Shahid, U., and Malavasi, F. (1996) *FASEB J.* **10,** 1408–1417
9. Franco, L., Guida, L., Bruzzone, S., Zocchi, E., Usai, C., and De Flora, A. (1998) *FASEB J.* **12,** 1507–1520
10. Sun, L., Adebanjo, O. A., Koval, A., Anandatheerthavarada, H. K., Iqbal, J., Wu, X. Y., Moonga, B. S., Wu, X. B., Biswas, G., Bevis, P. J., Kumegawa, M., Epstein, S., Huang, C. L., Avadhani, N. G., Abe, E., and Zaidi, M. (2002) *FASEB J.* **16,** 302–314
11. Partida-Sanchez, S., Cockayne, D. A., Monard, S., Jacobson, E. L., Oppenheimer, N., Garvy, B., Kusser, K., Goodrich, S., Howard, M., Harmsen, A., Randall, T. D., and Lund, F. E. (2001) *Nat. Med.* **7,** 1209–1216
12. Simons, K., and Toomre, D. (2000) *Nat. Rev. Mol. Cell. Biol.* **1,** 31–39
13. Brown, D. A., and London, E. (2000) *J. Biol. Chem.* **275,** 17221–17224
14. Xavier, R., Brennan, T., Li, Q., McCormack, C., and Seed, B. (1998) *Immunity* **8,** 723–732
15. Moran, M., and Miceli, M. C. (1998) *Immunity* **9,** 787–796
16. Janes, P. W., Ley, S. C., and Magee, A. I. (1999) *J. Cell Biol.* **147,** 447–461
17. Montixi, C., Langlet, C., Bernard, A. M., Thimonier, J., Dubois, C., Wurbel, M. A., Chauvin, J. P., Pierres, M., and He, H. T. (1998) *EMBO J.* **17,** 5334–5348
18. Cheng, P. C., Brown, B. K., Song, W., and Pierce, S. K. (2001) *J. Immunol.* **166,** 3693–3701

19. Cheng, P. C., Dykstra, M. L., Mitchell, R. N., and Pierce, S. K. (1999) *J. Exp. Med.* **190,** 1549–1560
20. Petrie, R. J., Schnetkamp, P. P., Patel, K. D., Awasthi-Kalia, M., and Deans, J. P. (2000) *J. Immunol.* **165,** 1220–1227
21. Field, K. A., Holowka, D., and Baird, B. (1997) *J. Biol. Chem.* **272,** 4276–4280
22. Deans, J. P., Robbins, S. M., Polyak, M. J., and Savage, J. A. (1998) *J. Biol. Chem.* **273,** 344–348
23. Yang, H., and Reinherz, E. L. (2001) *J. Biol. Chem.* **276,** 18775–18785
24. Ilangumaran, S., Briol, A., and Hoessli, D. C. (1998) *Blood* **91,** 3901–3908
25. Millan, J., Montoya, M. C., Sancho, D., Sanchez-Madrid, F., and Alonso, M. A. (2002) *Blood* **99,** 978–984
26. Yashiro-Ohtani, Y., Zhou, X. Y., Toyo-Oka, K., Tai, X. G., Park, C. S., Hamaoka, T., Abe, R., Miyake, K., and Fujiwara, H. (2000) *J. Immunol.* **164,** 1251–1259
27. Drevot, P., Langlet, C., Guo, X. J., Bernard, A. M., Colard, O., Chauvin, J. P., Lasserre, R., and He, H. T. (2002) *EMBO J.* **21,** 1899–1908
28. Zubiaur, M., Guirado, M., Terhorst, C., Malavasi, F., and Sancho, J. (1999) *J. Biol. Chem.* **274,** 20633–20642
29. Morra, M., Zubiaur, M., Terhorst, C., Sancho, J., and Malavasi, F. (1998) *FASEB J.* **12,** 581–592
30. Zubiaur, M., Izquierdo, M., Terhorst, C., Malavasi, F., and Sancho, J. (1997) *J. Immunol.* **159,** 193–205
31. Zubiaur, M., Fernandez, O., Ferrero, E., Salmeron, J., Malissen, B., Malavasi, F., and Sancho, J. (2002) *J. Biol. Chem.* **277,** 13–22
32. Brown, D. A., and London, E. (1998) *Annu. Rev. Cell Dev. Biol.* **14,** 111–136
33. Pralle, A., Keller, P., Florin, E. L., Simons, K., and Horber, J. K. (2000) *J. Cell Biol.* **148,** 997–1008
34. Varma, R., and Mayor, S. (1998) *Nature* **394,** 798–801
35. Deaglio, S., Dianzani, U., Horenstein, A. L., Fernandez, J. E., Kooten, C. V., Bragardo, M., Funaro, A., Garbarino, G., Virgilio, F. D., Banchereau, J., and Malavasi, F. (1996) *J. Immunol.* **156,** 727–734
36. Straus, D. B., and Weiss, A. (1992) *Cell* **70,** 585–593
37. Funaro, A., Monte, L. B. D., Dianzani, U., Forni, M., and Malavasi, F. (1993) *Eur. J. Immunol.* **23,** 2407–2411
38. Sancho, J., Franco, R., Chatila, T., Hall, C., and Terhorst, C. (1993) *Eur. J. Immunol.* **23,** 1636–1642
39. Poncelet, P., and Carayon, P. (1985) *J. Immunol. Methods* **85,** 65–74
40. Iyer, S. B., Hultin, L. E., Zawadzki, J. A., Davis, K. A., and Giorgi, J. V. (1998) *Cytometry* **33,** 206–212
41. Zubiaur, M., Sancho, J., Terhorst, C., and Faller, D. V. (1995) *J. Biol. Chem.* **270,** 17221–17228
42. Ilangumaran, S., Arni, S., van Echten-Deckert, G., Borisch, B., and Hoessli, D. C. (1999) *Mol. Biol. Cell* **10,** 891–905
43. Brown, D. A., and Rose, J. K. (1992) *Cell* **68,** 533–544
44. Melkonian, K. A., Chu, T., Tortorella, L. B., and Brown, D. A. (1995) *Biochemistry* **34,** 16161–16170
45. Millan, J., Cerny, J., Horejsi, V., and Alonso, M. A. (1999) *Tissue Antigens* **53,** 33–40
46. Delgado, P., Fernandez, E., Dave, V., Kappes, D., and Alarcon, B. (2000) *Nature* **406,** 426–430
47. Ilangumaran, S., and Hoessli, D. C. (1998) *Biochem. J.* **335,** 433–440
48. Roper, K., Corbeil, D., and Huttner, W. B. (2000) *Nat. Cell Biol.* **2,** 582–592
49. Kabouridis, P. S. (2003) *Biochem. J.* **371,** 907–915
50. Exley, M., Wileman, T., Mueller, B., and Terhorst, C. (1995) *Mol. Immunol.* **32,** 829–839
51. van Oers, N. S., Tohlen, B., Malissen, B., Moomaw, C. R., Afendis, S., and Slaughter, C. A. (2000) *Nat. Immun.* **1,** 322–328
52. Sloan-Lancaster, J., Shaw, A. S., Rothbard, J. B., and Allen, P. M. (1994) *Cell* **79,** 913–922
53. Madrenas, J., Wange, R. L., Wang, J. L., Isakov, N. A., Samelson, L. E., and Germain, R. N. (1995) *Science* **267,** 515–518
54. Kersh, E. N., Shaw, A. S., and Allen, P. M. (1998) *Science* **281,** 572–575
55. Hartley, D., and Corvera, S. (1996) *J. Biol. Chem.* **271,** 21939–21943
56. Chan, A. C., Dalton, M., Johnson, R., Kong, G. H., Wang, T., Thoma, R., and Kurosaki, T. (1995) *EMBO J.* **14,** 2499–2508
57. Lupher, M. L., Jr., Rao, N., Eck, M. J., and Band, H. (1999) *Immunol. Today* **20,** 375–382
58. Finco, T. S., Kadlecek, T., Zhang, W., Samelson, L. E., and Weiss, A. (1998) *Immunity* **9,** 617–626
59. Liu, S. K., Fang, N., Koretzky, G. A., and McGlade, C. J. (1999) *Curr. Biol.* **9,** 67–75
60. Salojin, K. V., Zhang, J., Meagher, C., and Delovitch, T. L. (2000) *J. Biol. Chem.* **275,** 5966–5975
61. Makover, D., Cuddy, M., Yum, S., Bradley, K., Alpers, J., Sukhatme, V., and Reed, J. C. (1991) *Oncogene* **6,** 455–460
62. Prior, I. A., and Hancock, J. F. (2001) *J. Cell Sci.* **114,** 1603–1608
63. Schade, A. E., and Levine, A. D. (2002) *J. Immunol.* **168,** 2233–2239
64. Cho, Y. S., Han, M. K., Choi, Y. B., Yun, Y., Shin, J., and Kim, U. H. (2000) *J. Biol. Chem.* **275,** 1685–1690
65. van't Hof, W., and Resh, M. D. (1999) *J. Cell Biol.* **145,** 377–389
66. Rodriguez-Tarduchy, G., Sahuquillo, A. G., Alarcon, B., and Bragado, R. (1996) *J. Biol. Chem.* **271,** 30417–30425
67. Sancho, J., Chatila, T., Wong, R. C., Hall, C., Blumberg, R., Alarcon, B., Geha, R. S., and Terhorst, C. (1989) *J. Biol. Chem.* **264,** 20760–20769
68. San Jose, E., Sahuquillo, A. G., Bragado, R., and Alarcon, B. (1998) *Eur. J. Immunol.* **28,** 12–21
69. Pitcher, L. A., Young, J. A., Mathis, M. A., Wrage, P. C., Bartok, B., and Van Oers, N. S. (2003) *Immunol. Rev.* **191,** 47–61
70. Guirado, M., de Aos, I., Orta, T., Rivas, L., Terhorst, C., Zubiaur, M., and Sancho, J. (2002) *Biochem. Biophys. Res. Commun.* **291,** 574–581
71. Bunnell, S. C., Hong, D. I., Kardon, J. R., Yamazaki, T., McGlade, C. J., Barr, V. A., and Samelson, L. E. (2002) *J. Cell Biol.* **158,** 1263–1275
72. Hartgroves, L. C., Lin, J., Langen, H., Zech, T., Weiss, A., and Harder, T. (2003) *J. Biol. Chem.* **278,** 20389–20394
73. Plyte, S., Majolini, M. B., Pacini, S., Scarpini, F., Bianchini, C., Lanfrancone, L., Pelicci, P., and Baldari, C. T. (2000) *Oncogene* **19,** 1529–1537
74. Prior, I. A., Harding, A., Yan, J., Sluimer, J., Parton, R. G., and Hancock, J. F. (2001) *Nat. Cell Biol.* **3,** 368–375
75. Song, K. S., Li, S., Okamoto, T., Quilliam, L. A., Sargiacomo, M., and Lisanti, M. P. (1996) *J. Biol. Chem.* **271,** 9690–9697
76. Roy, S., Luetterforst, R., Harding, A., Apolloni, A., Etheridge, M., Stang, E., Rolls, B., Hancock, J. F., and Parton, R. G. (1999) *Nat. Cell Biol.* **1,** 98–105
77. Matallanas, D., Arozarena, I., Berciano, M. T., Aaronson, D. S., Pellicer, A., Lafarga, M., and Crespo, P. (2003) *J. Biol. Chem.* **278,** 4572–4581
78. Hancock, J. F. (2003) *Nat. Rev. Mol. Cell. Biol.* **4,** 373–384
79. Exley, M., Varticovski, L., Markus, P., Sancho, J., and Terhorst, C. (1994) *J. Biol. Chem.* **269,** 15140–15146
80. de Aós, I., Metzger, M. H., Exley, M., Dahl, C. E., Misra, S., Zheng, D., Varticovski, L., Terhorst, C., and Sancho, J. (1997) *J. Biol. Chem.* **272,** 25310–25318
81. Shoelson, S. E., Sivaraja, M., Williams, K. P., Hu, P., Schlessinger, J., and Weiss, M. A. (1993) *EMBO J.* **12,** 795–802
82. Buhl, A. M., and Cambier, J. C. (1997) *Immunol. Rev.* **160,** 127–138
83. Wange, R. L. (2000) *Science STKE* http://www.stke.org/cgi/content/full/OC_sigtrans;2000/RE1
84. Kitanaka, A., Ito, C., Nishigaki, H., and Campana, D. (1996) *Blood* **88,** 590–598

Full Title: Antigen-induced clustering of surface CD38 and recruitment of intracellular CD38 to the immunological synapse[1]

Running title: CD38 clustering at the immunological synapse

Authors: Pilar Muñoz[*], María Mittelbrunn[†], Hortensia de la Fuente[†], Manuel Pérez[†], Mercedes Zubiaur[*], Francisco Sánchez-Madrid[†], Jaime Sancho[*2].

[*] Departamento de Biología Celular e Inmunología. Instituto de Parasitología y Biomedicina "López-Neyra". Consejo Superior de Investigaciones Científicas. 18100 Armilla. Spain.

[†] Servicio de Inmunología. Hospital Universitario de la Princesa. Universidad Autónoma de Madrid. 28006 Madrid. Spain.

Keywords: Cell Surface Molecules, T cells, Superantigens, Cell Activation, Signal Transduction.

ABSTRACT

The behavior of CD38 during immune synapse formation has not been elucidated. We determined herein that human CD38 redistributed to the contact area of T cell-APC conjugates in Ag-dependent manner, and occured with either B cells, or monocyte-derived dendritic cells (DCs)[3] as APC. Confocal microscopy studies showed that CD38 preferentially accumulated along the contact zone, whereas CD3-ζ redistributed toward the central zone of the immunological synapse (IS). Studies of T-APC conjugates with either human T cells, or B cells transiently expressing CD38-green fluorescent protein (GFP) revealed the presence of two pools of CD38, one at the cell-membrane and another in recycling endosomes. The recruitment of both pools to the T cell:APC contact site requires Ag-pulsed APC. In T cells CD38 recruitment to the synapse is Lck-dependent. Moreover, in T cells overexpressing CD38 there was an Ag-independent T cell-driven increase in CD38 ectoenzymatic activity upon T cell:APC contact, and an APC- and Ag-dependent increase in $[Ca^{2+}]_i$ that was more potent and sustained than that in $CD38^{normal}$ T cells. Preincubation of influenza HA-specific T cells with non-agonist anti-CD38 mAbs affected the kinetics of Ag-induced early signaling events such as phoshorylation of LAT at Tyr^{191}, or phosphorylation of PKCθ at the regulatory site Thr^{538}, impairment of IFN-γ production without affecting the kinetics of phosphorylation of Erk at the activation sites Thr^{202}/Tyr^{204}. These results reveal a new role for CD38 in Ag-mediated T cell responses during or before synapse formation leading to increased $[Ca^{2+}]_i$, phosphorylation of LAT, PKCθ activation, and IFN-γ production.

INTRODUCTION

The IS is the specialized contact surface that is formed between the T cell and the APC (1). Although it was originally coined to describe the contact area between a helper T cell and B cell, the term IS is today generically used to describe the contact surface between any lymphoid effector cell (T, B, or NK cell) and APC or target cell. This cell-cell contact area has two spatially segregated regions: The central supramolecular activation complex (c-SMAC) containing the TCR, costimulatory molecules, and signaling molecules, surrounded by the peripheral SMAC, which is enriched in adhesion molecules.

Human CD38 is a 45-kDa type II transmembrane glycoprotein with a short amino-terminal cytoplasmic domain and a long carboxy-terminal extracellular domain (2). CD38 expression is correlated with differentiation or activation of human T and B cells, and CD38 may serve as an adhesion and signal transduction molecule (3). Thus, a variety of cellular functions can be elicited by ligation of CD38 with specific mAbs including proliferation, lymphopoiesis, apoptosis, adhesion, cytokine production and tyrosine phosphorylation of proteins (4-8).

Human, mouse and rat CD38 extracellular domains display amino acid sequences similar to that of *Aplysia* ADP ribosyl cyclase, an enzyme that catalyzes the formation of cyclic ADP ribose (cADPR) from NAD^+ (9). CD38 not also catalyzes the formation of cADPR but also the formation of adenosine diphosphate ribose and nicotinic acid adenine dinucleotide phosphate, which are potent mediators of intracellular calcium release and/or influx of extracellular calcium by distinct mechanisms (10, 11). A long recognized paradox of the NAD^+/cADPR system is the compartmentalization in several mammalian cell types (for a review see De Flora et al., (12). Although most of cADPR produced by CD38 likely acts in the extracellular space, expression of CD38 in $CD38^-$ 3T3 fibroblasts increases basal levels of intracellular calcium and cADPR concentration (13), as well as the intracellular calcium ($[Ca^{2+}]_i$) mobilization in response to ATP (14). Moreover, decreased cADPR and increased NAD^+ has been observed in the $CD38^{-/-}$ mice (15). Whether this phenomenon could be

extended to other cell types, it remains to be seen. Elegant studies by Guse et al., have shown that there is a causal relation between increased cADPR concentrations, sustained calcium signaling and activation of T cells, (16), which correlated with increased ADP ribosyl cyclase detected in the cytosolic fractions, and not in particulate fractions (membrane-bound) from anti-CD3 stimulated T cells. This soluble enzyme found in the cytosolic fraction of Jurkat T cells is distinguishable from the plasma-membrane-bound ectoenzyme CD38 in terms of substrate usage (16, 17). However, in these studies the anti-CD3 mAb OKT3 was used to stimulate T cells and not antigen-pulsed APC, which did not allow examining the effect of cell to cell contact on the membrane-bound CD38-associated enzymatic activity in a more physiological context (intact cells vs cell fractions). Moreover, CD38 is highly enriched in membrane rafts (18, 19), which are only a relatively small proportion of the total membrane fractions used to measure ADP-ribosyl cyclases (16, 17).

CD38 signaling in T cells is functionally dependent on the TCR/CD3 complex (20, 21), and it is initiated in a subset of membrane rafts containing CD38, Lck and the CD3-ζ chain of the TCR (18, 19). On the other hand, it is likely that in monocytes CD38 and MHC Class II share a common activation pathway (22), and that in these cells CD38, HLA-DR, and CD9 are pre-associated without any interaction with T cells (23). Moreover, MHC class II molecules present in lipid rafts of APCs are concentrated at the synapse to facilitate antigen presentation (24, 25), tetraspanins as CD81 are also dynamically redistributed during synapse formation (26), and CD38 is laterally associated with CD81 in mature dendritic cells as judged by the simultaneous translocation of these molecules to a pole of the cells in co-capping experiments (4). Because Lck and CD3-ζ molecules are recruited to the IS upon successful T cell-APC conjugate formation, we hypothesized that accumulation of CD38 at the T cell:APC contact might occur. In this study we show that CD38 is recruited to the T cell-APC interface, and that T cells and, to a lesser extent APCs, contribute to the clustering of this molecule to the IS. The results also indicate that CD38 expression may contribute in

T cells to antigen-mediated Ca^{2+} responses, and to modulate the phosphorylation status of some intracellular signaling molecules as LAT and PKCθ.

MATERIAL AND METHODS

Cells

The Jurkat-derived human T cell line J77cl20 (TCR Vβ8$^+$) and the lymphoblastoid B cell line Raji (HLA-DR3/DR10) have been previously described (27). The Jurkat-derived clone D8 (TCR Vβ8$^+$) was obtained from wild-type Jurkat E6-1 by limiting dilution technique to get a variant with a relative high CD38 surface expression (7). The Jurkat-derived Lck-deficient JCaM1.6 was provided by Dr. A. Weiss (UCSF, San Francisco, CA) (28). Human monocyte derived-DCs were obtained as described (29). At day 6, maturation of DCs was induced by LPS (10 ng/ml, Sigma Chemical Co., St. Louis, MO). SEB specific polyclonal CD4$^+$ T lymphocytes were generated by incubating irradiated LG2 cells and peripheral blood monocytes with peripheral blood lymphocytes in medium supplemented with 0.5 μg/ml of SEB. Cells were restimulated every 2 weeks as described (27). CH7C17 cells derive from a TCR$^-$ Jurkat T cell clone permanently transfected with the cDNAs encoding the TCRα and the TCRβ chains from the DR1-HA-responsive human T cell clone HA1.7 (30). CH7C17 cells were grown in RPMI medium containing 10% FBS + Hygromycin B (0.44 mg/ml) + Puromicin (4.4μg/ml). The EBV-transformed B cell line HOM2 is homozygous for HLA-DR1 (DRB1*0101-positive) (31) was a gift of Dr. D. Jaraquemada (Instituto de Biotecnología y Biomedicina (IBB), Barcelona, Spain).

Antibodies and reagents

The following mAbs were used: FITC-conjugated OKT3 (anti-CD3), unconjugated or FITC-conjugated HB136 (anti-CD38), TP1/15.1 (anti-CD31), TP1/24 and HP2/19 (anti-ICAM-3), 448 (anti-CD3-ζ, a gift of Dr. B. Alarcón, (CBM-CSIC, Madrid, Spain), D3/9 (anti-CD45), AE-6 (anti-Golgi) was purchased from Calbiochem, DF 1513 (anti-CD71), and AC-40 (anti-α-actin) from Sigma-Aldrich, biotin-conjugated mouse anti-human Vβ8TCR, and anti-human CD19 from BD Pharmingen, anti-phospho-LAT (Tyr^{191}), anti-phospho-Erk E10 mAb (Thr^{202}/Tyr^{204}), anti-phospho-PKCθ (Thr^{538}), and anti-PKCθ from Cell Signaling, anti-phospho-Tyrosine (RC20-HRP) from BD Transduction Laboratories, secondary Alexa 488- and Rodamine Red X-labeled

Abs, streptavidin, and fluorescent trackers chloromethyl derivative of aminocoumarin (CMAC), chloromethyl-benzoylamino-tetramethylrhodamine (CM-TMR), and 4',6-diamidino-2-phenylindole, dihydrochloride were obtained from Molecular Probes (Eugene, OR). NGD^+, and Poly-L-lysine (PLL) were purchased from Sigma-Aldrich. Superantigens SEE, or SEB were obtained from Toxin Technology (Sarasota, FL). The influenza hemagglutinin (HA) peptide (HA 307-319, PKYVKQNTLKLAT) was synthesized and purified by HPLC by Genosphere Biotechnologies (Paris, France). The human CD38 cDNA and the anti-CD38 mAb IB6 was a gift from Dr. Fabio Malavasi (Torino University Medical Center, Torino, Italy).

CD38-GFP construct and transient transfections

CD38-GFP was obtained by PCR amplification of the human CD38 cDNA and cloned in the pEGFP-C1 vector (Clontech Laboratories, Palo Alto, CA). Raji B cells or J77 Jurkat T cells were resuspended at 1 x 10^7 cells in 400 µl of Optimem-1 (Life Technologies, Grand Island, NY) with 10 µg of pEGFP-C1-CD38 and electroporated at 975 µF/270 V/186Ω in a Electro Cell Manipulator 600 (BTX, Harvard Apparatus Inc., Holliston, MA). The pEGFP-C1 vector was used as a transfection control. Cells were used at 48 h after transfection. For CD38 overexpression experiments J77 Jurkat T cells were transfected with the pEGFP-C1-CD38, or pEGFP-C1 vectors using the human Cell line Nucleofector Kit V (Amaxa) according with manufacturer's specifications at the proportion of 2 x 10^6cells/5µg cDNA. Cells were used 24 h after transfection.

Conjugate formation and immunofluorescence microscopy

To distinguish APCs from T lymphocytes, the APCs were loaded with the fluorescent trackers CMAC, or CM-TMR (10 µM) (Molecular Probes). The APCs were then incubated for 20 min at 37°C with 1 µg/ml SEE (Raji). Jurkat (0.5 x 10^6 cells) were mixed with Raji cells (0.5 x 10^6 cells), centrifuged at 1,100 rpm for 5 min, and then incubated for 5 min at 37°C. Cells were plated onto PLL (50 µg/ml)-coated slides, incubated for 20 min at 37°C, and fixed in 2% p-formaldehyde. SEB specific polyclonal T cells were loaded with the blue fluorescent cell tracker CMAC (5 µM for 30 min at 37º C), washed and resuspended in HBSS-2% FBS. Human monocyte-derived mature

DCs ($5x10^4$), preloaded with SEB (1 μg/ml for 30 min, 37º C), were mixed with Polyclonal SEB-specific T cells ($1.5x10^6$), centrifuged and incubated for 15 min at 37º C. Then, cells were allowed to settle on coverslips for 30 min at 37º C. Cell conjugates were fixed for 5 min in 2% formaldehyde-PBS. After blocking with human γ-globulin (Sigma), immunofluorescence staining of cell surface molecules was performed with the appropriate primary mAb. Intracellular proteins were detected by permeabilizing cells in 0.5% Triton-X-100 prior staining with the specific antibody as described elsewhere (26, 27). Samples were then examined with either a DMR photomicroscope (Leica, Mannheim, Germany) using Leica QFISH 1.0 software, or an Olympus Cell R IX81 motorized system inverted microscope equipped with MT20 illumination system, a CCD camera (Hamamatsu), and Cell^R imaging software.

Confocal microscopy

Confocal images were acquired using a Leica TCS-SP confocal scanning laser microscope equipped with Ar and He-Ne laser beams and attached to a Leica DMIRBE inverted epi-fluorescence microscope. Serial fluorescence and DIC images were obtained simultaneously as previously described (26). Image analysis and subcellular colocalization fluorograms were generated and analyzed using the Leica confocal software package. Positive image masks of significant colocalization of two fluorophores were generated from the image fluorogram data sets by defining the specific regions of interest with a bounding box of the fluorogram.

Antigen-induced T cell activation, FACS and Western-blot analysis

For antigen-specific stimulation, HOM-2 were incubated at 37ºC for 2.5 h with the HA peptide (307-319) (67μM), or were left unpulsed. Then, HOM-2 cells were mixed with CH7C17 T cells at a ratio of 1:1, centrifuged for 1 min at 4,000 rpm in a microfuge, and incubated at 37ºC for various periods of time (1, 5, 20 and 40 min). Cells were then lysed and analyzed by Western blot as described in detail elsewhere (7, 18, 19).

Cells were analyzed for surface expression of TCR Vβ8, CD3, CD38, ICAM-3, CD31, and CD19 by flow cytometry as previously described (7). Samples were analyzed in a FACScalibur flow cytometer (Becton Dickinson, San Jose, CA), using the CellQuest

Software. The CELLQUANT Calibrator kit (BIOCYTEX, France) was used for leukocyte surface antigen quantification.

ADP-ribosyl cyclase activity

Ectocellular GDP-ribosyl cyclase activity was continuously measured in intact cells at 37ºC using 100 μM NGD^+ as a surrogate substrate for NAD^+ (32).

The production of the fluorescent cGDPR was measured fluorimetrically (excitation wavelength, 300 nm (BW 20 nm); emission wavelength, 430 nm (BW 35 nm) using a fluorescence plate reader Infinite F200 (TECAN, Switzerland). Cells were spun-down for 1 min at 4,000 rpm immediately prior to the assay to favor conjugate formation, and cells were placed in a 96-well black plate (Ref: 265301, NUNC). The reaction was measured over 90 min at 37ºC. The rates of cGDPR production were determined from the slopes of fluorescence increase.

Ca^{2+} analysis

J77 were nucleofected with CD38-GFP or pEGFP-C1 24 h before the experiment. Cells were then tested for GFP and/or CD38 expression by FACS. To eliminate dead cells and debris, cells were purified by Histopaque cell gradient centrifugation as previously described (33). Then, cells were loaded with Fura2-AM (Invitrogen) for 30 min in the dark (Fura2-AM loading solution: HBSS-BSA-Probenecid (2.5mM)-Fura2-AM (4μM)-Pluronic F-127 (20%)). Cells were then washed and mixed with an equal number of APCs previously pulsed with SEE or not as described above. After a 1 min spinning at 4,000 rpm, cells were placed in a 96-well black plate (Ref: 265301, NUNC), and fluorescence measurements were done on a fluorimeter plate reader (Infinite F200, TECAN, Switzerland) at 37ºC. Cells were consecutively excited at 340 and 380 nm at intervals of 30 s and emissions at 510 nm was recorded. $[Ca^{2+}]_i$ was determined by calculating the fluorescence ratio (340/380).

Cytokine production

IL-2, or IFN-γ production was measured in cell supernatants after overnight stimulation of T cells with antigen-pulsed or unpulsed APC by ELISA (Eli-pair, Diaclone), as previously described (34).

RESULTS

Surface CD38 clusters at the T cell-APC contact region

In Jurkat T cells about 60% of CD38 is located into raft fractions and co-immunoprecipitates with CD3-ζ and Lck (19). Moreover, CD38 in rafts is able to initiate and propagate several activating signaling pathways via its capacity to interact with Lck and CD3-ζ (18, 19). Because Lck and CD3-ζ molecules are recruited to the contact area of a T cell with an antigen-pulsed APC, known as the IS (35), we hypothesized that accumulation of CD38 at the T cell:APC contact might occur. To determine whether CD38 localized at the IS we first used the Jurkat T cell-Raji B cell system. Jurkat T cells expressing the Vβ8 gene segment of the TCRβ chain (Fig. 1A) are able to recognize the SEE superantigen bound to the human B cell line Raji, which acts as an APC, and form conjugates similar to genuine T cell-APC pairs (27, 36). We used two different Jurkat clones, D8 and J77, which only differ in the level of CD38 surface expression (Figure 1A).

The conjugates Jurkat:Raji formed were monitored for the distribution of the fluorescent label at the site of T:B cell contact after 5 min incubation in solution and 20 min onto PLL-coated cover slides at 37ºC, a time considered to be long enough for the establishment of mature synapses (27). Fig. 1B (upper panels) shows that, in the absence of SEE, CD38 was evenly distributed on the cell-surface of most Jurkat D8-Raji conjugates, while in the presence of SEE, CD38 accumulated at the contact area between the T cell and the APC in increased number of conjugates. The pattern of CD38 redistribution was clearly different from that of CD3-ζ, which is a marker of mature synapse formation. CD3-ζ was detected in a small cluster in the center of the synapse, the c-SMAC, whereas CD38 was enriched along the contact zone (Fig. 1B, middle panels). In contrast, CD45 was evenly distributed at the plasma membrane (Figure 1B, lower panels). The results on CD38 clustering along the T cell:APC contact area were confirmed by analysis of Jurkat D8 SEE-pulsed Raji conjugates by confocal microscopy (Fig. 1C).

In most conjugates formed between Jurkat J77 cells and SEE-pulsed Raji B cells the accumulation of CD38 was homogeneous throughout the contact region, but in some of them CD38 was concentrated at the outer zone (Fig. 1D), which resembled what occurs for ICAM-3 in Jurkat-Raji conjugates in the presence of SEE (Fig. 1D, and (27)).

We also determined the redistribution of CD38 in other T cell−APC system, such as the interaction of SEB-specific polyclonal T cells in interaction in interaction with monocyte-derived mature DCs. CD38 redistributed along the region of T cell contact with DCs that had been pulsed with staphylococcal enterotoxin B (SEB), (Fig. 1E). In contrast CD3-ζ was detected as a smaller cluster toward the center of the T-DC contact zone (Fig. 1E).

CD38 is detected at the plasma membrane and in intracellular compartments that co-distributes with CD3-ζ

Since both Jurkat T and Raji B cells express CD38 on the cell surface, the observed redistribution of surface CD38 to the interface formed by the Jurkat and Raji cells prompted us to investigate the cellular origin of CD38. J77 T cells were transfected with either a plasmid encoding a C-terminal fusion protein of CD38 with the GFP (CD38-GFP), or with a plasmid encoding the GFP protein alone, and expression of the CD38-GFP chimeric protein, or GFP in total cell lysates was assessed (Fig. 2A). CD38-GFP form migrated at an apparent molecular weight of 80 kDa while endogenous CD38 had an apparent molecular weight of 45 kDa as revealed by Western blotting with anti-CD38 mAb. The 80 kDa band was also detected by an anti-GFP mAb which was indicative that this band corresponded to the CD38-GFP fusion protein. In GFP-transfected cells only a band at 35 kDa was detected, which coincided with the expected molecular weight of the GFP protein.

Cellular distribution of transfected CD38-GFP and GFP clearly differed (Fig. 2B). While CD38-GFP localized at the plasma membrane and in a conspicuous intracellular compartment, GFP alone showed a cytoplasmic staining with no enrichment at the plasma membrane. The cellular localization of CD38-GFP was compared with that of endogenous CD3-ζ and CD38. As shown in Fig. 2C (upper

panels), in CD38-GFP-transfected J77 cells CD38-GFP co-localized with endogenous CD3-ζ both at the plasma membrane and in the subcellular compartment. Moreover, in non-transfected J77 cells the pattern of intracellular endogenous CD38 overlapped with that of CD3-ζ (Fig. 2C, lower panels). Note also that the pattern of CD38-GFP expression in transfected Raji B cells was very similar to that of endogenous CD38 in nontransfected Raji cells with dual expression at the plasma membrane and inside the cells (Fig. 2D). Altogether these results demonstrate that CD38-GFP distribution is not an artifact due to GFP tagging or a specificity of Jurkat T, or Raji B cell lines.

CD38 in recycling endosomes and in the Golgi apparatus is redistributed at the T cell side contacting the APC

Since it has previously shown that intracellular CD3-ζ is present in recycling endosomes and to lesser extent in the Golgi apparatus (37, 38), we assessed whether intracellular CD38-GFP co-distributed with specific markers of these compartments by confocal microscopy. The transferrin receptor (TfR, CD71) is normally present in the plasma membrane and recycling endosomes, and it has been used as a marker for the latter (39). In T cell-APC conjugates, the T cell CD71 endosomal pool relocates beneath the contact site, whereas surface CD71 localizes to the peripheral ring of the IS (38, 39). As shown in Fig. 3A (upper panels, arrows), in the absence of SEE, CD71 and CD38-GFP appeared at the cell surface with an even distribution. Note that staining of CD71 was done in permeabilized cells and, therefore, both CD71 pools were accessible for detection. In contrast, Jurkat T cells conjugated with SEE-pulsed APCs displayed a significant accumulation of CD38-GFP to the contact site that overlapped with the massive clustering of CD71 to the same zone (Fig. 3A, lower panels, arrowheads). As depicted in the example, in most T cell:SEE-pulsed APC conjugates, membrane CD71 and intracellular vesicles containing CD71 were in so close proximity that were difficult to discriminate between them. The merge images showed that most intracellular CD38-GFP (green) and CD71 (red) colocalized (yellow) into the same endosome-like vesicles (see also the close-up panel). A more quantitative assessment of the level of colocalization was done by analyzing the colocalization scatter plot and generating a

mask of the area of interest (AOI) (Fig. 3, right panels). In marked contrast, on B cells neither surface, nor intracellular CD71 moved toward the T cell:APC contact zone.

In the absence of superantigen, intracellular CD38-GFP partly but not entirely overlapped with the Golgi marker, far away from the T:APC contact zone (Fig. 3B, upper panels, indicated by arrowheads). The merge images of CD38-GFP and the Golgi marker indicated that most intracellular CD38-GFP was immediately adjacent but distinguishable from the Golgi apparatus. In the presence of superantigen, most T cells exhibited Golgi polarization toward the APC, although only partial overlapping with intracellular CD38-GFP was observed (Fig. 3B, lower panels, see also the close-up panel and colocalization masks). Overall, these data indicate that in T cells most of the intracellular pool of CD38 is associated with endosomes, whereas only a part of CD38 colocalizes with the Golgi apparatus.

Quantitation of TCR-dependent clustering and polarization of CD38 from T cells at the T cell-APC contact zone

In J77 Jurkat T cells reorientation of the CD38-GFP$^+$ intracellular compartment toward the cell-cell contact zone (polarization or recruitment) occurred in most cases in which surface CD38-GFP clustered at the same zone (clustering). Sometimes the intracellular compartment appeared fused with the one located at the plasma membrane, in particular in those conjugates were B cells were pulsed with SEE (Fig. 4A, lower panels). This made difficult to quantify the polarization of intracellular CD38 independently from the clustering of plasma membrane CD38 at the contact zone. Three independent experiments summarized in Figure 4B, showed that recruitment of CD38 at the T cell:APC contact zone occurred in 17 ± 0.6% of the conjugates formed with CD38-GFP$^+$ J77 cells and Raji cells not pulsed with SEE, while in the presence of SEE CD38 redistribution at the T cell:APC contact zone was increased up to 49 ± 2.9% of the conjugates ($P = 0.0004$). Redistribution of endogenous CD3-ζ (plasma membrane and intracellular) was checked as a positive control for mature synapse formation (Figure 4A). CD3-ζ redistribution occurred in 35 ± 3% of conjugates in the absence of SEE, whereas in the presence of SEE, CD3-ζ redistribution increased up to 77 ± 6% of

T:B cell conjugates (Fig. 4B, $P = 0.0039$). The intracellular pool of CD3-ζ redistributed towards the cell-cell contact zone, substantially overlapping with that of CD38-GFP (Fig. 4A).

We next studied the recruitment of the CD38-GFP fusion protein at the contact zone between live T cells and SEE-pulsed Raji APCs by time-lapse confocal microscopy. Clustering of surface CD38-GFP at the T/APC interface appeared very rapidly (within the first 30 seconds) and persisted for at least 20-25 min (Fig. 4C, upper panel, and Movie 1[4]). Intracellular CD38-GFP compartment polarized in the vicinity of the APC within 1-2 min of the T cell-APC contact in a SEE-dependent manner, where it appeared fused with surface CD38-GFP within 4-5 min of cell-cell contact (Fig. 4C, lower panel, and Movie 2).

Defective CD38 clustering at the immunological synapse in an Lck deficient T cell line

To determine the role of Lck in TCR-mediated CD38 clustering at the IS, we studied the behavior of CD38-GFP in the Lck-deficient JCaM1.6 T cells after interaction with APCs. In conjugates formed with Lck-deficient JCaM1.6 cells and Raji B cells non-pulsed with SEE, clustering of CD38-GFP, or CD3-ζ toward the T:APC contact zone was greatly reduced as compared with that in wild-type J77:APC conjugates (Fig. 5B vs Fig. 4B). Despite that, in T cell:SEE-pulsed APC conjugates CD38-GFP accumulation at the IS, and recruitment of endogenous CD3-ζ to the c-SMAC increased 2- and 6-fold respectively over the basal levels, although only the increased translocation of CD3-ζ to the synapse was statistically significant (Fig. 5B). Polarization of the intracellular GFP-CD38 and endogenous CD3-ζ towards the APC was detected in most of conjugates in which clustering of surface CD38-GFP or CD3-ζ occurred (Fig. 5A, middle panels). However, reorientation of the intracellular pools of CD38-GFP and CD3-ζ without apparent clustering of their corresponding surface counterparts was also observed (Fig. 5A, lower panels). Therefore, in these cells the formation of mature synapses and translocation of surface CD38 at the T cell:APC contact zone may occur although with lower efficiency than that in wild-type J77 cells.

These data suggest that CD38 is actively recruited at the synapse by mechanisms involving Lck-mediated signaling events.

TCR-dependent clustering of CD38 from B cells and CD31 from T cells at the T cell-APC contact zone

Raji B cells were transiently transfected with the CD38-GFP construct and assessed for their ability to cluster CD38 at the contact zone with the T cells (Fig. 6A and 6B). 4.6 ± 1.6% of conjugates, which were CD38-GFP$^+$, showed translocation of CD38-GFP to the T cell-APC contact zone in the absence of SEE. The translocation of CD38-GFP at the cell contact zone increased 2.6-fold in the presence of SEE up to 12 ± 0.3% of conjugates, indicating active translocation ($P = 0.0487$). Interestingly, in 80% of the conjugates in which CD38-GFP from the B cell clustered at the cell contact zone there was also a clear translocation of CD3-ζ from the apposed T cell (Figure 6A, lower panels). However, many other conjugates showed translocation of membrane CD3-ζ and polarization of intracellular CD3-ζ without the concomitant recruitment of CD38-GFP from the apposing B cell (Fig. 6A, middle panels). Therefore, the relative low number of B cells showing CD38-GFP clustering to the T cell:APC interface was not due to a failure to form mature synapses since translocation of CD3-ζ at the T cell:APC interface occurred in about 72% of the conjugates (Figure 6B), which was indicative of normal synapse formation and maturation.

Jurkat T cells express the counter receptor of CD38, CD31 (40), whereas the Raji B cells are almost CD31 negative (Fig. 6C). Therefore it was of interest to test whether the recruited CD38-GFP from B cells co-localized with CD31 from the opposing T cells. First, CD38 and CD31 surface antigen expression levels were quantified in both cells by flow cytometry using the Cellquant Calibrator Kit, which allows determining the number of antigenic sites per cell (Fig. 6D, and 6E). The number of CD38 antigenic sites on Raji cells (98,108 ± 12,940; n = 5) was significantly higher than the number of CD31 antigenic sites on Jurkat J77 cells (5,261 ± 474; n = 5). Then, CD38-GFP-transfected B cells were pulsed or not with SEE and incubated with Jurkat J77 cells. As shown in Fig. 6F, in the absence of SEE 2.8 ± 1.3% of the conjugates

CD38-GFP$^+$ showed translocation of CD31 to the IS. In these conjugates simultaneous clustering of CD38-GFP from the APCs was not observed (data not shown). In contrast, in response to SEE stimulation the recruitment of CD31 to the T:APC contact zone increased 5-fold up to 14 ± 1.6% of the CD38-GFP$^+$ conjugates (P = 0.0003). In about 40% of the conjugates in which CD38-GFP from the SEE-pulsed Raji B cell translocated to the T:APC contact zone, there was co-localization with CD31 from the T cell (Fig. 6B, middle panels), suggesting active recruitment caused by receptor-ligand interactions. Assuming that translocation of CD38 on B cells and CD31 on T cells is driven by receptor/counter-receptor interactions, the observed 18.6-fold difference in surface expression of these two receptors could explain the relative inefficiency of the process in B cells. However, recruitment of CD31 to the IS without the concomitant translocation of CD38-GFP also occurred (Fig. 6B, lower panels), which could be indicative of the existence of alternative mechanisms for CD31 clustering to the T:APC contact zone.

Effect of CD38 overexpression in T cell function

The redistribution of plasma membrane CD38 at the synapse with the extracellular domain of CD38 facing toward the APC opened the possibility that the enzymatic activity of CD38 outside the cell could concentrated in a small area on the T cell. To test whether the ADP-ribosyl cyclase activity of CD38 could be affected by conjugate formation, and/or CD38 translocation to the IS, J77 Jurkat T cells were transfected with the cDNAs coding for CD38-GFP, or GFP alone by nucleofection. By this method of transfection, not only a high efficiency was reached, as judged by the high percentage of cells transfected (GFP$^+$), but also a higher number of CD38 molecules per cell was obtained (double positives for GFP and CD38-PE) (Fig. 7A, and data not shown). 24 h upon transfection, cells were subjected to histopaque gradient centrifugation to get rid of dead cells and debris and then they were left alone, or put in contact with SEE-pulsed or unpulsed Raji B cells following a brief centrifugation step to favor conjugate formation. Ectocellular GDP-ribosyl cyclase activity was continuously measured at 37ºC using NGD$^+$ as a surrogate substrate for NAD$^+$ (32). Fig.

7B and 7C shows a typical fluorimetric tracing of GDP-ribosyl cyclase activity. In Fig. 7B, during the first 20 min of incubation with NGD^+ the individual cells (J77 CD38-GFP^+, or Raji cells alone) did not show any enzymatic activity, in contrast with the significant GDP-ribosyl cyclase activity observed when the same cells were put in contact (i.e. J77 CD38-GFP^+ cells with either SEE-pulsed, or with unpulsed Raji cells). At later time points, although individual cells showed measurable GDP-ribosyl cyclase activity, the sum of such activities was lower than that observed when the two cell-types were put together. In control experiments performed with J77 transfected with GFP (J77 pEGFP-C1) mixed and put in contact with SEE-pulsed or unpulsed Raji B cells (Fig. 7C), increased GDP-ribosyl cyclase activity relative to that in Raji B cells kept alone was only detected during the first 20 min, with no significant differences afterwards. GDP-ribosyl cyclase activity in J77 pEGFP-C1 cells alone was only detectable when higher number of cells was used in this assay (1×10^6 cells/point; data not shown), which is in agreement with the lower surface CD38 expression in these cells relative to that observed in J77 CD38-GFP^+ cells, or Raji B cells. Therefore, increased surface expression of CD38 in J77 CD38-GFP^+ cells and antigen-independent T-APC interactions favored by the centrifugation step might be involved in the dramatic changes in ecto-GDP-ribosyl cyclase activity observed.

To test whether overexpression of CD38 could affect intracellular calcium ($[Ca^{2+}]_i$) mobilization in antigen-stimulated T cells, either J77 CD38-GFP^+, or J77 pEGFP-$C1^+$ were loaded with the calcium indicator Fura-2 and then mixed with SEE-pulsed Raji B cells. No intracellular calcium mobilization $[Ca^{2+}]_i$ was observed (data not shown). Short centrifugation (1 min) followed by resuspension of the T:APC mixture resulted in a rapid increase in $[Ca^{2+}]_i$ immediately after T:APC contact and this was sustained throughout the experimental period (about 9 min, Fig. 7D). This calcium mobilization was higher in J77 CD38-GFP^+ cells than in J77 pEGFP-$C1^+$ used as controls. As revealed by control experiments, conjugation of these T cells with unpulsed Raji B cells resulted in relatively low increases in $[Ca^{2+}]_i$ (Fig. 7D) relative to that with SEE-pulsed B cells. These results demonstrate that CD38 overexpression in T cells

enhances TCR-mediated calcium mobilization in an APC- and antigen-dependent manner, if rapid conjugate formation between the T cell and the APC was supported by centrifugation. Moreover, the basal level of $[Ca^{2+}]_i$ in J77 CD38-GFP$^+$ cells was relatively higher than that in J77 pEGFP-C1$^+$ cells incubated alone (data not shown). These data resembled previous work showing that in CD38$^+$-transfected HeLa and 3T3 cells there was an elevation of the basal $[Ca^{2+}]_i$, which correlated with increased CD38 surface expression and increased surface cyclase activity (13).

Because sustained increase in $[Ca2^+]_i$ is required for TCR-induced IL-2 production by T cells, we next determined the effect of CD38 overexpression on IL-2 secretion by Jurkat T cells stimulated with SEE-pulsed Raji B cells. As shown in Fig. 7E, there was a consistent increase in IL-2 production by J77 CD38-GFP$^+$ in comparison with that by J77 pEGFP-C1$^+$ cells at a broad concentration range of SEE (from 10 ng/ml to 1 μg/ml), although the differences were not statistically significant. Therefore, CD38 overexpression seems not to be required for maximal IL-2 production induced upon SEE-stimulation.

Functional role of CD38 in antigen-stimulated T cells

To investigate the functional role of CD38 in T cell activation in a system closely mimicking physiological T cell stimulation by APC, we used Jurkat T cells expressing the HA 307-319 epitope-specific TCR (CH7-C17 cells), and B cells presenting the nominal antigenic peptide HA 307-319 (HOM-2 cells) as corresponding APCs. An additional advantage of this system is that, in contrast with Raji cells, HOM-2 cells are CD38 negative by FACS (Fig. 8A), and therefore the functional capabilities of the CD38 from the T cell could be easily tested without the interference of the CD38 from the B cell. We first assessed whether non-agonistic anti-CD38 mAbs could affect the overall increased protein tyrosine phosphorylation that occurs in T cells upon incubation with antigen-pulsed APCs. To this end, we used the anti-CD38 mAb, IB6, which is unable to induce PBMC proliferation, calcium fluxes, and IFN-γ secretion (41). As shown in Fig. 8B, IB6, which in the absence of HA antigen did not induce any detectable increase in tyrosine phoshorylation of any substrate (compare lanes 1-4 vs

lanes 5-8), had no clear effect in the kinetics of HA-mediated increased tyrosine phosphorylation of several proteins (compare lanes 9-12 vs lanes 13-16).

Next, we used phosphospecific antibodies to identify specific proteins that could be affected by IB6-induced blockade. As shown in Fig. 8C, stimulation of Jurkat CH7-C17 cells with HOM-2 cells pulsed with the HA specific peptide induced phosphorylation of the tyrosine residue Tyr^{191} of the adaptor protein LAT with relatively fast kinetics, reaching the maximum at 5 min upon stimulation and remaining stably high throughout the experiment, while stimulation of the same cells in the presence of the anti-CD38 mAb IB6 induced LAT tyrosine phosphorylation with slower kinetics, not reaching the maximum up to 20-40 min upon stimulation (see Fig. 8D, for quantification). In contrast, similar kinetics of Erk phosphorylation at Thr^{202} and Tyr^{204} were induced by HA-pulsed HOM-2 cells, either in the presence of absence of anti-CD38 mAb IB6 (Fig. 8E, lanes 9-12 vs lanes 13-16; and Fig. 8F).

The cellular function of PKCθ in T cells can be regulated by phosphorylation of a specific threonine residue (Thr^{538}) in the PKCθ activation loop (42), or by other mechanisms such as autophosphorylation of Thr^{219} (43). We used a phospho-specific antibody that recognizes Thr^{538}–phosphorylated PKCθ to test whether stimulation of CH7-C17 Jurkat T cells with HA-pulsed HOM-2 cells led to increased phosphorylation of Thr^{538} of PKCθ. As shown in Fig. 8G, (lanes 9-12) and Fig. 8H, increased phosphorylation of PKCθ at Thr^{538} was clearly observed after T cell stimulation with HA-pulsed HOM-2 cells, whereas no such increase was observed when the CH7-C17 cells were stimulated with pulsed HOM-2 cells in the presence of the anti-CD38 mAb IB6 (Fig. 8G, lanes 13-16, and Fig. 8H). This occurred despite the fact that the anti-CD38 mAb IB6 induced at 5 min a short-lived increased phosphorylation of PKCθ in CH7-C17 Jurkat T cells incubated with non-pulsed HOM-2 cells (Fig. 8G, lanes 5-8). It was also observed a low level of basal Thr^{538} phosphorylation on PKCθ in CH7-C17 cells incubated with non-pulsed HOM-2 cells throughout the duration of the experiment (Fig. 8G, lanes 1-4), which is consistent with the low level of constitutive phosphorylation of PKCθ at Thr^{538} observed in Jurkat T cells by others (43).

The above results prompted us to investigate whether there were any effects on later events such as cytokine production. As shown in Fig. 8I, two different anti-CD38 mAbs, IB6 or HB136, induced a partial but significant inhibition on the IFN-γ production induced in CH7-C17 T cells by HA-pulsed HOM-2 cells. Likewise, preincubation of CH7-C17 T cells with 100 μM 8-Br-cADPR, which is a cADPR antagonist, or 500 μM Nicotinamide, which is a negative feedback inhibitor of CD38 ADP-ribosyl cyclase activity, exerted a similar effect on IFN-γ production. In contrast, the addition of the 100 μM β-NAD^+, which is the natural substrate of CD38, had no effect.

DISCUSSION

In this study we show for the first time that in T cells CD38 forms two distinct cellular pools, one at the plasma membrane and a second in intracellular compartments, which are both redistributed towards the IS upon TCR engagement. Intracellular CD38-GFP displayed a similar distribution as endogenous intracellular CD3-ζ, or CD71, which are present in recycling endosomes, and recruited towards the IS formed between T cells and SEE-pulsed APCs. Recruitment of recycling endosomes containing CD3-ζ, Lck, LAT, and transferrin to the mature IS has been previously observed (37, 38, 44, 45). In this sense, in human T cells CD38 engagement with anti-CD38 mAbs induces CD38 internalization and its subsequent localization in early and late endosomes (46), processes that may be linked to increased c-Cbl tyrosine phosphorylation upon CD38 ligation (7, 19). Moreover, in human monocytes anti-CD38 mAbs induce internalization, shedding, and, more interestingly, new expression of CD38 on the cell surface (47). This newly expressed CD38 derives either from a pre-formed intracellular CD38 pool, or from surface CD38 that has been internalized and recycled back to the cell membrane (47). Therefore, and as it occurs for CD3-ζ (38), it is likely that intracellular CD38 might recycle back to the plasma membrane, providing an additional source of this protein to the mature synapse.

The presence of intracellular vesicles containing CD38 nearby the IS could have functional consequences due to the intrinsic enzymatic activity of CD38, which catalyzes the formation of cADPR from NAD^+. cADPR activates intracellular Ca^{2+} release via type 2 and 3 ryanodine receptors, and also induces extracellular Ca^{2+} entry via activation of capacitative Ca^{2+} entry and/or activation of the cation channel TRPM2 in conjunction with adenosine diphosphoribose (48). The redistribution of plasma membrane CD38 at the synapse with the extracellular domain of CD38 facing toward the APC opens the possibility that CD38-mediated production of cADPR outside the cell could concentrated in a small area on the T cell surface. Targeted release of NAD^+ from the cytosol to the extracellular space (reviewed in (12)), and the subsequent production of cADPR catalyzed by the CD38 accumulated at the IS could establish a

relatively high concentration of this metabolite in the synaptic space. The subsequent translocation of the in situ-generated cADPR inside the cell via CD38 itself, or via concentrative nucleoside transporters (12) may lead to preferential stimulation of the APC and the T cell itself. Our results, however, suggest that there is an antigen-independent T cell-driven increase in CD38 ectoenzymatic activity upon T cell:APC contact. Thus, this effect was only stabilized when the T cells expressed high levels of CD38 on their surface (i.e.: J77 CD38-GFP^{+}, CD38^{high}), and not in T cells with lower CD38 expression (J77 pEGFP-C1, CD38^{normal}), despite the fact that the number of CD38 molecules expressed on the cell surface of the APCs used (Raji B cells) clearly exceeded to those expressed on both T cell transfectants used. Moreover, the introduction of a centrifugation step to favor conjugate formation appeared to be crucial to see any differences on CD38 enzymatic activity, suggesting that the cell to cell contact is required for this process.

Whether this increase in CD38 ectoenzymatic activity has any effect on T cell activation remains to be proved, however, T cells overexpressing CD38 (CD38^{high}) had a higher basal level of cytosolic Ca^{2+} than the CD38^{normal} counterparts, which is likely due to increase intracellular cADPR as it occurs in CD38-transfected murine 3T3 fibroblasts (13). Moreover, in CD38^{high} T cells there was a more potent and more sustained increase in cytosolic Ca^{2+} in response to superantigen stimulation than that in CD38^{normal} Jurkat T cells. Increased tyrosine phosphorylation of PLC-γ1 was also observed (data not shown). Therefore, there is a causal relation between increased CD38 expression and sustained calcium signaling of antigen-stimulated T cells. However, CD38 overexpression had little effect on superantigen-stimulated production of IL-2, at least at the concentrations of SEE used in this study. It is important to note that Bueno et al., (49) have recently reported that bacterial superantigens can activate T cells by an alternative pathways bypassing the classical Lck-dependent tyrosine kinase phosphorylation events and activating instead a Gα11-dependent, PLC-β-mediated pathway, which has not been addressed in our study.

Remains to be seen, whether CD38 overexpression may modulate other T cell processes as proliferation, apoptosis, or cell survival. In this sense, in other cell types it has been observed increased survival potential of $CD38^+$ cells as compared with $CD38^-$ counterparts (4, 50). Moreover, cADPR, both exogenously added or paracrinally produced by $CD38^+$ feeder layer cells induce intracellular calcium mobilization, proliferation of human hemopoietic progenitors (51), and *in vivo* expansion of hemopoietic stem cells (52). It is important to point out that, in addition to membrane-bound cyclase activity linked to CD38, an, as yet unidentified, cytosolic ADP-ribosyl cyclase has been detected in Jurkat T cells and in peripheral blood T lymphocytes (16, 53). This cytosolic cyclase, or the intracellular CD38 located in recycling endosomes, which accumulates at IS, might also be reasonable candidates for inducing increased amounts of intracellular cADPR in response of T cells to the interaction with Ag-primed APCs. In the latter case, mechanisms for transport of NAD^+ inside the endosomes, and the subsequent release of the cADPR to the cytosol should be fully operational (12). In this regard, the polarized production of NO at the IS has been recently reported, with a modulating role on the strength of TCR-driven signaling (54). NO release at the IS requires increased intracellular Ca^{2+} (54), and although it has not been addressed in this study, it is very likely that this Ag-driven increased intracellular Ca^{2+} and subsequent NO response is mainly mediated by cADPR as it occurs in other cell systems (55).

To further address the question of how CD38 may contribute to T cell signaling in antigen-stimulated T cells, we investigated the impact of blocking CD38 with an anti-CD38 mAb, which acts as non-agonist in most functional assays tested (41). The data show that blocking CD38 affects the kinetics of antigen-induced phosphorylation of LAT at Tyr^{191}, results in inhibition of phosphorylation of PKCθ at Thr^{538} to basal levels, and partial although significant inhibition of IFN-γ production. However, phosphorylation of Erk at Thr^{202} and Tyr^{204} was unaffected. Moreover, another non-agonistic anti-CD38 mAb, HB136 also affected antigen-induced IFN-γ production. Since the APC used in these experiments is CD31 negative, it is unlikely that the anti-

CD38 mAb used may affect CD38/CD31 interaction, although they may affect the interaction of CD38 with an as jet unknown ligand expressed by the APC.

CD38 accumulates first along the T cell-APC contact zone and then at later time points rearranges to more peripheral sites colocalizing with adhesion molecules as ICAM-3 (Fig. 1, and data not shown) (27). This pattern of accumulation it is also similar to that of Lck, which is also enriched in the synapse periphery after an initial accumulation in the c-SMAC (45). In this sense, by using the cell line JCaM 1.6, which lacks of functional Lck, we have shown that the proportion of conjugates showing mature synapses and/or CD38 translocated to the interface between the T cell and the APC is greatly reduced as compared with that in wild-type Jurkat T cells. Likewise, CD38-mediated signaling is defective in JCaM1.6 cells (7). Consistently, Src-family protein tyrosine kinases were required for CD38 relocalization, as shown by the even lower accumulation of CD38 at the IS displayed by wild-type Jurkat T cells treated with the Src-family inhibitor PP-2 (data not shown). These results are in agreement with previous work by Morgan et al., (56) showing defective conjugate formation in JCaM1.6 cells, or PP2-treated wild-type Jurkat T cells, and failure to recruit F-actin and LFA-1 to the T cell:APC contact site. Moreover, ezrin, a member of the ezrin-radixin-moesin family of membrane-microfilament linkers that in wild-type Jurkat T cells is highly enriched in the F-actin-rich membrane protrusions at the periphery of the IS, shows poorly accumulation in JCaM1.6 cells (36). Hence, our results suggest that redistribution of CD38 to the IS strongly depends on Lck-mediated early signaling events that lead to actin polymerization and remodeling.

The formation of condensed membrane domains, which biophysically reflects membrane raft accumulation, is detected first in the central regions and later at the periphery of the productive IS (57). Therefore, the redistribution of CD38 and Lck, which are raft-associated proteins, to peripheral sites of the IS may also be linked to the dynamics of condensation of the T cell plasma membrane shown at the site of T cell activation, while most CD3-ζ remains in the c-SMAC. As pointed out elsewhere (45), different CD3-ζ and Lck accumulation patterns do not necessarily reflect an absolute

molecular segregation, rather changes in the relative distribution of these molecules, which could have a substantial effect on the signals transduced by them. In support of this concept are our own data showing that in Jurkat T cells, where CD38, Lck, and CD3-ζ are associated in a subset of lipid raft vesicles, CD38 engagement results in activating signals such as full CD3-ζ and CD3-ε ITAM phosphorylation, Ras activation and translocation of key signaling components as Sos and p85 PI-3 kinase into rafts (19). In contrast, in the non-raft microdomains, where CD38 is associated with CD3-ζ but not with Lck, CD38 engagement results in inhibitory signals such as partial CD3-ζ and CD3-ε ITAM phosphorylation, and strong c-Cbl phosphorylation (19). It is likely that the rearrangement of CD38 and Lck to more peripheral sites of the mature synapse away from CD3-ζ could generate different or reduced signals than those observed immediately after engagement of the T cell with an antigen-pulsed APC, just when the three molecules are associated in the same raft subset (19), and the earliest signaling events are taking place (45) by the active formation of TCR-containing microclusters (58, 59). Interestingly, T cell receptor-proximal signals are sustained in peripheral microclusters and terminated in the c-SMAC (60), therefore CD38 location at the periphery of the IS could be related with its signaling capabilities. Note that the blocking effect of anti-CD38 mAbs is exerted against signaling events that occur before maturation of the synapse. Likewise, the gain of function observed in T cells overexpressing CD38 has to do with calcium mobilization that is initiated immediately after T:APC conjugate formation.

In a small but significant proportion of T cell/APC conjugates formed with CD38-GFP-transfected Raji B cells pulsed with SEE, membrane CD38-GFP from Raji B cells clusters along the T cell/APC contact zone. In many of these conjugates translocation of its counter receptor CD31 from the T cells to the T cell:APC interface was clearly observed, suggesting active recruitment caused by ligand-receptor interactions. Interestingly CD31 contains functional ITIMs within its cytoplasmic domain, and co-ligation of CD31 with the TCR results in Lck-dependent tyrosine phosphorylation of CD31 ITIMs, recruitment of Src homology 2 domain-containing

protein tyrosine phosphatase-2, and attenuation of TCR-mediated cellular signaling (61). To our knowledge our data is the first physiological evidence that CD31 could be in the proximity of the TCR upon antigen-mediated T cell activation without artificially forcing such interaction with specific mAbs. The negative regulation of SEE-induced T cell activation played by Lck (62) is consistent with the requirement of Lck for CD31 tyrosine phosphorylation in response to cross-linking the TCR (61). It seems therefore likely that the proximity of CD31 to the TCR and Lck in the IS could favor the inhibitory function that CD31 plays on T cell activation. Whether CD38 in the APCs is involved in the recruitment of CD31 to the IS requires further investigation.

Relocation in APCs of MHC class II molecules to raft-rich microdomains or to tetraspanin-containing microdomains at the IS has been implicated in optimal peptide presentation and T lymphocyte activation (25, 63). Dynamic changes in these molecular associations, such as recruitment of other surface and/or signaling molecules, may occur during the formation and establishment of the relevant synapse(s). Thus, binding of ICAM-3, and ICAM-1 to a lesser extent, to LFA-1 expressed by mature but not immature DCs, induces MHC-II clustering into the immune synapse (64). Moreover, localization of CD38 in lipid rafts associated with Class II MHC molecules and the tetraspanin CD9 has been observed in monocytes (23), as well as with the tetraspanin CD81 in mature DCs (4). CD81 is indeed present in Raji B cells, and is actively recruited to the IS upon antigen stimulation (26). On the other hand, in Raji B cells a large proportion of CD38 is located in lipid raft microdomains (data not shown). The simultaneous presence of antigen-loaded Class II MHC complexes, tetraspanins and modulatory molecules as CD38 into physically distinguishable microdomains on the surface of APCs is likely to influence the ability of APCs to stimulate antigen-specific T cells. In this sense, CD38 expressed in monocytes seem to play a role in the transduction of signals involved in superantigen-induced T cell activation, operating in synergy with MHC Class II (22). Moreover, CD38-mediated signaling and its location in lipid rafts is required for the migration, survival, and polarization toward Th1 responses of mature DCs (4). Therefore, clustering of CD38 at the IS, and the

contribution of both T cells and APCs to this phenomenon suggests that CD38 may play an important role during antigen presentation.

ACKNOWLEDGMENTS

We thank Nieves de la Casa from the Confocal Core Facility of the University of Jaén, David Porcel from the CIC of the University of Granada, and Ana B. Martin and Antonio Mérida from the IPBLN for their technical assistance. We thank Dr. Balbino Alarcón, Dr. Arthur Weiss, and Dr. Fabio Malavasi for valuable reagents and cells.

DISCLOSURES

The authors have no financial conflict of interest.

FOOTNOTES

[1]This work was supported by the Ministerio de Educación y Ciencia (MEC) (Grants SAF2002-00721, and SAF2005-06056-C02-01), Consejería de Innovación, Ciencia y Empresa de la Junta de Andalucía (Grant P05-CVI-00908) to JS. MZ was supported by the Instituto Carlos III-FIS, Ministerio de Sanidad y Consumo (Grants FIS03/0389, and FIS06/1502) and by a Ramón y Cajal contract from MEC. PM was supported by a FPI Fellowship from MEC.

[2]Corresponding author: Jaime Sancho, Instituto de Parasitología y Biomedicina "López-Neyra", CSIC. PT de Ciencias de la Salud. Avenida del Conocimiento s/n, 18100 Armilla, Spain. Phone: +34 958 181664; FAX: +34 958181632; e-mail: granada@ipb.csic.es

[3]Abbreviations used in this paper: DC, dendritic cell; IS, immunological synapse; GFP, green fluorescent protein; cADPR, cyclic ADP ribose; CMAC, chloromethyl derivative of aminocoumarin; CM-TMR, chloromethyl-benzoylamino-tetramethylrhodamine; PLL, Poly-L-lysine; SEE, *Staphylococcus aureus* enterotoxin E; SEB, *Staphylococcus aureus* enterotoxin B; c-SMAC, central SupraMolecular Activation Cluster.

[4] The online version of this article contains supplemental material.

REFERENCES

1. Dustin, M. L. 2002. Membrane domains and the immunological synapse: keeping T cells resting and ready. *J Clin Invest* 109:155-160.
2. Jackson, D. G., and J. I. Bell. 1990. Isolation of a cDNA encoding the human CD38 (T10) molecule, a cell surface glycoprotein with an unusual discontinuous pattern of expression during lymphocyte differentiation. *J. Immunol.* 144:2811-2815.
3. Malavasi, F., A. Funaro, S. Roggero, A. Horenstein, L. Calosso, and K. Mehta. 1994. Human CD38: a glycoprotein in search of a function. *Immunol. Today* 15:95-97.
4. Frasca, L., G. Fedele, S. Deaglio, C. Capuano, R. Palazzo, T. Vaisitti, F. Malavasi, and C. M. Ausiello. 2006. CD38 orchestrates migration, survival, and Th1 immune response of human mature dendritic cells. *Blood* 107:2392-2399.
5. Deaglio, S., A. Capobianco, L. Bergui, J. Durig, F. Morabito, U. Duhrsen, and F. Malavasi. 2003. CD38 is a signaling molecule in B-cell chronic lymphocytic leukemia cells. *Blood* 102:2146-2155.
6. Lund, F. E., H. Muller-Steffner, H. Romero-Ramirez, M. E. Moreno-Garcia, S. Partida-Sanchez, M. Makris, N. J. Oppenheimer, L. Santos-Argumedo, and F. Schuber. 2006. CD38 induces apoptosis of a murine pro-B leukemic cell line by a tyrosine kinase-dependent but ADP-ribosyl cyclase- and NAD glycohydrolase-independent mechanism. *Int Immunol* 18:1029-1042.
7. Zubiaur, M., M. Izquierdo, C. Terhorst, F. Malavasi, and J. Sancho. 1997. CD38 ligation results in activation of the Raf-1/mitogen-activated protein kinase and the CD3-zeta/zeta-associated protein-70 signaling pathways in Jurkat T lymphocytes. *J Immunol* 159:193-205.
8. Campana, D., T. Suzuki, E. Todisco, and A. Kitanaka. 2000. CD38 in hematopoiesis. *Chem Immunol* 75:169-188.

9. States, D. J., T. F. Walseth, and H. C. Lee. 1992. Similarities in amino acid sequences of Aplysia ADP-ribosyl cyclase and human lymphocyte antigen CD38. *Trends Biochem. Sci.* 17:495.

10. Heiner, I., J. Eisfeld, and A. Luckhoff. 2003. Role and regulation of TRP channels in neutrophil granulocytes. *Cell Calcium* 33:533-540.

11. Lee, H. C. 2001. Physiological functions of cyclic ADP-ribose and NAADP as calcium messengers. *Annu Rev Pharmacol Toxicol* 41:317-345.

12. De Flora, A., E. Zocchi, L. Guida, L. Franco, and S. Bruzzone. 2004. Autocrine and paracrine calcium signaling by the CD38/NAD+/cyclic ADP-ribose system. *Ann N Y Acad Sci* 1028:176-191.

13. Zocchi, E., A. Daga, C. Usai, L. Franco, L. Guida, S. Bruzzone, A. Costa, C. Marchetti, and A. De Flora. 1998. Expression of CD38 increases intracellular calcium concentration and reduces doubling time in HeLa and 3T3 cells. *J Biol Chem* 273:8017-8024.

14. Bruzzone, S., S. Kunerth, E. Zocchi, A. De Flora, and A. H. Guse. 2003. Spatio-temporal propagation of Ca2+ signals by cyclic ADP-ribose in 3T3 cells stimulated via purinergic P2Y receptors. *J Cell Biol* 163:837-845.

15. Young, G. S., E. Choleris, F. E. Lund, and J. B. Kirkland. 2006. Decreased cADPR and increased NAD+ in the Cd38-/- mouse. *Biochem Biophys Res Commun* 346:188-192.

16. Guse, A. H., C. P. da Silva, I. Berg, A. L. Skapenko, K. Weber, P. Heyer, M. Hohenegger, G. A. Ashamu, H. Schulze-Koops, B. V. Potter, and G. W. Mayr. 1999. Regulation of calcium signalling in T lymphocytes by the second messenger cyclic ADP-ribose. *Nature* 398:70-73.

17. da Silva, C. P., K. Schweitzer, P. Heyer, F. Malavasi, G. W. Mayr, and A. H. Guse. 1998. Ectocellular CD38-catalyzed synthesis and intracellular Ca2+-signalling activity of cyclic ADP-ribose in T-lymphocytes are not functionally related. *FEBS Lett* 439:291-296.

18. Zubiaur, M., O. Fernandez, E. Ferrero, J. Salmeron, B. Malissen, F. Malavasi, and J. Sancho. 2002. CD38 is associated with lipid rafts and upon receptor stimulation leads to Akt/protein kinase B and Erk activation in the absence of the CD3-zeta immune receptor tyrosine-based activation motifs. *J Biol Chem* 277:13-22.

19. Munoz, P., M. D. Navarro, E. J. Pavon, J. Salmeron, F. Malavasi, J. Sancho, and M. Zubiaur. 2003. CD38 signaling in T cells is initiated within a subset of membrane rafts containing Lck and the CD3-zeta subunit of the T cell antigen receptor. *J Biol Chem* 278:50791-50802.

20. Morra, M., M. Zubiaur, C. Terhorst, J. Sancho, and F. Malavasi. 1998. CD38 is functionally dependent on the TCR/CD3 complex in human T cells. *Faseb J* 12:581-592.

21. Zubiaur, M., M. Guirado, C. Terhorst, F. Malavasi, and J. Sancho. 1999. The CD3-gamma delta epsilon transducing module mediates CD38-induced protein-tyrosine kinase and mitogen-activated protein kinase activation in Jurkat T cells. *J Biol Chem* 274:20633-20642.

22. Zilber, M. T., S. Gregory, R. Mallone, S. Deaglio, F. Malavasi, D. Charron, and C. Gelin. 2000. CD38 expressed on human monocytes: a coaccessory molecule in the superantigen-induced proliferation. *Proc Natl Acad Sci U S A* 97:2840-2845.

23. Zilber, M. T., N. Setterblad, T. Vasselon, C. Doliger, D. Charron, N. Mooney, and C. Gelin. 2005. MHC class II/CD38/CD9: a lipid-raft-dependent signaling complex in human monocytes. *Blood* 106:3074-3081.

24. Anderson, H. A., E. M. Hiltbold, and P. A. Roche. 2000. Concentration of MHC class II molecules in lipid rafts facilitates antigen presentation. *Nat Immunol* 1:156-162.

25. Hiltbold, E. M., N. J. Poloso, and P. A. Roche. 2003. MHC class II-peptide complexes and APC lipid rafts accumulate at the immunological synapse. *J Immunol* 170:1329-1338.

26. Mittelbrunn, M., M. Yanez-Mo, D. Sancho, A. Ursa, and F. Sanchez-Madrid. 2002. Cutting edge: dynamic redistribution of tetraspanin CD81 at the central zone of the immune synapse in both T lymphocytes and APC. *J Immunol* 169:6691-6695.

27. Montoya, M. C., D. Sancho, G. Bonello, Y. Collette, C. Langlet, H. T. He, P. Aparicio, A. Alcover, D. Olive, and F. Sanchez-Madrid. 2002. Role of ICAM-3 in the initial interaction of T lymphocytes and APCs. *Nat Immunol* 3:159-168.

28. Straus, D. B., and A. Weiss. 1992. Genetic evidence for the involvement of the lck tyrosine kinase in signal transduction through the T cell antigen receptor. *Cell* 70:585-593.

29. Sallusto, F., and A. Lanzavecchia. 1994. Efficient presentation of soluble antigen by cultured human dendritic cells is maintained by granulocyte/macrophage colony-stimulating factor plus interleukin 4 and downregulated by tumor necrosis factor alpha. *J Exp Med* 179:1109-1118.

30. Hewitt, C. R., J. R. Lamb, J. Hayball, M. Hill, M. J. Owen, and R. E. O'Hehir. 1992. Major histocompatibility complex independent clonal T cell anergy by direct interaction of Staphylococcus aureus enterotoxin B with the T cell antigen receptor. *J Exp Med* 175:1493-1499.

31. Long, E. O., S. Rosen-Bronson, D. R. Karp, M. Malnati, R. P. Sekaly, and D. Jaraquemada. 1991. Efficient cDNA expression vectors for stable and transient expression of HLA-DR in transfected fibroblast and lymphoid cells. *Hum. Immunol.* 31:229-235.

32. Graeff, R. M., T. F. Walseth, K. Fryxell, W. D. Branton, and H. C. Lee. 1994. Enzymatic synthesis and characterizations of cyclic GDP-ribose. A procedure for distinguishing enzymes with ADP-ribosyl cyclase activity. *J Biol Chem* 269:30260-30267.

33. Pavon, E. J., P. Munoz, M. D. Navarro, E. Raya-Alvarez, J. L. Callejas-Rubio, F. Navarro-Pelayo, N. Ortego-Centeno, J. Sancho, and M. Zubiaur. 2006. Increased association of CD38 with lipid rafts in T cells from patients with

systemic lupus erythematosus and in activated normal T cells. *Mol Immunol* 43:1029-1039.

34. Serrador, J. M., J. R. Cabrero, D. Sancho, M. Mittelbrunn, A. Urzainqui, and F. Sanchez-Madrid. 2004. HDAC6 deacetylase activity links the tubulin cytoskeleton with immune synapse organization. *Immunity* 20:417-428.

35. Lin, J., M. J. Miller, and A. S. Shaw. 2005. The c-SMAC: sorting it all out (or in). *J Cell Biol* 170:177-182.

36. Roumier, A., J. C. Olivo-Marin, M. Arpin, F. Michel, M. Martin, P. Mangeat, O. Acuto, A. Dautry-Varsat, and A. Alcover. 2001. The membrane-microfilament linker ezrin is involved in the formation of the immunological synapse and in T cell activation. *Immunity* 15:715-728.

37. Blanchard, N., V. Di Bartolo, and C. Hivroz. 2002. In the immune synapse, ZAP-70 controls T cell polarization and recruitment of signaling proteins but not formation of the synaptic pattern. *Immunity* 17:389-399.

38. Das, V., B. Nal, A. Dujeancourt, M. I. Thoulouze, T. Galli, P. Roux, A. Dautry-Varsat, and A. Alcover. 2004. Activation-induced polarized recycling targets T cell antigen receptors to the immunological synapse; involvement of SNARE complexes. *Immunity* 20:577-588.

39. Batista, A., J. Millan, M. Mittelbrunn, F. Sanchez-Madrid, and M. A. Alonso. 2004. Recruitment of transferrin receptor to immunological synapse in response to TCR engagement. *J Immunol* 172:6709-6714.

40. Deaglio, S., M. Morra, R. Mallone, C. M. Ausiello, E. Prager, G. Garbarino, U. Dianzani, H. Stockinger, and F. Malavasi. 1998. Human CD38 (ADP-ribosyl cyclase) is a counter-receptor of CD31, an Ig superfamily member. *J. Immunol.* 160:395-402.

41. Ausiello, C. M., F. Urbani, R. Lande, A. la Sala, B. Di Carlo, G. Baj, N. Surico, J. Hilgers, S. Deaglio, A. Funaro, and F. Malavasi. 2000. Functional topography of discrete domains of human CD38. *Tissue Antigens* 56:539-547.

42. Lee, K. Y., F. D'Acquisto, M. S. Hayden, J. H. Shim, and S. Ghosh. 2005. PDK1 nucleates T cell receptor-induced signaling complex for NF-kappaB activation. *Science* 308:114-118.

43. Gruber, T., M. Freeley, N. Thuille, I. Heit, S. Shaw, A. Long, and G. Baier. 2006. Comment on "PDK1 nucleates T cell receptor-induced signaling complex for NF-kappaB activation". *Science* 312:55; author reply 55.

44. Bonello, G., N. Blanchard, M. C. Montoya, E. Aguado, C. Langlet, H. T. He, S. Nunez-Cruz, M. Malissen, F. Sanchez-Madrid, D. Olive, C. Hivroz, and Y. Collette. 2004. Dynamic recruitment of the adaptor protein LAT: LAT exists in two distinct intracellular pools and controls its own recruitment. *J Cell Sci* 117:1009-1016.

45. Ehrlich, L. I., P. J. Ebert, M. F. Krummel, A. Weiss, and M. M. Davis. 2002. Dynamics of p56lck translocation to the T cell immunological synapse following agonist and antagonist stimulation. *Immunity* 17:809-822.

46. Funaro, A., M. Reinis, O. Trubiani, S. Santi, R. Di Primio, and F. Malavasi. 1998. CD38 functions are regulated through an internalization step. *J Immunol* 160:2238-2247.

47. Pfister, M., A. Ogilvie, C. P. da Silva, A. Grahnert, A. H. Guse, and S. Hauschildt. 2001. NAD degradation and regulation of CD38 expression by human monocytes/macrophages. *Eur J Biochem* 268:5601-5608.

48. Guse, A. H. 2005. Second messenger function and the structure-activity relationship of cyclic adenosine diphosphoribose (cADPR). *Febs J* 272:4590-4597.

49. Bueno, C., C. D. Lemke, G. Criado, M. L. Baroja, S. S. Ferguson, A. K. Rahman, C. D. Tsoukas, J. K. McCormick, and J. Madrenas. 2006. Bacterial superantigens bypass Lck-dependent T cell receptor signaling by activating a Galpha11-dependent, PLC-beta-mediated pathway. *Immunity* 25:67-78.

50. Deaglio, S., T. Vaisitti, S. Aydin, E. Ferrero, and F. Malavasi. 2006. In-tandem insight from basic science combined with clinical research: CD38 as both

marker and key component of the pathogenetic network underlying chronic lymphocytic leukemia. *Blood*.

51. Zocchi, E., M. Podesta, A. Pitto, C. Usai, S. Bruzzone, L. Franco, L. Guida, A. Bacigalupo, and A. De Flora. 2001. Paracrinally stimulated expansion of early human hemopoietic progenitors by stroma-generated cyclic ADP-ribose. *Faseb J* 15:1610-1612.

52. Podesta, M., A. Pitto, O. Figari, A. Bacigalupo, S. Bruzzone, L. Guida, L. Franco, A. De Flora, and E. Zocchi. 2003. Cyclic ADP-ribose generation by CD38 improves human hemopoietic stem cell engraftment into NOD/SCID mice. *Faseb J* 17:310-312.

53. Bruzzone, S., A. De Flora, C. Usai, R. Graeff, and H. C. Lee. 2003. Cyclic ADP-ribose is a second messenger in the lipopolysaccharide-stimulated proliferation of human peripheral blood mononuclear cells. *Biochem J* 375:395-403.

54. Ibiza, S., V. M. Victor, I. Bosca, A. Ortega, A. Urzainqui, J. E. O'Connor, F. Sanchez-Madrid, J. V. Esplugues, and J. M. Serrador. 2006. Endothelial nitric oxide synthase regulates T cell receptor signaling at the immunological synapse. *Immunity* 24:753-765.

55. Zhang, A. Y., and P. L. Li. 2006. Vascular physiology of a Ca(2+) mobilizing second messenger - cyclic ADP-ribose. *J Cell Mol Med* 10:407-422.

56. Morgan, M. M., C. M. Labno, G. A. Van Seventer, M. F. Denny, D. B. Straus, and J. K. Burkhardt. 2001. Superantigen-induced T cell:B cell conjugation is mediated by LFA-1 and requires signaling through Lck, but not ZAP-70. *J Immunol* 167:5708-5718.

57. Gaus, K., E. Chklovskaia, B. Fazekas de St Groth, W. Jessup, and T. Harder. 2005. Condensation of the plasma membrane at the site of T lymphocyte activation. *J Cell Biol* 171:121-131.

58. Yokosuka, T., K. Sakata-Sogawa, W. Kobayashi, M. Hiroshima, A. Hashimoto-Tane, M. Tokunaga, M. L. Dustin, and T. Saito. 2005. Newly generated T cell

receptor microclusters initiate and sustain T cell activation by recruitment of Zap70 and SLP-76. *Nat Immunol* 6:1253-1262.

59. Campi, G., R. Varma, and M. L. Dustin. 2005. Actin and agonist MHC-peptide complex-dependent T cell receptor microclusters as scaffolds for signaling. *J Exp Med* 202:1031-1036.

60. Varma, R., G. Campi, T. Yokosuka, T. Saito, and M. L. Dustin. 2006. T cell receptor-proximal signals are sustained in peripheral microclusters and terminated in the central supramolecular activation cluster. *Immunity* 25:117-127.

61. Newman, D. K., C. Hamilton, and P. J. Newman. 2001. Inhibition of antigen-receptor signaling by Platelet Endothelial Cell Adhesion Molecule-1 (CD31) requires functional ITIMs, SHP-2, and p56(lck). *Blood* 97:2351-2357.

62. Criado, G., and J. Madrenas. 2004. Superantigen stimulation reveals the contribution of Lck to negative regulation of T cell activation. *J Immunol* 172:222-230.

63. Kropshofer, H., S. Spindeldreher, T. A. Rohn, N. Platania, C. Grygar, N. Daniel, A. Wolpl, H. Langen, V. Horejsi, and A. B. Vogt. 2002. Tetraspan microdomains distinct from lipid rafts enrich select peptide- MHC class II complexes. *Nat Immunol* 3:61-68.

64. de la Fuente, H., M. Mittelbrunn, L. Sanchez-Martin, M. Vicente-Manzanares, A. Lamana, R. Pardi, C. Cabanas, and F. Sanchez-Madrid. 2005. Synaptic clusters of MHC class II molecules induced on DCs by adhesion molecule-mediated initial T-cell scanning. *Mol Biol Cell* 16:3314-3322.

FIGURE LEGENDS

Figure 1. Surface CD38 clusters at the T cell:APC contact region. *A,* FACS analysis. Jurkat D8 (upper panels), Jurkat J77 (middle panels), or Raji (lower panels) cells were stained with specific antibodies against CD38, CD3, ICAM-3 or TCR Vβ8 as indicated in Material and Methods. *B,* Raji cells were labeled with CMAC and incubated in the absence or in the presence of SEE (1 μg/ml). Raji and Jurkat D8 cells were mixed at 1:1 ratio, fixed, and double stained for CD38 (green), or CD3-ζ (red) (upper and middle panels), or double stained for CD45 (green), or CD3-ζ (red) (lower panels). *C,* Jurkat D8-Raji cell conjugates were generated in presence of SEE, double-stained for CD38 (green), and CD3-ζ (red), and analyzed by confocal microscopy. The panel shows the stacked pictures of 23 sections with 0.4 μm thickness. *D,* J77-Raji cell conjugates were generated in the absence or the presence of SEE, and double stained for ICAM-3 (green) and CD38 (red). Green fluorescence merged with red fluorescence images, and the corresponding DIC images superimposed on blue fluorescence images from CMAC-loaded Raji cells are shown. *E,* T cell-Dendritic cells (DC) conjugates were generated as described in material and methods.

Figure 2. Localization of CD38-GFP in Jurkat and Raji cells. *A,* Postnuclear cell lysates of non-transfected Jurkat J77 cells, J77 transfected with a GFP construct (pEGFP-C1), or J77 transfected with CD38-GFP were run on SDS-PAGE and Western blotted against GFP (left panel), or against CD38 (upper right panel), or against α-actin (lower right panel). *B,* Subcellular location of CD38-GFP (a), or pEGFP-C1 (c) in transfected Jurkat T cells. The corresponding DIC images (b and d) are shown. *C,* Upper panels: CD38-GFP-transfected J77 cells were permeabilized and labeled with an anti-CD3-ζ polyclonal antiserum followed by a Rodamine Red X-labeled secondary Ab. Green fluorescence (CD38-GFP) merged with red fluorescence (CD3-ζ) images are shown. Lower panels: Labeling of intracellular endogenous CD38 (red) and intracellular endogenous CD3-ζ (green) in nontransfected permeabilized J77 T cells. Green fluorescence merged with red fluorescence images are shown. *D,* Subcellular location of

CD38-GFP, or endogenous CD38 in Raji B cells. The corresponding DIC images are shown. In *B, C,* and *D* the white arrowheads point to the intracellular CD38-GFP, endogenous CD38, or CD3-ζ. The arrows point to plasma membrane CD38-GFP, or endogenous CD38.

Figure 3. In T cells the CD38-GFP present in recycling endosomes and in the Golgi apparatus is targeted to the T cell:APC contact zone. *A,* CD38-GFP-transfected J77 cells were incubated with Raji B cells pulsed with medium alone (upper panels) or with SEE (lower panels). Cells were then fixed, permeabilized and stained with anti-CD71 (TfR) mAb under permeabilizing conditions followed by a goat anti-mouse Rhodamine Red X-second antibody. Samples were analyzed by a Leica TCS-SP5 confocal scanning laser microscope. The white arrowheads point to intracellular CD38-GFP. The arrows point to the plasma membrane CD38-GFP, or CD71. *B,* CD38-GFP-transfected J77 cells were treated as in *A* except that after fixation and permeabilization cells were stained with an anti-Golgi mAb under permeabilizing conditions followed by a goat anti-mouse Rhodamine Red X-second antibody. Samples were analyzed by confocal microscopy. The white arrowheads point to the intracellular CD38-GFP, or the position of the Golgi apparatus. The arrows point to the plasma membrane CD38-GFP accumulated at the synapse. The acquired CD38-GFP (green), Golgi (red), the merge images, close-ups of some merge images, and Normasky images are shown. A semi-quantitative assessment of the level of colocalization was done by analyzing the colocalization scatter plot and generating a mask of the area of interest (AOI) (right panels).

Figure 4. TCR-dependent clustering and polarization of CD38-GFP from T cells at the T cell:APC contact zone. *A,* Jurkat J77 cells were transiently transfected with the CD38-GFP construct and allowed to conjugate with CMAC-labeled Raji cells not pulsed or pulsed with SEE. Then, cells were fixed, permeabilized and stained for CD3-ζ (red). The white arrowheads point to the intracellular CD38-GFP, or CD3-ζ. The arrows point to the plasma membrane CD38-GFP, or CD3-ζ accumulated at the synapse. *B,* Comparative analysis of the percentage of conjugates with CD38-GFP, or endogenous

CD3-ζ redistributed at the contact zone relative to the total number of CD38-GFP$^+$ J77:Raji conjugates in the absence (open bars), or in the presence (filled bars) of SEE. The data represent the mean+SEM of three independent experiments. In each experiment 50-70 conjugates were analyzed. *C,* Jurkat J77 cells transiently transfected with CD38-GFP were seeded onto FN-coated coverslips. Raji cells labeled in red with the probe CM-TMR were incubated with SEE and added to the chambers. Cells were monitored by time-lapse confocal microscopy at 30-s intervals. Representative images of two different T cell:SEE-pulsed APC conjugates are shown. Each time point shows the fluorescence images of Raji cells (red) and CD38-GFP fluorescence (green). The white arrowheads point to the intracellular CD38-GFP. The arrows point to the plasma membrane CD38-GFP.

Figure 5. Defective TCR-induced CD38 clustering at the immunological synapse in a Lck deficient T cell line. *A,* JCaM1.6 T cells were transiently transfected with the CD38-GFP construct and allowed to conjugate with CMAC-labeled Raji cells not pulsed or pulsed with SEE. Then, cells were fixed, permeabilized and stained for CD3-ζ (red). CD38-GFP (green), CD3-ζ (red), and the green fluorescence merged with red fluorescence images superimposed on blue fluorescence images from CMAC-loaded Raji cells are shown. The white arrowheads point to the intracellular CD38-GFP, or CD3-ζ. The arrow points to the plasma membrane CD38-GFP, or CD3-ζ. *B,* Comparative analysis of the percentage of conjugates with CD38-GFP, or endogenous CD3-ζ redistributed at the contact zone relative to the total number of CD38-GFP$^+$ JCaM 1.6:Raji conjugates in the absence (open bars), or in the presence (filled bars) of SEE. The data represent the mean+SEM of three independent experiments. In each experiment 50-70 conjugates were analyzed.

Figure 6. TCR-dependent clustering of CD38 from B cells and CD31 from T cells at the T cell:APC contact zone. *A,* Raji cells transiently transfected with the CD38-GFP construct were pulsed or not with SEE, and allowed to conjugate with Jurkat J77 T cells. Then, cells were fixed, permeabilized and stained for CD3-ζ (red). CD38-GFP (green), CD3-ζ (red), green fluorescence merged with red fluorescence images, and the

corresponding DIC images superimposed on blue fluorescence images from CMAC-loaded Raji cells are shown. The white arrowheads point to the intracellular CD38-GFP, or CD3-ζ. The arrow point to the plasma membrane CD3-ζ accumulated at the synapse. *B,* Comparative analysis of the percentage of conjugates with CD38-GFP, CD31, or CD3-ζ redistributed at the contact zone relative to the total number of J77:CD38-GFP+ Raji conjugates in the absence (open bars), or in the presence (filled bars) of SEE. The data represent the mean+SEM of three independent experiments. In each experiment 40-70 conjugates were analyzed. *C,* FACS analysis of Jurkat J77 cells (upper panels), or Raji B cells (lower panels). Cells were stained with specific antibodies against CD38 (left panels, or anti-CD31 (right panels). *D,* Quantification of the number of CD38, CD3, or CD31 molecules in Jurkat J77 T cells by using the CELLQUANT Calibrator kit (BIOCYTEX, France). *E,* Quantification of the number of CD38, CD19 and CD31 molecules in Raji B cells using the same kit as in D. *F,* CD38-GFP-transfeced Raji B cells were treated as in A except that after permeabilization cells were stained for CD31 (red). CD38-GFP (green), CD31 (red), green fluorescence merged with red fluorescence images, and the corresponding DIC images superimposed on blue fluorescence images from CMAC-loaded Raji cells are shown. The white arrowheads point to the intracellular CD38-GFP. The arrows point to the plasma membrane CD38-GFP or CD31 accumulated at the synapse.

Figure 7. Effect of CD38 overexpression in T cell function. *A,* Jurkat J77 cells were left untransfected, or transiently transfected with the pEGFP-C1, or the CD38-GFP constructs by nucleofection. 24 hours after transfection they were analyzed by FACS for GFP expression (FL1) and cell viability (FL3, Propidium iodide) (left panels), or for GFP expression (FL1) and CD38 expression (FL2, anti-CD38-PE: HB136) (right panels). Numbers in each quadrant are the percentage of cells positive for one or two markers. *B,* and *C,* Transfected ells were subjected to Histopaque-1077 centrifugation and then they were left alone, or mixed with SEE-pulsed, or unpulsed Raji B cells. After a brief centrifugation to favor conjugate formation ectocellular GDP-ribosyl cyclase activity was continuously measured at 37ºC using NGD^+ as a substrate. The cGDPR

production in fluorescence units was plotted against time (min). (●) J77 CD38-GFP$^+$ T cells incubated with SEE-pulsed Raji B cells, (○) J77 CD38-GFP$^+$ T cells incubated with unpulsed Raji B cells, (■) Raji B cells alone, (◆) J77 CD38-GFP$^+$ T cells alone, (▼) J77 pEGFP-C1$^+$ T cells incubated with SEE-pulsed Raji B cells, (▽) J77 pEGFP-C1$^+$ T cells incubated with unpulsed Raji B cells, (▲) J77 pEGFP-C1$^+$ T cells. *D,* Ag-induced Ca^{2+} released in J77 CD38-GFP$^+$ T (● and ○) and J77 pEGFP-C1$^+$ T cells (▼ and ▽). Fura-2/AM-loaded J77 CD38-GFP$^+$ T, or J77 pEGFP-C1$^+$ T cells were mixed with SEE-pulsed (closed symbols), or unpulsed (open symbols) Raji B cells. $[Ca2^+]_i$ changes were measured using a fluorescence plate reader, as described in Material and Methods. Characteristic tracings are shown (mean of three independent experiments). *E,* IL-2 production in in J77 CD38-GFP$^+$ T (■) and J77 pEGFP-C1$^+$ T cells (□) incubated with Raji B cells pulsed with various concentrations of SEE as indicated.

Figure 8. Effect of anti-CD38 mAb on antigen-induced T cell early signaling and IFN-γ production. *A,* FACS analysis of CH7C17 T cells (upper panels), or HOM-2 B cells (lower panels) cells were stained with specific antibodies against CD38 (left panels), anti-CD31 (middle panels), or anti-CD3 (right panels). *B,* Western-blot analysis with the anti-phosphotyrosine mAb RC-20HRP of whole cell lysates of CH7C17 T cells incubated with unpulsed (-HA), or HA-pulsed (+HA) HOM-2 B cells for the period of times indicated. The CH7C17 T cells were either preincubated with vehicle (-IB6), or preincubated for 15 min at 37ºC with the anti-CD38 mAb IB6 (+IB6), before mixing them with the HOM-2 B cells as indicated above. The picture is representative of three independent experiments. *C,* Western-blot analysis with the anti-phospho LAT (Tyr^{191}), followed by anti-α-actin for protein loading-control of an aliquot of the same experiment as in *B*. *D,* Densitometric analysis of the blot in *C* corrected by protein-loading control (pErk:Actin ratio x100). (■) CH7C17 T cells incubated with unpulsed HOM-2 cells for the indicated periods of time, (□) CH7C17 T cell preincubated with anti-CD38 mAb IB6 and then, with unpulsed HOM-2 cells, (●) CH7C17 cells incubated with HA-pulsed HOM-2 cells, (○) CH7C17 cells preincubated with IB6 and then incubated with HA-pulsed HOM-2 cells. *E,* Western-blot analysis with anti-phosphoErk

(Thr^{202}/Tyr^{204}), followed by anti-α-actin for protein-loading control. *F,* Densitometric analysis of the blot in *E* was corrected by protein-loading control. Symbols as in *D*. *G,* Western-blot analysis with anti-phosphoPKCθ (Thr^{538}), followed by anti-PKCθ for protein-loading control. *H,* Densitometric analysis of the blot in *G* was corrected by protein-loading control. Symbols as in *D*. *I,* IFN-γ production by CH7C17 T cells incubated overnight with HA peptide-pulsed (+), or unpulsed (-) HOM-2 B cells. CH7C17 T cells were preincubated for 15 min at 37ºC with the indicated anti-CD38 mAb, or with reagents at the concentrations indicated in the Results section. Representative experiment out of three independent experiments performed in triplicates. Statistical analysis: unpaired *t-test*.

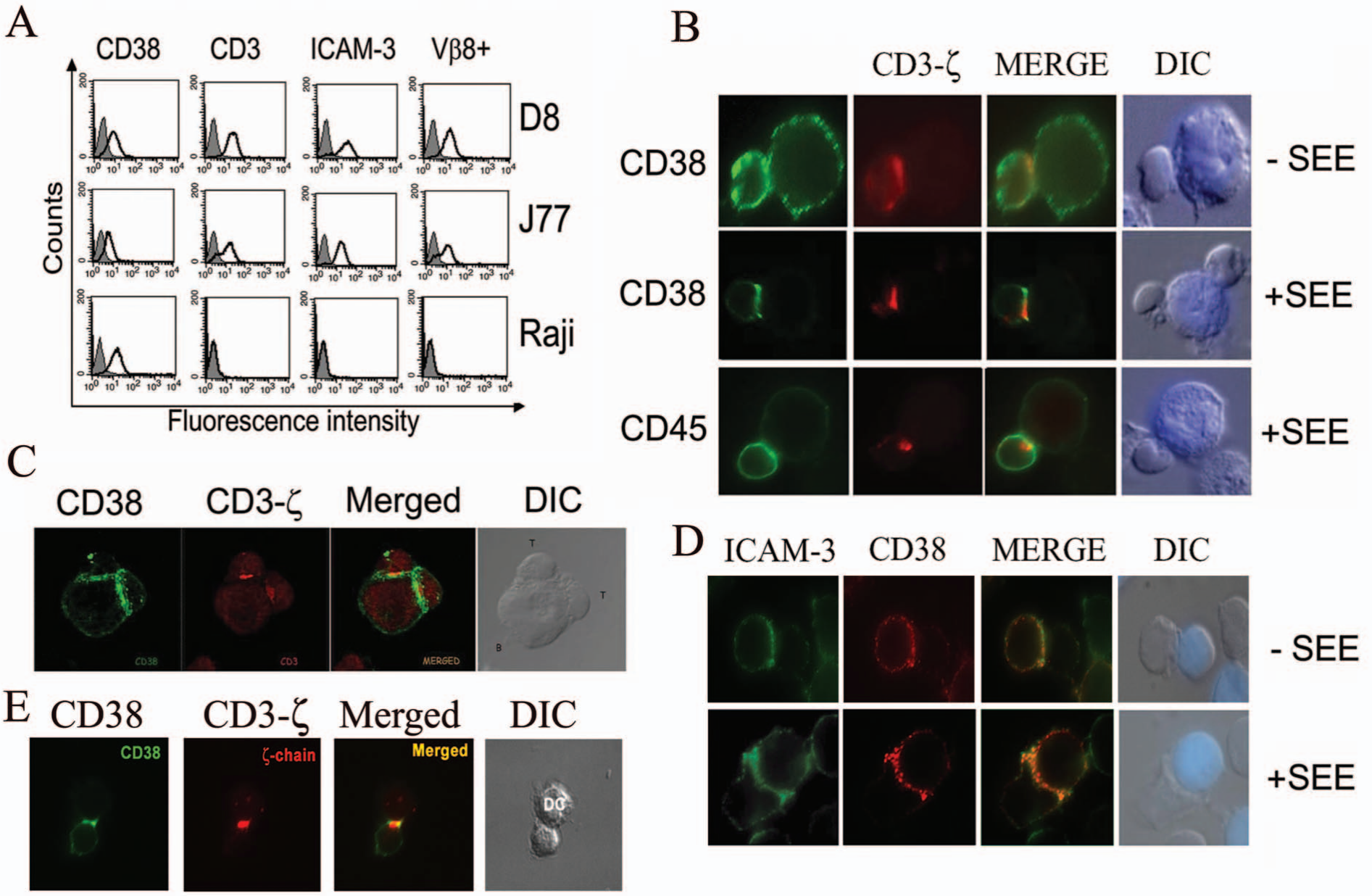

Figure 1, Muñoz et al.

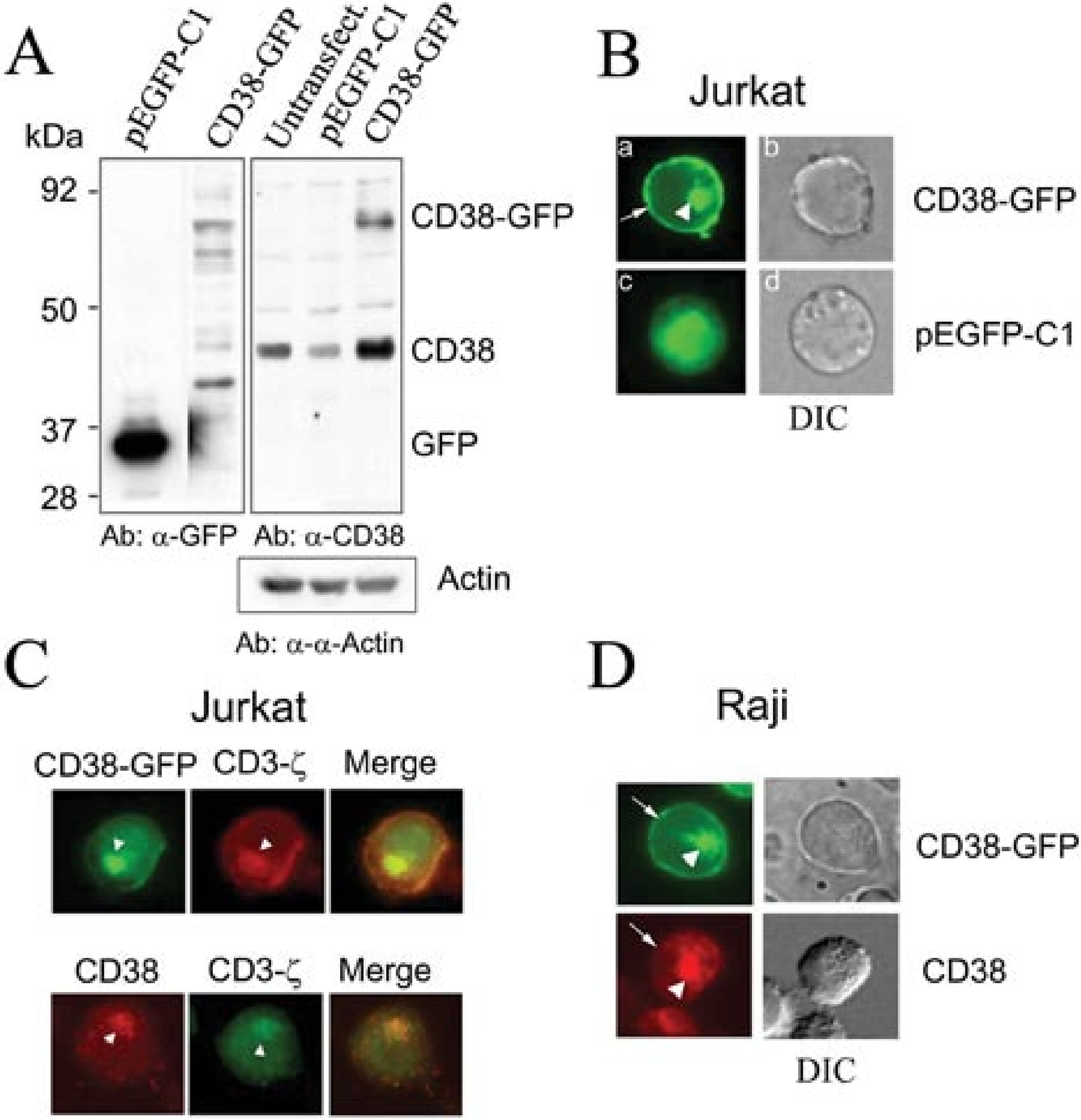

Figure 2, Muñoz et al.,

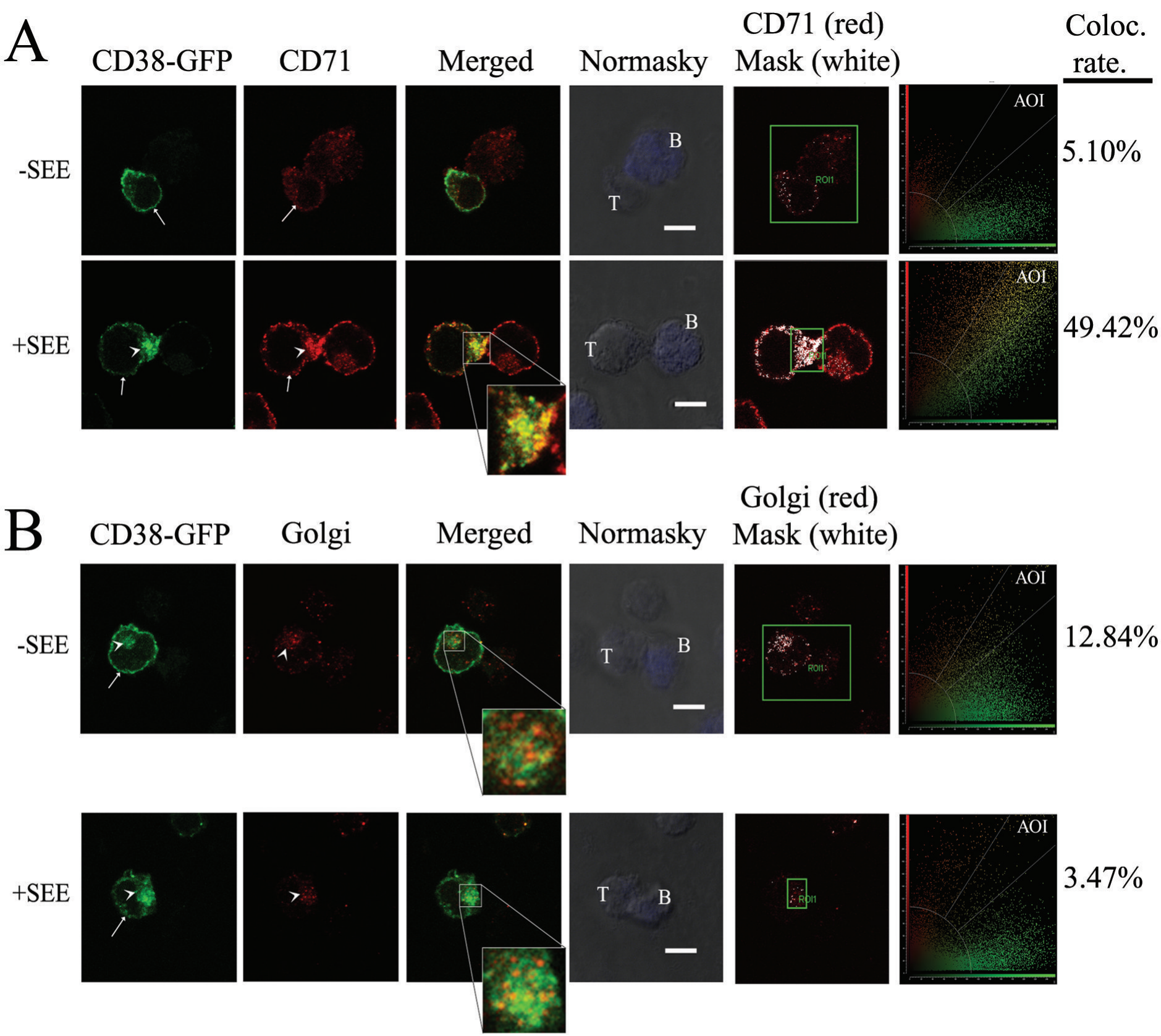

Figure 3, Muñoz et al.

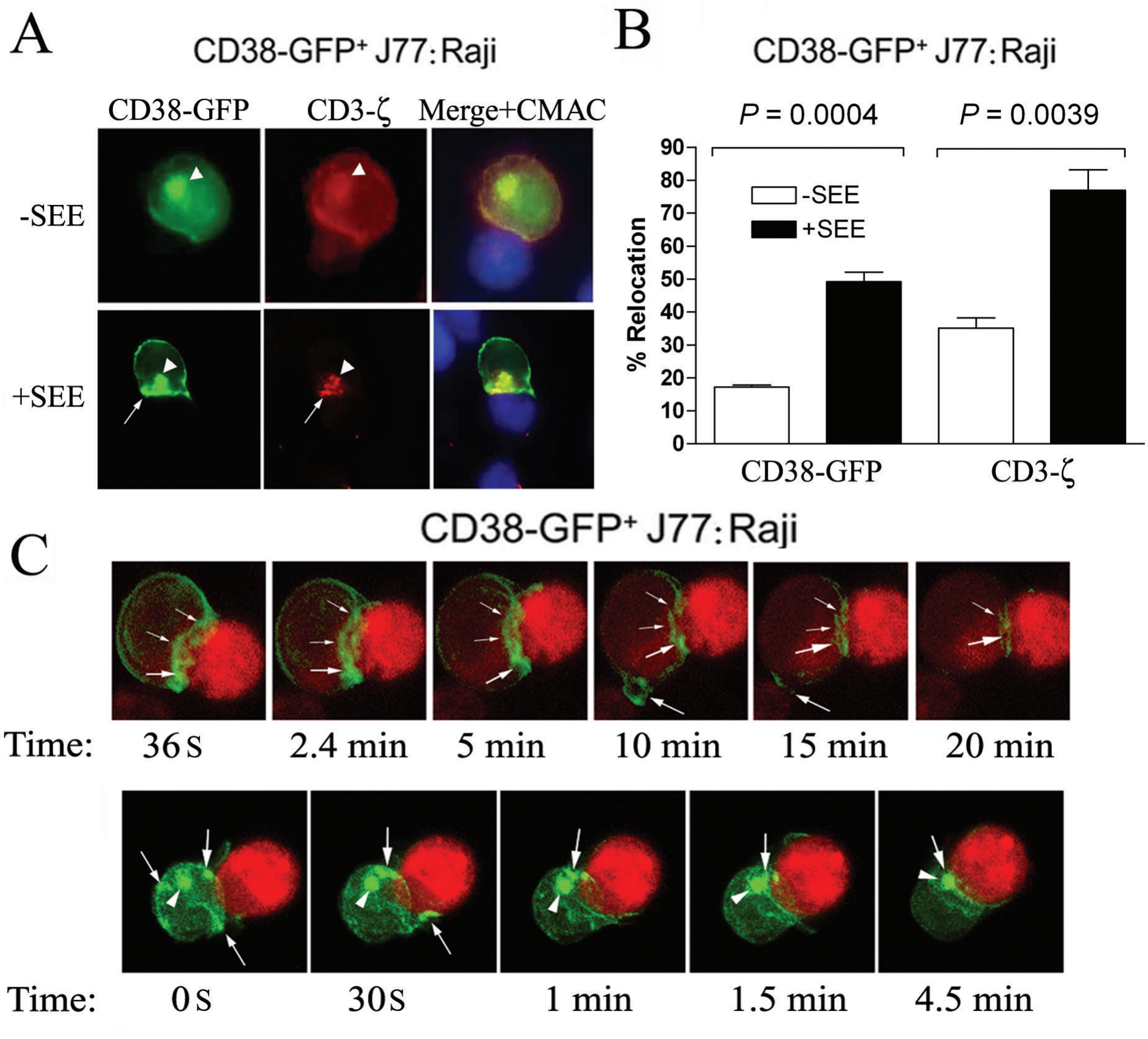

Figure 4, Muñoz et al.,

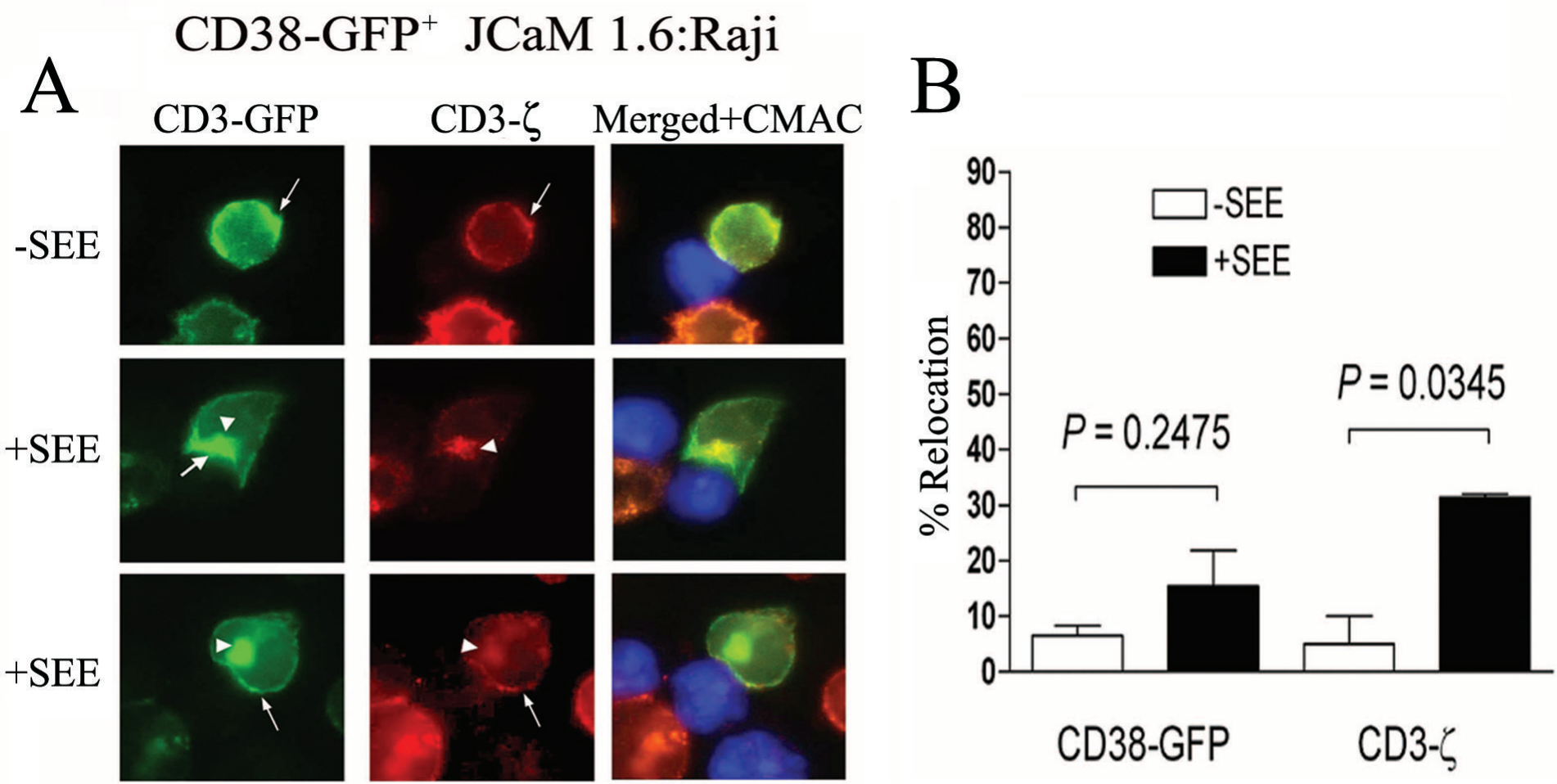

Figure 5, Muñoz et al.,

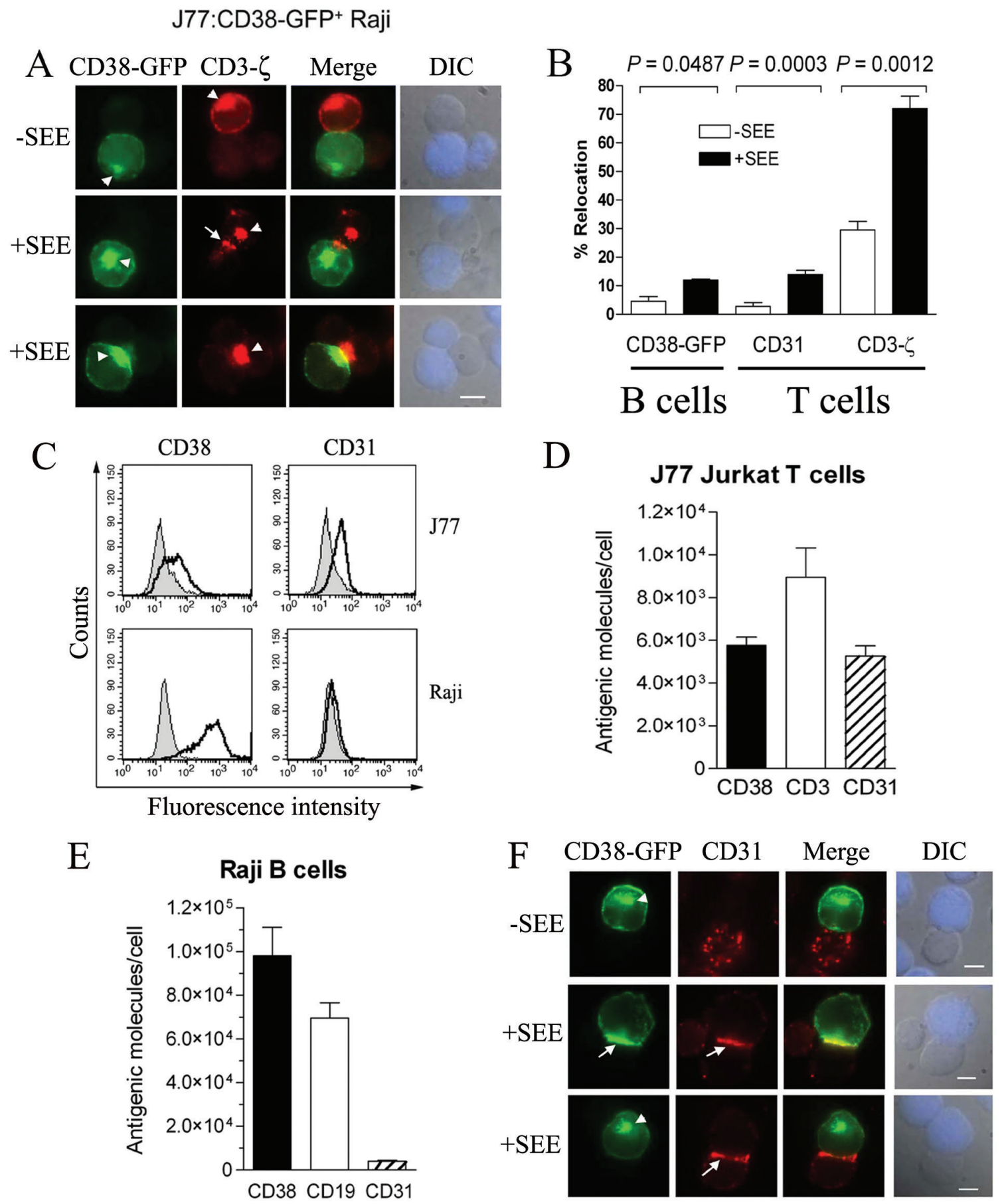

Figure 6, Muñoz et al.

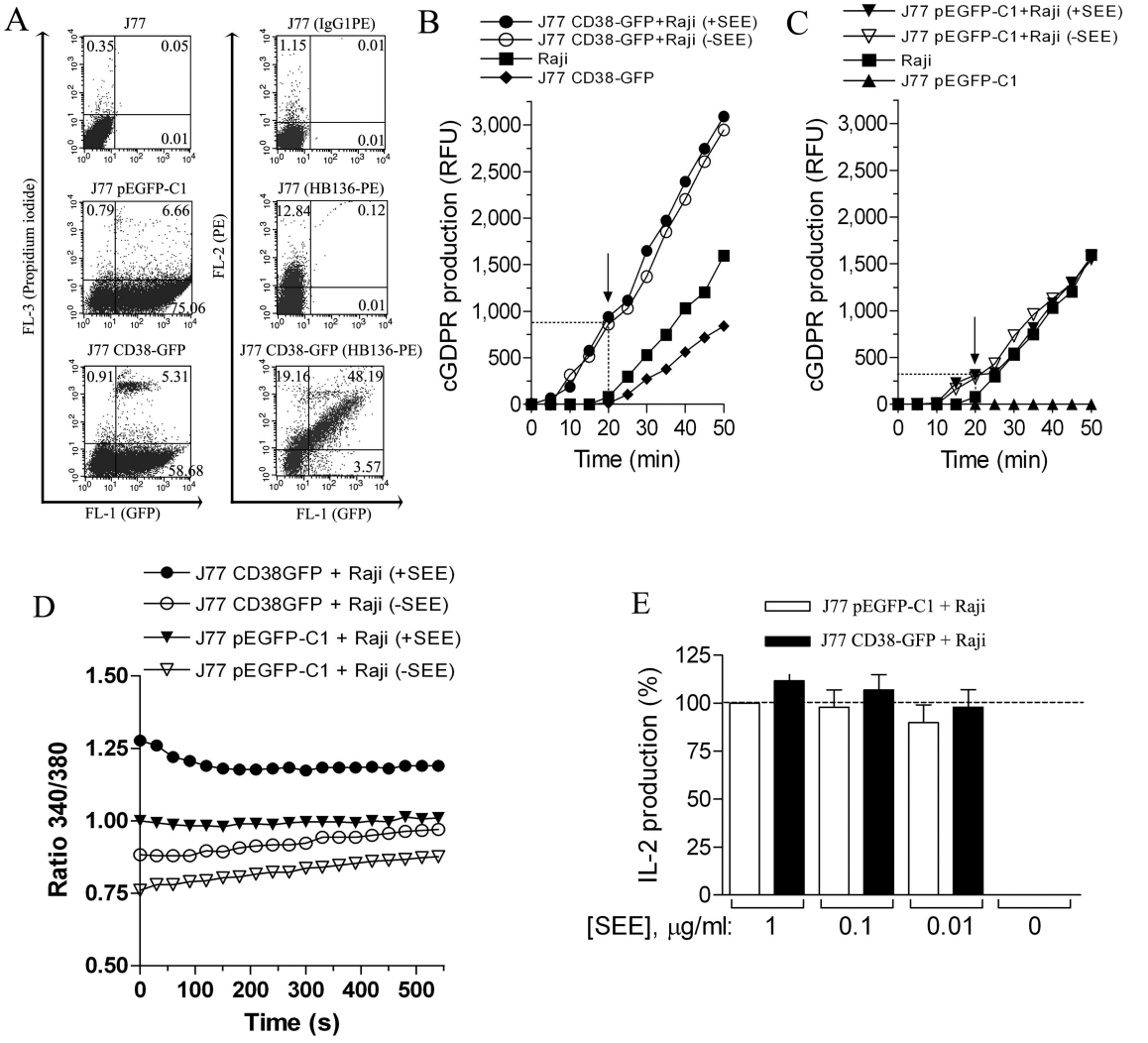

Figure 7, Muñoz et al.

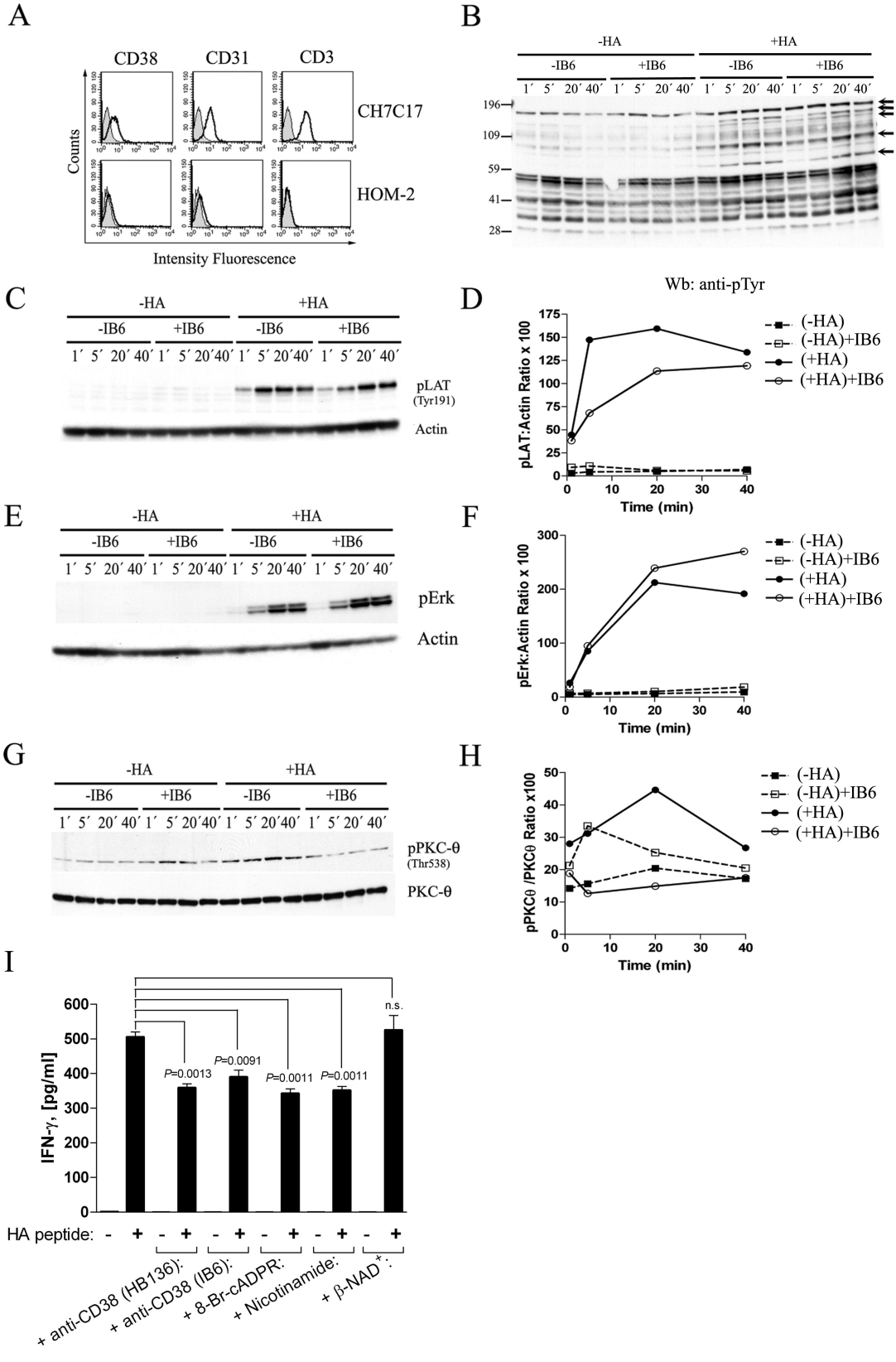

Figure 8, Muñoz et al.

Anexo II

Artículos publicados (Colaboraciones)

Available online at www.sciencedirect.com
SCIENCE DIRECT
Molecular Immunology 43 (2006) 1029–1039
Molecular Immunology
www.elsevier.com/locate/molimm

Increased association of CD38 with lipid rafts in T cells from patients with systemic lupus erythematosus and in activated normal T cells

Esther J. Pavón [a], Pilar Muñoz [a], María-del-Carmen Navarro [a], Enrique Raya-Alvarez [b], José-Luis Callejas-Rubio [b], Francisco Navarro-Pelayo [b], Norberto Ortego-Centeno [b], Jaime Sancho [a,*], Mercedes Zubiaur [a]

[a] *Departamento de Biología Celular e Inmunología, Instituto de Parasitología y Biomedicina "López-Neyra", CSIC, Parque Tecnológico de Ciencias de la Salud, Avenida del Conocimiento s/n, 18100 Armilla, Granada, Spain*
[b] *Unidad de Enfermedades Autoinmunes Sistémicas, Hospital Clinico San Cecilio, Granada, Spain*

Received 15 March 2005
Available online 16 June 2005

Abstract

In this study we have determined whether there is a relationship between CD38 expression on T cells, its distribution in different membrane microdomains, and T cell activation in SLE patients. The data show that CD38 expression is augmented in ex vivo $CD3^+$, $CD4^+$, $CD8^+$, and $CD25^+$ SLE T cells, which correlates with its increased insolubility in Brij 98 detergent, and its translocation into lipid rafts. Moreover, SLE T cells show an altered CD4:CD8 ratio, which is due to a decreased proportion of $CD4^+$ T cells and a concomitant increase in the proportion of $CD8^+$ T cells. These data are consistent with the increased CD38 expression and lipid raft formation, and the significant reduction in the CD4:CD8 ratio observed in mitogen-stimulated normal T cells as compared with that in *ex vivo* untouched normal T cells. Increased expression of CD38 in floating rafts from SLE T cells, or from activated normal T cells may modulate TCR signaling by providing or sequestering signaling molecules to the engaged TCR.

Keywords: CD38; TCR; Signaling; Lipid rafts; T cells; Lupus; Autoimmunity

1. Introduction

SLE is a multisystemic autoimmune disease characterized by the production of high levels of autoantibodies against nuclear antigens resulting, at least in part, from a dysregulated T lymphocyte response to autoantigens (Janeway et al., 2001; Kammer et al., 2002; Kong et al., 2003). Although SLE etiopathology is poorly understood, there is likely a role for environmental triggers, for instance viruses, acting in the context of susceptibility genes (Rozzo et al., 2001; Wakeland et al., 2001). In both, European-American, and Iceland populations it has been identified a SLE susceptibility locus on human region 4p15 (Gray-McGuire et al., 2000; Lindqvist and Alarcon-Riquelme, 1999). Located within human 4p15 region are a number of interesting candidate genes including CD38 and CD157, which are both ectoenzymes members of the ADP-ribosyl cyclase family that are directly involved with T and B lymphocyte activity (Deaglio et al., 2001; Ortolan et al., 2002). There is an association between a polymorphism located at position 182 of intron 1 of the CD38 gene, and the development of discoid rash in Spanish SLE patients (Gonzalez-Escribano et al., 2004).

Previous studies have defined B cell subsets from inflamed secondary lymphoid tissue, such as tonsil, or the periphery of active-SLE patients that are defined by very high expression of CD38 and the presence of intracellular immunoglobulin (Grammer and Lipsky, 2003). On the other hand, increased expression of CD38 on T cells has been found in SLE patients (Alcocer-Varela et al., 1991; al-Janadi and Raziuddin, 1993; Erkeller-Yuksel et al., 1997). In certain tumor types, up-regulation of CD38 in tumor-associated non-neoplastic T

* Corresponding author. Tel.: +34 958 181664; fax: +34 958 181632.
E-mail address: granada@ipb.csic.es (J. Sancho).

0161-5890/$ – see front matter © 2005 Elsevier Ltd. All rights reserved.
doi:10.1016/j.molimm.2005.05.002

cells could be useful as a marker of persistent T cell activation as well as a surrogate marker of disease progression (Lin et al., 2004). Likewise, up-regulation of CD38 on $CD8^+$ T cells could be a marker of ongoing viral replication during acute or chronic viral infections (Belles-Isles et al., 1998; Carbone et al., 2000; Lynne et al., 1998; Ramzaoui et al., 1995).

Plasma membranes of many cell types, including T cells, contain specialized microdomains, or lipid rafts, enriched in sphingolipids, cholesterol, sphingomyelin and glycosylphophatidylinositol-anchored proteins. These membrane domains are characterized by detergent-insolubility at low temperatures and low buoyant density (Brown and London, 2000; Simons and Toomre, 2000). Lipid rafts play a central role in signal-transduction, in the immune response and in many pathological situations on the basis of two important raft properties, their capacity to incorporate or exclude proteins selectively, and their ability to coalesce into larger domains (Manes et al., 2003; Simons and Ehehalt, 2002). The densely packed, liquid-ordered environment of rafts excludes most integral membrane proteins. However, we have demonstrated that in T cells CD38 is constitutively associated with lipid rafts resistant to solubilization in 1% NP-40 at 4 °C (Zubiaur et al., 2002), or in 1% Brij 98 at 37 °C (Munoz et al., 2003). Furthermore, CD38 in rafts is able to initiate and propagate several activating signaling pathways, possibly by facilitating critical associations within other raft subsets, per example LAT rafts, via its capacity to interact with Lck and CD3-ζ (Munoz et al., 2003).

Changes in the properties or composition of lipid rafts may lead to inappropriate T lymphocyte signaling and ultimately to the development of pathological conditions, including autoimmunity (Gringhuis et al., 2000; Salojin et al., 1998). In this sense, in SLE T cells there are qualitative alterations in the protein composition of lipid rafts, alterations in actin dynamics, and increased calcium responses (Krishnan et al., 2004). Moreover, reduced expression of Lck in SLE T cells (Jury et al., 2003) is associated with increased expression of GM1 and increased localization of CD45, a molecule important in regulating Lck activity (Jury et al., 2004).

In this study we found that CD38 expression is augmented in $CD3^+$ T cells from patients with SLE, which correlates with its increased translocation into lipid rafts. These data are consistent with increased lipid raft formation in activated normal T cells, and the evidence that SLE T cells display activation phenotypes.

2. Material and methods

2.1. Patients and healthy controls

Fifty-one consecutive outpatients fulfilling the revised American College of Rheumatology (ACR) criteria for the diagnosis of SLE (Tan et al., 1982), and routinely followed in the Systemic Autoimmune Diseases Unit (Hospital Clínico San Cecilio, Granada, Spain) could participate in this study between December 2002 and May 2004. Thirty-six healthy, age-matched healthy volunteers served as controls. Disease activity was scored and the SLE Disease Activity Index (SLEDAI) was calculated (Bombardier et al., 1992). Our study included 22 inactive SLE patients, 29 active patients with SLEDAI ranging from one to 20, and 36 healthy control volunteers (Table 1). All of them were Caucasians. Patients who were being treated with prednisone were asked not to take this medication 24 h before blood was drawn. For each patient, data were recorded on age, duration of the disease defined as the period from the disease onset (time when patients fulfilled the ACR criteria) to the time of the study, current and cumulative gluco-corticoid doses by review of patient records. Complete blood cell count, serum complement and serum anti-nuclear and anti-DNA antibodies were measured in all patients. Because the paucity of cell numbers obtained from the disease group, many of whom were leukopenic, different sets of experiments were performed with different patient groups but care was taken to include patients of SLEDAI score ranging from low (0–4 range) to high (5–20) in each group. Within each group, patient samples were matched with normal samples of similar ages and gender. The study protocol was approved by the Hospital Clínico San Cecilio, and CSIC Review Board and Ethics Committees. Written informed consent was obtained from all participating patients and volunteers according to the Declaration of Helsinki.

Table 1
Clinical and demographic characteristics of the study subjects

	SLE ($N = 51$)	Healthy controls ($n = 36$)
Women	45 (88%)	21 (58%)
Age (y)	38.1 (20–77)	38.1 (20–77)
Caucasian	51 (100%)	36 (100%)
Disease duration (y)	4.1 (1–15)	NA
SLEDAI	3.35 (0–20)	NA
SLEDAI = 0	22 (43.1%)	NA
SLEDAI = 1–4	14 (27.4%)	NA
SLEDAI > 4	15 (29.4%)	NA

2.2. T lymphocyte isolation

PBMC were obtained by density gradient centrifugation over HISTOPAQUE®-1077 (Sigma-Aldrich Química, S.A., Spain). T cells were isolated from PBMC by magnetic separation after depletion of non-T cells by negative selection with the Pan T Cell Isolation Kit II (Miltenyi Biotec, GmbH, Germany) following the manufacturer's instructions. In all the cases, the percentage of T cells in the isolated subpopulation was >98% as determined by anti-CD3-ε mAb staining and fluorescence-activated cell sorter (FACS) analysis. T cells were stimulated with 5 μg/ml PHA-L and and 50 U/ml IL-2 (Sigma-Aldrich, Química, S.A.) for 3 days.

2.3. Antibodies and reagents

Anti-human CD3-ε mAb OKT3 (IgG_{2a}), or the CD38 mAbs HB136 (IgG_1) and OKT10 (IgG_1) were prepared, pu-

rified, and labeled with fluorescein isothiocyanate (FITC) as previously described (Zubiaur et al., 1999). Affinity purified anti-human CD4-PE and CD8-FITC antibodies, the CTB-FITC conjugate and the affinity purified mouse mAb to α-Actin (clone AC40) were obtained from Sigma-Aldrich. Affinity purified anti-human mAb CD19-PE ($IgG_{1\kappa}$), anti-human mAb CD38- PE ($IgG_{1\kappa}$), and mouse immunoglobulin isotype controls were purchased from BD Biosciences (San Jose, CA). Affinity purified mAb anti-human CD56-PE (IgG_1) was purchased from Miltenyi Biotec, GmbH (Germany). Affinity purified, FITC-conjugated, $F(ab')_2$ fraction of rabbit antibody to mouse immunoglobulins was purchased from DAKO (Glostrup, Denmark). The affinity-purified rabbit polyclonal antibody anti-Fyn was purchased from Santa Cruz Biotechnology (Santa Cruz, CA). An affinity purified rabbit antibody to CD3-ε was purchased from Dako (Denmark). Polyclonal antibody anti-LAT was from UBI Upstate Biotechnology (Upstate, NY). Anti-CD3-ζ antiserum 448 was a gift from Dr. B. Alarcón (Centro de Biología Molecular, CSIC, Madrid, Spain). Affinity purified goat anti-rabbit IgG (Fc) HRP Conjugate, and goat anti-mouse IgG (H + L) HRP Conjugate were from Promega (Madison, WI). Prestained SDS-PAGE Standards (broad and precision range), and ImmunoStart reagents were from Bio-Rad (Hercules, CA).

2.4. FACS analysis

PBMC or purified T cells were analyzed for surface expression of CD3, CD4, CD8, CD38, CD19 and CD56 by single or double-staining using FITC-, or PE-labeled anti-CD3, anti-CD38, anti-CD19, and anti-CD56 mAbs in the relevant combinations. Compensation settings were adjusted using single stained PBMC, or T cell samples. Isotype-matching labeled antibodies were used to calculate the non-specific staining. PBMC and lymphocytes were gated according with their forward and scatter characteristics (Munoz et al., 2003; Zubiaur et al., 1997). Two color immunofluorescence analysis was performed on a FACScan flow cytometer (BD Biosciences, San Jose, CA), using the CellQuest Pro (BD Biosciences), and FlowJo (Tree Star, Inc. San Carlos, CA) software.

2.5. Detergent solubilization of cells at 37 °C

Cells ($1–5 \times 10^6$) were lysed in 1% Brij 98 at 37 °C as described previously (Munoz et al., 2003). Lysates were centrifuged at 13,000 rpm for 15 min at 4 °C, and supernatant (SN) and pellet (P) were diluted in 3× non-reducing Laemmli sample buffer. Both fractions were resolved on a 12.5% SDS-PAGE, transferred to PVDF and immunoblotted with specific antibodies, followed by the ECL system, as previously described (Munoz et al., 2003; Zubiaur et al., 2002).

2.6. Fractionation of floating rafts by sucrose gradient ultracentrifugation

Detergent-insoluble and -soluble fractions were separated in a discontinuous sucrose gradient as described (Munoz et al., 2003; Zubiaur et al., 2002) with minor modifications. Two pools of the sucrose gradient fractions were then collected. First, the low-density fractions corresponding to the 5/30% interface (fractions 2 and 3, along fraction 4) and referred to as *Floating Rafts* (R). Second, the high-density soluble material corresponding to fractions 7 and 8 of the gradient and referred to as *Soluble* (S). The two pools were diluted with 3× non-reducing Laemmli sample buffer and resolved on 12.5% SDS-PAGE, transferred to PVDF and immunoblotted with specific antibodies, followed by the ECL system, as previously described (Zubiaur et al., 1999). Except where otherwise noted, 27 μl of each sample was loaded onto gels.

2.7. Densitometric and statistical analysis

Densitometric analysis was performed on a PC using the Quantity One 1-D Analysis Software Version 4.4 (Bio-Rad Laboratories, Inc., USA). To compare sample groups statistical analysis were performed using the Student's *t*-test, the Mann–Whitney U test, or the Fisher's exact test when appropriate. *P* values less than 0.05 were considered significant. The tests were performed using the GraphPad Prism software version 4.02 (GraphPad Software, Inc. San Diego, CA).

3. Results

3.1. A significant percentage of CD38 is insoluble in Brij 98 at 37 °C in PBMC from SLE patients

The non-ionic detergent Brij 98 has been successfully used to selective isolate, at physiological temperatures, detergent-insoluble microdomains with the biochemical characteristics of rafts (Drevot et al., 2002; Munoz et al., 2003; Schuck et al., 2003). Therefore, we first investigated in PBMC whether CD38 was associated with the membrane raft vesicles that are recovered as detergent-insoluble complexes upon cell lysis in Brij 98 detergent at 37 °C and centrifugation at $13,000 \times g$ for 15 min at 4 °C. After this treatment, cytosolic and fully solubilized membrane proteins were found in the supernatant (referred to as SN), whereas lipid rafts and associated proteins, as well as cytoskeletal components remained in the pellet (referred to as P) (Munoz et al., 2003). The presence of CD38 in the P and SN fractions was determined by Western blotting. Equal number of cell equivalents (0.5×10^6) were loaded in patients and control samples, and the proportion of CD38 present in the P fraction relative to the total amount of CD38, (SN + P) was calculated. CD38 was present in the P fraction from either the SLE patients and the healthy controls (Fig. 1A, lanes 2 and 4), although its proportion, relative to the total amount of CD38 was significantly higher in SLE than in controls ($P = 0.0090$, Fig. 1B). In contrast, similar proportions of Fyn, or actin relative to controls were detected when the same membranes were re-blotted with anti-Fyn, or anti-α-actin antibodies, respectively (Fig. 1A). Both SLE patients with high or low SLEDAI scores displayed a sta-

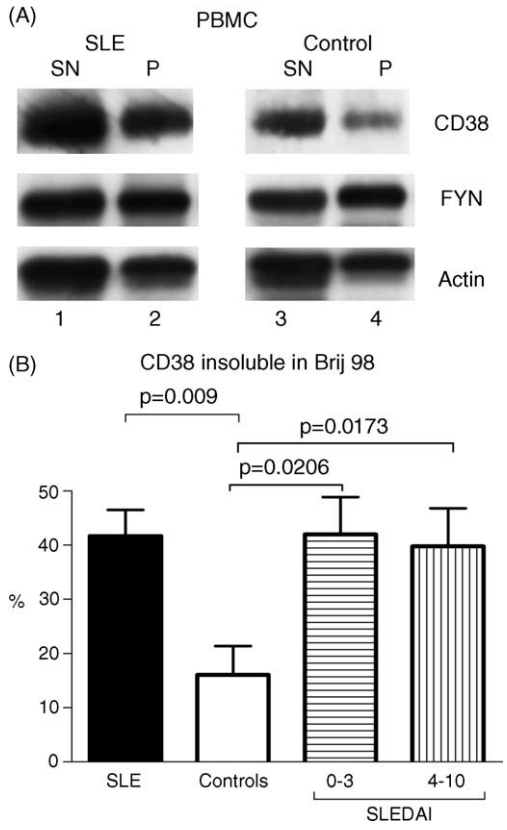

Fig. 1. A significant proportion of CD38 is insoluble in 1% Brij 98 in PBMC from SLE patients. (A) PBMC from SLE patients, or healthy controls were lysed in 1% Brij 98 at 37 °C as described in Section 2, and the detergent-insoluble fraction was separated from the soluble fraction by centrifugation at 13,000 × *g*. Supernatant (SN) and pellet (P) were diluted in 3× SDS non-reducing sample buffer and proteins were separated by 12% SDS-PAGE, transferred, and immunoblotted for the indicated proteins on the right of each panel. (B) bands intensities were quantified by densitometry, and the densitometric units on CD38 in pellet were presented as percentage of the sum of the densitometric units of supernatant + pellet. Values are the mean and S.E.M. The mean percentage of CD38 insoluble in Brij 98 was significantly increased in 29 SLE patients (black histograms) compared with nine healthy controls (open histograms). Likewise, SLE patients segregated according their SLEDAI scores as low (0–3) (horizontal stripped histograms, $n = 18$), or high (4–10) (vertical stripped histograms, $n = 11$), showed significantly increased percentages of CD38 insoluble in Brij 98 compared with controls (two-tailed unpaired *t*-test).

tistically significant higher proportion of CD38 in the Brij 98-insoluble fraction as compared with that in healthy controls ($P = 0.0173$ and 0.0206, respectively, Fig. 1B). These results strongly suggested that in SLE PBMC a large fraction of CD38 was associated with the membrane raft vesicles recovered as Brij 98-insoluble complexes.

3.2. Increased association of CD38 with floating rafts in PBMC from SLE patients

Insolubility of a membrane protein in a detergent as Brij 98 can be due to its association with detergent-resistant lipid rafts and/or its anchoring to cytoskeletal elements (Munoz et al., 2003). Proteins associated with detergent-insoluble lipid rafts float in a sucrose density gradient, while cytoskeleton-associated proteins remain at the bottom of the ultracentrifuge tube (Brown and Rose, 1992; London and Brown, 2000; Simons and Ikonen, 1997). Therefore, if CD38 is associated with Brij 98-insoluble lipid rafts, this CD38 should also float in a sucrose density gradient (Drevot et al., 2002; Munoz et al., 2003). To address this issue, rafts and non-raft fractions were isolated by sucrose gradient ultracentrifugation upon lysis of PBMC in Brij 98 at 37 °C (see Section 2, and (Munoz et al., 2003)). In floating rafts (referred to as R), five out of nine lupus patients studied showed percentages of CD38 above the upper 99% confidence interval (upper CI = 9.9%) of the mean values for six normal individuals (Fig. 2A, *left panel* 1 and 3). Application of the Fisher's exact test revealed a statistically significant difference (Fig. 2A, *right panel*, $13.7 \pm 4.6\%$ in SLE, $n = 9$ versus $3.6 \pm 1.6\%$ in controls, $n = 6$, $P = 0.0440$). In contrast, five out of nine patients studied showed percentages of CD3-ζ below the lower 95% confidence interval (lower CI = 4.2%) of the mean values for six normal healthy controls (Fig. 2A, *left panel*, lanes 1 and 3), although these differences were not statistically significant (Fig. 2B, *left panel*, $7.0 \pm 2.6\%$ in SLE, $n = 9$ versus $12.7 \pm 3.0\%$ in controls, $n = 6$, $P = 0.2867$, Fisher's exact test). Likewise, LAT that is constitutively associated with lipid rafts (Zhang et al., 1998), was always detected in floating rafts from both SLE patients and controls (Fig. 2A, *left panel*, lanes 1 and 3), and the minor differences observed between them were not statistically significant (Fig. 2B, *right panel*, $20.7 \pm 5.9\%$ in SLE, $n = 9$ versus $26.9 \pm 4.1\%$ in controls, $n = 6$). Therefore, these results demonstrate that SLE PBMC express an increased proportion of CD38 associated with floating lipid rafts, while similar proportions of CD3-ζ and LAT were present compared with that in PBMC from healthy controls.

3.3. Increased CD38 expression in SLE T cells and T cell subsets

Highly purified untouched T cells were obtained from PBMC by depletion of non-T cells by magnetic separation (see Section 2). T lymphocytes from eight patients with SLE and seven healthy controls were analyzed for expression of CD38 in $CD3^+$, $CD4^+$, $CD8^+$, and $CD25^+$ cells. The proportion of $CD38^+$ cells in the whole T cell population ($CD3^+$), as well as in the three T cell subsets studied ($CD4^+$, $CD8^+$, and $CD25^+$), was significantly increased in SLE patients as compared with that in healthy controls (Fig. 3). These increases seemed to be specific for T cells since neither the B or the NK cell compartments showed significant differences in CD38 expression between SLE patients and healthy controls when evaluated in PBMC by dual staining for CD38 and CD19 (B cells), or CD38 and CD56 (NK cells) (data not shown). No significant differences were observed in the proportion of CD3, CD19, or CD56 subsets within the PBMC population (data not shown). These results support the observation that the altered distribution and expression

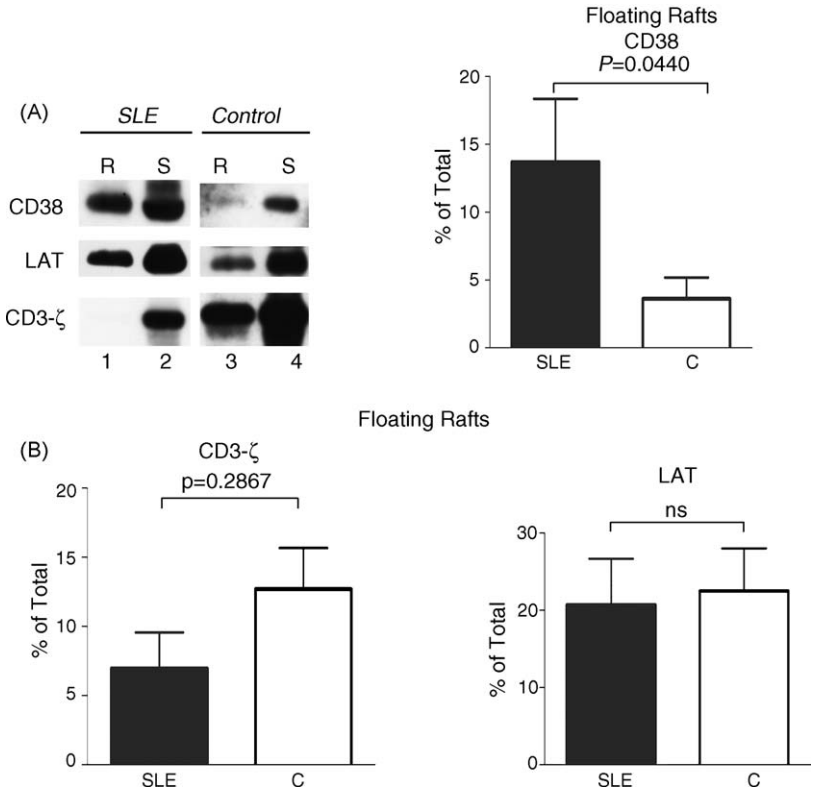

Fig. 2. Increased association of CD38 with floating rafts in PBMC from SLE patients. (A) *Left panel*, floating rafts (R) and soluble (S) fractions from one SLE (lanes 1 and 2) and one healthy control (lanes 3 and 4) PBMC were isolated as described in Section 2. Proteins were separated on SDS-PAGE, transferred to PVDF membranes, and immunoblotted with anti-CD38, anti-LAT, or anti-CD3-ζ antibodies. *Right panel*, graph displaying cumulative results for CD38 expression in PBMC floating rafts from nine SLE patients (closed histograms), and five healthy controls (open histograms). Densitometric data on CD38 in floating rafts (R) are presented as percentage of the sum of all sucrose gradient fractions ($P = 0.0440$, Fisher's exact text). (B) The mean percentages for CD3-ζ ($P = 0.2867$, not significant, Fisher's exact text) and LAT expression (*left and right panels*, respectively) in PBMC floating rafts from SLE patients and healthy controls was calculated as in A.

of CD38 in PBMC from lupus patients are unique to SLE T cells.

3.4. CD38 is associated with floating rafts in ex vivo SLE T cells

3.4.1. Increased CD38 expression and insolubility in Brij 98 upon mitogenic stimulation

Next, we analyzed CD38 distribution in raft and non-raft compartments in untouched T cells in isolation. Floating rafts were isolated by sucrose gradient ultracentrifugation as described for PBMC. A representative experiment is shown in Fig. 4A (*upper panels*, lane 1 versus lane 3). CD38 was readily detected in the floating raft pool from SLE T cells in five out of eight SLE patients ($16.9 \pm 7.5\%$), whereas very little, if any, was detected in eight healthy control T cells ($0.0 \pm 0.0\%$). In contrast, the mean values for the percentages of CD3-ζ ($13.7 \pm 4.8\%$, in SLE versus $17.9 \pm 5.6\%$, in controls), and CD3-ε ($7.0 \pm 1.8\%$ in SLE versus $10.8 \pm 4.6\%$ in controls) in floating rafts were somewhat lower in SLE than in normal T cells, although the differences were not statistically significant (either by the Fisher's exact test, or unpaired *t*-test).

PHA acts as a potent and specific T cell activator by binding to cell membrane glycoproteins including the TCR/CD3 complex and the CD2 co-receptor, and exogenous IL-2 provides further T cell expansion (Kay, 1991). Moreover, stimulation of resting human T cells with PHA results in a significant increase in proportion of the plasma membrane that adopts a raft structure as judged by the dramatic increase on the cell surface expression of the raft-associated glycosphingolipid GM1 (Tuosto et al., 2001), which has previously been shown a reliable marker for detection of lipid raft domains (Janes et al., 1999). We next explored whether mitogenic stimulation could affect raft CD38 expression and distribution in SLE T cells compared with normal T cells. Thus, T cells were stimulated in vitro with PHA and IL-2 for 3 days (see Section 2) and then analyzed for CD38 expression by Western blotting of Brij 98-insoluble and -soluble fractions from whole cell extracts. Equal number of cell equivalents (0.5×10^6) were loaded in patients and control samples, and the proportion of CD38 present in the P fraction relative to the total amount of CD38, (SN + P) was calculated. As shown in Fig. 4B, there was a dramatic increase in the total amount of CD38 (SN + P) in PHA-stimulated T cells from both SLE patients (lanes 3 and 4) and healthy controls (lanes 7 and 8)

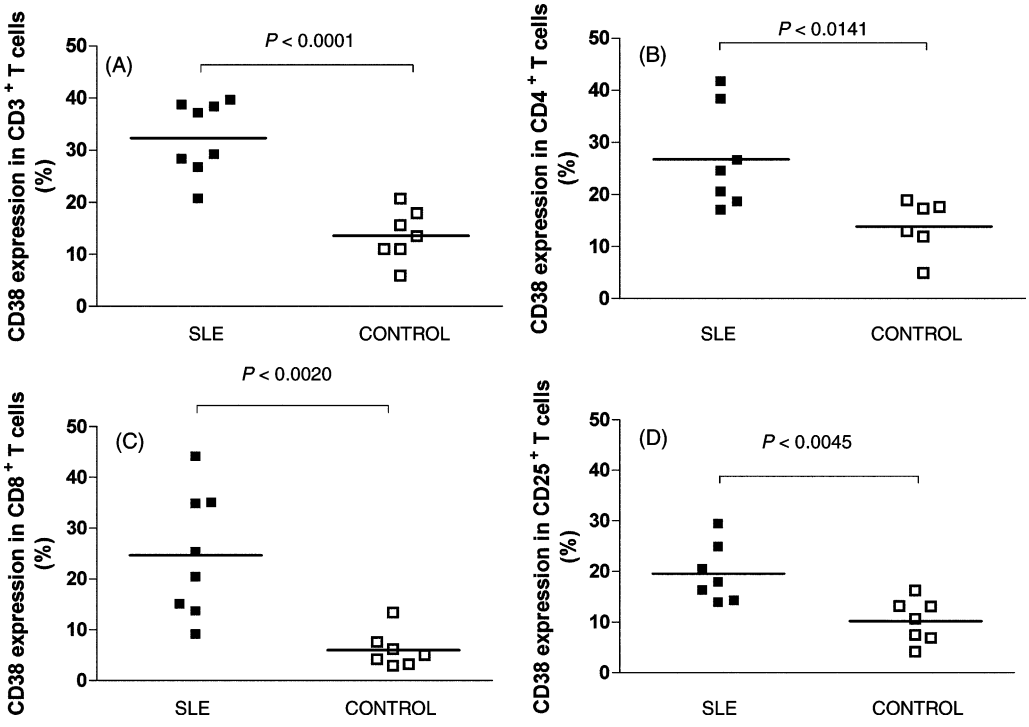

Fig. 3. Increased CD38 expression in SLE T cells and SLE T cell subsets. (A) Percentage of purified $CD3^+$ T cells expressing CD38. (B) Percentage of $CD4^+$ T cells expressing CD38. (C) Percentage of $CD8^+$ T cells expressing CD38. (D) Percentage of $CD25^+$ T cells expressing CD38. Scattered plots of percent of double positive cells are shown for SLE patients (filled squares), and healthy controls (open squares). Each symbol represents one patient or control, and the bar within each group represents the mean percentage value. The *P* values are indicated in each panel (two-tailed unpaired Student's *t*-test).

as compared with that in ex vivo untouched T cells (lanes 1, 2, 5, and 6). Moreover, in PHA-stimulated SLE and control T cells there was a significant shift of CD38 into the Brij 98-insoluble fraction (lanes 3 and 7) as compared with that in ex vivo cells (lanes 1 and 5). In contrast, the amount of Fyn, or actin and its distribution between soluble and insoluble fractions remained constant upon PHA stimulation, which was indicative of equal protein loading (Fig. 4B). Therefore, PHA stimulation induced quantitative and qualitative changes in the amount and distribution of CD38 between raft and non-raft fractions.

3.5. Increased lipid raft expression and altered CD4:CD8 ratio in ex vivo SLE T cells

3.5.1. Recapitulation in normal T cells upon mitogenic stimulation

Next, to visualize rafts on the cell surface, ex vivo and mitogen-stimulated T cells were analyzed for GM1 surface expression with fluorescent-labeled CTB and flow cytometry. CTB binds the raft-associated glycosphingolipid GM1, previously shown to be a reliable marker for detection of lipid raft domains (Janes et al., 1999). The analysis (Fig. 5A) revealed an increased proportion of ex vivo SLE T cells that bound CTB compared with that in normal T cells ($2.5 \pm 0.4\%$, $n = 18$, in SLE versus $0.9 \pm 0.1\%$, $n = 10$, in controls, $P = 0.0095$). PHA stimulation resulted in dramatic increases in the percentages of $GM1^+$ cells in both SLE and normal T cells (Fig. 5A). However, although the percentages of $GM1^+$ SLE T cells were increased as compared with that in normal T cells, these differences were not statistically significant ($18.5 \pm 3.7\%$, $n = 6$, in SLE versus 13.0 ± 2.4, $n = 8$, in controls, $P = 0.2180$). Interestingly in PHA-stimulated T cells about 35–40% of the $CD38^+$ cells were also $GM1^+$ (Fig. 5B), which suggested the selective expansion of a subset that expressed both markers. Moreover, these data were indicative that in both SLE and normal T cells an increased proportion of the plasma membrane adopts a lipid raft structure upon mitogenic stimulation.

Ex vivo and PHA-stimulated T cells were analyzed for CD4:CD8 ratio by flow cytometry. Patients with SLE had a significantly reduced CD4:CD8 ratio compared with that of healthy controls (Fig. 5C, $P = 0.0022$), as described previously (Jury et al., 2004). This was due to a significant reduction in the number (%) of $CD4^+$ T cells ($P < 0.0001$, Fig. 5D), and to a significant augmentation in the proportion of $CD8^+$ T cells ($P = 0.0447$, Fig. 5E). Interestingly, in healthy controls PHA-stimulated T cells had a significantly reduced CD4:CD8 ratio compared with that of ex vivo T cells (Fig. 5C, $P = 0.0052$), which was caused by a significant reduction in the percentage of $CD4^+$ T cells (Fig. 5D, $P = 0.0145$), and an increase in the percentage of $CD8^+$ T cells (Fig. 5E, $P = 0.0156$). This altered phenotype paralleled the one obtained in untouched *ex vivo* SLE T cells. In contrast, in SLE patients, PHA-stimulation did not induce significant changes in the CD4:CD8 ratio, neither in the number

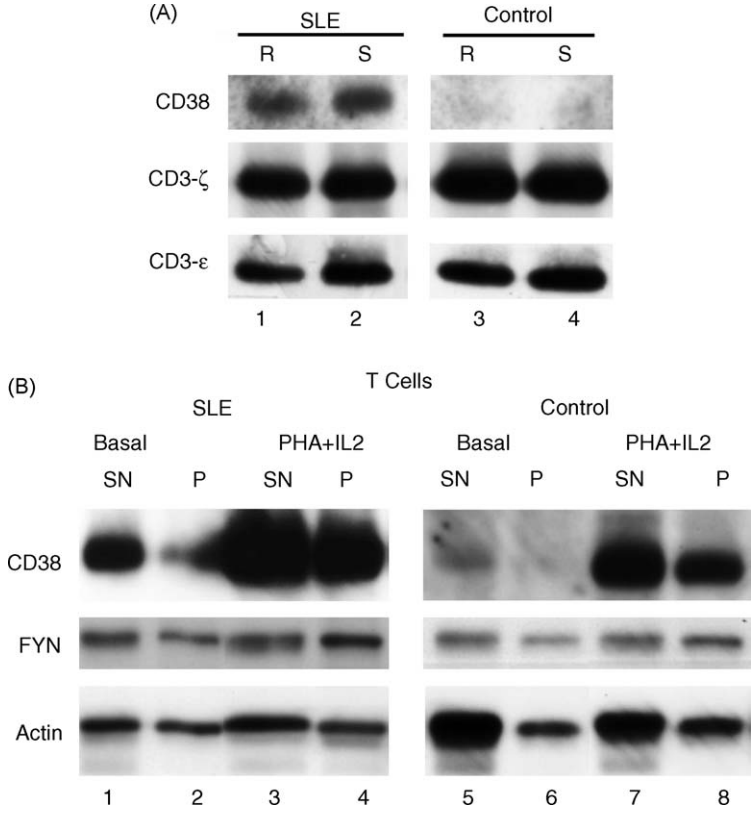

Fig. 4. (A) CD38 is associated with floating rafts in ex vivo SLE T cells. Floating rafts (R), and Soluble fractions (S) were prepared from untouched T cells purified by immunomagnetic depletion of non-T cells (see Section 2) from one SLE patients (lanes 1 and 2) and one healthy control (lanes 3 and 4) without any ex vivo stimulation. Proteins were separated on SDS-PAGE and analyzed by Western blotting with anti-CD38, anti-CD3-ζ, and anti-CD3-ε antibodies. This is a representative experiment out of eight experiments done in eight different SLE patients and eight healthy controls. Densitometric data on CD38, CD3-ζ, and CD3-ε in floating rafts (R) were calculated as in Fig. 2A (see Section 3 for specific numbers). (B) Increased CD38 expression and translocation into the Brij 98-insoluble fraction in T cells upon PHA stimulation. SN and P fractions were prepared as in Fig. 1A from: ex vivo untouched SLE T cells (lanes 1 and 2), ex vivo normal healthy control T cells (lanes 5 and 6), PHA + IL-2-stimulated SLE T cells (lanes 3 and 4), or PHA + IL-2-stimulated normal T cells (lanes 7 and 8). Proteins were separated by 12% SDS-PAGE, transferred, and analyzed by Western blotting with anti-CD38, anti-Fyn, and anti-α-actin antibodies. This is a representative experiment out of eight experiments done with cells from eight different SLE patients and eight healthy controls.

of $CD4^+$, nor $CD8^+$ T cells compared with that of ex vivo SLE T cells (Fig. 5C–E, respectively).

Taken together, these results on Figs. 4 and 5 indicate that ex vivo SLE T cells show an increased raft expression and altered phenotype, which can be recapitulated by PHA stimulation of normal T cells. PHA stimulation also induces increased CD38 expression, and active recruitment of CD38 to lipid rafts. This may be associated with an augmentation in the proportion of the plasma membrane adopting a lipid raft structure, as judged by the increased expression of GM1 on the cell surface, and the distinct expansion of the $CD38^+GM1^+$ T cells.

4. Discussion

In this study, we provide evidence of increased insolubility of CD38 in the non-ionic detergent Brij 98 at physiological temperatures in SLE PBMC as compared with normal PBMC, which correlated with an increased proportion of CD38 in floating rafts in both SLE PBMC and T cells. Consistent with previous reports (Alcocer-Varela et al., 1991; al-Janadi and Raziuddin, 1993), the percentage of $CD3^+$ T cells that express CD38 is significantly higher in SLE patients than in healthy controls. Moreover, we have found a significant increased percentage of $CD8^+CD38^+$, $CD4^+CD38^+$, and $CD25^+CD38^+$ T cells in patients with SLE in comparison to normal controls. $CD8^+CD38^+$ T cells are increased in advanced viral infections (Belles-Isles et al., 1998), and $CD8^+CD38^+$ lymphocyte percent is a useful immunological marker for monitoring HIV-1-infected patients (Mocroft et al., 1997). In this regard, PHA-stimulation of normal T cells results in reduced CD4:CD8 ratio and increased CD38 expression, which paralleled the altered phenotype of ex vivo SLE T cells. The contribution of the increased $CD8^+CD38^+$ T cells to the pathology of the SLE disease remains unclear (Erkeller-Yuksel et al., 1997), but together with increased $CD4^+CD38^+$ and $CD25^+CD38^+$ T cells could be indicative of persistent T cell activation.

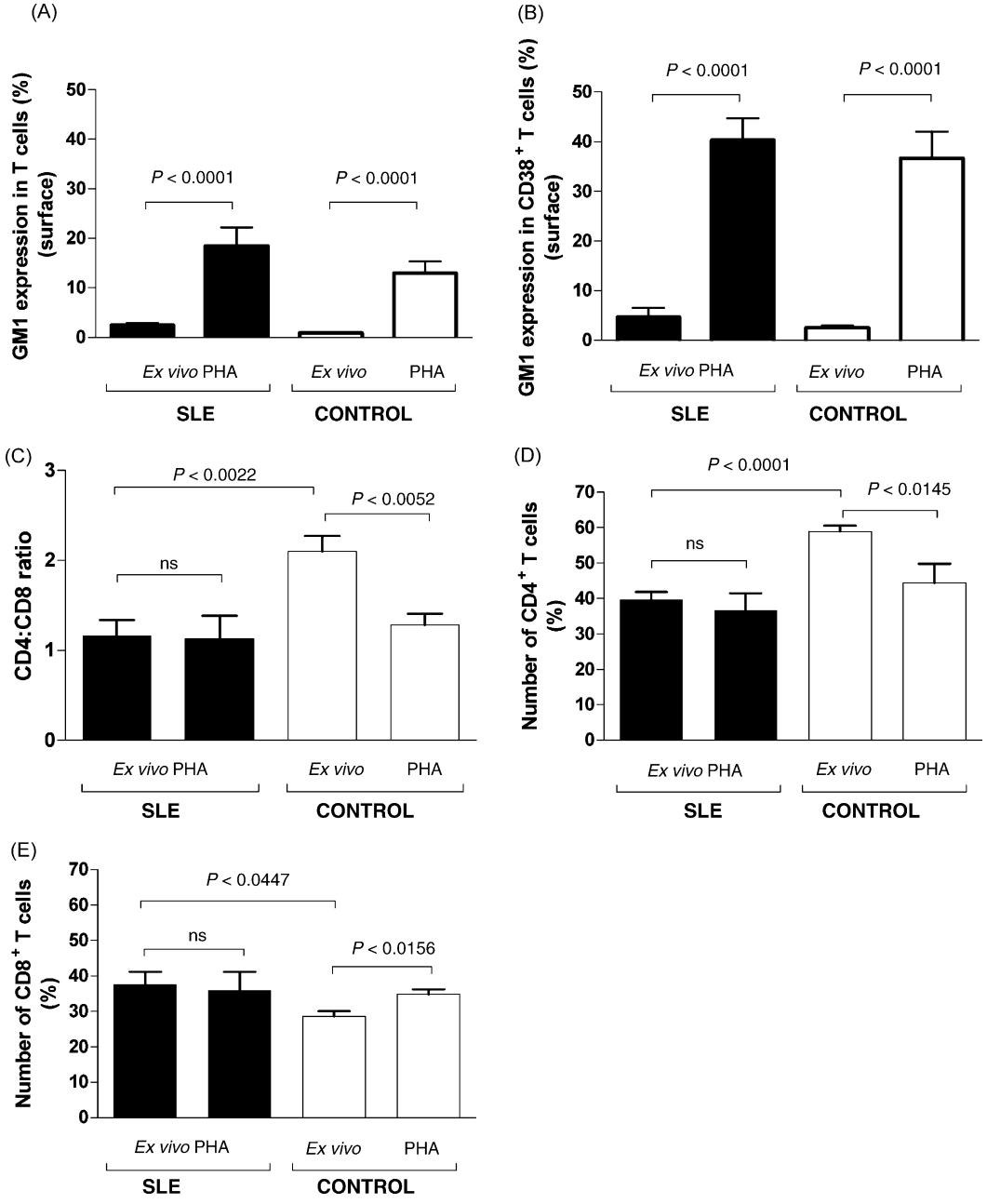

Fig. 5. Increased lipid raft expression and altered phenotype in ex vivo SLE T cells. Effect of PHA stimulation. Number (%) of $CD3^+$ cells (panel A), or $CD38^+$ cells (panel B) expressing GM1 on the cell surface in ex vivo or PHA-stimulated T cells from 18 SLE patients (black histograms) and 10 healthy controls (open histograms). The relative proportions of T cells expressing CD4 or CD8 (panel C) were expressed as a ratio (CD4:CD8) on ex vivo or PHA-stimulated T cells from eight SLE patients (black histograms) or from seven healthy controls (open histograms). The number (%) of $CD4^+$ (panel D), or $CD8^+$ (panel E) T cells. All results are expressed as mean + S.E.M. The *P* values are indicated in each panel (two-tailed unpaired Student's *t*-test).

CD38 function in T cells is mediated by cell-surface association with the TCR/CD3 complex (Morra et al., 1998; Zubiaur et al., 1997, 1999), and the localization of CD38 to lipid raft domains is essential for CD38-mediated signaling in CD38-transfected murine T cell lines (Zubiaur et al., 2002), or in Jurkat T cells, which constitutively express CD38 (Munoz et al., 2003). In these T cell lines, CD38 appears to localize to the rafts without the need for ligation (Munoz et al., 2003; Zubiaur et al., 2002). Therefore, it was to some extent surprising that in normal resting T cells CD38 was detected exclusively in soluble fractions. The mechanism by which CD38 in T cells is included or excluded from rafts is not known, but it may be related rather with the significant differences in the lipid raft composition and dynamics between resting and activated/effector T cells, and not with the level of expression of CD38. Thus, the organization of GM1-lipid rafts on the T cell membrane appears developmentally regulated (Hare et al., 2003). Interestingly, in rest-

ing human T cells from peripheral blood Lck and the raft glycosphingolipid GM1 reside in intracellular membranes, while in activated/effector T cells the amount of these markers at the plasma membrane increases significantly (Tuosto et al., 2001). These dramatic increases in GM1 cell surface expression can be recapitulated in vitro by a number of different stimuli including PHA (Tuosto et al., 2001), TCR/CD3 cross-linking with a soluble CD3 ligand (Thomas et al., 2003b), or with anti-CD3/CD28 beads (Slaughter et al., 2003; Tuosto et al., 2001). Likewise, murine and human T cell lines, which have an effector phenotype, express high levels of GM1 on the cell surface, and CD38 is readily detected in lipid rafts (Zubiaur et al., 2002; Munoz et al., 2003). Our present findings are significant in this regard, as the dramatic changes in the distribution of CD38 into Brij 98-insoluble and -soluble fractions upon mitogenic stimulation of normal T cells (Fig. 4B) correlated with increased GM1 expression on the cell surface (Fig. 5A), and a distinct expansion of $GM1^{+}CD38^{+}$ T cells (Fig. 5B). Likewise, in untouched SLE T cells a significant proportion of CD38 is associated with lipid rafts, which again correlates with increased basal expression of GM1 on the cell surface (Fig. 5A). Note that we have just measured the GM1 pool that is on the cell surface, which is only a fraction of the total GM1 pool (surface + intracellular). Increased basal expression of total GM1 has been reported previously in SLE T cells compared with normal T cells (Jury et al., 2004; Krishnan et al., 2004). Therefore, SLE T cells possess more extensive basal levels of lipid rafts than normal T cells, which may be indicative of their "activated" phenotype that could result from the exposure of SLE T cells to the abnormal frequency of differentiated dendritic cells found in these patients (Blanco et al., 2001).

Increased lipid raft expression on the plasma membrane may constitute a means by which effector T cells acquire an improved signaling machinery (Tuosto et al., 2001). In contrast, displacement of the CD4:Lck signalosome from the lipid rafts by a soluble, dimeric peptide-MHC Class II chimera induces Ag-specific T cell anergy (Thomas et al., 2003a), suggesting that the defective partitioning of signaling molecules in lipid rafts is an early, negative signaling event in T cells. The study of raft protein composition in the Jurkat T cell line have revealed that CD38, Lck and CD3-ζ reside in a subset of lipid rafts separately from LAT and other key signaling molecules (Munoz et al., 2003), which is compatible with other studies showing that in resting T cells Lck and LAT are located in different raft subsets (Drevot et al., 2002; Schade and Levine, 2002; Slaughter et al., 2003). After cellular activation, these rafts coalesce, leading to Lck and LAT colocalization in the same raft population (Drevot et al., 2002; Schade and Levine, 2002; Slaughter et al., 2003). CD38 residency in a subset of lipid rafts together with Lck and CD3-ζ provides a structural basis for initiating CD38-mediated signaling in this compartment, where fully phosphorylation of CD3-ζ, CD3-ε, Lck and LAT occurs, as well as the translocation of key signaling molecules as Sos and p85-phosphatidylinositol 3-kinase into rafts (Munoz et al., 2003).

The low number of cells used in this study precluded the analysis of the protein composition of CD38-containing rafts in either resting or activated SLE T cells but it is likely that the anomalous expression or changes in membrane location of signaling molecules as CD3-ζ, or Lck found in these patients (Jury et al., 2003; Krishnan et al., 2004) may lead to anomalous lipid raft-mediated signaling. It has been shown that ligand-mediated cross-linking of GM1 moieties in lipid rafts facilitates an exchange of proteins including the redistribution of the TCR and adhesion molecules in T cells (Mitchell et al., 2002). We speculate that the increased expression of CD38 in floating rafts from SLE T cells, or from activated T cells may modulate TCR signaling by providing or sequestering signaling molecules to the engaged TCR. This aspect will require further study and may help in searching for new molecular mechanisms of positive or negative regulation in T cells.

Acknowledgments

Dr. Sancho's work was supported by Ministerio de Educación y Ciencia (former Ministerio de Ciencia y Tecnología) grant SAF2002-00721. Dr. Zubiaur's work was supported by Instituto Carlos III-FIS, Ministerio de Sanidad y Consumo, grant FIS03/0389, by a "Ramón y Cajal" contract from the Ministerio de Educación y Ciencia, and by a Grant 209/02 from the Consejería de Salud de la Junta de Andalucía. Esther J. Pavón was supported by a fellowship from grant SAF2002-00721. Pilar Muñoz was supported by a fellowship FPI (Formación de Personal Invesigador) from the Ministerio de Educación y Ciencia, Spain. María del Carmen Navarro was supported by a contract I3P from the Consejo Superior de Investigaciones Científicas.

References

Alcocer-Varela, J., Alarcon-Riquelme, M., Laffon, A., Sanchez-Madrid, F., Alarcon-Segovia, D., 1991. Activation markers on peripheral blood T cells from patients with active or inactive systemic lupus erythematosus. Correlation with proliferative responses and production of IL-2. J. Autoimmun. 4, 935–945.

al-Janadi, M., Raziuddin, S., 1993. B cell hyperactivity is a function of T cell derived cytokines in systemic lupus erythematosus. J. Rheumatol. 20, 1885–1891.

Belles-Isles, M., Houde, I., Lachance, J.G., Noel, R., Kingma, I., Roy, R., 1998. Monitoring of cytomegalovirus infections by the $CD8^{+}CD38^{+}$ T-cell subset in kidney transplant recipients. Transplantation 65, 279–282.

Blanco, P., Palucka, A.K., Gill, M., Pascual, V., Banchereau, J., 2001. Induction of dendritic cell differentiation by IFN-alpha in systemic lupus erythematosus. Science 294, 1540–1543.

Bombardier, C., Gladman, D.D., Urowitz, M.B., Caron, D., Chang, C.H., 1992. Derivation of the SLEDAI. A disease activity index for lupus patients. The Committee on Prognosis Studies in SLE. Arthritis Rheum. 35, 630–640.

Brown, D.A., London, E., 2000. Structure and function of sphingolipid- and cholesterol-rich membrane rafts. J. Biol. Chem. 275, 17221–17224.

Brown, D.A., Rose, J.K., 1992. Sorting of GPI-anchored proteins to glycolipid-enriched membrane subdomains during transport to the apical cell surface. Cell 68, 533–544.

Carbone, J., Gil, J., Benito, J.M., Navarro, J., Munoz-Fernandez, A., Bartolome, J., Zabay, J.M., Lopez, F., Fernandez-Cruz, E., 2000. Increased levels of activated subsets of CD4 T cells add to the prognostic value of low CD4 T cell counts in a cohort of HIV-infected drug users. AIDS 14, 2823–2829.

Deaglio, S., Mehta, K., Malavasi, F., 2001. Human CD38: a (r)evolutionary story of enzymes and receptors. Leuk. Res. 25, 1–12.

Drevot, P., Langlet, C., Guo, X.J., Bernard, A.M., Colard, O., Chauvin, J.P., Lasserre, R., He, H.T., 2002. TCR signal initiation machinery is pre-assembled and activated in a subset of membrane rafts. Embo. J. 21, 1899–1908.

Erkeller-Yuksel, F.M., Lydyard, P.M., Isenberg, D.A., 1997. Lack of NK cells in lupus patients with renal involvement. Lupus 6, 708–712.

Gonzalez-Escribano, M.F., Aguilar, F., Torres, B., Sanchez-Roman, J., Nunez-Roldan, A., 2004. CD38 polymorphisms in Spanish patients with systemic lupus erythematosus. Hum. Immunol. 65, 660–664.

Grammer, A.C., Lipsky, P.E., 2003. B cell abnormalities in systemic lupus erythematosus. Arthritis Res. Ther. 5 (Suppl. 4), S22–S27.

Gray-McGuire, C., Moser, K.L., Gaffney, P.M., Kelly, J., Yu, H., Olson, J.M., Jedrey, C.M., Jacobs, K.B., Kimberly, R.P., Neas, B.R., Rich, S.S., Behrens, T.W., Harley, J.B., 2000. Genome scan of human systemic lupus erythematosus by regression modeling: evidence of linkage and epistasis at 4p16-15.2. Am. J. Hum. Genet. 67, 1460–1469.

Gringhuis, S.I., Leow, A., Papendrecht-Van Der Voort, E.A., Remans, P.H., Breedveld, F.C., Verweij, C.L., 2000. Displacement of linker for activation of T cells from the plasma membrane due to redox balance alterations results in hyporesponsiveness of synovial fluid T lymphocytes in rheumatoid arthritis. J. Immunol. 164, 2170–2179.

Hare, K.J., Pongracz, J., Jenkinson, E.J., Anderson, G., 2003. Modeling TCR signaling complex formation in positive selection. J. Immunol. 171, 2825–2831.

Janes, P.W., Ley, S.C., Magee, A.I., 1999. Aggregation of lipid rafts accompanies signaling via the T cell antigen receptor. J. Cell Biol. 147, 447–461.

Janeway, C.A., Travers, P., Walport, M., Shlomechik, M., 2001. Immunobiology. Garland Publishing, New York.

Jury, E.C., Kabouridis, P.S., Abba, A., Mageed, R.A., Isenberg, D.A., 2003. Increased ubiquitination and reduced expression of LCK in T lymphocytes from patients with systemic lupus erythematosus. Arthritis Rheum. 48, 1343–1354.

Jury, E.C., Kabouridis, P.S., Flores-Borja, F., Mageed, R.A., Isenberg, D.A., 2004. Altered lipid raft-associated signaling and ganglioside expression in T lymphocytes from patients with systemic lupus erythematosus. J. Clin. Invest. 113, 1176–1187.

Kammer, G.M., Perl, A., Richardson, B.C., Tsokos, G.C., 2002. Abnormal T cell signal transduction in systemic lupus erythematosus. Arthritis Rheum. 46, 1139–1154.

Kay, J.E., 1991. Mechanisms of T lymphocyte activation. Immunol. Lett. 29, 51–54.

Kong, P.L., Odegard, J.M., Bouzahzah, F., Choi, J.Y., Eardley, L.D., Zielinski, C.E., Craft, J.E., 2003. Intrinsic T cell defects in systemic autoimmunity. Ann. NY Acad. Sci. 987, 60–67.

Krishnan, S., Nambiar, M.P., Warke, V.G., Fisher, C.U., Mitchell, J., Delaney, N., Tsokos, G.C., 2004. Alterations in lipid raft composition and dynamics contribute to abnormal T cell responses in systemic lupus erythematosus. J. Immunol. 172, 7821–7831.

Lin, P., Medeiros, L.J., Wilder, R.B., Abruzzo, L.V., Manning, J.T., Jones, D., 2004. The activation profile of tumour-associated reactive T-cells differs in the nodular and diffuse patterns of lymphocyte predominant Hodgkin's disease. Histopathology 44, 561–569.

Lindqvist, A.K., Alarcon-Riquelme, M.E., 1999. The genetics of systemic lupus erythematosus. Scand. J. Immunol. 50, 562–571.

London, E., Brown, D.A., 2000. Insolubility of lipids in triton X-100: physical origin and relationship to sphingolipid/cholesterol membrane domains (rafts). Biochim. Biophys. Acta 1508, 182–195.

Lynne, J.E., Schmid, I., Matud, J.L., Hirji, K., Buessow, S., Shlian, D.M., Giorgi, J.V., 1998. Major expansions of select $CD8^+$ subsets in acute Epstein-Barr virus infection: comparison with chronic human immunodeficiency virus disease. J. Infect. Dis. 177, 1083–1087.

Manes, S., del Real, G., Martinez, A.C., 2003. Pathogens: raft hijackers. Nat. Rev. Immunol. 3, 557–568.

Mitchell, J.S., Kanca, O., McIntyre, B.W., 2002. Lipid microdomain clustering induces a redistribution of antigen recognition and adhesion molecules on human T lymphocytes. J. Immunol. 168, 2737–2744.

Mocroft, A., Bofill, M., Lipman, M., Medina, E., Borthwick, N., Timms, A., Batista, L., Winter, M., Sabin, C.A., Johnson, M., Lee, C.A., Phillips, A., Janossy, G., 1997. $CD8^+$, $CD38^+$ lymphocyte percent: a useful immunological marker for monitoring HIV-1-infected patients. J. Acq. Immun. Def. Synd. Hum. Retrovirol. 14, 158–162.

Morra, M., Zubiaur, M., Terhorst, C., Sancho, J., Malavasi, F., 1998. CD38 is functionally dependent on the TCR/CD3 complex in human T cells. Faseb. J. 12, 581–592.

Munoz, P., Navarro, M.D., Pavon, E.J., Salmeron, J., Malavasi, F., Sancho, J., Zubiaur, M., 2003. CD38 signaling in T cells is initiated within a subset of membrane rafts containing Lck and the CD3-zeta subunit of the T cell antigen receptor. J. Biol. Chem. 278, 50791–50802.

Ortolan, E., Vacca, P., Capobianco, A., Armando, E., Crivellin, F., Horenstein, A., Malavasi, F., 2002. CD157, the Janus of CD38 but with a unique personality. Cell Biochem. Funct. 20, 309–322.

Ramzaoui, S., Jouen-Beades, F., Michot, F., Borsa-Lebas, F., Humbert, G., Tron, F., 1995. Comparison of activation marker and TCR V beta gene product expression by $CD4^+$ and $CD8^+$ T cells in peripheral blood and lymph nodes from HIV-infected patients. Clin. Exp. Immunol. 99, 182–188.

Rozzo, S.J., Allard, J.D., Choubey, D., Vyse, T.J., Izui, S., Peltz, G., Kotzin, B.L., 2001. Evidence for an interferon-inducible gene, Ifi202, in the susceptibility to systemic lupus. Immunity 15, 435–443.

Salojin, K.V., Zhang, J., Madrenas, J., Delovitch, T.L., 1998. T-cell anergy and altered T-cell receptor signaling: effects on autoimmune disease. Immunol. Today 19, 468–473.

Schade, A.E., Levine, A.D., 2002. Lipid raft heterogeneity in human peripheral blood T lymphoblasts: a mechanism for regulating the initiation of TCR signal transduction. J. Immunol. 168, 2233–2239.

Schuck, S., Honsho, M., Ekroos, K., Shevchenko, A., Simons, K., 2003. Resistance of cell membranes to different detergents. Proc. Natl. Acad. Sci. U.S.A. 100, 5795–5800.

Simons, K., Ehehalt, R., 2002. Cholesterol, lipid rafts, and disease. J. Clin. Invest. 110, 597–603.

Simons, K., Ikonen, E., 1997. Functional rafts in cell membranes. Nature 387, 569–572.

Simons, K., Toomre, D., 2000. Lipid Rafts and Signal Transduction. Nat. Rev. Mol. Cell Biol. 1, 31–39.

Slaughter, N., Laux, I., Tu, X., Whitelegge, J., Zhu, X., Effros, R., Bickel, P., Nel, A., 2003. The flotillins are integral membrane proteins in lipid rafts that contain TCR-associated signaling components: implications for T-cell activation. Clin. Immunol. 108, 138–151.

Tan, E.M., Cohen, A.S., Fries, J.F., Masi, A.T., McShane, D.J., Rothfield, N.F., Schaller, J.G., Talal, N., Winchester, R.J., 1982. The 1982 revised criteria for the classification of systemic lupus erythematosus. Arthritis Rheum. 25, 1271–1277.

Thomas, S., Kumar, R., Preda-Pais, A., Casares, S., Brumeanu, T.D., 2003a. A model for antigen-specific T-cell anergy: displacement of CD4-p56(lck) signalosome from the lipid rafts by a soluble, dimeric peptide-MHC class II chimera. J. Immunol. 170, 5981–5992.

Thomas, S., Kumar, R.S., Casares, S., Brumeanu, T.D., 2003b. Sensitive detection of GM1 lipid rafts and TCR partitioning in the T cell membrane. J. Immunol. Meth. 275, 161–168.

Tuosto, L., Parolini, I., Schroder, S., Sargiacomo, M., Lanzavecchia, A., Viola, A., 2001. Organization of plasma membrane functional rafts upon T cell activation. Eur. J. Immunol. 31, 345–349.

Wakeland, E.K., Liu, K., Graham, R.R., Behrens, T.W., 2001. Delineating the genetic basis of systemic lupus erythematosus. Immunity 15, 397–408.

Zhang, W., Trible, R.P., Samelson, L.E., 1998. LAT palmitoylation: its essential role in membrane microdomain targeting and tyrosine phosphorylation during T cell activation. Immunity 9, 239–246.

Zubiaur, M., Fernandez, O., Ferrero, E., Salmeron, J., Malissen, B., Malavasi, F., Sancho, J., 2002. CD38 is associated with lipid rafts and upon receptor stimulation leads to Akt/protein kinase B and Erk activation in the absence of the CD3-zeta immune receptor tyrosine-based activation motifs. J. Biol. Chem. 277, 13–22.

Zubiaur, M., Guirado, M., Terhorst, C., Malavasi, F., Sancho, J., 1999. The CD3-gamma delta epsilon transducing module mediates CD38-induced protein-tyrosine kinase and mitogen-activated protein kinase activation in Jurkat T cells. J. Biol. Chem. 274, 20633–20642.

Zubiaur, M., Izquierdo, M., Terhorst, C., Malavasi, F., Sancho, J., 1997. CD38 ligation results in activation of the Raf-1/mitogen-activated protein kinase and the CD3-ζ/ζ-associated protein-70 signaling pathways in Jurkat T lymphocytes. J. Immunol. 159, 193–205.

DOI 10.1002/pmic.200500404 *Proteomics* 2006, *6,* S282–S292

RESEARCH ARTICLE

Proteomic analysis of plasma from patients with systemic lupus erythematosus: Increased presence of haptoglobin α2 polypeptide chains over the α1 isoforms

Esther J. Pavón[1], Pilar Muñoz[1], Antonio Lario[2], Victoria Longobardo[2], Montserrat Carrascal[3], Joaquín Abián[3], Ana B. Martin[1], Salvador A. Arias[1], José-Luis Callejas-Rubio[4], Ricardo Sola[5], Francisco Navarro-Pelayo[4], Enrique Raya-Alvarez[6], Norberto Ortego-Centeno[4], Mercedes Zubiaur[1] and Jaime Sancho[1]

[1] Departamento de Biología Celular e Inmunología, Instituto de Parasitología y Biomedicina "López-Neyra", CSIC, Armilla, Spain
[2] Servicio de Proteómica y Genómica, Instituto de Parasitología y Biomedicina "López-Neyra", CSIC, Armilla, Spain
[3] Unidad de Espectrometría de Masas Estructural y Biológica, Instituto de Investigaciones Biomédicas de Barcelona (IIBB), CSIC-IDIBAPS, Barcelona, Spain
[4] Unidad de Enfermedades Autoinmunes Sistémicas, Hospital Clínico San Cecilio, Granada, Spain
[5] Servicio de Hematología, Hospital Clínico San Cecilio, Granada, Spain
[6] Servicio de Reumatología, Hospital Clínico San Cecilio, Granada, Spain

In the present study plasma samples from 15 systemic lupus erythematosus (SLE) patients and 16 healthy controls of initially unknown haptoglobin (Hp) phenotype were separated by 2-DE, and tryptic digests of the excised Hpα polypeptide chain spots were analyzed by MALDI-TOF-MS. Selected tryptic peptides were sequenced by nano-(n)ESI-IT MS/MS. The six major Hp phenotypes were present, although with distinct frequencies in controls and SLE patients. Thus, there were an increased proportion of SLE patients with Hp 2–2, or Hp 2–1S phenotypes. The Hp phenotype distribution resulted in allele frequencies of 0 625 *(Hp^2)*, 0.281 *(Hp^{1S})*, and 0.093 *(Hp^{1F})* in healthy controls, correlating fairly well with the allele frequencies of European populations. In contrast, the Hp allele frequencies of the SLE patients were 0.733 *(Hp^2)*, 0.233 *(Hp^{1S})*, and 0.033 *($Hp1^{1F}$)*, which clearly indicated an increased frequency of Hp^2, a similar proportion of Hp^{1S} and a diminished proportion of Hp^{1F} in SLE patients compared with that in healthy controls. Preferential Hpα2 expression in SLE patients may contribute to some of the clinical manifestations of the disease such as hypergammaglobulinemia, systemic vasculitis, and cardiovascular disorders.

Received: June 1, 2005
Revised: November 11, 2005
Accepted: November 14, 2005

Keywords:
Autoimmune disease / Differential protein expression / Haptoglobin / MALDI-TOF MS / Serum biomarkers

Correspondence: Dr. Jaime Sancho, Instituto de Parasitología y Biomedicina, CSIC, Parque Tecnológico de Ciencias de la Salud, Avenida del Conocimiento s/n, 18100 Armilla, Granada, Spain
E-mail: granada@ipb.csic.es
Fax: +34-958-181-632

Abbreviations: aa, amino acid; **Hp**, haptoglobin; **SLE**, systemic lupus erythematosus; **SLEDAI**, SLE disease activity index

1 Introduction

Haptoglobin (Hp) consists of two different polypeptide chains, the α and β chain. The β chain (40 kDa) is heavier than the α chain and is identical in all Hp types. The *Hp*α gene, located on chromosome 16q22, consists of three structural alleles: Hp^{1F}, Hp^{1S}, and Hp^2 [1]. The gene products of the $Hp^{1F}$and Hp^{1S} alleles, the α1F and α1S chains, are of the

equal length but differ in the number of charged residues. The α1F chain carries aspartic acid and lysine residues at positions 52 and 53, whereas at these positions asparagine and glutamic acid residues are located in the α1S chain. All other amino acids (aa) are identical in both Hpα1 proteins. The Hp^2 allele originates from fusion of the $Hp^{1F}$and Hp^{1S} alleles, presumably by a non-homologous crossing-over between the structural alleles during meiosis [2]. Therefore, this allele codes for a polypeptide chain, Hpα2, that is almost twice as much longer as the α1 chains. The three alleles are responsible for six Hp phenotypes: 1F-1F, 1S-1S, 1F-1S, 2–1F, 2–1S, and 2–2 [2, 3]. However, due to the sequence similarity of the α1S and α1F chains, often only the three major phenotypes Hp 1–1, Hp 2–2, and Hp 2–1 are described in the literature [1, 4]. The Hp 1–1 phenotype express only α1 variants (~9 kDa), while the α2 chains (16 kDa) are present in both Hp 2–2 and Hp 2–1 phenotypes. The Hpα chains form varying spot patterns in 2-DE gels, which can only be fully identified by MS, and MS/MS analysis [2, 3].

Hp, one of the acute phase proteins induced in response to infection, tissue injury, and malignancy, was originally described as functioning by the absorption of free hemoglobin and thus preventing kidney damage [1]. However, it has subsequently become apparent that the physiological role of Hp is not restricted to the trapping of free hemoglobin. Bacteriostatic and angiogenic effects and antibody-like and antioxidative properties have also been suggested [1, 4]. Hp inhibits lectin-induced lymphocyte transformation [1] and may selectively bind to CD22, a B cell-specific lectin that mediates the interactions of mature B cells with erythrocytes, lymphocytes, monocytes, neutrophils, and endothelial cells [5]. Hp binds to human peripheral blood neutrophils via a specific membrane receptor [6]. Adding Hp to culture medium together with stimulatory agents such as formyl-methionyl-leucyl-phenylalanine (fMLP), arachidonic acid, and opsonized zymosan, specifically inhibits the neutrophil respiratory burst activity [6]. These cell interactions are likely to be affected by changing levels of Hp.

The Hp1–1 phenotype is associated with a higher binding and antioxidant capacity compared with the Hp 2–2, or Hp 2–1 phenotypes. In contrast, the Hp 2–2 phenotype is associated with a higher immune reactivity and ability to form antibodies. Moreover, the possession of a particular phenotype has been associated with the prevalence and clinical evolution of many inflammatory diseases including infections as tuberculosis, vaccination, viral hepatitis, atherosclerosis, cardiovascular and autoimmune diseases [1, 3–5, 7]. However, the association of the two allelic α1S and α1F variants or α2 and α1 PTM that lead to structurally distinct protein species with different clinical conditions has not been studied.

Systemic lupus erythematosus (SLE) is a systemic autoimmune disease characterized by a waxing and waning course and the involvement of multiple organs, including skin, kidneys, and CNS [8]. SLE patients display multiple abnormalities in T cell antigen-mediated signaling that lead to B cell hyper-responsiveness, increased apoptosis, skewed cytokine production, and breakdown of immunological tolerance (reviewed in [9], and [10]). Although SLE ethiopathology is poorly understood, there is likely a role for environmental triggers, for instance viruses, acting in the context of susceptibility genes [11, 12]. A significant increase of the haptoglobin type 2–2 and a concomitant decrease in the percentage of the 2–1 phenotype has been found in SLE patients [13]. Since the method used to determine the Hp phenotypes did not allow distinguishing between the two α1 isoforms, and even less, to detect PTM [13], the contribution of either α1F, or α1S and derivatives to these abnormalities is lacking. In this study, SLE patients show increased presence of the Hp 2–2 and Hp 2–1S phenotypes, and decreased Hp 2–1F phenotype. This results in both, increased frequency of the Hp^2 allele and diminished frequency of the Hp^{1F} allele.

2 Materials and methods

2.1 Patients and healthy controls

Fifteen outpatients fulfilling the revised American College of Rheumatology (ACR) criteria for the diagnosis of SLE [14], and routinely followed in the Systemic Autoimmune Diseases Unit (Hospital Clínico San Cecilio, Granada, Spain) participated in this study. Sixteen healthy, age-matched volunteers served as controls. Disease activity was scored and the SLE Disease Activity Index (SLEDAI) was calculated [15]. All subjects participating in the study were Caucasians. Complete blood cell count, serum complement and serum anti-nuclear and anti-DNA antibodies were measured in all patients. The study protocol was approved by the Hospital Clínico San Cecilio, and CSIC Review Board and Ethics Committees. Written informed consent was obtained from all participating patients and volunteers according to the Declaration of Helsinki.

2.2 Plasma sample collection

Blood was collected by the BD Vacutainer system into K_2-EDTA tubes (BD Diagnostics, NJ) and plasma was separated from cells by density gradient centrifugation over HISTOPAQUE®-1077 (Sigma-Aldrich Química, Spain). The supernatant was collected, checked for the absence of cells by light microscopy, and fractionated in aliquots that were stored at −80°C.

2.3 Albumin and IgG depletion

Plasma samples were albumin and IgG depleted by using the Aurum™ Serum Protein kit (Bio-Rad, Hercules, CA) following the manufacturer's instructions. Briefly, 60 μL of plasma was mixed with 180 μL of binding-buffer and the solution was deposited onto the column, mixed with the sorbent and allowed to stand for 5 min. This mixing step was

repeated twice and the protein extract was eluted by centrifugation at 10 000 × *g* (20 s). The column was washed with 200 μL of binding buffer followed by a second centrifugation at the same speed. The two eluates were mixed and stored for analysis. Protein concentration was determined in each sample by using the Protein Assay kit (Bio-Rad).

2.4 2-DE

2-DE was carried out using the Protean IEF cell and Criterion electrophoresis cell systems (Bio-Rad). Plasma samples depleted of albumin and IgG were diluted in 185 μL of rehydratation/sample buffer containing 8 M urea, 2% w/v CHAPS, 50 mM DTT, 0.2% Biolyte® 3/10 ampholytes, and Bromophenol Blue (trace) (Bio-Rad). First-dimension IPG strips (Bio-Rad: 11 cm, linear pH 4–7 gradient) were loaded with the solubilized samples through passive in-gel rehydration 12–18 h at 20°C. The 11-cm IPG strips were focused in a one-step procedure, at 8000 V for 30 000 Vh at 20°C with a current limit of 50 μA. Prior to the second-dimension separation, the focused strips were equilibrated for 10 min in Equilibration Buffer I (6 M urea, 2% SDS. 0.375 M Tris-HCl pH 8.8, 20% glycerol, and 2% w/v DTT) followed by another 10 min in Equilibration Buffer II (Equilibration Buffer I with 2.5% w/v iodoacetamide instead of DTT). The equilibrated IPG strips were positioned on Criterion XT Precast Gels (4–12% gradient in XT MES buffer) and the separation was performed at 150 V at room temperature. The gels were fixed for 30 min in 10% methanol, 7% acetic acid and stained overnight with SYPRO Ruby fluorescent stain (Bio-Rad) according to the manufacturer's instructions. The stained gels were scanned with a Typhoon 9400 system (Amersham Biosciences). Then gels were washed with double-distilled H_2O and stained for 60 min with Bio-Safe stain (Bio-Rad) and scanned using a GS-800 Calibrated densitometer (Bio-Rad). Digitalized gel images were analyzed with the PDQuest software version 7.2 (Bio-Rad)

2.5 In-gel digestion of proteins

Gel pieces containing the proteins of interest were manually excised and subjected to in-gel digestion using a 96-well ZipPlate kit for sample preparation (Millipore Ibérica SA Madrid, Spain). Proteins were reduced, alkylated, and digested with sequence grade trypsin (Promega, Madison, WI) according to the manufacturer's protocol. Peptides were eluted by the centrifugation using 5–10 μL of 60% v/v ACN/0.1% v/v TFA.

2.6 Protein identification by MS

2.6.1 Protein identification methods

Proteins were identified either by PMF by MALDI-TOF MS or by peptide sequencing using nano(n)ESI-IT MS/MS.

2.6.2 MALDI-TOF MS

MALDI-TOF MS analysis of the tryptic digest was performed using a Voyager DE-PRO (Applied Biosystems, Barcelona, Spain) instrument in the reflectron mode. Spectra were externally mass calibrated using a standard peptide mixture. For the analysis, 0.5 μL of the peptide extract and 0.5 μL of matrix (CHCA, 3 mg/mL) were loaded in the MALDI plate and were let to dry.

2.6.3 nESI-IT MS/MS

Selected peptides from the tryptic digest were sequenced on a Finnigan LCQ IT mass spectrometer (ThermoQuest, Finnigan MAT, San Jose, CA) equipped with a nanospray source (Protana, Odense, Denmark). The spray voltage applied was 0.85 kV and the capillary temperature was 110°C. For MS/MS experiments, the isolation window was three mass units wide and the relative collision energy was 30%. Samples were desalted prior to the analysis with C18 ZipTip pipette tips (Millipore, MA) following standard procedures.

2.6.4 Database search

MASCOT (Matrix Science, London, UK) and the Protein Prospector v 3.4.1 (UCSF Mass Spectrometry Facility, University of California) were used for protein identification from the PMF or peptide fragment-ion data obtained from MALDI-TOF-MS and MS/MS analysis, respectively. The Swiss-Prot (European Bioinformatics Institute, Heidelberg, Germany, Update 02/20/02), MSDB, and NCBInr databases were used for the search.

2.7 Statistical analysis

Statistical analysis of Hp plasma levels was performed using the non-parametric two-tailed Mann-Whitney test (GraphPad Software, Version 4.02, San Diego, CA). Statistical significance was set at $p < 0.05$. To evaluate whether the gene frequencies fulfilled the Hardy-Weinberg equilibrium, a chi-square test was used to compare the observed number of subjects with the expected number.

3 Results

3.1 2-DE analysis of control and SLE plasma samples

The protein profile of plasma samples from 16 controls and 15 SLE patients of unknown Hp phenotype were examined by 2-DE. Very few proteins from plasma were observed in 2-D gels to migrate below pH 4. Above pH 7, gels were dominated by light and heavy chain immunoglobulin proteins (data not shown). Moreover, removal of albumin and IgG from plasmas allowed a higher sample load and

improved the visualization of less abundant proteins (data not shown). Therefore, for proteome analyses of the albumin- and Ig-removed plasmas, proteins were separated in IPG strips ranging from pH 4 to 7. At first glance, the protein patterns visualized by Bio-Safe Coomassie-stained gels from healthy controls and SLE patients resemble each other closely (Fig. 1). However, upon closer examination, significant differences between the protein compositions in healthy controls and SLE patients became evident. The differences found in the low-molecular mass region boxed in Fig. 1 will be described in detail below. Since several spots were difficult to visualize by Coomassie staining, the differential protein analyses that follow were performed from SYPRO Ruby-stained gels.

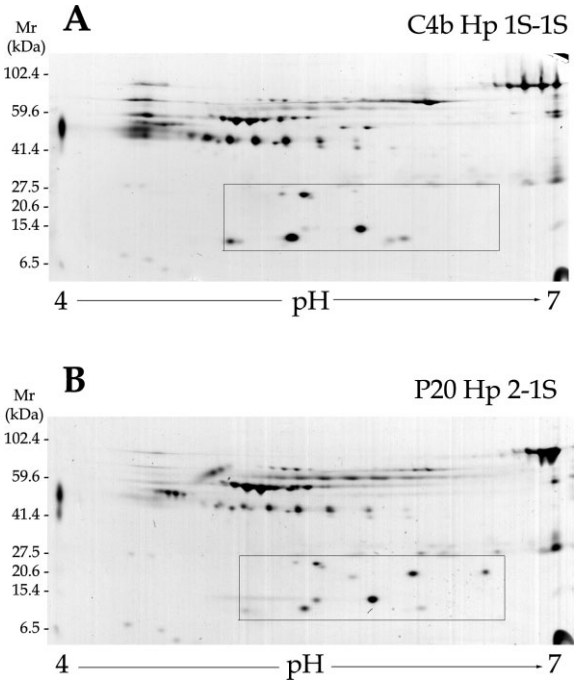

Figure 1. Plasma from a healthy control (A) and from an SLE patient (B) upon depletion of albumin and Ig. The region where prominent differences in protein expression patterns occur is boxed (see Fig. 2). Total protein amount was 35 μg. pH range 4–7, 11-cm IPG strips in the first dimension, 4–12% Criterion PreCast XT Gels in XT MES buffer in the second dimension. Bio-Safe Coomassie staining.

3.2 Interindividual differences in the haptoglobin α species

Differences in several spots in the low-mass region were observed and identified as Hpα derivatives after visual inspection of the spot pattern of SYPRO Ruby-stained gels (Fig. 2). The Hpα spots locations and patterns were comparable to those in the Swiss-2-D database plasma map (www.expasy.org/ch2d/), however, given the similarity of the sequences of the different Hp isoforms, assignation of each

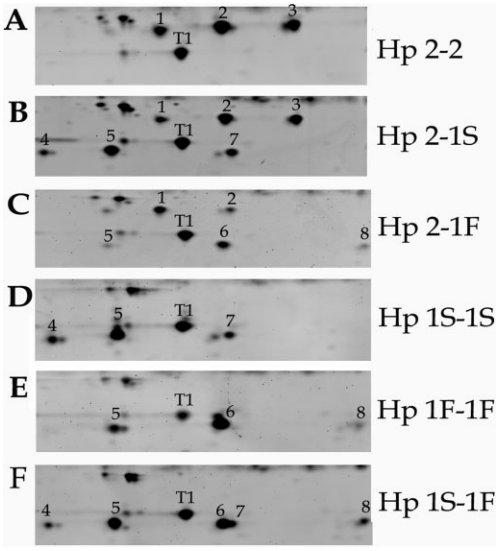

Figure 2. Comparison of 2-DE protein patterns in the low mass region of albumin- and Ig-depleted plasmas showing haptoglobin α chains. (A) Hp 2–2, (B) Hp 2–1S, (C) Hp 2–1F, (D) Hp 1S-1S, (E) Hp 1F-1F, and (F) Hp 1S-1F phenotypes. Numbers 1, 2 and 3 indicate spots of haptoglobin α2 chains; numbers 4, 5, and 7 are spots of haptoglobin α1S chains; numbers 5, 6, and 8 contains haptoglobin α1F, and spot T1 contained transthyretin protein species. Same running conditions as in Fig. 1 except that about 100 μg of total protein was loaded per gel. SYPRO Ruby staining.

isoform could only be done on the basis of specific tryptic peptide signals observed in the MALDI spectra [2, 3] (see below).

Samples belonging to the phenotype Hp 2–2 showed α2 spots only (Fig. 2 and Table 1), with three prominent spots separated in the first dimension, each with a distinct p*I*, (spots 1–3; molecular masses of about 16 kDa). The central spot usually was the most prominent. In the 2-D gels representing the phenotypes Hp 1S-1S, Hp 1F-1F, and Hp 1S-1F

Table 1. Human plasma haptoglobin α chain derivatives characterized in this study

Spot location[a)]	Description	Number of aa	p*I*[b)]	M_r[b)]
1	Hpα2,N5D	142	5.37	15 946.7
2	Hpα2	142	5.57	15 945.7
3	Hpα2,R143	143	5.82	16 101.9
4	Hpα1S,N5D	83	4.99	9 193.1
5	Hpα1S	83	5.23	9 192.1
7	Hpα1S,R84	84	5.6	9 348.4
5	Hpα1F,N5D	83	5.22	9 193.2
6	Hpα1F	83	5.58	9 192.1
8	Hpα1F,R84	84	6.1	9 348.4

a) See Fig. 2.

b) Theoretical values were calculated using the Compute p*I*/M_r tool (www.expasy.org/tools/pi_tool.html).

samples, the spots 1–3 are missing, indicating that Hp α2 isoform and derivatives are not present. In contrast in the Hp 2–1S and Hp 2–1F phenotypes, the α2 chains (spots 1–3), as well as the α1 chains (spots 4, 5 and 7 in Hp 2–1S, or spots 5, 6, and 8 in Hp 2–1F; molecular masses about 9 kDa) were visible as the main spots. Note that in the Hp 2–1S and Hp 1S-1S phenotypes an identical pattern of α1 spots was shown (spots 4, 5 and 7 were present, whereas spots 6 and 8 were missing), spot 5 being the most prominent. This pattern is consistent with the identification of these spots as the α1S isoform and derivatives.

In Hp 2–1F and Hp 1F-1F samples spots 4 and 7 were missing, while spots 5, 6 and 8 were usually present, the spot 6 being the most prominent, which is consistent with the presence of α1F derivatives only. In contrast, in the Hp 1S-1F sample all α1 spots were present (spots 4, 5, 6, 7 and 8), which is consistent with the presence of both α1S and α1F chains and derivatives. In this sample spots 6 and 7 appeared very close with a more intensely stained left spot (α1F isoform). Thus, three up to five different forms of α1 chains are separated in 2-D gels of the Hp 2–1S, Hp 2–1F, Hp 1S-1S, Hp 1F-1F, or Hp 1S-1F phenotypes.

In this study, the six major Hp phenotypes were present although with distinct frequencies in controls as compared with those in SLE patients (Table 2). Nevertheless the selection of samples in healthy controls, with allele frequencies of 0 625 *(Hp^2)*, 0.281 *(Hp^{1S})* and 0.093 *(Hp^{1F})* correlated fairly well with the allele frequencies of European populations [16–18]. In contrast, the Hp allele frequencies of the SLE patients were 0.733 *(Hp^2)*, 0.233 *(Hp^{1S})*, and 0.033 *(Hp^{1F})*, indicating clearly an increased frequency of Hp^2, a similar proportion of Hp^{1S} and a diminished frequency of Hp^{1F} in SLE patients compared with that in healthy controls. Note that in SLE patients the frequency of Hp^1 (Hp^{1S} + Hp^{1F}) was 0.266, while in controls it was 0.374 (Table 2).

Table 2. Haptoglobin phenotype distribution and *Hp* allele frequencies in healthy controls and SLE patients

Phenotype	Controls[a] $n = 16$[c]	SLE[a] $n = 15$[c]	Haplotype	Controls[b] $n = 16$[c]	SLE[b] $n = 15$[c]
Hp 1S-1F	0 (0)	1 (6.7)	*Hp2*	0.625	0.733
Hp 1S-1S	2 (12.5)	0 (0)	*Hp1S*	0.281	0.233
Hp 1F-1F	1 (6.25)	0 (0)	*Hp1F*	0.093	0.033
Hp 2–1F	1 (6.25)	0 (0.0)	*Hp1*	0.374[d]	0.266
Hp 2–1S	5 (31.25)	6 (40)			
Hp 2–2	7 (43.75)	8 (53.3)	Hp^2/Hp^1 ratio	1.67[e]	2.75[e]

a) The entries indicate the number of individuals with a particular phenotype. Data in parentheses represent percentage.
b) The calculation of gene frequencies is based on the gene counting method, assuming that haptoglobins are codominantly inherited and therefore, phenotype = genotype. The gene frequencies are in agreement with the Hardy-Weinberg equilibrium.
c) Number of controls or SLE patients analyzed by 2-DE.
d) The Hp^1 allele frequency (the sum of Hp^{1S} and Hp^{1F} allele frequencies) in European populations is ~0.40 [4], including the Spanish population [16].
e) In balanced polymorphism, the Hp^2/Hp^1 allele ratio should remain constant [1].

3.3 Protein identification by MS

3.3.1 General observations

To gain insight into the composition of these spots, the MALDI peptide maps of the corresponding tryptic digests were then analyzed in detail. PMF searching identified these spots as belonging to the Hp precursor family (Table 3). However, the sequence database entries of haptoglobins are for the least processed forms, comprising the signal peptide (aa 1–18) followed directly by the α subunit, and with the β subunit located in the C-terminal portion of a single polypeptide chain [19], whereas in the mature Hp α subunits, both the signal peptide and the β chain are not present. Therefore, in a regular PMF database search, the experimental peptide masses derived from Hpα2 and α1 subunits, of about 16 and 9 kDa, are confronted with the theoretical peptide masses of their corresponding precursors (42 and 39 kDa, respectively), which necessarily leads to relatively low sequence coverage when compared with other proteins of similar size as transthyretin, and, eventually, low P scores (Table 3).

In contrast, manual inspection of each Hp precursor hit indicated that the ion signals were for tryptic peptides corresponding exclusively to the portion of the Hp precursor sequence where the α2 or α1 subunits were located [2], leading to almost full-sequence coverage (Tables 4 and 5). Moreover, we noticed that the N-terminal and C-terminal tryptic peptides of most of the Hp proteins analyzed by MALDI-TOF had no matching peptides in the Hp precursors. Thus, the additional 18 aa of the signal peptide lead to a theoretical N-terminal tryptic peptide at m/z 5204.57, which cannot be cleaved by trypsin into smaller peptides due to the absence of arginine or lysine residues between the first aa of the signal peptide and the first aa of the mature protein. In contrast, the N-terminal tryptic peptide of the mature Hp α isoforms lacking the signal peptide, yields ion signals at m/z 3349.6 (Fig. 3B–D) that, indeed, will never match with those generated by the Hp precursors. Likewise, an ion signal at m/z 2578.3 (Fig. 3A, B and D) that corresponds to the C-terminal peptide of the α chains (aa 119–142 of the mature α2 isoform, or aa 60–83 of the mature α1 isoforms), has no matching peptide in any of the annotated Hp precursors. The corresponding peptide (aa 137–161 of the Hp-2 precursor, or aa 78–102 of the Hp-1 precursor) yields ion signals at m/z 2734.37. This is due to an additional arginine at the C terminus that is removed from the mature α chains by a circulating carboxipeptidase of unknown nature [20]. Only the α species that migrate to the more basic location conserve this arginine [2].

Table 3. Database search results with MALDI PMF data (see also Fig. 2 for spot location)

Spot[a)]	Mass (kDa)/p*I* theoretical	Protein	Score	Sequence coverage	Acc. number
1	45.86/6.13	Haptoglobin precursor	84	20	P00738[b)]
2	42.12/6.25	Hp-2 alpha	126	27	Q6LBY9[c)]
3	45.86/6.13	Haptoglobin precursor	120	23	P00738[b)]
4	38.94/6.13	Haptoglobin precursor	70	18	HPHU1[c)]
5	38.94/6.13	Haptoglobin precursor	66	12	P00738[b)]
6	45.86/6.13	Haptoglobin precursor	62	14	P00738[b)]
7	45.86/6.13	Haptoglobin precursor	101	19	P00738[b)]
8	38.94/6.13	Haptoglobin precursor	38	14	P00738[b)]
T1	12.99/5.33	Transthyretin	247	91	2ROXA[c)]

a) A total of 63 different spots from 12 controls and 7 SLE patients were analyzed (see Tables 4 and 5).
b) Swiss-Prot.
c) MSDB.

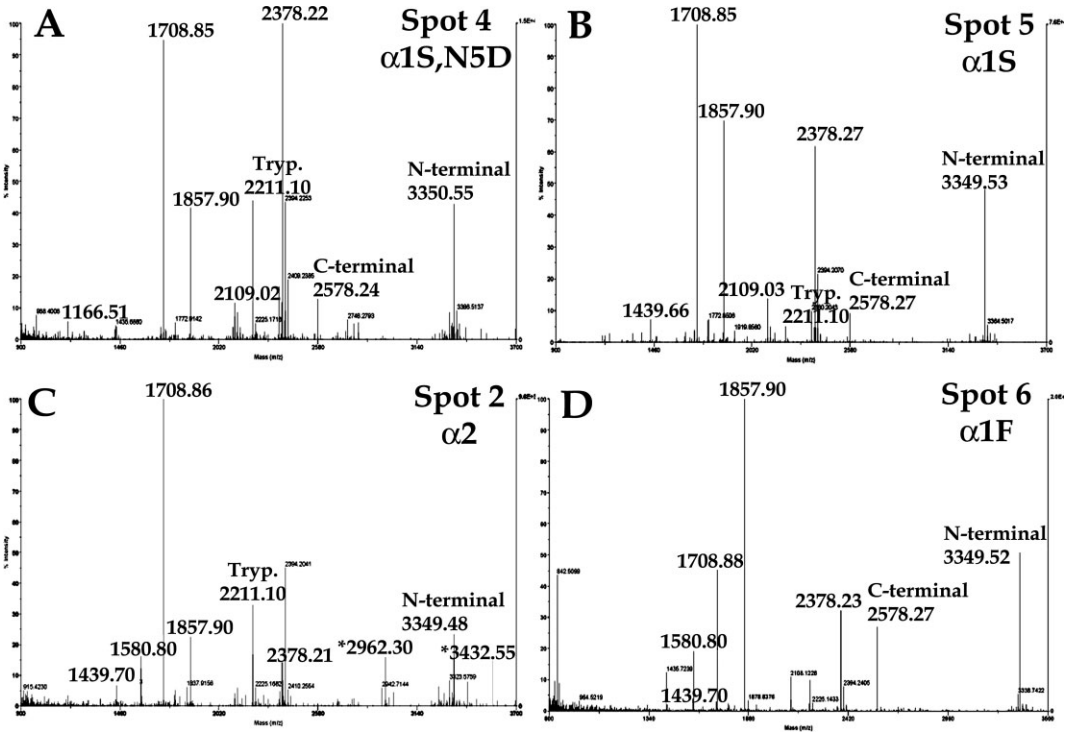

Figure 3. MALDI-TOF-MS peptide mapping analyses from tryptic digests of (A) spot 4, (B) spot 5, (C) spot 2, and (D) spot 6 shown in Fig. 2. Large numbers in the mass spectrum give precise *m/z* values for the detected peptide ion signals that are specific for Hpα chains. *m/z* values of the N-terminal ad C-terminal peptides are indicated. Trypsin autoproteolysis peptide at *m/z* 2211.10 is labeled as Tryp. In panel (C), ion signals resulting from peptides that are specific for Hpα2 protein are indicated with an asterisk.

3.3.2 Hpα2 spot family

We first analyzed the protein structures of the corresponding spots 1–3 from 10–13 samples from either controls or SLE patients (Table 4). Significant differences between the mass spectra from the haptoglobin α2 proteins in the three spots were found in the analyzed samples. As mentioned above, the first 31 aa of mature Hpα comprise a characteristic tryptic peptide at *m/z* 3349.5 that was detectable in all samples analyzed from spots 2 and 3 (Table 4 and Fig. 3C). However, the masses of the N-terminal peptides from spot 1 were found to be heavier by 1 Da (*m/z* 3350.6) due to deamidation of the asparagine residue at position 5 to aspartic acid [2]. The mass differences of 1 Da were clearly identified in most samples analyzed.

Table 4. Most pronounced tryptic peptides of haptoglobin α2 polypeptide chains identified by MALDI-TOF-MS

$[M+H]^{+a)}$	Haptoglobin α2 chain			
	Position[b)]	Relative abundance[c)]		
		Spot 1 (α2,N5D) (n = 11)[d)]	Spot 2 (α2) (n = 14)[d)]	Spot 3 (α2,R143) (n = 12)[d)]
3349.54	1–31	12.5	100.0	100.0
3350.52[e)]	1–31	75.0	0	0
1166.53	32–39	18.2	14.3	0
1580.79	40–53	63.6	78.6	75.0
1708.89	40–54	100.0	100.0	100.0
2378.25	40–59	90.9	92.9	83.3
1439.70	42–54	27.3	57.1	58.3
2109.06	42–59	54.5	71.4	66.7
3432.60[f)]	60–90	81.8	100.0	87.5
2962.35[f)]	65–90	81.8	92.8	75.0
1166.53	91–98	18.2	14.3	0
1708.85	99–113	100.0	100.0	100.0
2378.21	99–118	90.9	92.9	83.3
1439.70	101–113	27.3	57.1	58.3
2109.03	101–118	54.5	71.4	66.7
1857.92	119–135	90.9	92.8	91.7
2578.27	119–142	36.4	50.0	0
2734.38[g)]	119–143	0	0	50.0
895.47[g)]	136–143	0	0	50.0

a) Calculated values.
b) Sequence position.
c) The entries indicate the percentage of samples in which the respective peptide masses were detected in the corresponding mass spectra relative to the total number of spots analyzed.
d) Numbers in parenthesis indicate the number of different spots analyzed, each one corresponding to a different plasma sample from a different individual.
e) N-terminal peptide in which N5 is deaminated.
f) Peptides only present in α2 and derivatives.
g) C-terminal peptide with an additional arginine residue.

The masses of the C-terminal peptides from spots 2 and 3 were found at m/z 2578.28 (aa 119–142) whereas in the Hpα2 protein species that migrated to a more basic location (spot 3), a distinct ion signal at m/z 2734.38 was found in 6 out of 12 samples analyzed. According to Mikkat *et al.* [2], this corresponds to the mass of the C-terminal peptide (aa 119–143), which contains an additional arginine residue at the C terminus (Table 4). Furthermore, in 6 out of 12 samples analyzed an ion signal at m/z 895.47 was detected, which also indicated a C-terminal peptide with the arginine-containing C terminus (aa 136–-143). The presence of these peptides has been reported for the α2 protein most basically located spot [2], in agreement with our results.

Spots 1, 2 and 3 of most samples analyzed showed ion signals at m/z 2962.3, corresponding to a peptide that is specific for α2 species (aa 65–90), and therefore, it is not found in tryptic maps of α1 polypeptide chains [2]. Another peptide that is also α2 specific, and showed an ion signal at m/z 3432.6 (aa 60–90) was also detectable in tryptic maps from most samples analyzed (Table 4). Other ion signals at m/z 1708.85, 2378.21, 1439.7, and 2109.03 matched to two tryptic peptides, because the sequence of the α2 chain is composed of two nearly identical sequence stretches [20]. These ion signals and the one at m/z 1857.92 (aa 119–135) were found in most samples analyzed.

MS sequence data using the nESI-ITMS/MS technique (Fig. 4A) confirmed that peptide at m/z 1580.9 from spot 2 corresponded to aa 40–53 of haptoglobin α2, or α1F (Tables 4 and 5). Likewise, a peptide at m/z 1439.7 from spots 1, 2, and 3 was also analyzed by nESI-ITMS/MS and showed fragment

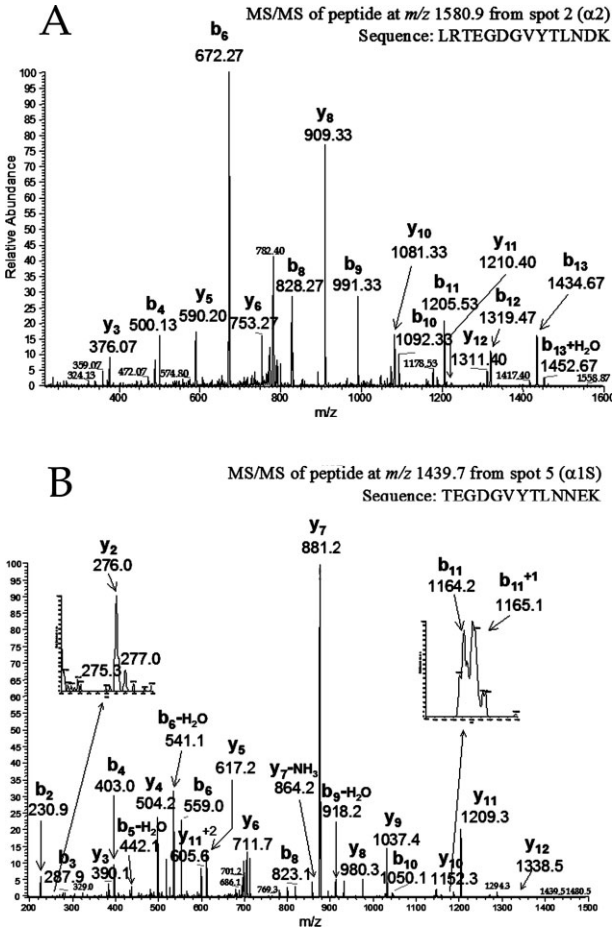

Figure 4. (A) nESI-ITMS/MS analysis of peptide with ion signal at m/z 1580.9 from spot 2. The MS fragment ions from the y-type and b-type ion series are indicated. The determined partial aa sequence is depicted on top and was assigned to a haptoglobin peptide comprising aa40–53 of haptoglobin α1, or α2. (B) nESI-ITMS/MS analysis of peptide with ion signal at m/z 1439.7 from spot 5. The MS fragment ions from the y-type and b-type ion series are indicated. Magnification showed the enlarged regions around the y_2 (m/z 276), and b11 (m/z 1164.2) ions. The determined partial aa sequence is depicted on top and was assigned to a haptoglobin peptide comprising aa 42–54 of haptoglobin α1S.

Table 5. Most pronounced tryptic peptides of haptoglobin α1 polypeptide chains identified by MALDI-TOF-MS

$[M+H]^{+a)}$	Haptoglobin α1 chains						
	Position[b)]	Relative abundance[c)]					
		Spot 4 (α1S,N5D) ($n = 5$)[d)]	Spot 5 (α1S) ($n = 8$)[d)]	Spot 5 (α1F,N5D) ($n = 2$)[d)]	Spot 6 (α1F) ($n = 5$)[d)]	Spot 7 (α1S,R84) ($n = 5$)[d)]	Spot 8 (α1F,R84) ($n = 1$)[d)]
3349.54	1–31	0	100	0	100	100	100
3350.52[e)]	1–31	100	0	100	0	0	0
1166.53	32–39	20	12.5	50	0	20	0
1580.79[f)]	40–53	0	0	50	100	0	100
1708.89	40–54	80	100	100	100	100	100
2378.25	40–59	100	100	100	100	100	100
1439.70	42–54	0	50	50	60	20	0
2109.06	42–59	60	87.5	100	80	60	0
1857.92	60–76	80	100	100	80	80	100
2578.27	60–83	60	62.5	100	40	0	0
2734.38[g)]	60–84	0	0	0	0	60	100
895.47[g)]	77–84	0	0	0	0	40	0

a) Calculated values.
b) Sequence position.
c) The entries indicate the percentage of samples in which the respective peptide masses were detected in the corresponding mass spectra relative to the total number of spots analyzed.
d) Numbers in parenthesis indicate the number of different spots analyzed, each one corresponding to a different plasma sample from a different individual.
e) N-terminal peptide in which N5 is deaminated.
f) Peptide that is not generated in the α1S chain.
g) C-terminal peptide with an additional arginine residue.

ions corresponding to aa 42–54 of either Hpα2, or α1F (data not shown). The apparent molecular weights of spots 1, 2, and 3 (Fig. 2) are closer to that of α2 and derivatives (Table 1), and, therefore, these spots could represent distinct PMF of the haptoglobin α2 chain.

3.3.3 Hpα1S protein spot family

In general, spectra from Hpα1 proteins resemble those from α2 species with the main exception that the ion signals at *m/z* 2962.3 and *m/z* 3432.6 are missing, because the corresponding tryptic peptides do not occur in α1 chains (Tables 4 and 5). Thus, Hpα1 and α2 species can easily be distinguished in the PMF spectra. Moreover, the aa sequences of Hpα1S and α1F differ in a double aa exchange at positions 52 and 53. Accordingly, the tryptic peptide aa 40–53 that generates an ion signal at *m/z* 1580.8 is contained in Hpα1F, but is missing in the α1S protein, where a glutamic acid residue at position 53 does not allow tryptic cleavage [1].

As neither the ion at *m/z* 1580.8 (Fig. 3 and Table 5), nor other signals related to tryptic cleavage at the C terminus of aa 53 were present in the PMF spectra from spot 5 in any of the samples analyzed, we concluded that spot 5 represents the unmodified Hpα1S chain (Table 5). To confirm this assumption, the nESI-ITMS/MS spectrum from the peptide at *m/z* 1439.7 from spot 5 was submitted to database search and yielded the identification of the corresponding peptide sequence comprising aa 42–54 from the Hpα1S (Fig. 4B). The ion signals in the y2 (*m/z* at 276.0) and b11 (*m/z* at 1164.2) ions showed the expected mass difference of 1 Da as compared with the y_2 (*m/z* at 275) and b_{11} (*m/z* at 1165.1) ions of the corresponding fragmentation of peptide 42–54 from Hpα1F (Fig. 5B). These differences in the masses of y_2 and b_{11} ion fragments allow the unambiguous identification of spot 5 as α1S and spot 6 as α1F.

Of note is that spot 7 from most samples analyzed showed ion signals at *m/z* 2734.4 and at *m/z* 895.48 that indicated the presence of C-terminal peptides aa 60–84 and aa 77–84, respectively, with an additional arginine at position 84 (Table 5). The absence of signal at *m/z* 1580.8 led us to conclude that this spot corresponded to the Hpα1S,R84 form (Table 1). In contrast, spot 4 of most samples analyzed showed ion signals at *m/z* 2578.23, indicating the presence of a normal C-terminal peptide (aa 60–83). The absence of ion signals at *m/z* 1580.8, and the presence of ion signals at *m/z* 3350.55, which is the increase of 1 Da in the N-terminal peptide of the protein migrating on the acidic side (Fig. 3 and Table 5) due to deamidation of the asparagine residues at position 5 to aspartic acid [2], strongly suggested that this α1S derivative corresponds to Hpα1S,N5D (Table 1). Therefore, the MALDI spectra revealed the same three structural modifications for Hpα1S proteins as for the α2 chain spots.

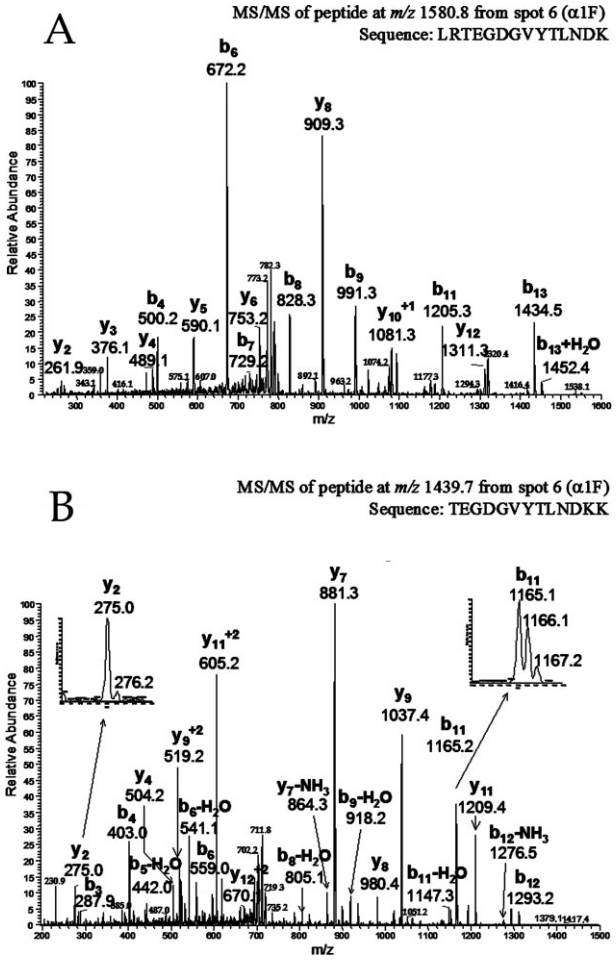

Figure 5. (A) nESI-ITMS/MS analysis of peptide with ion signal at m/z 1580.8 from spot 6. The MS fragment ions from the y-type and b-type ion series are indicated. The determined partial aa sequence is depicted on top and was assigned to a haptoglobin peptide comprising aa 40–53 of haptoglobin α1, or α2. (B) nESI-ITMS/MS analysis of peptide with ion signal at *m/z* 1439.7 from spot 6. The MS fragment ions from the y-type and b-type ion series are indicated. Magnification showed the enlarged regions around the y_2 (*m/z* 275), and b11 (*m/z* 1165.2) ions. The determined partial aa sequence is depicted on top and was assigned to a haptoglobin peptide comprising aa 42–54 of haptoglobin α1, or α2.

3.3.4 Hpα1F spot family

Spot 6 showed the characteristic ion signal at *m/z* 1580.8 in all five samples analyzed (Table 5), strongly suggesting the presence of α1F in this spot. nESI-ITMS/MS analysis of this peptide (Fig. 5B) clearly revealed the sequence of the peptide corresponding to aa 40–53 of α1F, or α2 (Tables 5 and 4). Likewise, as mentioned above, nESI-ITMS/MS analysis of a peptide at *m/z* 1439.7 (Fig. 5A) produced fragment ions belonging to the haptoglobin sequence ranging aa 42–54, which is present in α1F, and α2, but not in α1S. Spot 6 also showed an ion signal at *m/z* 2578.3, characteristic of the normal C-terminal peptide without arginine at the C terminus (aa 60–83). The absence of the ion signal at *m/z* 2734.4 was also consistent with the presence of α1F and not α1S,R84 in that spot. Therefore, the protein in spot 6 will be referred to as Hpα1F (Table 1).

Ion signals at *m/z* 3350.5 were detected in spot 5 of two samples analyzed (one with Hp 1F-1F phenotype and the other with Hp 2–1F), and in both cases this spot was likely to correspond to the N-terminally deaminated form of the α1F chain (Hpα1F,N5D), and not to Hpα1S. The MALDI-TOF spectrum from spot 8 showed the ion signal of the unmodified N-terminal peptide (*m/z* 3349.6) and of the C-terminal peptide with the additional arginine residue (*m/z* 2734.4) and, thus the protein in spot 8 will be referred to as Hpα1F,R84 (Table 5).

In conclusion, the MS analysis discovered three main structural variants of both haptoglobin α1S and α1F.

3.4 Haptoglobin levels

The median Hp plasma levels were significantly higher in SLE patients with high SLEDAI scores (127.5 mg/dL) than in SLE patients with low or not disease activity (69 mg/dL) (p = 0.0411) (Fig. 6). However, these differences were at the limit of significance when compared with the Hp levels of the normal healthy population (79.2 mg/dL), probably due to the low number of individuals analyzed (p = 0.0549) (Fig. 6).

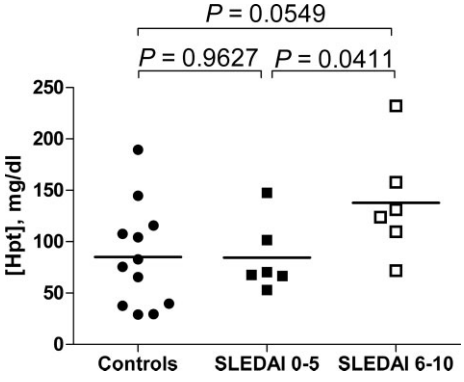

Figure 6. Hp plasma levels were measured by nephelometry. SLE patients were segregated according to their SLEDAI scores, which is highly indicative of the disease activity [15]. p Values were calculated by the Mann-Whitney test (two-tailed).

4 Discussion

Plasma samples from healthy controls and SLE patients have been comparatively analyzed by 2-DE. There are remarkable interindividual differences in the Hp patterns of SLE patients compared with those of healthy controls. Thus, Hpα1F protein is only present in one of the patients studied, whereas the Hpα2 isoform is detected in all but one SLE patients studied. This results in an Hp^2 allele frequency

(0.733), which is significantly higher than that in healthy controls (0.625). Moreover, the frequency of the Hp^{1F} allele is drastically diminished (0.033 in SLE *vs.* 0 093 in controls). As the Hp^{1S} frequency in our study is relatively normal, the overall diminished Hp^{1} frequency must be attributed to the Hp^{1F} allele. Interestingly, in a previous study on Hp distribution in SLE patients from Sweden [13], the Hp^{1} frequency in SLE patients was 0.278, which is quite similar to the one found in the present study (0.266). However, in the Swedish study no distinction was made between Hp 2–1S and Hp 2–1F phenotypes because only the three major Hp phenotypes (Hp 2–2, Hp 2–1, and Hp 1–1) were tested. Note that the Hp^{1} allelic frequency in different European populations is about 0.4 [1], including the Spanish population ([16], and this study).

SLE is a chronic, multisystem autoimmune disease characterized by the differentiation of short- and long-lived immunoglobulin secreting plasma cells that secrete pathogenic autoantibodies [21]. In this sense, the association of the Hp^{2} allele with SLE may be connected with the superior ability of individuals with the Hp 2–2 phenotype to produce antibodies [1, 4]. Moreover, individuals with the Hp 2–2 phenotype show an unbalanced number of B cells between the periphery and bone marrow [4]. Hp binds to the CD22 receptor on human B cells [4], which is implicated in B cell activation and survival. Although the affinity of the binding is the same for the three phenotypes, the number of free CD22-binding sites in the circulation is estimated to be higher in Hp 2–2 individuals. Increased B cell expression of CD22 promotes the presence of autoreactive B cells in the mature repertoire [22]. In addition, murine CD22 is located within the *sle3* susceptibility locus [23], and a polymorphism of *cd22* associates with SLE in a study of Japanese patients [24]. It is likely that the Hp/CD22 interaction can modulate B cell function. Thus, soluble Hp could inhibit the interaction of $CD22^{+}$ B cells with the activated endothelial cells, which upon treatment with pro-inflammatory cytokines such as tumor necrosis factor-alpha (TNF-α) display increased expression of cell-surface CD22 ligands [5]. Overall, there are no dramatic changes in the plasma Hp levels in the SLE patients studied (Fig. 6), although the patients with higher disease activity showed significant higher Hp levels than those with lower or no activity. Despite that a larger number of samples should be included, increased Hp levels may correlate with increased disease activity, which is when the release of pro-inflammatory cytokines and the resultant acute-phase response may occur.

The Hp polymorphism is related to the prevalence and the outcome of various pathological conditions with altered iron metabolism such as hemochromatosis, infections, and atherosclerotic vascular disease. Free hemoglobin promotes the accumulation of hydroxyl radical and harmful reactive oxygen species (free radicals), because iron can generate extremely reactive hydroxyl radicals in the presence of H_2O_2 [25]. Hp functions as an antioxidant and an essential endothelial protector by binding to free hemoglobin [26]. However, both the hemoglobin-binding and the antioxidant capacity of Hpα1 is higher compared with that of Hpα2 [1, 5]. The lower Hb-binding capacity of individuals with the Hp 2–2 phenotype results in more renal damage and higher serum iron levels, at least in males [27].

The increased antioxidant function of Hp1 is thought to confer protection from angiopathies. Thus, following a myocardial infarction, the severity and extent of myocardial damage is greater in patients with Hp 2–2 phenotype than in those with Hp 1–1, or Hp 2–1 [28]. In addition, the survival time in patients with Hp 2–2 who have undergone coronary artery bypass graft is shorter than for people with other Hp phenotypes [4]. These data suggest that Hp 2–2 protects less against oxidative stress in arterial vessels. Interestingly, the Hp 2–2 phenotype is an independent risk factor for cardiovascular disease in individuals with diabetes [29]. This is probably due to the increased generation of redox active iron induced preferentially by Hp 2–2-Hb complexes [30]. In Hp-null mice, free hemoglobin accumulates predominantly in the kidney instead in the liver and spleen as in wild-type mice [31]. In Hp-null mice, induction of severe hemolysis by phenylhydrazine causes greater mortality rate and oxidative tissue damage than in normal mice [32].

Cardiovascular disease is an important complication in patients with SLE, and the increased risk of cardiovascular disease in these patients is not fully accounted for by traditional atherosclerotic risk factors [33]. Moreover, several studies indicate that atherosclerosis is an active inflammatory and immune-mediated process [34], and that this dyslipoproteinemia, which is characterized by high serum triglyceride levels and low serum levels of high-density lipoprotein, correlates with increased disease activity in patients with SLE [33]. Factors, capable of modulating the inflammatory response in patients with SLE, are, therefore, likely to be of interest with regard to the pathogenesis of cardiovascular disease in these patients. Knowledge of the haptoglobin phenotypes and their PMF by 2-DE and MS in SLE patients can help predicting or preventing cardiovascular disorders and determining a more precise prognosis and better treatment.

Dr. Sancho's work was supported by Ministerio de Educación y Ciencia (former Ministerio de Ciencia y Tecnología) grants SAF2002–00721 and SAF2005–06056-C02–01. Dr. Zubiaur's work was supported by Instituto Carlos III-FIS, Ministerio de Sanidad y Consumo, grant FIS03/0389, by a "Ramón y Cajal" contract from the Ministerio de Educación y Ciencia, and by a Grant 209/02 from the Consejería de Salud de la Junta de Andalucía. Esther J. Pavón was supported by a fellowship from grant SAF2002–00721. Pilar Muñoz was supported by a fellowship FPI (Formación de Personal Invesigador) from the Ministerio de Educación y Ciencia, Spain. Ana B. Martin was supported by a contract I3P from the Consejo Superior de Investigaciones Científicas. Salvador A. Arias was supported by a fellowship "Introducción a la investigación" from the Consejo Superior de Investigaciones Científicas.

5 References

[1] Langlois, M. R., Delanghe, J. R., *Clin. Chem* 1996, *42*, 1589–1600.

[2] Mikkat, S., Koy, C., Ulbrich, M., Ringel, B. *et al.*, *Proteomics* 2004, *4*, 3921–3932.

[3] Quero, C., Colome, N., Prieto, M. R., Carrascal, M. *et al.*, *Proteomics* 2004, *4*, 303–315.

[4] Van Vlierberghe, H., Langlois, M.Delanghe, J., *Clin. Chim. Acta* 2004, *345*, 35–42.

[5] Hanasaki, K., Powell, L. D.Varki, A., *J. Biol. Chem.* 1995, *270*, 7543–7550.

[6] Oh, S. K., Pavlotsky, N., Tauber, A. I., *J. Leukoc. Biol.* 1990, *47*, 142–148.

[7] Sadrzadeh, S. M., Bozorgmehr, J., *Am. J. Clin. Pathol.* 2004, *121 Suppl*, S97–104.

[8] Janeway, C. A., Travers, P., Walport, M., Shlomechik, M., *Immunobiology*, Garland Publishing, New York 2001.

[9] Kammer, G. M., Perl, A., Richardson, B. C., Tsokos, G. C., *Arthritis Rheum.* 2002, *46*, 1139–1154.

[10] Kong, P. L., Odegard, J. M., Bouzahzah, F., Choi, J. Y. *et al.*, *Ann. NY Acad. Sci.* 2003, *987*, 60–67.

[11] Rozzo, S. J., Allard, J. D., Choubey, D., Vyse, T. J. *et al.*, *Immunity* 2001, *15*, 435–443.

[12] Wakeland, E. K., Liu, K., Graham, R. R., Behrens, T. W., *Immunity* 2001, *15*, 397–408.

[13] Rantapaa Dahlqvist, S., Beckman, G., Beckman, L., *Hum. Hered.* 1988, *38*, 44–47.

[14] Tan, E. M., Cohen, A. S., Fries, J. F., Masi, A. T. *et al.*, *Arthritis Rheum.* 1982, *25*, 1271–1277.

[15] Bombardier, C., Gladman, D. D., Urowitz, M. B., Caron, D. *et al.*, *Arthritis Rheum.* 1992, *35*, 630–640.

[16] Alonso, A., Visedo, G., Sancho, M., Fernandez-Piqueras, J., *Electrophoresis* 1990, *11*, 321–324.

[17] Thymann, M., Svensmark, O., Masumba, G., Brokso, H. *et al.*, *Electrophoresis* 1990, *11*, 61–65.

[18] Teige, B., Olaisen, B., Teisberg, P., *Hum. Hered.* 1992, *42*, 93–106.

[19] Hanley, J. M., Haugen, T. H., Heath, E. C., *J. Biol. Chem.* 1983, *258*, 7858–7869.

[20] Yang, F., Brune, J. L., Baldwin, W. D., Barnett, D. R. *et al.*, *Proc. Natl. Acad. Sci. USA* 1983, *80*, 5875–5879.

[21] Grammer, A. C., Lipsky, P. E., *Arthritis Res. Ther.* 2003, *5 Suppl 4*, S22–27.

[22] Grimaldi, C. M., Cleary, J., Dagtas, A. S., Moussai, D. *et al.*, *J. Clin. Invest.* 2002, *109*, 1625–1633.

[23] Morel, L., Tian, X. H., Croker, B. P.Wakeland, E. K., *Immunity* 1999, *11*, 131–139.

[24] Hatta, Y., Tsuchiya, N., Matsushita, M., Shiota, M. *et al.*, *Immunogenetics* 1999, *49*, 280–286.

[25] Gutteridge, J. M., *Clin. Chem.* 1995, *41*, 1819–1828.

[26] Gutteridge, J. M., *Biochim. Biophy. Acta* 1987, *917*, 219–223.

[27] Delanghe, J. R.Langlois, M. R., *Clin. Chem. Lab. Med.* 2002, *40*, 212–216.

[28] Chapelle, J. P., Albert, A., Smeets, J. P., Heusghem, C. *et al.*, *N. Engl. J. Med.* 1982, *307*, 457–463.

[29] Levy, A. P., Hochberg, I., Jablonski, K., Resnick, H. E. *et al.*, *J. Am. Coll. Cardiol.* 2002, *40*, 1984–1990.

[30] Asleh, R., Guetta, J., Kalet-Litman, S., Miller-Lotan, R. *et al.*, *Circ. Res.* 2005, *96*, 435–441.

[31] Fagoonee, S., Gburek, J., Hirsch, E., Marro, S. *et al.*, *Am. J. Pathol.* 2005, *166*, 973–983.

[32] Lim, S. K., Kim, H., bin Ali, A., Lim, Y. K. *et al.*, *Blood* 1998, *92*, 1870–1877.

[33] Ohlenschlaeger, T., Garred, P., Madsen, H. O., Jacobsen, S., *N. Engl. J. Med.* 2004, *351*, 260–267.

[34] Kao, A. H., Sabatine, J. M., Manzi, S., *Curr. Opin. Rheumatol.* 2003, *15*, 519–527.

DC-SIGN ligation on dendritic cells results in ERK and PI3K activation and modulates cytokine production

Esther Caparrós, Pilar Munoz, Elena Sierra-Filardi, Diego Serrano-Gómez, Amaya Puig-Kröger, José L. Rodríguez-Fernández, Mario Mellado, Jaime Sancho, Mercedes Zubiaur, and Angel L. Corbí

The generation of pathogen-specific immune responses is dependent on the signaling capabilities of pathogen-recognition receptors. DC-SIGN is a C-type lectin that mediates capture and internalization of viral, bacterial, and fungal pathogens by myeloid dendritic cells. DC-SIGN–interacting pathogens are thought to modulate dendritic cell maturation by interfering with intracellular signaling from Toll-like receptor molecules. We report that engagement of DC-SIGN by specific antibodies does not promote dendritic cell maturation but induces ERK1/2 and Akt phosphorylation without concomitant p38MAPK activation. DC-SIGN ligation also triggers PLCγ phosphorylation and transient increases in intracellular calcium in dendritic cells. In agreement with its signaling capabilities, a fraction of DC-SIGN molecules partitions within lipid raft–enriched membrane fractions both in DC-SIGN–transfected and dendritic cells. Moreover, DC-SIGN in dendritic cells coprecipitates with the tyrosine kinases Lyn and Syk. The relevance of the DC-SIGN–initiated signals was demonstrated in monocyte-derived dendritic cells, as DC-SIGN cross-linking synergizes with TNF-α for IL-10 release and enhances the production of LPS-induced IL-10. These results demonstrate that DC-SIGN–triggered intracellular signals modulate dendritic cell maturation. Since pathogens stimulate Th2 responses via preferential activation of ERK1/2, these results provide a molecular explanation for the ability of DC-SIGN–interacting pathogens to preferentially evoke Th2-type immune responses. (Blood. 2006;107:3950-3958)

Introduction

The functional consequences of the dendritic cell (DC)–T lymphocyte interactions are critically dependent on the maturation state of the DC.[1] In the steady state, immature DCs capture and process antigens and promote either deletion of self-specific T cells or the generation and expansion of regulatory T cells, thus resulting in tolerance and preventing autoimmune responses. By contrast, in the presence of pathogens, DCs acquire the capacity to initiate potent immune responses (DC maturation).[2] Pathogen recognition is accomplished by pathogen-associated molecular patterns (PAMPs) receptors, which include members of the Toll-like receptor (TLR) and lectin protein families[3] and endow DCs with the ability to respond to exogenous agents and microbes.

The DC maturation program exhibits a huge degree of plasticity, thus allowing the generation of pathogen-tailored immune responses. Indeed, gene expression profile analysis of DCs exposed to pathogens or pathogen-derived products has confirmed that DC maturation is pathogen specific.[4] The intracellular signaling pathways that regulate DC maturation are beginning to be unraveled. In the case of TLR ligands, activation of NF-κB is an absolute requirement for DC maturation,[5] but the modulation of NF-κB–dependent gene transcription by other signaling routes contributes to the generation of pathogen-specific responses.[6] As an example, the differential ability of maturation-inducing agents to promote IL-12p70 release depends on their distinct capacity to activate p38MAPK, which "conditions" the IL-12p35 regulatory region for NF-κB occupancy.[7] Unlike p38MAPK, activation of the MEK-ERK signaling axis impairs the acquisition of maturation parameters,[8] and PI3K activation also modulates NF-κB–induced dendritic cell maturation.[9] Comparison of the intracellular signals from TLR4 and TLR2 has recently suggested that TLR agonists differentially instruct dendritic cells to initiate Th responses via modulation of intracellular signaling pathways[10]: TLR4 ligation favors pro-Th1 dendritic cell maturation through the p38MAPK-dependent synthesis of IL-12p70, whereas TLR2 ligands stimulate Th2 responses via preferential activation of ERK1/2 and c-fos.[11]

DCs display a large array of cell surface lectins and lectinlike molecules whose contribution to the maturation program is not completely understood. DC-SIGN is a C-type lectin implicated in

From the Centro de Investigaciones Biológicas and the Centro Nacional de Biotecnología, Consejo Superior de Investigaciones Cientificas (CSIC), Madrid, Spain; and the Instituto de Parasitología y Biomedicina "López-Neyra," Granada, Spain.

Submitted March 28, 2005; accepted January 5, 2005. Prepublished online as *Blood* First Edition Paper, January 24, 2006; DOI 10.1182/blood-2005-03-1252.

Supported by the Ministerio de Educación y Ciencia (Ministerio de Educación Ciencia [MEC]; grants SAF2005-0021, GEN2003-20649-C06-01/NAC, and AGL2004-02148-ALI), Fundación para la Investigación y Prevención del SIDA en España (FIPSE 36422/03) to A.L.C., and grant SAF2002-00721 to J.S. M.Z. was supported by Instituto Carlos III–Fondo de Investigaciones Sanitarias (FIS), by Ministerio de Sanidad y Consumo (grant FIS03/0389), and by a Ramón y Cajal contract from the Ministerio de Educación y Ciencia. E.C., P.M., and D.S.-G. were supported by Formación de Personal Investigador (FPI) Fellowships from MEC.

E.C. and P.M. contributed equally to this work.

M.Z. and A.L.C. contributed equally to this work.

E.C., P.M., E.S.-F., D.S.-G., A.P.-K., J.L.R.-F., M.M., and M.Z. performed research; M.Z. and A.L.C. designed research; M.Z. and J.S. contributed reagents; and A.L.C. wrote the paper.

Reprints: Angel L. Corbí, Centro de Investigaciones Biológicas, CSIC. Ramiro de Maeztu, 9. Madrid 28040 Spain; e-mail: acorbi@cib.csic.es.

The publication costs of this article were defrayed in part by page charge payment. Therefore, and solely to indicate this fact, this article is hereby marked "advertisement" in accordance with 18 U.S.C. section 1734.

capture and uptake of viral (HIV, hepatitis C virus [HCV], Ebola, dengue), bacterial, fungal, and parasite pathogens by DCs.[3,12] Most DC-SIGN–interacting microbes elicit Th2-type responses that result in impaired pathogen clearance and the establishment of chronic infections. This has led to the proposal that pathogens subvert DC-SIGN functions as a means to avoid immunosurveillance and the generation of effective immune responses.[3,12] In this regard, the shift of the immune responses toward Th2 caused by *Mycobacterium tuberculosis* appears to depend on lipoarabinomannan, which increases IL-10 release from DCs by interacting with DC-SIGN.[12] Therefore, the determination of DC-SIGN–initiated intracellular signals might facilitate the development of therapeutic strategies against the pathogens recognized by this lectin. We now present evidence that DC-SIGN ligation triggers activation of PI3K and ERK1/2, and a rapid and transient increase in intracellular calcium mobilization, in both dendritic cells and transfected cells, and that DC-SIGN colocalizes with protein tyrosine kinases in specialized membrane microdomains. The functional relevance of these intracellular signals is illustrated by the enhanced release of IL-10 observed in maturing dendritic cells upon DC-SIGN cross-linking. These results demonstrate that DC-SIGN–triggered intracellular signals modulate dendritic cell maturation and provide a molecular explanation for the ability of DC-SIGN–interacting pathogens to preferentially provoke Th2-type immune responses.

Materials and methods

Cell culture

Human peripheral blood mononuclear cells (PBMCs) were isolated from buffy coats from healthy donors over a Lymphoprep (Nycomed Pharma, Oslo, Norway) gradient according to standard procedures. Monocytes were purified from PBMCs by a 1-hour adherence step at 37°C in complete medium or by magnetic cell sorting using CD14 microbeads (Miltenyi Biotech, Bergisch Gladbach, Germany). To generate monocyte-derived dendritic cells (MDDCs), adherent or $CD14^+$ cells (> 95% monocytes) were cultured at 0.5 to 1 × 10^6 cells/mL in RPMI with 10% fetal calf serum (FCS), 25 mM HEPES, and 2 mM glutamine (complete medium), at 37°C in a humidified atmosphere with 5% CO_2. Complete medium was supplemented with 1000 U/mL granulocyte-macrophage–colony-stimulating factor (GM-CSF, Leucomax; Schering-Plough, Kenilworth, NJ) and 1000 U/mL IL-4 (PreProtech, Rocky Hill, NJ) for 5 to 7 days, with cytokine addition every second day. MDDC maturation was induced with either TNF-α (20 ng/mL; Peprotech EC, London, England), ultrapure LPS from *Escherichia coli* 0111:B4 (10 ng/mL), or Pam3Cys (20 μg/mL; InvivoGen, San Diego, CA). The human cell lines Jurkat (T-cell lymphoma) and THP-1 (monocytic leukemia) were cultured in complete medium. DC-SIGN–expressing Jurkat cells (Jurkat-DC-SIGN) were generated after electroporation of the pCDNA3-DC-SIGN plasmid,[13] selection in complete medium with 600 μg/mL G418 (Gibco, Grand Island, NY), and cell sorting with the MR-1 antibody. A similar procedure was done to generate Jurkat-mock cells, which are stably transfected with an empty pCDNA3.1(−) vector. Cells were observed under a Zeiss Axiovert 25 microscope equipped with a 32 ×/0.4 Ph1 lens (Zeiss, Jena, Germany), and were photographed with a RICOH XR-X3000 camera (Ricoh, West Caldwell, NJ). Image acquisition was performed with Dell photographic editor software in the Dell AIO printer (Dell, Round Rock, TX); subsequent processing was done with Adobe Photoshop 7.0 software (Adobe Systems, San Jose, CA).

Flow cytometry and antibodies

Phenotypic analysis of MDDCs and cell lines was carried out by immunofluorescence. Monoclonal antibodies used for cell surface staining included phycoerythrin-labeled anti-CD83 (BD Biosciences, San Diego, CA), FITC-FA6-152 (anti-CD36; Immunotech, Marseille, France), and MR1 (anti–DC-SIGN, CD209).[13] In this case, incubation with the unlabeled primary antibody was followed by incubation with FITC-labeled $F(ab')_2$ goat anti–mouse IgG. All incubations were done in the presence of 50 μg/mL human IgG to prevent binding through the Fc portion of the antibodies. P3X63 myeloma supernatant was included as negative control, and flow cytometry analysis was performed with an EPICS-CS (Coulter, Madrid, Spain) using log amplifiers.

Determination of IL-10 levels

Immature MDDCs (10^6/mL complete medium) were treated with maturing agents (LPS at 10 ng/mL, Pam3Cys at 20 μg/mL, or TNF-α at 20 ng/mL) and either in the absence or presence of purified antibody against DC-SIGN (MR-1) or purified mouse IgG as control. After 18 hours, cell supernatants were collected and IL-10 levels determined using the IL-10 ELISA Set (Immunotools, Friesoythe, Germany) following the manufacturer's recommendations. MDDC supernatants were assayed undiluted and diluted 1:3 in complete medium.

DC-SIGN cross-linking experiments

MDDCs or Jurkat cells were washed extensively in RPMI and cultured in RPMI containing 0.5% FCS to reduce the basal level of activation. Preliminary experiments indicated that MDDCs cultured overnight in RPMI 0.5% FCS exhibited a low level of ERK phosphorylation, whereas Jurkat cells required a 24/36-hour culture period. Then cells were transferred to a 37°C water bath and treated with the stimulatory agents for 5 minutes or the indicated period of time. In all cases, 2 × 10^6 MDDCs or Jurkat cells was used for each experimental condition. Stimulatory antibodies were added at 20 μg/mL, and included purified monoclonal antibodies against DC-SIGN (MR-1),[13] CD38 (HB136), CD70 (qa32), CD11c (HC1/1), and c-Myc (9E10). As positive control, cells were treated with either TNF-α (20 ng/mL), PMA (10 ng/mL), or a monoclonal antibody against CD3 at 20 μg/mL (OKT3). In some experiments, negative controls also included purified human IgG (AP3D11). After stimulation, cells were immediately lysed with 2 × lysis buffer (40 mM HEPES [pH 7.6], 300 mM NaCl, 2 mM EGTA, 1% NP-40, 100 μM phenylarsine oxide, 100 mM NaF, 2 mM Na_3VO_4, 2 mM Pefabloc, 20 mM iodoacetamide, and 2 μg/mL aprotinin, antipain, leupeptin, and pepstatin), and cell lysates subjected to Western blot with antibodies specific for the activated/phosphorylated forms of various signaling pathways.

Western blot

Cell lysates (10 μg) were subjected to sodium dodecyl sulfate–polyacrylamide gel electrophoresis (SDS-PAGE) under reducing conditions and transferred onto an Immobilon polyvinylidene difluoride membrane (PVDF; Millipore, Bedford, MA). After blocking with 1% BSA in 50 mM Tris-HCl (pH 7.6), 150 mM NaCl, 0.1% Tween-20, protein detection was performed using the Supersignal West Pico Chemiluminescent system (Pierce, Rockford, IL). For reprobing, membranes were incubated in stripping buffer (62.5 mM Tris-HCl [pH 6.7], 100 mM β-mercaptoethanol, 2% SDS) for 30 minutes at 50°C with occasional agitation. Detection of phosphotyrosine, phospho-p38MAPK, phospho-PI3K, phospho-PLCγ, phospho-ERK, and phospho-ZAP70 was carried out using polyclonal antibodies specific for antiphosphotyrosine (RC20-HRP; BD Biosciences), anti–phospho-p38MAPK (T180/Y182, no. 9211; Cell Signaling Technology, Beverly, MA), anti–phospho-Akt (no. 9271; Cell Signaling Technology), anti–phospho-PLCγ (sc-12943; Santa Cruz Biotechnology, Santa Cruz, CA), anti–phospho-ZAP70 (Y493, no. 9212; Cell Signaling Technology), and a monoclonal antibody anti–phospho-p44/42 MAPK (T202-Y204, no. 9101; Cell Signaling Technology). As a control for protein loading, blots were reprobed with polyclonal antisera against ERK (no. 9102; Cell Signaling Technology), p38MAPK (no. 9212; Cell Signaling Technology), PLCγ (sc-423; Santa Cruz Biotechnology), or tubulin (clone DM 1A; Sigma, Barcelona, Spain).

Isolation of detergent-insoluble and -soluble cell membrane fractions by sucrose gradient ultracentrifugation and membrane distribution of DC-SIGN

Detergent solubilization of cells ($7\text{-}9 \times 10^7$) at 37°C with 1% Brij 98 (Sigma Aldrich, St Louis, MO) was carried out as described.[14] Cell lysates were mixed with an equal volume of 80% sucrose and transferred to Sorvall ultracentrifuge tubes (Sorvall, Asheville, NC). The following were overlaid: 2 mL 30% sucrose, followed by 1 mL 5% sucrose in 20 mM HEPES (pH 7.6), 150 mM NaCl, 1 mM EGTA, 50 mM sodium fluoride, 1 mM sodium orthovanadate, 20 μM phenylarsine oxide, 1 mM phenylmethylsulfonyl fluoride, 10 mM iodoacetamide, and a mixture of small peptide protease inhibitors at 1 μg/mL each. All the sucrose solutions were prepared in the same buffer without detergent and in the presence of small peptide protease inhibitors at 1 μg/mL. Samples were centrifuged for 18 to 20 hours at 200 000*g* in a Sorvall AH-650 rotor. Eight 0.5-mL fractions were collected on ice, from the top to the bottom of the gradients. Aliquots of each fraction (18 μL) of the gradient were diluted with 9 μL 3 × Laemmli sample buffer and resolved on 12.5% SDS-PAGE under nonreducing conditions, transferred to PVDF, and immunoblotted with specific antibodies, which included polyclonal antibodies against DC-SIGN,[15] Lck (sc-13; Santa Cruz Biotechnology), ZAP-70 (sc-574; Santa Cruz Biotechnology), LAT (06-807; Upstate Biotechnology, Charlottesville, VA), CD3ε (A0452; Dako, Glostrup, Denmark), Syk (AW 1373-13, kindly provided by Dr Arthur Weiss), Lyn (sc-15; Santa Cruz Biotechnology), ERK (sc-154; Santa Cruz Biotechnology), cholera toxin–HRP (C4672; Sigma) for ganglioside GM1 detection, or a monoclonal antibody against Ras (RAS10; Upstate Biotechnology). In indicated experiments, pools of the sucrose gradient fractions were collected: the pool of the low-density fractions corresponding to the 5%/30% interface (fractions 2-4) was referred to as rafts; the pool of fractions 5 and 6 was termed intermediate (intrm.); and the pool of the high-density soluble material corresponding to fractions 7 and 8 was referred to as soluble. Cytoskeletal-associated rafts (CARs) were extracted from the pellet by treatment with 60 mM octyl D-glucoside (ODG) and 1% Brij 98, and the supernatant was collected after centrifugation at 13 000*g*.[16,17] In indicated experiments, immunoprecipitation under solubilizing conditions was carried out on pooled rafts, intermediate and soluble. Those pools were diluted with lysis buffer containing 1% Brij 98 + 60 mM ODG to less than 20% sucrose.

Immunoprecipitation of protein assemblies was performed by incubation of these pools with purified monoclonal antibodies against DC-SIGN (MR-1) or anti-Lyn (sc-7274; Santa Cruz Biotechnology) followed by capture of the immune complexes on Protein G superparamagnetic Microbeads (Miltenyi Biotech) as described elsewhere.[14] Immunoprecipitates were then subjected to Western blot using polyclonal antibodies against DC-SIGN (DSG-1),[15] Syk (AW 1373-13), Lyn (sc-15), or antiphosphotyrosine (RC20-HRP). In some experiments, cells were surface-labeled with biotin. To that end, cells were washed in PBS (pH 8.0) and incubated in 0.5 mg/mL biotinamidohexanoic acid 3-sulfo-*N*-hydroxysuccinimide ester sodium salt (B1022; Sigma Aldrich) for 30 minutes at room temperature. After labeling, cells were extensively washed in PBS, lysed, and subjected to fractionation by sucrose gradient ultracentrifugation as indicated.[14] After separation, lipid raft–containing and soluble fractions were pooled and immunoprecipitated with Streptavidin-agarose (Sigma Aldrich), and immunoprecipitated material was analyzed by SDS-PAGE and Western blot with antibodies specific for DC-SIGN or LAT.

Intracellular calcium determination

MDDCs (2.5×10^6 cells/mL) were resuspended in complete medium and incubated with Fluo-3AM (Calbiochem, San Diego, CA; 300 μM in DMSO, 10 μL/10^6 cells) for 30 minutes at 37°C. Cells were then washed, resuspended in RPMI containing 2 mM $CaCl_2$, and maintained at 37°C before addition of purified anti–DC-SIGN MR-1 monoclonal antibody (20 μg/mL) or an isotype-matched control. Calcium flux was measured in an EPICS XL flow cytometer at 525 nm (Coulter, Madrid, Spain). Fluo-3AM loading was controlled using ionomycin as ionophore (5 μg/mL). In some experiments SDF-1α (50 mM; Preprotech) was added before addition of the monoclonal antibody.

Results

DC-SIGN engagement leads to ERK and Akt activation but does not induce MDDC maturation

To evaluate the signaling capability of DC-SIGN, we initially assessed the influence of an anti–DC-SIGN antibody on the MDDC maturation state. Whereas LPS induced MDDC maturation parameters (CD83 induction and loss of CD36), purified MR-1 (anti–DC-SIGN) or HB136 (anti-CD38) antibodies at 20 μg/mL (1X) or 60 μg/mL (3X) for 24 hours neither altered cell morphology (data not shown) nor affected the expression of CD83 or CD36 (Figure 1A). Therefore, ligation of DC-SIGN on the cell surface with the MR-1 antibody does not lead to overt MDDC maturation. However, cross-linking of DC-SIGN with MR-1 induced a change in the profile of phosphotyrosine-containing proteins in MDDCs (Figure 1B). The change occurred within 1 minute (data not shown) and was not further amplified upon cross-linking with a secondary antibody, which, per se, did not induce any change in the phosphotyrosine profile (Figure 1B). We reasoned that the observed effect of cross-linking was unlikely to be due to endotoxin

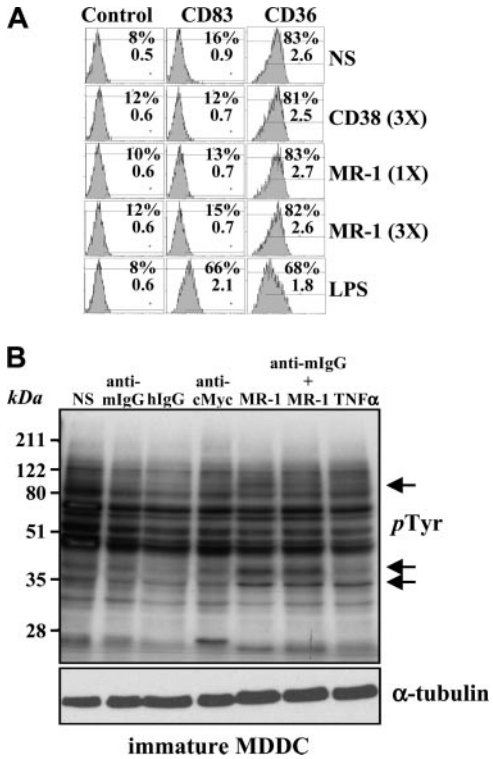

Figure 1. DC-SIGN ligation on MDDCs does not induce maturation but alters the profile of phosphotyrosine-containing proteins. (A) Immature MDDCs were isolated and either not stimulated (NS) or treated with lipopolysaccharide (LPS) or monoclonal antibodies against CD38 (HB136) or DC-SIGN (MR-1) at 20 μg/mL (1X) or 60 μg/mL (3X). After 48 hours, cells were collected and the cell surface expression of CD83 and CD36 was determined by flow cytometry, using an isotype-matched anti–c-Myc antibody (9E10) as control. The percentage of marker-positive cells and the mean fluorescence intensity are indicated in each case. Three experiments were performed on MDDCs from independent donors, and a representative experiment is shown. (B) DC-SIGN ligation induces changes in the pattern of tyrosine phosphorylation in MDDCs. Cells were either left untreated (not stimulated, NS) or incubated with monoclonal antibodies against DC-SIGN (MR-1) as ligation agent, or with MR-1 plus a cross-linking secondary antibody (anti–mouse $F(ab')_2$, anti–mouse IgG). After 5 minutes, cells were lysed, and the lysates were probed for phosphotyrosine residues by Western blot using the RC20-HRP monoclonal antibody. As a control, a monoclonal antibody against c-Myc (anti–c-Myc) was used. Two experiments on MDDCs from independent donors rendered similar results, and one of them is shown.

contamination of the antibody, because neither primary nor secondary control antibodies alone mimicked the stimulatory effect and MDDCs exposed to the anti–DC-SIGN antibody did not exhibit any maturation-specific parameters (Figure 1A).

Analysis of the pattern of tyrosine phosphorylation after DC-SIGN cross-linking revealed an increased phosphorylation in the 42 to 50 kDa range, suggesting that ERK1/2 MAP kinases might be candidate substrate proteins. To determine whether this was the case, immature MDDCs were treated with MR-1 and probed for the presence of phosphorylated ERK. DC-SIGN ligation promoted ERK activation after 5 minutes, whereas an antibody against CD70 was without effect and antibodies against CD11c triggered significant ERK phosphorylation only upon cross-linking with a secondary antibody (Figure 2A). Of interest, further cross-linking of DC-SIGN with an anti–mouse IgG resulted in weaker ERK activation (Figure 2A). By contrast, DC-SIGN ligation did not induce p38 phosphorylation, whereas TNF-α promoted both ERK and p38 activation (Figure 2A).

Kinetic experiments on MDDCs from an independent donor indicated that DC-SIGN ligation-induced ERK phosphorylation is a transient event that takes place as early as 1 minute after stimulation and vanishes after 30 minutes, a time point at which p38 activation also appears to be diminished by DC-SIGN ligation (Figure 2B). Moreover, DC-SIGN ligation promoted a weak and transient activation of PI3K, as evidenced by the appearance of phosphorylated Akt only 1 minute after stimulation (Figure 2B). Altogether, these results indicate that antibody ligation of DC-SIGN on the cell surface of MDDCs induces a wave of intracellular signaling that results in transient activation of ERK and PI3K, 2 kinases critically involved in dendritic cell maturation.[9,18]

DC-SIGN engagement was further evaluated for its capacity to modulate MDDC maturation signals initiated from other cell surface receptors. To this purpose, we initially focused on TNF-α, which induces maturation markers on MDDCs.[19] Whereas TNF-α and DC-SIGN ligation induced ERK activation to a similar extent (3.5-fold and 5.8-fold increase, respectively, over background levels), addition of both stimuli to MDDCs resulted in further enhanced phosphorylation of ERK (to 11.5-fold), whereas the combination of TNF-α and a control antibody did not result in any enhancement (Figure 2C). Analysis of MDDCs from an independent donor produced essentially similar results and indicated that DC-SIGN cross-linking is capable of inducing ERK phosphorylation even in the presence of ultrapure LPS, which failed to promote significant ERK activation by itself (Figure 2D). Altogether, these results demonstrate that DC-SIGN is capable of modulating the intracellular signals originated from maturation-inducing factors.

DC-SIGN engagement triggers intracellular signaling in myeloid and lymphoid cell lines

Next, we tested whether the signaling capability of DC-SIGN is restricted to dendritic cells, where it is expressed in very high levels, or can be observed in other cell types. To that end, DC-SIGN was engaged with the MR-1 antibody on the surface of THP-1 cells, which exhibit a weak basal level of the lectin (Figure 3A). Although to a lower extent than in MDDCs, engagement of DC-SIGN on the surface of THP-1 also resulted in enhanced ERK activation, which was comparable with the phosphorylation level induced upon phorbol ester treatment (Figure 3B).

To extend these findings to a different cell lineage, the signaling ability of DC-SIGN was evaluated in Jurkat-DC-SIGN transfectants, which exhibit a high level of DC-SIGN cell surface expression (Figure 3C). Like K562 cells,[20] Jurkat cells overexpressing DC-SIGN formed large homotypic aggregates (Figure 3D) and showed rapid lectin down-regulation upon ligation on the cell

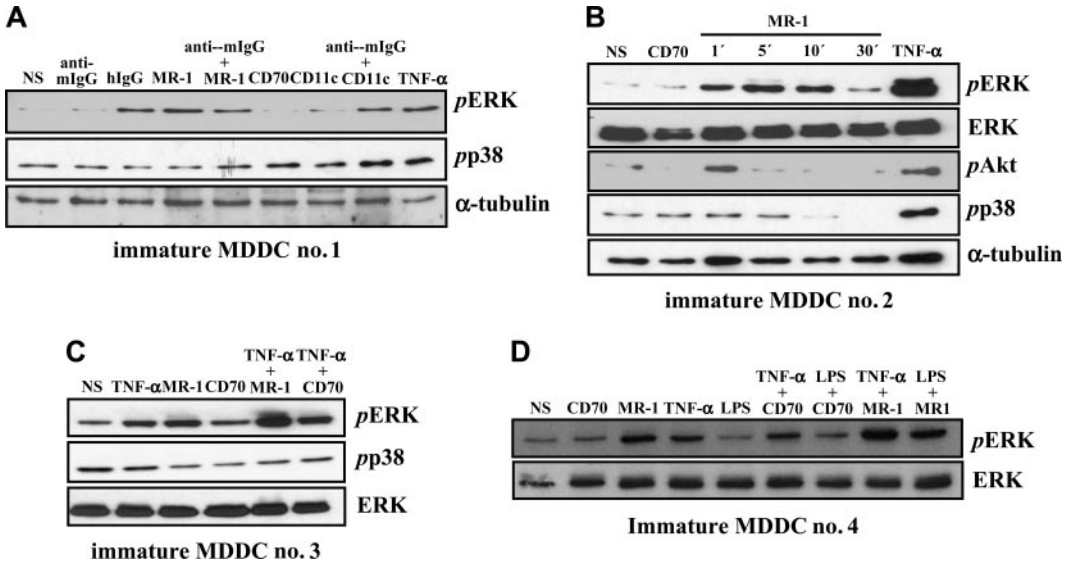

Figure 2. DC-SIGN ligation on MDDCs induces ERK phosphorylation and collaborates with TNF-α–initiated signals for enhanced ERK activation. (A) Activation of ERK by DC-SIGN engagement. DC-SIGN on MDDCs was engaged by the anti–DC-SIGN MR-1 antibody and the cells were incubated at 37°C for 5 minutes. For comparison, cells were treated with the indicated combinations of antibodies or TNF-α (20 ng/mL). Following cell lysis, phosphorylated ERK and phosphorylated p38 were detected using specific polyclonal antisera. Blots were then stripped and probed for α-tubulin levels as a control for protein loading (bottom panel). (B) DC-SIGN on MDDCs was engaged by the anti–DC-SIGN MR-1 antibody, and the cells were incubated at 37°C for the indicated periods of time. For comparison, cells were treated with an antibody against CD70 or TNF-α (20 ng/mL) for 5 minutes. Following cell lysis, phosphorylated ERK, p38, and Akt, and total ERK were detected using specific polyclonal antisera. Blots were then stripped and probed for α-tubulin levels as a control for protein loading. (C-D) Immature MDDCs from 2 independent donors were incubated with an antibody against DC-SIGN (MR-1) or against CD70, either alone or in combination with TNF-α (20 ng/mL) or LPS (10 ng/mL), and the cells were incubated at 37°C for 5 minutes. For comparison, cells were treated with either LPS (10 ng/mL) or TNF-α (20 ng/mL) for 5 minutes. Following cell lysis, phosphorylated ERK (pERK), phosphorylated p38 (pp38), or total ERK content (ERK) was detected using specific polyclonal antisera. Each experiment was done on MDDCs from at least 4 independent donors, and representative experiments are shown. In all panels, NS refers to cells that were not stimulated.

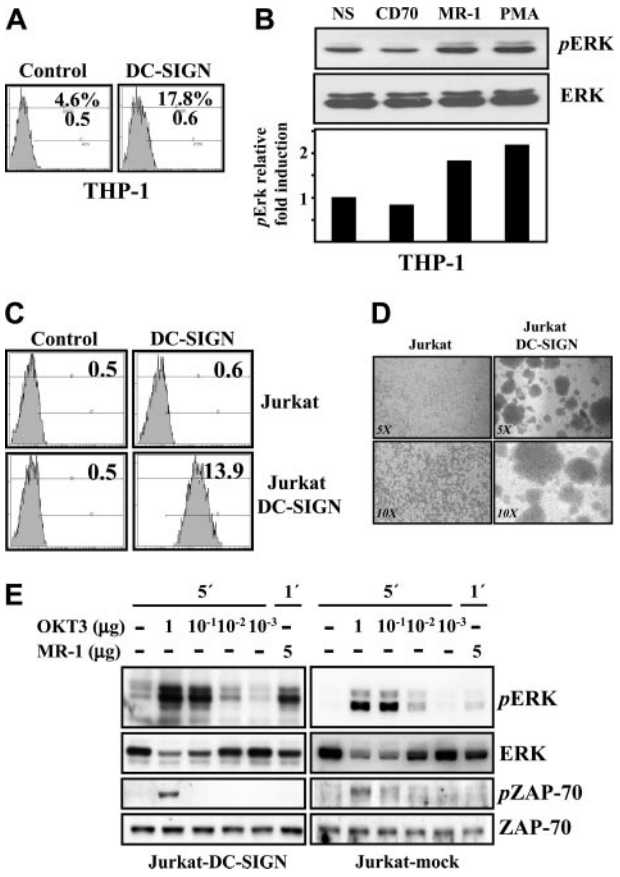

Figure 3. DC-SIGN ligation in myeloid and lymphoid cell lines results in ERK activation. (A) Cell surface expression of DC-SIGN in THP-1 cells, as determined by flow cytometry. The percentage of marker-positive cells and the mean fluorescence intensity are indicated in each case. (B) DC-SIGN on THP-1 cells was engaged by the anti–DC-SIGN MR-1 antibody (20 μg/mL), and the cells were incubated at 37°C for 5 minutes. As a control, cells were either incubated with an anti-CD70 monoclonal antibody or with PMA (10 ng/mL). After cell lysis, phosphorylated ERK (pERK, top panel) and total ERK (ERK, middle panel) were detected using specific polyclonal antisera. The bottom panel illustrates the level of pERK relative to the level of total ERK under each condition, as determined by densitometric analysis. NS indicates not stimulated. (C) Cell surface expression of DC-SIGN in mock-transfected (Jurkat) and DC-SIGN–transfected Jurkat cells (Jurkat-DC-SIGN) as determined by flow cytometry, using an isotype-matched anti–c-Myc antibody (9E10) as control. The mean fluorescence intensity is indicated in each case. (D) Homotypic aggregation of mock-transfected (Jurkat) and DC-SIGN–transfected (Jurkat-DCSIGN) Jurkat cells, as observed by reverse-phase microscopy at 2 different amplifications (5 ×, 10 ×). (E) DC-SIGN on Jurkat-DC-SIGN transfectants was ligated by the anti–DC-SIGN MR-1 antibody alone or in the presence of an anti-CD3 monoclonal antibody as control, and the cells were incubated at 37°C for 1 or 5 minutes. Mock-transfected Jurkat cells were subjected to the same treatments for control purposes. After cell lysis, phosphorylated ERK (pERK), phosphorylated ZAP-70 (pZAP-70), and total content of ERK and ZAP-70 were detected using specific polyclonal antisera. Each experiment was done 3 times with similar results. Representative results are shown.

surface (data not shown), thus confirming that DC-SIGN retains its adhesive and antigen-capture capabilities in Jurkat cells.[21] Accordingly, ligation of DC-SIGN in Jurkat cells led to ERK activation but had no effect on the phosphorylation state of ZAP-70 (Figure 3E) or p38MAPK (Figure 6A). Therefore, engagement of DC-SIGN on myeloid (MDDC, THP-1) or lymphoid (Jurkat) results in ERK phosphorylation.

DC-SIGN is found in lipid-rich regions on the cell surface of transfected lymphoid cells

Lipid rafts are specialized membrane regions that facilitate outside-in signaling by generating a physical environment rich in kinases, adaptors, and intracellular effectors.[22] The ability of DC-SIGN to trigger intracellular signals prompted us to analyze its membrane distribution in immature MDDCs and Jurkat-DC-SIGN cells. In agreement with a previous report,[23] analysis of Jurkat-DC-SIGN transfectants revealed the presence of DC-SIGN in lipid rafts (Figure 4A). Although DC-SIGN was mainly found in the soluble fractions, a percentage of the molecules was detected in GM1-rich lipid rafts, where Lck and LAT, but not ZAP-70, were also detected (Figure 4A). To examine potential interactions of DC-SIGN with signaling proteins, DC-SIGN was immunoprecipitated from the

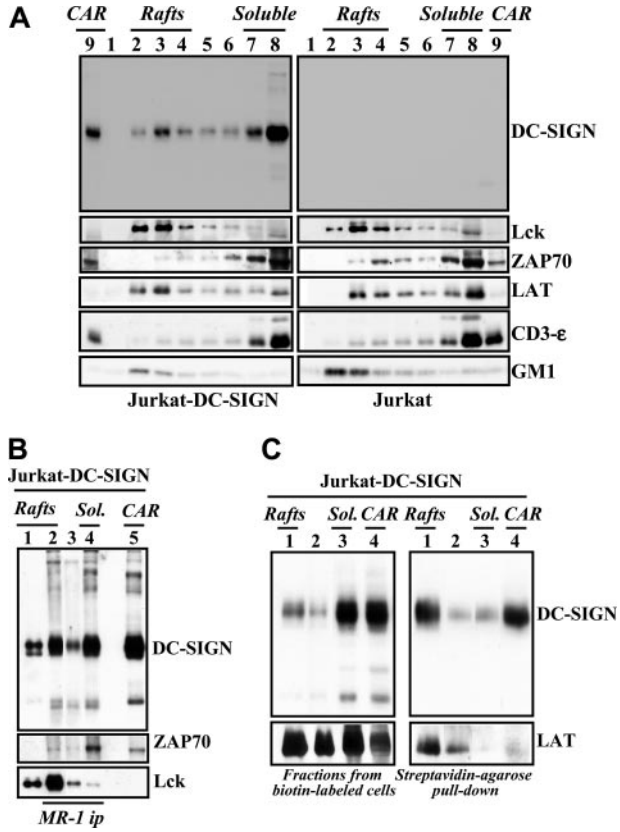

Figure 4. DC-SIGN is present within lipid rafts in lymphoid cells and coprecipitates with tyrosine kinases. (A) Jurkat-DC-SIGN (left panels) and mock-transfected Jurkat cells (right panels) were lysed in 1% Brij 98 lysis buffer at 37°C, and Brij 98–insoluble fractions 2 to 4 (lanes 2-4, rafts) and the high-density Brij 98–soluble fractions 7 to 8 (lanes 7-8, soluble) were separated by 12.5% SDS-PAGE under nonreducing conditions. Cytoskeletal-associated rafts (CARs), obtained by solubilization of the cell pellet with Brij 98 + octyl D-glucoside in lysis buffer, were analyzed in parallel (lane 9). The distribution of DC-SIGN, Lck, ZAP-70, LAT, CD3ε, and ganglioside GM1 in the distinct fractions was determined by immunoblotting with specific antibodies or cholera toxin–HRP (for GM1). (B) Coprecipitation of DC-SIGN and tyrosine kinases. DC-SIGN was immunoprecipitated with the MR-1 antibody (MR1 ip) from lipid raft–containing fractions 2 to 4 (rafts, lane 2), fractions 5 to 6 (between the rafts and the soluble material, lane 3), and the 7 to 8 soluble fractions (sol., lane 4), and the immunoprecipitated material was subjected to SDS-PAGE and immunoblotting with antibodies against DC-SIGN, Lck, or ZAP-70. As a control, fractions containing either rafts (lane 1) or cytoskeletal-associated rafts (CARs, lane 5) were analyzed in parallel. (C) Jurkat-DC-SIGN cells were cell-surface labeled with biotin, lysed in 1% Brij 98 lysis buffer at 37°C, and Brij 98–insoluble fractions (lanes 1, rafts), intermediate fractions (lanes 2), high-density Brij 98–soluble fractions (lanes 3, sol.), and cytoskeletal-associated raft-containing fractions (CARs, lane 4) were obtained. An aliquot from each fraction was removed and analyzed by 12.5% SDS-PAGE under nonreducing conditions and subjected to Western blot with anti–DC-SIGN or anti-LAT polyclonal antisera (left panel). Then, fractions were subjected to pull-down with Streptavidin-agarose, and the immunoprecipitated material was separated by 12.5% SDS-PAGE under nonreducing conditions and subjected to Western blot with anti–DC-SIGN or anti-LAT polyclonal antisera (right panel). Each experiment was performed twice with similar results, and one of the experiments is shown.

distinct membrane fractions in the presence of 1% Brij 98 + 60 mM octyl D-glucoside (ODG), which efficiently disrupts many lipid raft–protein associations. As shown in Figure 4B (lane 2), Lck tyrosine kinase was coimmunoprecipitated with DC-SIGN from the lipid raft–containing fractions, whereas ZAP-70 was detectable in DC-SIGN immunoprecipitates from the soluble pool (Figure 4B lane 4). These results suggest that DC-SIGN can be found in 2 distinct microdomain localizations that differ in their content of signaling molecules. Next, to determine the microdomain location of cell surface DC-SIGN, lipid raft–containing and soluble membrane fractions were generated from biotin-labeled Jurkat-DC-SIGN cells, and the resulting fractions were immunoprecipitated with Streptavidin-agarose. In agreement with experiments using unlabeled cell lysates, a large proportion of DC-SIGN was found in the soluble fraction pool (Figure 4C left panel). However, pull down of cell surface molecules by immunoprecipitation with Streptavidin-agarose revealed that most biotin-labeled DC-SIGN molecules partitioned within the lipid raft– and cytoskeletal-associated raft-containing fractions (Figure 4C right panel). Densitometric analysis of the results shown in Figure 4C indicated that 80% of the total cell surface expression of DC-SIGN (biotin-labeled DC-SIGN) is found within the lipid raft–containing fractions. These results indicate that most DC-SIGN molecules on the cell surface are included in lipid rafts, whereas DC-SIGN molecules in the soluble fraction pool are not accessible for biotin labeling and might be contained in intracellular compartments.

DC-SIGN is found in lipid-rich regions on MDDCs and coprecipitates with tyrosine kinases

To determine the membrane distribution of DC-SIGN in myeloid cells, detergent-insoluble and -soluble membrane fractions were isolated from MDDCs. Although a high percentage of the molecule appeared in soluble fractions, a fraction of DC-SIGN also partitioned within lipid rafts on MDDCs (Figure 5A). Fractionation of MDDCs from an independent donor further confirmed this DC-SIGN distribution and revealed that most of the intracellular membrane-bound tyrosine kinase Lyn partitioned into low-density fractions 2 to 4, which is consistent with its residency in floating lipid rafts, whereas the signaling molecules Syk, ERK, and Ras were partly localized in the lipid-rich regions on MDDCs (Figure 5B). Since DC-SIGN coprecipitates with ZAP-70 and Lck in lymphoid cells, we next evaluated whether DC-SIGN associated with related molecules in MDDC membranes. As shown in Figure 5C, DC-SIGN brought down phosphotyrosine-containing molecules from lipid raft fractions. Moreover, a significant amount of Lyn and a lesser amount of Syk tyrosine kinases could be detected in the DC-SIGN precipitates from lipid rafts (Figure 5C), indicating that DC-SIGN colocalizes with signaling molecules in glycolipid-enriched membranes from MDDCs. Conversely, neither Syk nor Lyn was detected in DC-SIGN immunoprecipitates from the soluble membrane fractions, in spite of the fact that DC-SIGN is more abundant in this fraction (Figure 5C). In addition, analysis of membrane fractions from an independent MDDC donor demonstrated the presence of DC-SIGN and Syk in Lyn immunoprecipitates (Figure 5D), further confirming the relationship between DC-SIGN and these 2 kinases within lipid rafts. However, not all DC-SIGN molecules are associated to Lyn since DC-SIGN can be easily pulled down with the MR-1 antibody from the post–anti-Lyn immunoprecipitation flow-through from either lipid rafts or soluble membrane fractions (Figure 5E).

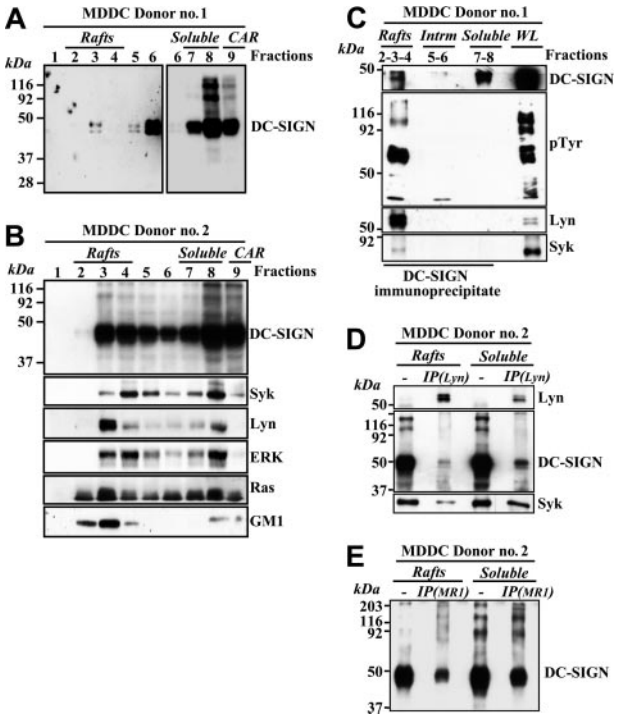

Figure 5. DC-SIGN is present within lipid rafts in MDDCs and coprecipitates with Lyn and Syk tyrosine kinases. (A-B) Immature MDDCs from 2 independent donors were lysed in 1% Brij 98 lysis buffer at 37°C and fractionated by sucrose density gradient centrifugation as described in "Materials and methods."[14] The low-density Brij 98–insoluble fractions 2 to 4 (lanes 2-4, rafts) and the high-density Brij 98–soluble fractions 6 to 8 (lanes 6-8, soluble) were separated by 12.5% SDS-PAGE under nonreducing conditions, and the distribution of DC-SIGN was determined by immunoblotting. Cytoskeletal-associated rafts (CARs), obtained by solubilization of the cell pellet with Brij 98 + octyl D-glucoside in lysis buffer, were analyzed in parallel (lane 9). (A) The left panel was intentionally exposed for longer than the blot section shown in the right panel. (B) The distribution of Syk, Lyn, ERK, Ras, and ganglioside GM1 in the distinct fractions was determined by immunoblotting with specific antibodies or cholera toxin–HRP (for GM1). (C) Coprecipitation of DC-SIGN, Lyn, and Syk tyrosine kinases. DC-SIGN was immunoprecipitated with the MR-1 antibody from lipid raft–containing fractions 2 to 4 (rafts), fractions 5 to 6 (intrm. indicates intermediate between the rafts and the soluble material), and the 7 to 8 soluble fractions (soluble), and the precipitated material was subjected to SDS-PAGE and immunoblotting with antibodies specific for DC-SIGN, Lyn, Syk, and phosphotyrosine-containing proteins. As a control, an aliquot from the whole lysate before fractionation (WL indicates whole lysate) was analyzed in parallel. (D) Presence of DC-SIGN and Syk in Lyn immunoprecipitates. Lyn was immunoprecipitated (IP(Lyn)) from the lipid raft–containing fraction pool (rafts) or the soluble material–containing fraction pool (soluble), and the precipitated material was subjected to SDS-PAGE and immunoblotting with antibodies specific for Lyn, DC-SIGN, and Syk. As a control, aliquots from the rafts and soluble fraction pools before immunoprecipitation were analyzed in parallel. (E) Presence of DC-SIGN in the post–anti-Lyn immunoprecipitation flow-through. Post–anti-Lyn immunoprecipitation flow-through from either lipid rafts or soluble membrane fraction pools (those indicated in D) were subjected to a further immunoprecipitation with a monoclonal antibody against DC-SIGN (IP(MR1)), and the precipitated material was subjected to SDS-PAGE and immunoblotting with a polyclonal antibody against DC-SIGN (DSG1). As a control, aliquots from the rafts and soluble fraction pools before immunoprecipitation were analyzed in parallel.

Additional intracellular signals initiated upon DC-SIGN engagement

The maturation state of dendritic cells is a critical parameter that determines not only whether an immune response is generated but the type of immune response.[2] Besides NF-κB activation, other signaling pathways have an impact on dendritic cell maturation, including MEK-ERK[8] and PI3K[9] activation, and transient calcium increases.[24] Given its ability to prompt ERK and Akt phosphorylation, we tested whether DC-SIGN–initiated signals also affected intracellular calcium levels. Engagement of DC-SIGN in Jurkat-DC-SIGN cells triggered PLC-γ phosphorylation, an effect that was not

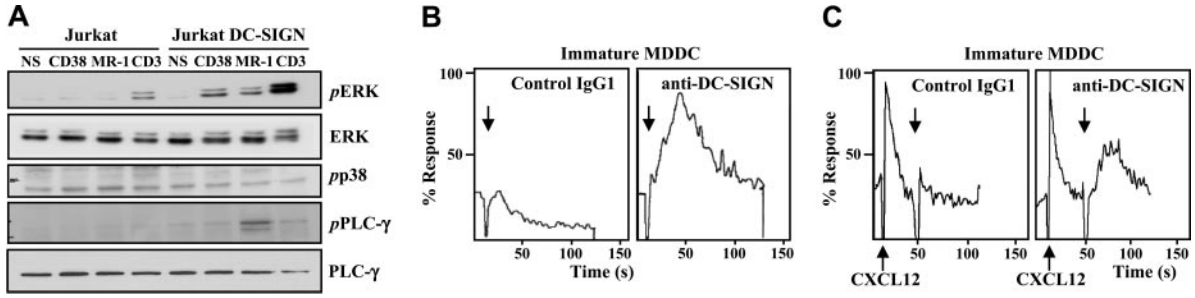

Figure 6. DC-SIGN ligation results in ERK and PLC-γ activation in transfected Jurkat cells and promotes transient calcium mobilization in MDDCs. (A) DC-SIGN on Jurkat-DC-SIGN transfectants was ligated by the anti–DC-SIGN MR-1 antibody, and the cells were incubated at 37°C for 5 minutes. As a control, cells were incubated with either anti-CD38 or anti-CD3 monoclonal antibodies. Mock-transfected cells were subjected to the same treatments for control purposes. After cell lysis, phosphorylated ERK (pERK), p38 (pp38), and PLC-γ (pPLC-γ), and total levels of ERK and PLC-γ were detected using specific polyclonal antisera. The experiment was performed twice with similar results, and one of the experiments is shown. NS indicates not stimulated. (B-C) Calcium determination in MDDCs after DC-SIGN ligation. Fluo-3AM–loaded MDDCs were left untreated (B) or treated with 50 nM SDF-1α (C), and subsequently incubated with anti–DC-SIGN MR-1 monoclonal antibody (20 μg/mL) (right panel) or an isotype-matched control antibody (left panel). Calcium flux was determined by flow cytometry at the indicated time points. Arrows indicate the time of addition of the MR-1 monoclonal antibody. Similar results were obtained from 3 independent experiments, and 1 of them is shown.

observed with either anti-CD38 or anti-CD3 antibodies (Figure 6A). In accordance with this finding, DC-SIGN ligation on the surface of immature MDDCs promoted a transient calcium mobilization (Figure 6B). Therefore, DC-SIGN engagement on the cell surface promotes phosphorylation of ERK, Akt, and PLC-γ, and leads to transient changes in intracellular calcium concentration.

DC-SIGN engagement influences cytokine production during MDDC maturation

The ability of DC-SIGN to modify the activation state of 3 key signaling molecules (ERK, Akt, and PLC-γ) suggested that DC-SIGN ligation might exert a modulatory effect on MDDC maturation. Since ERK activation has been linked to Th2-type polarization and enhanced IL-10 production,[11,25] the release of IL-10 in response to DC-SIGN ligation was determined. Immature MDDCs did not produce detectable IL-10 in response to either TNF-α, Pam3Cys (a synthetic TLR2 ligand), MR-1 antibody, or a control mouse IgG, and only LPS was capable of inducing the production of moderate levels of IL-10 (Figure 7). However, the presence of MR-1 antibody enhanced LPS-induced IL-10 release (Figure 7). Moreover, and although each agent alone had no effect, the simultaneous presence of MR-1 and TNF-α resulted in high levels of IL-10 production (Figure 7). These results are in agreement with the enhanced ERK phosphorylation observed upon MDDC treatment with anti–DC-SIGN and TNF-α, and demonstrate that DC-SIGN engagement on the membrane of immature dendritic cells modulates the maturation program initiated by other cell surface receptors.

Discussion

The generation of pathogen-specific immune responses is based on the plasticity of the dendritic cell maturation process, which results from the integration of all the intracellular signals initiated after recognition of PAMPs by pathogen-recognition receptors. Intracellular signaling from the distinct TLR exhibits the common property of NF-κB activation, but, for DCs, their differential coupling to adapter molecules, their differential activation of MAPKs, and the modulation of their signals by other PAMP receptors contribute to the generation of pathogen-specific dendritic cell maturation and pathogen-tailored immune responses.[25] One of the dendritic cell PAMP receptors is the C-type lectin DC-SIGN, which participates in the recognition and capture of numerous viral, bacterial, and fungal pathogens.[3] In the present report, we demonstrate that DC-SIGN engagement on the dendritic cell surface induces phosphorylation of ERK and Akt, but not p38MAPK, and promotes a transient calcium flux, which correlates with its ability to trigger PLCγ phosphorylation in transfected lymphoid cells. In agreement with its signaling capability, DC-SIGN in lipid rafts associates with tyrosine kinases of the Src and Syk/ZAP-70 families in both dendritic cells and transfected lymphoid cells. All these signaling events might explain the ability of DC-SIGN–engaging ligands to shift MDDC maturation toward the acquisition of pro-Th2/protolerogenic polarizing capability, which is also exemplified by the fact that DC-SIGN ligation synergizes with TNF-α receptor–initiated signals for enhanced IL-10 release.

The signaling and functional consequences of DC-SIGN ligation here reported are in agreement with the results of Geijtenbeek et al, who showed that *Mycobacterium* Man-LAM enhanced IL-10

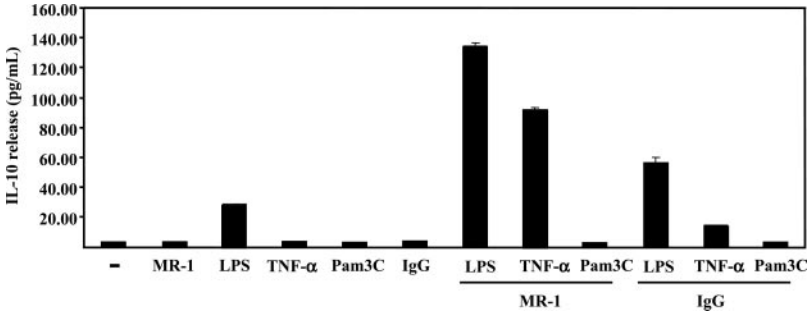

Figure 7. DC-SIGN ligation in immature MDDCs enhances maturation-dependent IL-10 production. MDDCs were incubated with LPS, TNF-α, Pam3Cys, MR-1, or an isotype-matched antibody (IgG), either alone or in the indicated combinations, for 18 hours in complete medium. After incubation, supernatants from MDDCs were collected and IL-10 content was determined by enzyme-linked immunosorbent assay (ELISA). The data indicate means (SD of triplicate samples from 1 representative experiment of 3 experiments on MDDCs from independent donors).

production by MDDCs in a DC-SIGN–dependent manner.[12] The comparison of the intracellular signaling pathways activated by TLR4 and TLR2 has demonstrated that preferential activation of p38MAPK leads to IL-12p70–dependent pro-Th1 dendritic cell maturation, while a high ERK/p38MAPK activation ratio promotes pro-Th2 maturation via increased IL-10 release and reduced IL-12p70 synthesis.[10,11,25] Therefore, the DC-SIGN–mediated ERK activation fits with the enhanced release of IL-10 seen in maturing MDDCs after DC-SIGN engagement, and is also compatible with the inhibitory action of ERK activation on IL-12p70 release by dendritic cells[8] and macrophages.[26] Apart from ERK and p38MAPK, other intracellular signals modulate the pro-Th1/Th2 balance during MDDC maturation. In this regard, (1) PI3K activation in dendritic cells has been shown to negatively regulate IL-12 synthesis and, therefore, prevents Th1 polarization[27]; (2) calcium signaling antagonizes IL-12 production by mature dendritic cells, negatively regulates pro-Th1 maturation, and preferentially promotes the acquisition of pro-Th2/Tc2 characteristics[24]; and (3) lysophosphatidic acid–induced increase of intracellular calcium inhibits IL-12 secretion and enhances secretion of IL-10 from mature dendritic cells.[28] Therefore, the intracellular signaling triggered upon DC-SIGN engagement (ERK and PI3K activation, transient rise in intracellular calcium concentration) would impair IL-12 and enhance IL-10 release and, consequently, might explain why DC-SIGN ligation favors a pro-Th2/protolerogenic dendritic cell maturation.

The relevance of the DC-SIGN cell surface distribution for pathogen binding has been previously demonstrated.[23] In the present report, and in line with recent observations,[23] biochemical analysis of MDDC and DC-SIGN transfectants has revealed that a fraction of DC-SIGN molecules is located within lipid raft–enriched membrane fractions in both cell types (Figures 4-5) and that most DC-SIGN molecules on the plasma membrane reside within lipid raft–enriched microdomains (Figure 4C). Therefore, it is reasonable to assume that the microlocalization of DC-SIGN on the plasma membrane should also contribute to its signaling ability. In this regard, DC-SIGN coprecipitates with Lck or Lyn, 2 Src-family kinases involved in immunoreceptor signaling in lymphoid and myeloid cells.[29] The colocalization of DC-SIGN, Lyn, and Syk provides additional structural support for the regulatory role of DC-SIGN during dendritic cell maturation, as both kinases have been found to modulate murine dendritic cell maturation.[30-32] In fact, Lyn appears to positively regulate IL-12 production in mice and has been proposed to act as a negative regulator of Th2 immunity.[33] Therefore, future experiments are required to determine the functional significance of the DC-SIGN association with Lyn and Syk in dendritic cells, as well as to find out whether the association between DC-SIGN and both kinases reflects direct or indirect interactions. The latter appears as a likely alternative, given the lack of an obvious ITAM motif in the DC-SIGN cytoplasmic tail and the fact that no tyrosine phosphorylation of DC-SIGN has been detected after engagement by either antibodies or pathogenic ligands (data not shown).

Besides DC-SIGN, other lectin receptors expressed on myeloid (Dectin-1) and plasmacytoid (BDCA-2) dendritic cells have been shown to promote intracellular signaling and to modulate TLR signaling. Yeast binding to the β-glucan receptor Dectin-1 synergizes with TLR2 to enhance activation of NF-κB and production of IL-12.[34] In addition, Dectin-1 can also promote IL-10 synthesis via recruitment of Syk to its ITAM motif.[35] Similarly to DC-SIGN, antibody ligation of the plasmacytoid-specific BDCA2 lectin induces calcium mobilization and protein-tyrosine phosphorylation, resulting in suppression of IFN-α/β induction by plasmacytoid dendritic cells.[36] These results, combined with the diversity of their cytoplasmic sequences, suggest that lectins and lectinlike receptors expressed on dendritic cells might exhibit a large degree of variability in the intracellular signaling pathways they activate, providing an additional level of plasticity for the generation of pathogen-specific immune responses. In the case of DC-SIGN, the intracellular signals initiated by this lectin would result in increased pro-Th2/protolerogenic effector functions and might contribute to evasion from immunosurveillance of DC-SIGN–interacting pathogens.[3] However, since mice deficient in the DC-SIGN–related molecule SIGNR1 exhibit increased susceptibility to *Streptococcus pneumoniae*,[37] the dissection of the intracellular signals triggered upon DC-SIGN engagement deserves further investigation, as it might clarify the role of the lectin family on the generation of pathogen-specific immune responses.

References

1. Steinman RM, Hawiger D, Liu K, et al. Dendritic cell function in vivo during the steady state: a role in peripheral tolerance. Ann N Y Acad Sci. 2003; 987:15-25.
2. Kapsenberg ML. Dendritic-cell control of pathogen-driven T-cell polarization. Nat Rev Immunol. 2003;3:984-993.
3. Geijtenbeek TB, van Vliet SJ, Engering A, t'Hart BA, van Kooyk Y. Self- and nonself-recognition by C-type lectins on dendritic cells. Annu Rev Immunol. 2004;22:33-54.
4. Huang Q, Liu D, Majewski P, et al. The plasticity of dendritic cell responses to pathogens and their components. Science. 2001;294:870-875.
5. Ouaaz F, Arron J, Zheng Y, Choi Y, Beg AA. Dendritic cell development and survival require distinct NF-kappaB subunits. Immunity. 2002;16: 257-270.
6. Medzhitov R, Preston-Hurlburt P, Janeway CA Jr. A human homologue of the *Drosophila* Toll protein signals activation of adaptive immunity. Nature. 1997;388:394-397.
7. Saccani S, Pantano S, Natoli G. p38-Dependent marking of inflammatory genes for increased NF-kappa B recruitment. Nat Immunol. 2002;3:69-75.
8. Puig-Kroger A, Relloso M, Fernandez-Capetillo O, et al. Extracellular signal-regulated protein kinase signaling pathway negatively regulates the phenotypic and functional maturation of monocyte-derived human dendritic cells. Blood. 2001; 98:2175-2182.
9. Ardeshna KM, Pizzey AR, Devereux S, Khwaja A. The PI3 kinase, p38 SAP kinase, and NF-kappaB signal transduction pathways are involved in the survival and maturation of lipopolysaccharide-stimulated human monocyte-derived dendritic cells. Blood. 2000;96:1039-1046.
10. Agrawal S, Agrawal A, Doughty B, et al. Cutting edge: different Toll-like receptor agonists instruct dendritic cells to induce distinct Th responses via differential modulation of extracellular signal-regulated kinase-mitogen-activated protein kinase and c-Fos. J Immunol. 2003;171:4984-4989.
11. Dillon S, Agrawal A, Van Dyke T, et al. A Toll-like receptor 2 ligand stimulates Th2 responses in vivo, via induction of extracellular signal-regulated kinase mitogen-activated protein kinase and c-Fos in dendritic cells. J Immunol. 2004;172: 4733-4743.
12. Geijtenbeek TB, Van Vliet SJ, Koppel EA, et al. Mycobacteria target DC-SIGN to suppress dendritic cell function. J Exp Med. 2003;197:7-17.
13. Relloso M, Puig-Kroger A, Pello OM, et al. DC-SIGN (CD209) expression is IL-4 dependent and is negatively regulated by IFN, TGF-beta, and anti-inflammatory agents. J Immunol. 2002;168: 2634-2643.
14. Munoz P, Navarro MD, Pavon EJ, et al. CD38 signaling in T cells is initiated within a subset of membrane rafts containing Lck and the CD3-zeta subunit of the T cell antigen receptor. J Biol Chem. 2003;278:50791-50802.
15. Puig-Kroger A, Serrano-Gomez D, Caparros E, et al. Regulated expression of the pathogen receptor dendritic cell-specific intercellular adhesion molecule 3 (ICAM-3)-grabbing nonintegrin in THP-1 human leukemic cells, monocytes, and macrophages. J Biol Chem. 2004;279:25680-25688.
16. Brown DA, Rose JK. Sorting of GPI-anchored proteins to glycolipid-enriched membrane subdomains during transport to the apical cell surface. Cell. 1992;68:533-544.
17. Millan J, Montoya MC, Sancho D, Sanchez-Madrid F, Alonso MA. Lipid rafts mediate biosynthetic transport to the T lymphocyte uropod subdomain and are necessary for uropod integrity and function. Blood. 2002;99:978-984.

18. Yu Q, Kovacs C, Yue FY, Ostrowski MA. The role of the p38 mitogen-activated protein kinase, extracellular signal-regulated kinase, and phosphoinositide-3-OH kinase signal transduction pathways in CD40 ligand-induced dendritic cell activation and expansion of virus-specific CD8+ T cell memory responses. J Immunol. 2004;172:6047-6056.
19. Banchereau J, Steinman RM. Dendritic cells and the control of immunity. Nature. 1998;392:245-252.
20. de la Rosa G, Yáñez-Mó M, Serrano-Gómez D, et al. The role of DC-SIGN in the nonopsonic recognition of zymosan by dendritic cells. J Leuk Biol. 2005;77:699-709.
21. Alvarez CP, Lasala F, Carrillo J, Muniz O, Corbi AL, Delgado R. C-type lectins DC-SIGN and L-SIGN mediate cellular entry by Ebola virus in cis and in trans. J Virol. 2002;76:6841-6844.
22. Simons K, Toomre D. Lipid rafts and signal transduction. Nat Rev Mol Cell Biol. 2000;1:31-39.
23. Cambi A, de Lange F, van Maarseveen NM, et al. Microdomains of the C-type lectin DC-SIGN are portals for virus entry into dendritic cells. J Cell Biol. 2004;164:145-155.
24. Faries MB, Bedrosian I, Xu S, et al. Calcium signaling inhibits interleukin-12 production and activates CD83(+) dendritic cells that induce Th2 cell development. Blood. 2001;98:2489-2497.
25. Pulendran B. Modulating vaccine responses with dendritic cells and Toll-like receptors. Immunol Rev. 2004;199:227-250.
26. Hacker H, Mischak H, Hacker G, et al. Cell type-specific activation of mitogen-activated protein kinases by CpG-DNA controls interleukin-12 release from antigen-presenting cells. EMBO J. 1999;18:6973-6982.
27. Fukao T, Tanabe M, Terauchi Y, et al. PI3K-mediated negative feedback regulation of IL-12 production in DCs. Nat Immunol. 2002;3:875-881.
28. Panther E, Idzko M, Corinti S, et al. The influence of lysophosphatidic acid on the functions of human dendritic cells. J Immunol. 2002;169:4129-4135.
29. Latour S, Veillette A. Proximal protein tyrosine kinases in immunoreceptor signaling. Curr Opin Immunol 2001;13:299-306.
30. Setterblad N, Blancheteau V, Delaguillaumie A, et al. Cognate MHC-TCR interaction leads to apoptosis of antigen-presenting cells. J Leukoc Biol. 2004;75:1036-1044.
31. Chu CL, Lowell CA. The Lyn tyrosine kinase differentially regulates dendritic cell generation and maturation. J Immunol. 2005;175:2880-2889.
32. Sedlik C, Orbach D, Veron P, et al. A critical role for Syk protein tyrosine kinase in Fc receptor-mediated antigen presentation and induction of dendritic cell maturation. J Immunol. 2003;170:846-852.
33. Beavitt SJ, Harder KW, Kemp JM, et al. Lyn-deficient mice develop severe, persistent asthma: Lyn is a critical negative regulator of Th2 immunity. J Immunol. 2005;175:1867-1875.
34. Gantner BN, Simmons RM, Canavera SJ, Akira S, Underhill DM. Collaborative induction of inflammatory responses by dectin-1 and Toll-like receptor 2. J Exp Med. 2003;197:1107-1117.
35. Rogers NC, Slack EC, Edwards AD, et al. Syk-dependent cytokine induction by Dectin-1 reveals a novel pattern recognition pathway for C type lectins. Immunity. 2005;22:507-517.
36. Dzionek A, Sohma Y, Nagafune J, et al. BDCA-2, a novel plasmacytoid dendritic cell-specific type II C-type lectin, mediates antigen capture and is a potent inhibitor of interferon alpha/beta induction. J Exp Med. 2001;194:1823-1834.
37. Lanoue A, Clatworthy MR, Smith P, et al. SIGN-R1 contributes to protection against lethal pneumococcal infection in mice. J Exp Med. 2004;200:1383-1393.

The DC-SIGN–related lectin LSECtin mediates antigen capture and pathogen binding by human myeloid cells

Angeles Dominguez-Soto,[1] Laura Aragoneses-Fenoll,[1] Enrique Martin-Gayo,[2] Lorena Martinez-Prats,[3] Maria Colmenares,[1] Marisa Naranjo-Gomez,[4] Francesc E. Borras,[4] Pilar Munoz,[5] Mercedes Zubiaur,[5] Maria L. Toribio,[2] Rafael Delgado,[3] and Angel L. Corbi[1]

[1]Centro de Investigaciones Biológicas, Consejo Superior de Investigaciones Científicas (CSIC), Madrid; [2]Centro de Biología Molecular "Severo Ochoa," Consejo Superior de Investigaciones Científicas, Madrid; [3]Hospital Doce de Octubre, Madrid; [4]Hospital Universitari Germans Trias i Pujol, Badalona; [5]Instituto de Parasitología y Biomedicina, Consejo Superior de Investigaciones Científicas, Granada, Spain

Liver and lymph node sinusoidal endothelial cell C-type lectin (LSECtin [CLEC4G]) is a C-type lectin encoded within the liver/lymph node–specific intercellular adhesion molecule-3–grabbing nonintegrin (L-SIGN)/dendritic cell–specific intercellular adhesion molecule-3–grabbing nonintegrin (DC-SIGN)/CD23 gene cluster. LSECtin expression has been previously described as restricted to sinusoidal endothelial cells of the liver and lymph node. We now report LSECtin expression in human peripheral blood and thymic dendritic cells isolated ex vivo. LSECtin is also detected in monocyte-derived macrophages and dendritic cells at the RNA and protein level. In vitro, interleukin-4 (IL-4) induces the expression of 3 LSECtin alternatively spliced isoforms, including a potentially soluble form (Δ2 isoform) and a shorter version of the prototypic molecule (Δ3/4 isoform). LSECtin functions as a pathogen receptor, because its expression confers Ebola virus–binding capacity to leukemic cells. Sugar-binding studies indicate that LSECtin specifically recognizes N-acetylglucosamine, whereas no LSECtin binding to Mannan- or N-acetyl-galactosamine–containing matrices are observed. Antibody or ligand-mediated engagement triggers a rapid internalization of LSECtin, which is dependent on tyrosine and diglutamic-containing motifs within the cytoplasmic tail. Therefore, LSECtin is a pathogen-associated molecular pattern receptor in human myeloid cells. In addition, our results suggest that LSECtin participates in antigen uptake and internalization, and might be a suitable target molecule in vaccination strategies. (Blood. 2007;109:5337-5345)

Introduction

The identification of the lectin gene cluster at chromosome 19p13.2[1] has led to the realization that some C-type lectins are capable of mediating intercellular adhesion, pathogen-binding, and antigen internalization for induction of T cell responses.[2] The paradigmatic example of this type of lectin is dendritic cell-specific intercellular adhesion molecule-3-grabbing nonintegrin (DC-SIGN), which efficiently internalizes antigens,[3] mediates dendritic cell intercellular adhesions,[4] and recognizes a wide range of microorganisms through binding to mannose- and Lewis-containing glycans.[5] C-type lectins on dendritic cells enhance their ability for pathogen recognition[6] and contribute to modulation of toll-like receptor (TLR)-initiated signals.[7] Consequently, the definition of the range of dendritic cell lectins and their binding specificities might provide adequate targets for immune intervention and prevention of pathogen entrance and spreading.

The lectin gene cluster at chromosome 19p13.2 includes the genes encoding for the type II C-type lectins DC-SIGN, liver/lymph node-specific intercellular adhesion molecule-3-grabbing integrin (L-SIGN), CD23, and liver and lymph node sinusoidal endothelial cell C-type lectin (LSECtin).[1,4,8,9] DC-SIGN is expressed on myeloid dendritic cells,[4,10] and alternatively activated in vitro on macrophages.[11] In vivo it is found on interstitial dendritic cells,[12] a subset of CD14+ peripheral blood DC,[13] human microvascular endothelial cells,[8] and on synovial, placenta, lymph node, and alveolar macrophages.[14-16] By contrast, L-SIGN is exclusively expressed on endothelial cells of the liver, lymph nodes, and placenta,[17,18] but not on myeloid cells.

The LSECtin (CLEC4G) gene is located between the CD23 and DC-SIGN genes with the three genes arranged in the same orientation.[9] LSECtin encodes a protein with a lectin domain followed by a 110-residue stalk region, a transmembrane domain, and a 31-residue cytoplasmic domain.[9] LSECtin has been previously detected on liver and lymph node sinusoidal endothelial cells at the protein and RNA level.[9] LSECtin functions as an attachment factor for Ebola virus and SARS, but it does not bind HIV or hepatitis C virus.[19] We now describe the expression of LSECtin isoforms in ex vivo isolated human peripheral blood and thymic dendritic cells as well as in dendritic cells and macrophages generated in vitro. LSECtin exhibits ligand-induced internalization, and its sugar recognition specificity differs from that of DC-SIGN. The presence of LSECtin on myeloid cells should therefore contribute to expanding their antigen-capture and pathogen-recognition capabilities.

Submitted September 21, 2006; accepted February 23, 2007. Prepublished online as *Blood* First Edition Paper, March 5, 2007; DOI 10.1182/blood-2006-09-048058.

The publication costs of this article were defrayed in part by page charge payment. Therefore, and solely to indicate this fact, this article is hereby marked "advertisement" in accordance with 18 USC section 1734.

Materials and methods

The study described was approved by the Centro de Investigaciones Biologicas (CSIC) Institutional Review Board. The study did not involve any direct contact with human subjects.

Cell culture

Human peripheral blood mononuclear cells were isolated from buffy coats from normal donors over a Lymphoprep (Nycomed Pharma, Oslo, Norway) gradient according to standard procedures.[20] Monocytes were purified from peripheral blood mononuclear cells by magnetic cell sorting using CD14 microbeads (Miltenyi Biotech, Bergisch Gladbach, Germany). Monocyte-derived dendritic cells (MDDC), monocyte-derived macrophages, and alternatively (AAMØ) or classically (CAMØ) activated macrophages were generated as previously described.[11,20] Isolation of peripheral blood myeloid dendritic cells (MyDC)was done with a Blood DC isolation kit (MACS; Miltenyi Biotec) with some modifications. First, peripheral blood mononuclear cells were depleted of T cells, NK cells, and monocytic cells by magnetic separation, and the remaining population was incubated with monoclonal antibodies (mAbs) to fluorescein isothiocyanate (FITC)-CD4, phycoerythrin (PE)-labelled CD11c, PE-Cy5-CD14, and PE-Cy5-CD19 and sorted in a FACSVantage cell sorter (BD Biosciences, Franklin Lakes, NJ). PE-Cy5-positive cells were discarded, and double-positive cells for CD4 and CD11c were sorted as MyDC (CD11c+ BDCA2-CD123-). The purity of the resulting population was confirmed by additional antibody staining.

Human thymic dendritic cells and macrophages were isolated from thymus fragments removed during corrective cardiac surgery of patients aged 1 month to 4 years. After Lymphoprep centrifugation, thymocyte cell suspensions were depleted of T, B, NK cells and CD34+ precursors by magnetic cell sorting (AutoMacs; Miltenyi Biotech) as described.[21] Macrophages were isolated from the depleted cell fraction by using PE-labeled anti-CD14mAb and anti-PE microbeads, and exhibited a CD13+, CD11c+, CD14+ phenotype. Thymic pDC were isolated from the macrophage-depleted fraction with PE-labeled antiCD123 and antiPE microbeads, and showed a CD11c-, CD13-, BDCA2+, CD123+ phenotype. Thymic MyDC (CD13+, $CD11c^{dim}$, $CD14^{-}$) were isolated from the CD123-negative fraction with PE-labeled antiCD13 and anti-PE microbeads. Sorted populations proved to be over 97% pure on reanalysis. Phenotypic analysis was carried out by indirect immunofluorescence as described.[20]

The K562 (chronic myelogenous leukemia) and THP-1 (monocytic leukemia) cell lines were cultured as described[20] and THP-1 differentiation induced with phorbol myristate acetate (PMA) at 10 ng/mL.[11] HEK293T and COS-7 cells were grown in Dulbecco modified eagle medium (DMEM) with 10% fetal calf serum (FCS) and transfected with Superfect (Qiagen, Hilden, Germany). Transfection of the pCDNA3.1(-)-based constructs in K562 cells was accomplished with Superfect or by nucleofection (Amaxa GmbH, Cologne, Germany). Mutation of residues Y^{6} $E^{14}E^{15}$, $W^{21}GRW^{24}VHW^{27}$, and both Y^{6} and $E^{14}E^{15}$ were done by site-directed mutagenesis on LSECtin cDNA cloned in pCDNA3.1(-), which resulted in the generation of LSECtin Y/F, LSECtin EE/AA, LSECtin 3W/3A, and LSECtin DM constructs.

Isolation and detection of LSECtin isoform mRNA in distinct cell types

LSECtin isoforms were isolated by reverse transcriptase-polymerase chain reaction (RT-PCR) on RNA from MDDC of a healthy donor. Total cellular RNA was isolated with RNeasy columns (Qiagen). Two micrograms of RNA was reverse-transcribed and amplification was carried out on 5 μL of each cDNA synthesis reaction in 50 μL of solution. After a 5 minute denaturation step, LSEctin was optimally amplified after 35 cycles of denaturation (95°C, 45 seconds), annealing (65°C, 30 seconds), and extension (72°C, 90 seconds), followed by a 10-minute extension step at 72°C. Oligonucleotides used for amplification of the coding region of the prototypical LSECtin isoform (LSECtin full-length) were LSECtin sense 5′-GGGAATTCGCCTGCATCGCCATGGACACC-3′) and LSECtin antisense 5′-CCCAAGCTTGGGCGGGGTCAGCAGTTGTGC -3′). Amplification of LSECtin isoforms was accomplished using the primer pairs LSECtin sense/LSECtin antisense, LSECtin Δ3/4sense/LSECtin antisense, and LSECtin Δ2sense/LSECtin antisense. The oligonucleotide LSECtin Δ3/4sense 5′-CCTATTGTCCAAGGGCTCGGG -′3 spans through the exon 2/exon 5 junction. Oligonucleotide LSECtin Δ2sense 5′-CCGAGGAGGTC-CCCGGAGCCT-′3 spans through the exon 1/exon 3 junction. PCR fragments were resolved in 1.2% agarose gels, purified, cloned, and sequenced. For eukaryotic expression, the selected LSECtin cDNA isoforms were excised from TOPO cloning vectors (Invitrogen, Paisley, UK) with *Eco*RI and HindIII, gel purified, and ligated into *Eco*RI- and *Hin*dIII-digested pCDNA3.1(-). As a control in RT-PCR experiments, GAPDH mRNA was amplified using oligonucleotides 5′-GGCTGAGAACGGGAAGCTTGTCA-3′ and 5′-CGGCCAT-CACGCCACAGT TTC-3′, which together amplify a 417 bp fragment. Images were captured with GelDoc XR (BioRad, Hercules, CA) using Quantity One-4.5.2 software.

Detection and cell-surface distribution of LSECtin

The cDNA region coding for the extracellular portion of LSECtin (residues 55-293) was generated by polymerase chain reaction with the primers 5′-CACCGCCTCCACGGAGCGCGCGG-3′ and 5′-CCCAAGCTT-GGGCGGGGTCAGCA GTTGTGC-3′. The resulting fragment, which contains the neck and lectin domains of LSECtin, was cloned in-frame downstream of the hexahistidine sequence of pET100/D-TOPO (Invitrogen) and sequenced. The resulting vector, as well as a positive control encoding β-galactosidase (pET100/D/lacZ), were transformed into BL21 bacteria, and HIS-LSECtin and HIS-β-gal fusion proteins were purified on Ni^{2+}-nitrilotriacetic acid-agarose (Qiagen). The purified HIS-LSECtin fusion protein was injected intraperitoneally (three times) into Balb/c mice. After a final intraperitoneal boost, splenocytes were removed and fused to SP2 cells at a 1:1 ratio using PEG 1500 (Sigma, Barcelona, Spain), as described.[10] Screening for anti-LSECtin antibodies was done by enzyme-linked immunosorbent assay using 96-well plates coated with HIS-LSECtin or HIS-β-gal (negative control) fusion proteins. Final selection of the selected hybridoma (SOTO1) was done by immunofluorescence on HEK293T transiently transfected with an LSECtin-expression vector.

Peptides based on the sequence of the LSECtin neck region (AQAK-LMEQESALRELREEVTQGLA) and cytoplasmic tail (MDT-TRYSKWGGSSEEVPGGP WGRWVHWSRR) were synthesized using the multiple antigen peptide system. New Zealand white rabbits were immunized by subcutaneous injection of each individual peptide or the HIS-LSECtin protein (0.5 mg of a 1-mg/mL solution in phosphate-buffered saline) in complete Freud's adjuvant 1:1 on day 0 and in incomplete Freud's adjuvant 1:1 on days 21 and 42. Rabbits were bled on day 49, and serum was assayed for LSECtin recognition by Western blot. The resulting antisera (ADS-1 against the neck domain, ADS-3 against the cytoplasmic tail and ADS-4 against the HIS-LSECtin protein) were subsequently validated by Western blot on 10 μg of cell lysates, as described.[20] DC-SIGN was detected using a polyclonal antiserum against the neck region of the molecule.[22] Isolation of detergent-insoluble and soluble MDDC cell membrane fractions was done by sucrose gradient ultracentrifugation as described.[23]

Gene-expression profiling in dendritic cells

RNA from immature and LPS-mature MDDC from two independent donors, and monocyte-derived macrophages from three independent donors generated in the presence of either granulocyte macrophage-colony stimulating factor (GM-CSF) or macrophage-colony stimulating factor (M-CSF), were labeled, processed, and independently hybridized on Codelink human whole genome DNA chip of the Codelink microarray platform (Amersham Biosciences, Uppsala, Sweden) containing 55 000 human gene targets. Scanned images were processed using the Codelink Expression Analysis Software. Raw data were normalized by the quantile method. Data corresponding to the experimental groups were analyzed by the Student *t* test. The raw *P* values obtained were adjusted using the control of the false discovery rate-based procedure and implemented in the multitest package within the Bioconductor set of routines (www.bioconductor.org).

Sugar-binding assays

For precipitation of Mannan-, N-acetyl-glucosamine-, and N-acetyl-galactosamine-binding proteins, K562 cells stably transfected with different LSECtin isoforms (3×10^6) were collected, washed with phosphate-buffered saline and 1 mM EDTA, and lysed. Then, each lysate was incubated with 50 μL of Mannan-agarose (Sigma), N-acetyl-glucosamine-agarose (Sigma), or N-acetyl-galactosamine-agarose (Sigma) for 12 hours at 4°C. After extensive washing, bound proteins were eluted either by incubation with an excess of the sugars or boiling the agarose beads in 3× Laemmli's sample buffer. SDS-eluted material was resolved by SDS-PAGE and LSECtin detection accomplished with specific polyclonal antibodies.

Ebola glycoprotein (GP)1 and virus-binding assays

Ebola virus binding was determined using lentiviral particles pseudotyped with Ebola virus GP according to a transient transfection protocol previously described.[24] K562 transfectants were challenged with Ebola virus GP pseudotypes or controls: 25×10^4 cells were resuspended in 250 μL complete medium and incubated overnight with 250 μL of transfection supernatants. Cells were assayed for luciferase expression 48 hours postinfection. For inhibition experiments, cells were preincubated for 10 minutes at room temperature with the preimmune or ADS-1 polyclonal antibodies.

Ebola virus GP1 (envelope glycoprotein of the Zaire strain of Ebola virus, provided by Dr. Anthony Sanchez, CDC, Atlanta, GA) was fused with human IgG-Fc by subcloning into pEF-Fc (provided by Dr. J. M. Casasnovas, CNB, CSIC, Madrid, Spain). The pSyngp120IgG plasmid, which encodes strain JR-FL HIV gp120 fused to human IgG1Fc, was obtained from the National Institutes of Health AIDS Research and Reference Reagent Program (Germantown, MD). For binding experiments, envelope constructions were transfected into 293T cells and supernatants collected after 72 hours. MDDC were incubated for 30 minutes at room temperature with 1:10 dilution of the supernatants in phosphate-buffered saline, 2% FCS, 4 mM $CaCl_2$. Cells were then washed twice and incubated with a PE-conjugated goat antihuman IgG-Fc antibody (Immunotech, Marseille, France). Cells were analyzed in an EPICS-XL cytometer using the Expo32 software.

LSECtin internalization assays

K562 cells were transiently transfected with LSECtin by Nucleofection (Amaxa). After 24 hours, cells were washed, resuspended in complete medium, and incubated with either SOTO1 (for LSECtin), P5D2 (for CD29), or TS1/18 (for CD18) antibodies for 30 minutes at 4°C to prevent internalization. After extensive washing, cells were placed at 37°C to allow internalization to occur, and aliquots were removed after 2, 5, and 15 minutes and immediately placed at 4°C. Then, cells were incubated with a 1:100 dilution of a FITC-labeled goat anti-mouse antibody (Serotec) to detect cell surface-bound antibodies. All incubations were done in the presence of 50 μg/mL of human IgG to prevent binding through the Fc portion of the antibodies. In some cases, and to detect internalized antibodies, cells were fixed and permeabilized (CytoFIX/CytoPerm; BD Biosciences) before addition of the secondary antibody. Flow cytometry analysis was performed with an EPICS-CS (Coulter Científica, Madrid, Spain) using log amplifiers.

Results

LSECtin mRNA is found in monocyte-derived dendritic cells and is induced by IL-4

The LSECtin gene lies within the C-type lectin-encoding DC-SIGN/L-SIGN/CD23 gene cluster on chromosome 19p13.2.[1] Although reported to be exclusively expressed on liver and lymph node sinusoidal endothelial cells,[9] its chromosomal location prompted us to determine whether LSECtin was found in myeloid cells. Microarray gene profiling experiments showed that LSECtin mRNA is expressed in immature and mature human MDDC (Figure 1A). MDDC contained significantly higher levels of LSECtin RNA than macrophages generated either in the presence of GM-CSF or M-CSF (Figure 1B). This set of data was verified by RT-PCR, because LSECtin mRNA was readily detected in MDDC but was

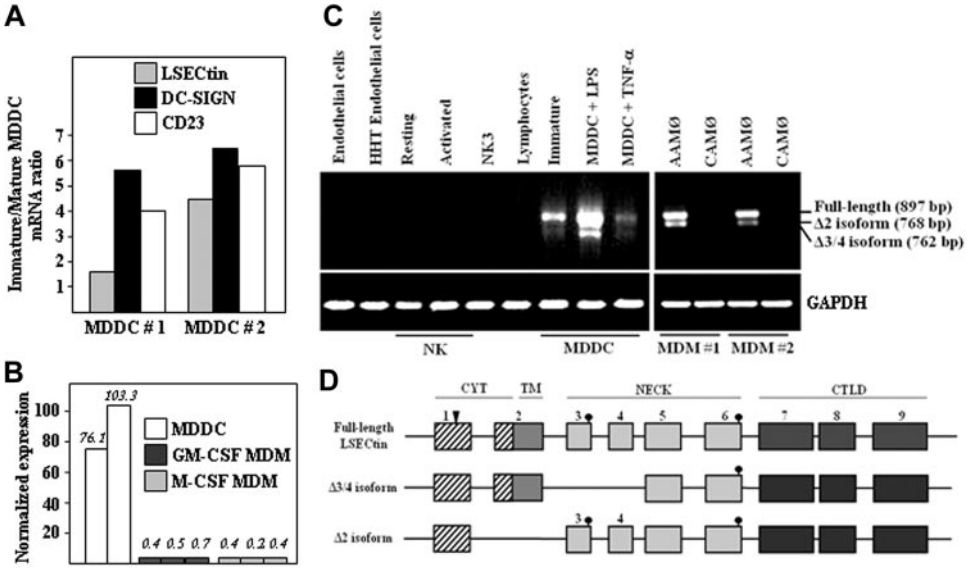

Figure 1. Expression of LSECtin mRNA in human MDDC. (A) Relative levels of LSECtin, DC-SIGN, and CD23 mRNA in immature and mature MDDC as determined by gene expression profiling using Codelink Whole Genome Bioarrays. (B) Relative levels of LSECtin mRNA in immature MDDC from two independent donors and monocyte-derived macrophages generated in the presence of either GM-CSF or M-CSF from three independent donors, as determined by gene expression profiling using Codelink Whole Genome Bioarrays. Values represent the intensity of expression normalized with the median of all the intensity values in the microarray. (C) Detection of LSECtin mRNA in hematopoietic cells, cell lines, and in vitro–generated monocyte-derived macrophages and dendritic cells. Total RNA was isolated from the indicated cells and cell lines and subjected to RT-PCR for amplification of the LSECtin coding region and GAPDH (as control). Analyzed RNA was obtained from endothelial cells from normal and HHT donors, resting and activated NK cells, the NK3 NK cell clone, peripheral blood T lymphocytes, MDM (interferon-γ-activated, CAMØ; IL-4-activated, AAMØ), immature or mature (with either lipopolysaccharide or tumor necrosis factor-α) MDDC, and the THP-1 and K562 leukemic cell lines. (D) Schematic representation of the structure of LSECtin mRNA species amplified by RT-PCR from monocyte-derived dendritic cells. Boxes represent the individual exons, and the arrowhead marks the position of the initiation methionine. Dark circles indicate the potential N-glycosylation sites.

absent from peripheral blood lymphocytes, resting or activated NK cells, or CD34+-derived endothelial-like cells (Figure 1C).

LSECtin mRNA was seen in AAMØ but absent in either naive or CAMØ (Figure 1C). Sequencing of the two RT-PCR fragments routinely generated from MDDC and AAMØ revealed the existence of three LSECtin mRNA species, which encode the prototypic isoform (full-length, 879 bp), an isoform lacking the transmembrane region (Δ2, 768 bp), and an isoform lacking the first two exons encoding the stalk region (Δ3/4, 762 bp) (Figure 1D). The full-length isoform was amplified from more than 20 unrelated MDDC donors, whereas the shorter isoforms were variably detected (data not shown). Therefore, LSECtin mRNA is differentially expressed in monocyte-derived macrophages and dendritic cells, with the latter containing three distinct mRNA species. Moreover, LSECtin expression can be detected in macrophages activated in the presence of IL-4 (AAMØ).

The presence of LSECtin mRNA in AAMØ, and the proximity of the LSECtin gene to that of DC-SIGN, whose expression is IL-4-dependent,[4,10] led us to explore the cytokine responsiveness of the LSECtin gene. LSECtin mRNA was induced during GM-CSF + IL-4-promoted MDDC differentiation and was found to be responsive to the presence of IL-4 (Figure 2A). Besides, and in agreement with the microarray data, LSECtin mRNA was detected in MDDC matured with either lipopolysaccharide or tumor necrosis factor-α (Figure 2A). Similarly, IL-4 induced the appearance of LSECtin mRNA on proliferating or PMA-differentiated THP-1 cells, where the three LSECtin alternatively spliced isoforms were detected (Figure 2B). Because the combined addition of PMA and IL-4 promotes THP-1 cells to acquire a dendritic cell-like phenotype,[11] these results are compatible with the presence of LSECtin in MDDC. More importantly, LSECtin mRNA was detected in ex vivo isolated peripheral blood myeloid dendritic cells (CD11c+ BDCA2-CD123-) (Figure 2C) as well as in myeloid and plasmacytoid thymic dendritic cells and thymic macrophages (Figure 2D). Sequencing of the amplified fragments confirmed the presence of the full-length and Δ2 isoforms in both thymic macrophages and myeloid dendritic cells, which were also seen in human liver RNA as control (Figure 2D). Altogether, these results indicate that LSECtin RNA is induced by IL-4 and is expressed by dendritic cells in vivo.

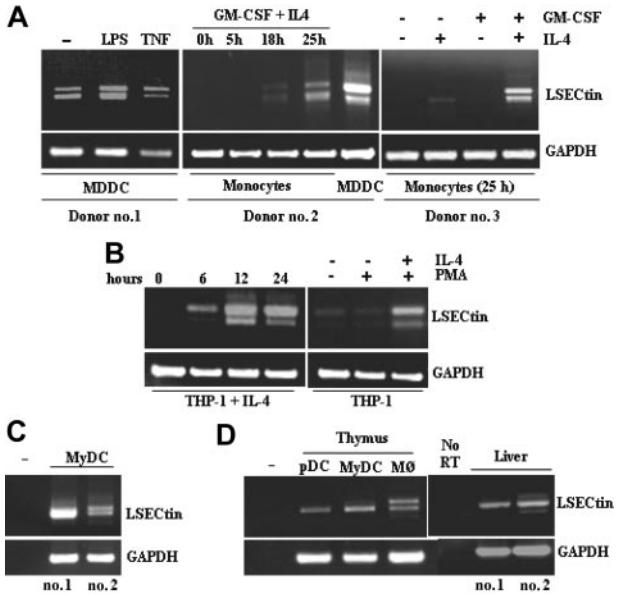

Figure 2. Cytokine-dependence of LSECtin mRNA levels in MDDC and detection of LSECtin mRNA in ex vivo peripheral blood and thymic dendritic cells. (A) Monocytes from three independent donors were treated for the indicated periods of time with either GM-CSF, IL-4, or both cytokines, or allowed to differentiate into MDDC and further matured with lipopolysaccharide or tumor necrosis factor-α. After RNA extraction from the distinct cell types, the coding region of the LSECtin mRNA was amplified and the resulting fragments resolved by agarose gel electrophoresis. (B) THP-1 leukemic myeloid cells were treated for the indicated periods of time with IL-4 alone (left panel) or for 96 hours in the presence of IL-4 and the differentiation-inducing agent PMA (right panel). After RNA extraction from the distinct cell types, the coding region of the LSECtin mRNA was amplified and the resulting fragments resolved by agarose gel electrophoresis. (C) RNA was extracted from human myeloid peripheral blood dendritic cells from three independent donors and LSECtin mRNA detected by RT-PCR. (D) RNA was extracted from human myeloid and plasmacytoid thymic dendritic cells, thymic macrophages, or liver biopsies from three independent donors and LSECtin mRNA detected by RT-PCR. In all cases, GAPDH mRNA was amplified as a control.

LSECtin protein expression in dendritic cells and macrophages

To confirm these results at the protein level, LSECtin-specific polyclonal antisera were raised and their specificity tested by enzyme-linked immunosorbent assay on purified recombinant HIS-LSECtin. Whereas an anti-HIS serum detected HIS-LSECtin and HIS-β-gal to a similar extent, ADS-1 (stalk region-specific) and ADS-4 antiserum (raised against the extracellular region of the molecule) exclusively reacted with HIS-LSECtin (Figure 3A). By contrast, and as expected, ADS-3 antiserum (specific for the LSECtin cytoplasmic tail) showed no reactivity against the HIS-LSECtin recombinant protein (Figure 3A). The LSECtin specificity of the ADS-1 and ADS-4 antisera was further demonstrated by Western blot after transient transfection of the full-length and the Δ2 isoforms in COS7 cells (Figure 3B).

The availability of the anti-LSECtin polyclonal antisera allowed us to address the presence of LSECtin protein in dendritic cells. Analysis of immature and mature MDDC demonstrated the presence of an ADS1-reactive protein band that comigrates with the LSECtin protein generated in COS-7 cells after transient transfection (Figure 3C). The specificity of the recognition was further demonstrated by the fact that the detected band was not observed in the presence of an excess of the immunizing peptide (Figure 3C, right panel). Moreover, and like DC-SIGN,[23] a significant percentage of LSECtin molecules were detected in lipid raft-enriched membrane fractions (Figure 3D), suggesting that LSECtin might also act as a signaling molecule. Therefore, LSECtin is expressed in monocyte-derived dendritic cells, where it might contribute to increase their pathogen-recognition capability.

Detection of LSECtin protein during MDDC differentiation and macrophage activation confirmed the mRNA data. The IL-4-dependent in vitro generation of AAMØ resulted in up-regulation of LSECtin, which was not expressed by CAMØ (Figure 4A). On the other hand, LSECtin was barely expressed in monocytes, increased after 48 hours in the presence of GM-CSF and IL-4, and reached maximal levels in immature MDDC (5-day treatment with GM-CSF + IL-4; Figure 4A). Analysis of MDDC from additional donors confirmed the presence of LSECtin protein in all cell extracts (data not shown). The presence of LSECtin was further evaluated by flow cytometry (Figure 4B) and confocal microscopy (Figure 4C), which revealed the presence of variable levels of LSECtin protein on the cell surface of monocyte-derived dendritic cells. Furthermore, flow cytometry revealed high levels of LSECtin on the cell surface of $CD13^+$ $CD14^+$ thymic macrophages, whereas weak levels were found on both thymic myeloid ($CD13^+$ $CD14^-$) and plasmacytoid ($BDCA2^+$ $CD123^+$) dendritic cells (Figure 4D). Therefore, LSECtin is expressed on the cell surface of in vitro differentiated (MDDC) and ex vivo isolated (thymic macrophages) myeloid cells.

Functional characterization of LSECtin

To evaluate the recognition capabilities of LSECtin, stable transfectants were generated in K562 cells (K562-LSECtin), where the

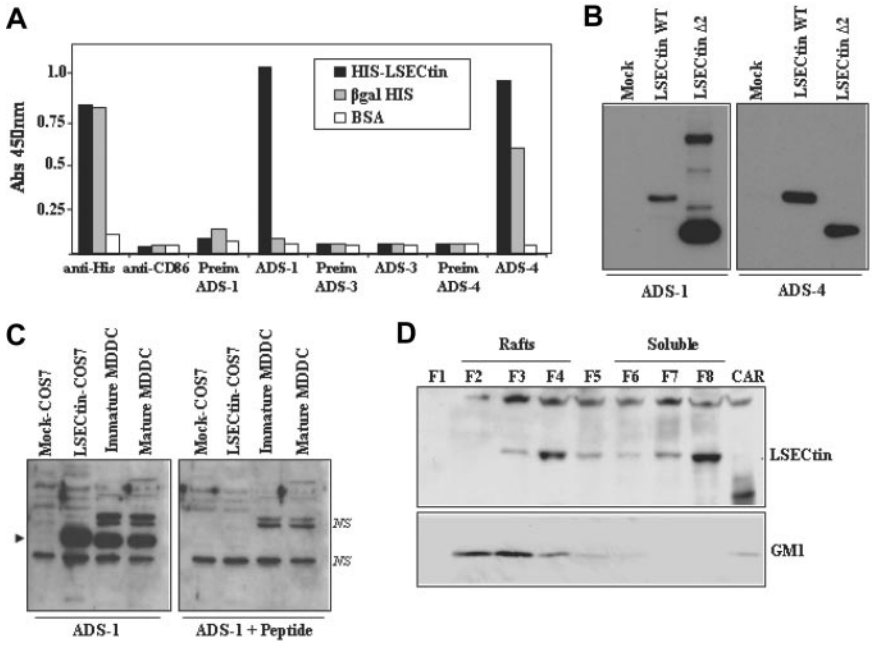

Figure 3. Expression of LSECtin in human MDDC. (A) Specificity of polyclonal antisera against LSECtin by enzyme-linked immunosorbent assay. High protein-binding 96-well plates were coated with either purified HIS-LSECtin, purified βgal-HIS, or BSA. After washing, wells were treated with either a monoclonal antibody against the HIS epitope (anti-His), a control monoclonal antibody (antiCD86), polyclonal antisera against LSECtin (ADS-1, ADS-3, ADS-4), or the corresponding preimmune sera. Bound antibodies were detected using HRP-conjugated goat antirabbit and goat antimouse polyclonal antisera. Quantification was done on a microplate enzyme-linked immunosorbent assay reader at 450 nm. (B) Specificity of polyclonal antisera against LSECtin by Western blot. Whole cell extracts were obtained from COS-7 cells transiently transfected with full-length LSECtin, the Δ2 LSECtin isoform (LSECtin Δ2), or mock-transfected cells (Mock). Ten micrograms of each whole cell extract was subjected to Western blot using the ADS-1 or ADS-4 polyclonal antisera specific for LSECtin. (C) Whole cell lysates were obtained from immature and mature MDDC, and 10 μg of each extract was subjected to Western blot using the ADS-1 anti-LSECtin polyclonal antiserum either alone (left panel) or in the presence of an excess of the immunizing peptide (right panel). Lysates from mock- and LSECtin-transfected COS-7 cells were included as controls. The position of the LSECtin protein is indicated by an arrowhead, and nonspecific bands are denoted as *NS*. (D) Immature MDDC were lysed in 1% Brij 98 lysis buffer at 37°C and fractionated by sucrose density gradient centrifugation. The low-density Brij 98-insoluble fractions 2-4 (lanes 2-4, Rafts) and the high-density Brij 98-soluble fractions 6-8 (lanes 6-8, soluble) were separated by 12.5% SDS-PAGE under reducing conditions, and the distribution of LSECtin was determined by immunoblotting. Cytoskeletal-associated Rafts (CAR), obtained by solubilization of the cell pellet with Brij98 + Octyl D-glucoside in lysis buffer, were analyzed in parallel (lane 9, CAR). Ten micrograms of each fraction was subjected to Western blot, and the distribution of LSECtin and ganglioside GM1 in the distinct fractions was determined by immunoblotting with the ADS-1 polyclonal antisera (LSECtin) or cholera toxin-HRP (GM1). The experiment was done on MDDC from two independent donors, and one of them is shown.

lectin was readily detectable on the cell surface either by flow cytometry (Figure 5A) or by immunoprecipitation of biotin-labeled cell surface proteins (Figure 5B) with polyclonal antisera (ADS-3, ADS-4) or the anti-LSECtin SOTO1 monoclonal antibody. Whereas K562-LSECtin and mock-transfected cells exhibited similar binding of VSV, expression of full-length LSECtin conferred K562 cells the ability to bind viral particles pseudotyped with Ebola or Marburg virus GP (Figure 5C). The viral binding to full-length LSECtin was almost completely abrogated in the presence of the ADS-1 polyclonal antiserum (Figure 5D), confirming the specificity of the interaction. In agreement with these results, K562-LSECtin cells specifically bound soluble Ebola virus glycoprotein GP1 (see subsequently). LSECtin also displayed Ebola GP1-binding ability when expressed on in vitro generated dendritic cells. Although HIV gp120 binding to MDDC was exclusively inhibited by anti-DC-SIGN antibodies, Ebola GP1 binding to MDDC was partially dependent on LSECtin (Figure 5E). In fact, complete abrogation of GP1 binding to MDDC was only observed in the presence of anti-LSECtin antiserum (ADS-1) and anti-DC-SIGN antibodies (MR1) (Figure 5E). Therefore, LSECtin displays pathogen-recognition capability when expressed on hematopoietic cells.

To compare the sugar-specificity of LSECtin with that of DC-SIGN, which acts as an Ebola virus attachment factor,[25] we performed sugar affinity experiments by incubation of extracts from DC-SIGN- and LSECtin-transfected K562 cells with Mannan-, N-acetyl-glucosamine-, and N-acetyl-galactosamine-agarose. Both the full-length and the Δ3/4 isoform were not retained by Mannan-agarose, whereas DC-SIGN bound to this matrix (Figure 6A). However, both LSECtin isoforms were specifically retained by N-acetyl-glucosamine-agarose (Figure 6B) but not by N-acetyl-galactosamine-agarose (Figure 6C). LSECtin from MDDC exhibited the same sugar specificity, because it was retained by N-acetyl-glucosamine-agarose but not by Mannan-agarose (Figure 6D). Therefore, and in agreement with the results of pathogen-binding experiments, LSECtin exhibits a sugar-binding specificity that differs from that of the structurally related DC-SIGN lectin on both K562 transfectants and in vitro generated dendritic cells.

Finally, we evaluated the ability of LSECtin to act as an antigen-capturing receptor by performing internalization experiments with LSECtin-specific ligands. Engagement of LSECtin by SOTO1 led to a rapid loss of the molecule from the cell surface (50% reduction after 2 minutes, 80% after 15 minutes) but did not affect the cell surface levels of CD29 (Figure 7A). To find out whether antibody engagement triggered LSECtin internalization or shedding, a similar experiment was performed using permeabilized cells. No reduction in LSECtin levels was observed when cells were permeabilized before the addition of the secondary fluorescent antibody (Figure 7A), although to a lower extent, the addition of GP1 onto K562-LSECtin cells also resulted in down-regulation of LSECtin without affecting the expression of the CD29 integrin subunit (Figure 7B). Altogether, these results indicate that LSECtin is internalized on ligation on the cell surface and might thus participate in antigen binding and uptake at the early stages of an immune response.

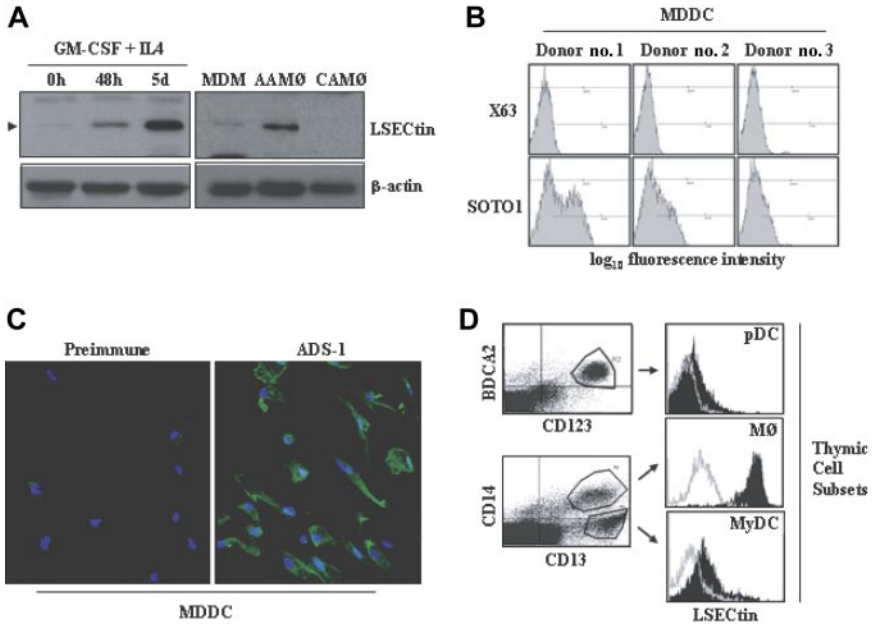

Figure 4. LSECtin expression on the cell surface of monocyte-derived dendritic cells and thymic-cell subsets. (A) Cell extracts were obtained from monocytes along the MDDC differentiation pathway by treating them with GM-CSF plus IL-4 for the indicated periods of time. In parallel, extracts were obtained from GM-CSF-generated macrophages after a 48-hour treatment with medium (MDM), IL-4 (AAMØ), or interferon-γ (CAMØ). In all cases, 10 μg of each lysate was subjected to Western blot for detection of LSECtin with the ADS-1 polyclonal antiserum and β-actin expression determined in parallel for loading control purpose. (B) Cell surface expression levels of LSECtin in monocyte-derived dendritic cells from three independent donors as determined with the antiLSECtin SOTO1 monoclonal antibody. The supernatant from the P3 × 63 myeloma was used as negative control (X63). (C) MDDC were allowed to differentiate on glass coverslips, fixed (paraformaldehyde 2%), washed, and incubated with either a polyclonal antiserum against LSECtin (ADS-1) or preimmune serum. After washing, cells were incubated with a 1:500 dilution of Alexa 488-labeled goat anti-rabbit IgG ($F(ab')_2$) antiserum. Nuclei were counterstained with 4′,6-diamidino-2-fenilindol diclorhidrato (DAPI). Coverslips were mounted in Dako Cytomation fluorescent mounting medium (Dako, Glostrup, Denmark) and representative fields photographed through an HCX PL APO lens (63.0 × 1.40 oil objective), with a 1.400000 numerical aperture on a TCS-SP2-ADBS confocal laser LEICA scanning system (LEICA MICROSYSTEMS GmbH, Wetzlar, Germany). (D) Expression of LSECtin in human thymic cell populations. Human thymic cell preparations were depleted of thymocytes by centrifugation on Ficoll after rosetting with sheep erythrocytes. The resulting population was then stained with either PE-labeled anti-CD123 and FITC-labeled BDCA2 or with FITC-labeled anti-CD14 and PE-labeled anti-CD13 antibodies. The $BDCA2^+$ $CD123^+$ (plasmacytoid DC [pDC]), $CD14^+$ $CD13^+$ (macrophages [MØ]), and $CD14^-CD13^+$ (myeloid DC [MyDC]) subsets (left panels) were simultaneously stained with the anti-LSECtin SOTO1 monoclonal antibody followed by incubation with an APC-labeled goat anti-mouse antiserum (right panels).

Ligand-induced endocytosis is a property shared by lectins involved in antigen capture and presentation and is dependent on the presence of internalization motifs in the cytoplasmic tail.[2] To determine the molecular basis for the antibody-induced LSECtin internalization, two potential internalization motifs similar to those present in other lectins (Y^6SKW and $E^{14}E^{15}$) were mutated and assayed for internalization capability. Mutation of either Y^6 (to F^6) or $E^{14}E^{15}$ (to $A^{14}A^{15}$) significantly reduced the ligand-induced internalization of LSECtin (Figure 7C). Although mutation of Y^6 exhibited a stronger effect at early time points (2 minutes), disruption of both motifs (LSECtin DM) reduced internalization to a higher extent than each individual mutations (after 5 or 15 minutes) (Figure 7C). By contrast, mutation of the three tryptophan residues within the cytoplasmic tail ($W^{21}GRW^{24}VHW$,[27] LSECtin 3W/3A) had no effect (Figure 7C). Therefore, the ability of LSECtin to be internalized on ligand binding is dependent on the integrity of both Y^6SKW and $E^{14}E^{15}$ motifs in the cytoplasmic tail. LSECtin was found to be internalized at a similar rate in MDDC, because only 20% of LSECtin molecules remain on the cell membrane 15 minutes after antibody engagement (Figure 7D). Therefore, LSECtin is internalized after engagement in both transfectants and monocyte-derived dendritic cells, suggesting its involvement in antigen capture and internalization by myeloid cells.

Discussion

The gene cluster in chromosome 19p13.2 includes the C-type lectin-encoding genes CD23, DC-SIGN (CD209), LSECtin, and DC-SIGNR, with the first three of them arranged adjacent to one another and in the same orientation. In the present report, we demonstrate that LSECtin, originally defined as a liver and lymph node sinusoidal-specific lectin,[9] can be induced by IL-4 on human peripheral blood monocytes and is expressed by in vitro generated dendritic cells and alternatively activated macrophages as well as by ex vivo thymic myeloid cells. The IL-4 dependence of LSECtin expression resembles the cytokine responsiveness of the DC-SIGN and CD23 genes, whose expression is either induced or up-regulated by IL-4,[10,26] and suggests a common mechanism for their coordinated up-regulation in IL-4-treated monocytes. Moreover, and like DC-SIGN and CD23, LSECtin is internalized on ligand binding. Therefore, DC-SIGN, CD23, and LSECtin comprise a cluster of structurally related lectin genes expressed on myeloid cells regulated by IL-4 and involved in antigen capture. At present, we have no explanation for the discrepancy between the previously reported lack of LSECtin mRNA detection in MDDC[9] and the data presented in this article, especially considering that MDDC were generated following an identical protocol. LSECtin expression in MDDC is consistent with its induction in alternatively activated macrophages, which share a number of membrane markers with MDDC,[11] and with the presence of LSECtin mRNA in peripheral blood and thymic dendritic cells. Therefore, it can be concluded that LSECtin exhibits a wider cell type distribution than DC-SIGN and CD23 being expressed in both hematopoietic and nonhematopoietic cell lineages.

Like in the case of other C-type lectins,[27] three distinct alternatively spliced isoforms can be predicted for LSECtin based on the sequences of the amplified mRNAs. The LSECtin gene gives

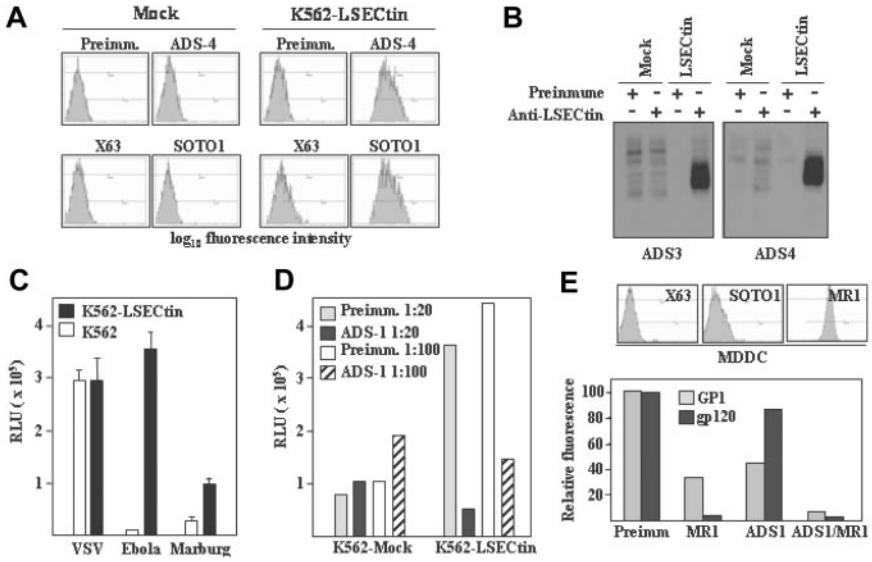

Figure 5. Pathogen-recognition ability of LSECtin. (A) Generation of LSECtin stable transfectants. K562 cells were transfected with an empty vector (Mock) or with an LSECtin expression vector (LSECtin) and grown in G418-containing selective medium. LSECtin expression was determined by indirect immunofluorescence with a polyclonal antiserum against LSECtin (ADS-4) or the SOTO1 anti-LSECtin monoclonal antibody. Preimmune polyclonal antiserum (Preimm.) and the supernatant from the P3 × 63 myeloma (X63) were used as controls. (B) Mock-transfected K562 cells (Mock) or K562-LSECtin cells stably transfected with full-length LSECtin (LSECtin) were surface-labeled with a water-soluble and membrane-impermeable biotin derivative (EZ-linked Sulfo-NHS-LC-Biotin; Pierce, Rockford, IL), washed, lysed, and immunoprecipitated with polyclonal antisera against LSECtin (left panel, ADS-3; right panel, ADS-4) or preimmune serum. Precipitated material was resolved by SDS-PAGE under reducing conditions and subjected to Western blot with HRP-streptavidin. (C) Binding of Ebola and Marburg pseudovirus to LSECtin-transfected cells. Mock-transfected and K562-LSECtin transfectants were challenged with vesicular stomatitis virus (VSV), Marburg or Ebola virus GP pseudotypes, and cells were assayed for luciferase expression 48 hours postinfection. (D) Inhibitory effect of the ADS-1 anti-LSECtin polyclonal antiserum on the Ebola pseudovirus binding to LSECtin. The experiment was performed like in D, but cells were preincubated for 10 minutes at room temperature with the preinmune or ADS-1 polyclonal antibodies before viral addition. (E) Binding of Ebola virus GP1 and HIV gp120 to MDDC. Cells were incubated with the recombinant proteins either in the absence or in the presence of antibodies against DC-SIGN (MR1), LSECtin (ADS-1), or both and binding measured by flow cytometry. Protein binding is measured as relative fluorescence, which indicates the binding observed in each experimental condition relative to the binding detected in the presence of preimmune antiserum (considered as 100). The level of expression of LSECtin and DC-SIGN in the assayed MDDC is illustrated in the upper panel.

rise to both membrane-bound and a transmembrane-lacking potentially soluble isoform (Δ2 isoform). The relative levels of the distinct LSECtin mRNA species appear to be dependent on the cell type: thymic macrophages exhibit equivalent amounts of LSECtin mRNA coding for full-length and truncated (Δ2 and Δ3/4) molecules, whereas thymic dendritic cells almost exclusively contain LSECtin mRNA for the shorter versions of the molecule. Interestingly, and as in the case of DC-SIGN,[27] a significant percentage of LSECtin mRNA species coding for a transmembrane domain-lacking potentially soluble isoform (LSECtin Δ2) have been detected not only in dendritic cells (generated in vitro and isolated ex vivo), but also in alternatively activated macrophages and even in the THP-1 cell line. In fact, and unlike full-length LSECtin, the LSECtin Δ2 isoform can be detected in the supernatant of transfected cells (data not shown), suggesting that it is stable in the extracellular milieu and that it might function as an opsonizing agent. In this regard, a large number of cell surface lectins and lectin-like molecules exhibit potentially soluble isoforms,[28] and several soluble lectins display pathogen-recognition capability.[29] The soluble form of CD23 is found in serum and is generated by endogenous or exogenous proteases that cleave CD23 from the cell surface[26] and has been described as regulating IgE synthesis.[30] The availability of the reagents described in the present article will allow us to determine whether LSECtin can be

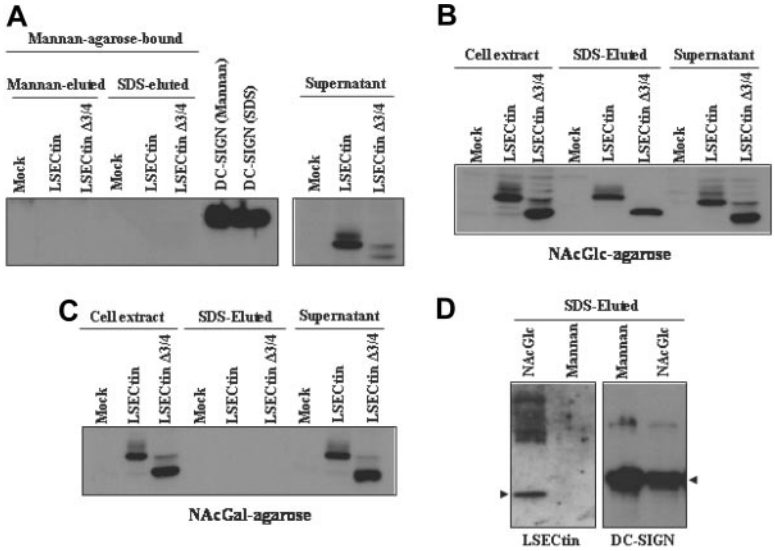

Figure 6. Binding specificity of LSECtin in dendritic cells and transfectants. Whole cell lysates from K562 cells stably transfected with full-length LSECtin(LSECtin), the Δ3/4 isoform (LSECtin Δ3/4), DC-SIGN, or mock-transfected (Mock) were loaded onto Mannan- (A), N-acetyl-glucosamine- (NAcGlc, B), or N-acetyl-galactosamine (NAcGal)-agarose (C) and retained proteins eluted with SDS sample buffer (SDS-eluted) and analyzed by Western blot using the ADS-1 anti-LSECtin polyclonal antiserum. As a control, aliquots from nonretained material (supernatant) were analyzed in parallel. (D) Whole cell lysates from monocyte-derived dendritic cells were loaded onto Mannan- or N-acetyl-glucosamine- (NAcGlc)-agarose and retained proteins eluted with SDS sample buffer (SDS-eluted) and analyzed by Western blot using polyclonal antisera against LSECtin (ADS-1) or DC-SIGN (DSG1).

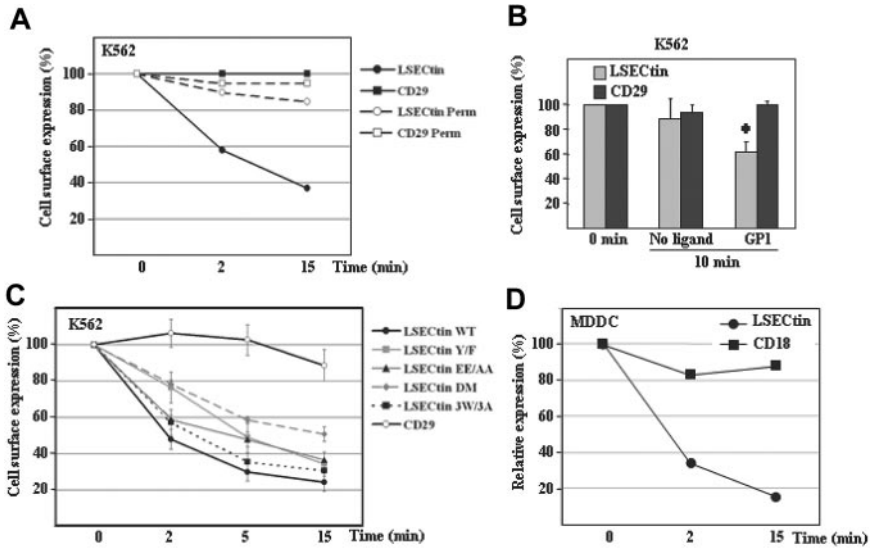

Figure 7. Ligand-induced internalization of LSECtin in transfectants and monocyte-derived dendritic cells. (A) Monoclonal antibody-induced internalization of LSECtin in K562 transfectants. K562-LSECtin cells were incubated with either the SOTO1 (antiLSECtin) or the P5D2 (antiCD29) antibodies for 30 minutes at 4°C. After extensive washing in cold phosphate-buffered saline, cells were transferred to 37°C for the indicated time points, fixed, and the presence of cell surface-bound antibodies detected with FITC-labeled $F(ab')_2$ anti-mouse IgG. Where indicated, cells were fixed and permeabilized before addition of the fluorescent secondary antibody (Perm). Values represent the fluorescence intensity of the cells at the distinct time points relative to the fluorescence intensity of control cells maintained at 4°C. One representative experiment of two is shown. (B) Ebola GP1-induced internalization of LSECtin. K562-LSECtin cells were either untreated or incubated with Ebola virus GP1-Fc (GP1) for 10 minutes at 37°C, transferred to 4°C, and the expression of LSECtin or the CD29 integrin (negative control) determined by indirect immunofluorescence with SOTO1 or P5D2 monoclonal antibodies and FITC-labeled F(ab′)2 anti-mouse IgG. Values represent the fluorescence intensity of the cells at the distinct time points relative to the fluorescence intensity of control cells maintained at 4°C. Mean ± standard deviation of three independent experiments is shown (*$P = 0.001$). (C) Cytoplasmic motifs involved in LSECtin ligand-induced internalization. K562 cells were transiently transfected with expression vectors for WT LSECtin or LSECtin mutated at Y^6 (LSECtin Y/F), $E^{14}E^{15}$ (LSECtin EE/AA), $W^{21}GRW^{24}VHW^{27}$ (LSECtin 3W/3A), or at both Y^6 and $E^{14}E^{15}$ (LSECtin DM). Twenty-four hours later, cells were washed and incubated with the SOTO1 (anti-LSECtin) or the P5D2 (anti-CD29) antibodies for 30 minutes at 4°C. After extensive washing in cold phosphate-buffered saline, cells were transferred to 37°C for the indicated time points (2, 5, 15 minutes), placed on ice, and the presence of cell surface-bound antibodies detected with FITC-labeled $F(ab')_2$ anti-mouse IgG. Values represent the fluorescence intensity of the cells at the distinct time points relative to the fluorescence intensity of control cells maintained at 4°C. Shown are the mean and standard deviation of three independent experiments. (D) Monoclonal antibody-induced internalization of LSECtin in MDDC. MDDC were incubated with either the SOTO1 (anti-LSECtin) or the TS1/18 (anti-CD18) antibodies for 30 minutes at 4°C. After extensive washing in cold phosphate-buffered saline, cells were transferred to 37°C for the indicated time points and immediately transferred to 4°C. The presence of cell surface-bound antibodies was detected with FITC-labeled $F(ab')_2$ anti-mouse IgG. Relative expression of each protein was measured by multiplying the percentage of marker-positive cells by their mean fluorescence intensity and is referred to the value obtained for control cells maintained at 4°C (considered as 100). One representative experiment of two is shown.

detected in serum and whether soluble LSECtin might also influence the IgE network.

Evaluation of the sugar specificity in precipitation assays has revealed that LSECtin interacts with N-acetyl-glucosamine (NAcGlc) but is not retained by N-acetyl-galactosamine (NAcGal) or Mannan. Although previously described to interact with Mannan,[9] our results are in agreement with the lack of Mannan-binding reported by Gramberg et al,[19] despite the presence of the EPN motif in calcium-binding site 2 that mediates Mannose/NAcGlc binding in other C-type lectins.[31] Thus, LSECtin specificity is distinct from CD23, which binds better to Gal-NAcGal-containing structures than to Gal-NAcGlc-structures,[26] and would also differ from DC-SIGN in their ability to be retained by Mannose-containing matrices (Figure 6). Therefore, available data suggest that the three lectins encoded within the 19p13.2 gene cluster are not functionally redundant in terms of sugar-binding specificity. The different carbohydrate specificity of DC-SIGN and LSECtin is further suggested by the distinct aggregation behavior of their corresponding transfectants in K562 cells.[32]

The nonredundant sugar specificity of the three lectins would also imply that DC-SIGN, CD23, and LSECtin differ in their pathogen-recognition capabilities. In fact, our results and those of others[19] indicate that this is indeed the case, because LSECtin does not mediate the binding and uptake of DC-SIGN-interacting pathogens such as HIV, hepatitis C virus,[19] *Leishmania*, *Candida,* or *Aspergillus* (data not shown). However, although the failure of K562-LSECtin to capture these pathogens is in agreement with the inability of Mannan-agarose matrix to retain LSECtin, these results should be interpreted with caution, because DC-SIGN-dependent pathogen-recognition activities are greatly dependent on the cell surface level of expression.[22] Therefore, an extensive analysis of the sugar-binding specificity of LSECtin should be performed before ruling out its ability to interact with DC-SIGN-interacting pathogens.

Several distinct motifs (tyrosine-based, dileucine-based, glutamic-rich sequences) have been identified as responsible for the internalization of dendritic cell lectins involved in antigen capture for subsequent presentation.[33] In the case of LSECtin, its ligand-induced internalization ability is dependent on two internalization motifs (Y^6SKW and $E^{14}E^{15}$) within the cytoplasmic tail of the molecule, which is devoid of a dileucine motif. Analysis of the LSECtin cytoplasmic tail reveals the presence of a tryptophan-rich sequence that conforms to the consensus WXYWXYWXY, where X is a small amino acid and Y is a positively charged residue. Although this sequence resembles motifs found in cytoskeletal and extracellular proteins, its disruption had no effect on LSECtin internalization, which leads us to hypothesize its involvement in signal transduction. The internalization ability of LSECtin fits well with the effector functions of macrophages and dendritic and sinusoidal cells, which constitutively capture extracellular material either for scavenging purposes or for antigen processing and presentation. Along this line, the presence of LSECtin in thymic macrophages and dendritic cells, which are involved in central tolerance induction,[34] is suggestive of a role for LSECtin in antigen presentation and tolerance. On the other hand, the expression of LSECtin in MDDC indicates that the molecule could be a potential

target molecule in vaccination strategies, a capacity already demonstrated for DEC-205 and DC-SIGN.[35,36] If so, determination of the LSECtin specificity might be helpful to understand whether the molecule participates in triggering immune responses (through recognition of PAMPs) or preferentially acts as a tolerance-inducing receptor (through capture of self-antigens).

Acknowledgments

This work was supported by the Ministerio de Educación y Ciencia (grants SAF2005-0021, AGL2004-02148-ALI, and GEN2003-20649-C06-01/NAC) and Fundación para la Investigación y Prevención del SIDA en España (FIPSE 36422/03) to ALC. A.D.S. was supported by a FPI predoctoral grant (BES2004-4405) from Ministerio de Educación y Ciencia (Spain).

Authorship

Contribution: A.D.S. designed the research and performed the experiments; L.A.F., E.G.M., L.M.P., and P.M. performed the research (lipid raft preparation, thymic cell separation, Ebola-binding assays); M.L.T., M.C., M.Z., R.D., and F.B. provided reagents and supervised individual experiments; and A.L.C. supervised research and wrote the paper.

Conflict-of-interest disclosure: The authors declare no competing financial interests.

Correspondence: Angel L. Corbí, Centro de Investigaciones Biológicas, Consejo Superior de Investigaciones Científicas, Velázquez 144, 28 006 Madrid, Spain; e-mail: acorbi@cib.csic.es.

References

1. Soilleux EJ, Barten R, Trowsdale J. DC-SIGN; a related gene, DC-SIGNR; and CD23 form a cluster on 19p13. J Immunol. 2000;165:2937-2942.
2. Cambi A, Figdor CG. Dual function of C-type lectin-like receptors in the immune system. Curr Opin Cell Biol. 2003;15:539-546.
3. Schjetne KW, Thompson KM, Aarvak T, Fleckenstein B, Sollid LM, Bogen B. A mouse C kappa-specific T cell clone indicates that DC-SIGN is an efficient target for antibody-mediated delivery of T cell epitopes for MHC class II presentation. Int Immunol. 2002;14:1423-1430.
4. Geijtenbeek TB, Torensma R, van Vliet SJ, et al. Identification of DC-SIGN, a novel dendritic cell-specific ICAM-3 receptor that supports primary immune responses. Cell. 2000;100:575-585.
5. Feinberg H, Mitchell DA, Drickamer K, Weis WI. Structural basis for selective recognition of oligosaccharides by DC-SIGN and DC-SIGNR. Science. 2001;294:2163-2166.
6. Figdor CG, van Kooyk Y, Adema GJ. C-type lectin receptors on dendritic cells and Langerhans cells. Nat Rev Immunol. 2002;2:77-84.
7. van Kooyk Y, Geijtenbeek TB. DC-SIGN: escape mechanism for pathogens. Nat Rev Immunol. 2003;3:697-709.
8. Bashirova AA, Geijtenbeek TB, van Duijnhoven GC, et al. A dendritic cell-specific intercellular adhesion molecule 3-grabbing nonintegrin (DC-SIGN)-related protein is highly expressed on human liver sinusoidal endothelial cells and promotes HIV-1 infection. J Exp Med. 2001;193:671-678.
9. Liu W, Tang L, Zhang G, et al. Characterization of a novel C-type lectin-like gene, LSECtin: demonstration of carbohydrate binding and expression in sinusoidal endothelial cells of liver and lymph node. J Biol Chem. 2004;279:18748-18758.
10. Relloso M, Puig-Kroger A, Pello OM, et al. DC-SIGN (CD209) expression is IL-4 dependent and is negatively regulated by IFN, TGF-beta, and anti-inflammatory agents. J Immunol. 2002;168:2634-2643.
11. Puig-Kroger A, Serrano-Gomez D, Caparros E, et al. Regulated expression of the pathogen receptor dendritic cell-specific intercellular adhesion molecule 3 (ICAM-3)-grabbing nonintegrin in THP-1 human leukemic cells, monocytes, and macrophages. J Biol Chem. 2004;279:25680-25688.
12. Soilleux EJ, Morris LS, Leslie G, et al. Constitutive and induced expression of DC-SIGN on dendritic cell and macrophage subpopulations in situ and in vitro. J Leukoc Biol. 2002;71:445-457.
13. Engering A, Van Vliet SJ, Geijtenbeek TB, Van Kooyk Y. Subset of DC-SIGN(+) dendritic cells in human blood transmits HIV-1 to T lymphocytes. Blood. 2002;100:1780-1786.
14. van Lent PL, Figdor CG, Barrera P, et al. Expression of the dendritic cell-associated C-type lectin DC-SIGN by inflammatory matrix metalloproteinase-producing macrophages in rheumatoid arthritis synovium and interaction with intercellular adhesion molecule 3-positive T cells. Arthritis Rheum. 2003;48:360-369.
15. Engering A, van Vliet SJ, Hebeda K, et al. Dynamic populations of dendritic cell-specific ICAM-3 grabbing nonintegrin-positive immature dendritic cells and liver/lymph node-specific ICAM-3 grabbing nonintegrin-positive endothelial cells in the outer zones of the paracortex of human lymph nodes. Am J Pathol. 2004;164:1587-1595.
16. Granelli-Piperno A, Pritsker A, Pack M, et al. Dendritic cell-specific intercellular adhesion molecule 3-grabbing nonintegrin/CD209 is abundant on macrophages in the normal human lymph node and is not required for dendritic cell stimulation of the mixed leukocyte reaction. J Immunol. 2005;175:4265-4273.
17. Mukhtar M, Harley S, Chen P, et al. Primary isolated human brain microvascular endothelial cells express diverse HIV/SIV-associated chemokine coreceptors and DC-SIGN and L-SIGN. Virology. 2002;297:78-88.
18. Pohlmann S, Soilleux EJ, Baribaud F, et al. DC-SIGNR, a DC-SIGN homologue expressed in endothelial cells, binds to human and simian immunodeficiency viruses and activates infection in trans. Proc Natl Acad Sci USA. 2001;98:2670-2675.
19. Gramberg T, Hofmann H, Moller P, et al. LSECtin interacts with filovirus glycoproteins and the spike protein of SARS coronavirus. Virology. 2005;340:224-236.
20. Dominguez-Soto A, Puig-Kroger A, Vega MA, Corbi AL. PU.1 regulates the tissue-specific expression of dendritic cell-specific intercellular adhesion molecule (ICAM)-3-grabbing nonintegrin. J Biol Chem. 2005;280:33123-33131.
21. de Yebenes VG, Carrasco YR, Ramiro AR, Toribio ML. Identification of a myeloid intrathymic pathway of dendritic cell development marked by expression of the granulocyte macrophage-colony-stimulating factor receptor. Blood. 2002;99:2948-2956.
22. Serrano-Gomez D, Dominguez-Soto A, Ancochea J, Jimenez-Heffernan JA, Leal JA, Corbi AL. Dendritic cell-specific intercellular adhesion molecule 3-grabbing nonintegrin mediates binding and internalization of *Aspergillus fumigatus* conidia by dendritic cells and macrophages. J Immunol. 2004;173:5635-5643.
23. Caparros E, Munoz P, Sierra-Filardi E, et al. DC-SIGN ligation on dendritic cells results in ERK and PI3K activation and modulates cytokine production. Blood. 2006;107:3950-3958.
24. Wool-Lewis RJ, Bates P. Characterization of Ebola virus entry by using pseudotyped viruses: identification of receptor-deficient cell lines. J Virol. 1998;72:3155-3160.
25. Alvarez CP, Lasala F, Carrillo J, Muniz O, Corbi AL, Delgado R. C-type lectins DC-SIGN and L-SIGN mediate cellular entry by Ebola virus in cis and in trans. J Virol. 2002;76:6841-6844.
26. Kijimoto-Ochiai S. CD23 (the low-affinity IgE receptor) as a C-type lectin: a multidomain and multifunctional molecule. Cell Mol Life Sci. 2002;59:648-664.
27. Mummidi S, Catano G, Lam L, et al. Extensive repertoire of membrane-bound and soluble dendritic cell-specific ICAM-3-grabbing nonintegrin 1 (DC-SIGN1) and DC-SIGN2 isoforms. Inter-individual variation in expression of DC-SIGN transcripts. J Biol Chem. 2001;276:33196-33212.
28. Cambi A, Koopman M, Figdor CG. How C-type lectins detect pathogens. Cell Microbiol. 2005;7:481-488.
29. Ji X, Gewurz H, Spear GT. Mannose binding lectin (MBL) and HIV. Mol Immunol. 2005;42:145-152.
30. Shakib F, Schulz O, Sewell H. A mite subversive: cleavage of CD23 and CD25 by Der p 1 enhances allergenicity. Immunol Today. 1998;19:313-316.
31. Drickamer K. Engineering galactose-binding activity into a C-type mannose-binding protein. Nature. 1992;360:183-186.
32. de la Rosa G, Yanez-Mo M, Samaneigo R, et al. Regulated recruitment of DC-SIGN to cell-cell contact regions during zymosan-induced human dendritic cell aggregation. J Leukoc Biol. 2005;77:699-709.
33. Mahnke K, Knop J, Enk AH. Induction of tolerogenic DCs: 'you are what you eat.' Trends Immunol. 2003;24:646-651.
34. Wu L, Shortman K. Heterogeneity of thymic dendritic cells. Semin Immunol. 2005;17:304-312.
35. Bonifaz L, Bonnyay D, Mahnke K, Rivera M, Nussenzweig MC, Steinman RM. Efficient targeting of protein antigen to the dendritic cell receptor DEC-205 in the steady state leads to antigen presentation on major histocompatibility complex class I products and peripheral CD8+ T cell tolerance. J Exp Med. 2002;196:1627-1638.
36. Tacken PJ, de Vries IJ, Gijzen K, et al. Effective induction of naive and recall T-cell responses by targeting antigen to human dendritic cells via a humanized anti-DC-SIGN antibody. Blood. 2005;106:1278-1285.